Exploring the Role of Zeb1 in the Haematopoietic System

Hamed Ahmad Alzahrani

Presented to the Cardiff University in partial

Fulfilment of the requirements for the degree of PhD at

CARDIFF UNIVERSITY

School of Biosciences

July 2023

ACKNOWLEDGMENTS

ABSTRACT

Zeb1 is a zinc finger transcription factor that plays a critical role in embryonic development, tissue regeneration, and stem cell biology. While *Zeb1* has been suggested to be involved in regulating the self-renewal and differentiation of hematopoietic stem cells (HSCs), the cellular and molecular mechanisms by which *Zeb1* may regulate HSC function are not fully understood.

We initially identified potential ZEB1 target genes in HSCs by RNA-sequencing of adult HSCs after Mx1-Cre mediated deletion of *Zeb1*. We found *Zeb1* regulates cell adhesion and cytoskeletal organization related genes as well as lipid metabolism related genes. Our studies identified cell adhesion molecule EpCAM as a critical ZEB1 target in HSCs. We analysed the impact of *Zeb1* mediated regulation of EpCAM expression on the transcriptional programming and molecular fate of HSCs and found that EpCAM expression in *Zeb1* knock-out (KO) HSCs increased cell survival and decreased transcriptional markers for mitochondrial metabolism, RNA synthesis, and differentiation.

To investigate the role of *Zeb1* in the long-term maintenance of HSCs, we conditionally deleted *Zeb1* using the Vav-iCre system, which deletes *Zeb1* gene expression in HSCs during embryonic development at E11.5. *Zeb1* KO mice were born with reduced Mendelian inheritance, demonstrating *Zeb1* KO in HSCs during embryonic development causes perinatal lethality. We found *Zeb1* KO mice that survived into young adulthood (8-12 weeks) displayed expanded HSC numbers but with reduced repopulation activity in transplantation experiments. Young adult *Zeb1* KO HSCs displayed widespread myeloid and lymphoid differentiation defects including B-cell maturation and erythroid differentiation. Disrupted erythroid differentiation in *Zeb1* KO HSCs led to the development of anaemia. In addition to the well-described critical role for Zeb1 in T-cell development, we found that loss of *Zeb1* in HSCs impaired positive selection of thymocytes and the cell survival of T-cell subpopulations, resulting in a pronounced expansion in effector and memory T-cell frequency and a reduction in naive T-cells. Our RNA-seq analysis of young adult *Zeb1* KO HSCs revealed altered transcriptional programming related to erythropoiesis, immunodeficiency, HSC maintenance pathways and inflammation. Heightened expression of

inflammatory cytokines IL-6, TNF-alpha and IFN-gamma in the plasma of young adult *Zeb1* KO mice was observed, identifying *Zeb1* as a critical mediator of inflammation. Ageing of adult *Zeb1* KO mice lead to fatality with almost complete penetrance, and evidence of profound anaemia and preliminary evidence suggesting the development of pre-leukaemia (MDS/MPN-like) was observed. In addition, a single aged *Zeb1 KO* mouse appeared to develop a CD4+ T-cell driven lymphoproliferative syndrome. This suggests that *Zeb1* depletion in HSCs can drive both myeloid and lymphoid malignancies/pre-malignancies. Overall, these data support the notion that *Zeb1* acts as a tumour suppressor in select haematologic malignancies.

In summary, this study reveals that *Zeb1* is critical regulator of long-term HSC integrity, and that lack of *Zeb1* in HSCs leads to the development of haematologic malignancies. These findings shed light on the complex molecular mechanisms underlying *Zeb1* regulation of HSC function, which may have important implications for the development of novel therapies for hematopoietic disorders where *ZEB1* expression is downregulated.

TABLE OF CONTENTS

Table of Contents

LIST OF TABLES

LIST OF FIGURES

ABBREVIATIONS

aa	amino acid
AGM	aorta-gonad-mesonephros
AICD	activation-induced cell death
AML	acute myeloid leukaemia
ANOVA	Analysis of Variance
AP	alkaline phosphatase
BCL	B-cell lymphoma
BCL-xl	B-cell lymphoma-extra large
BM	bone marrow
bp	base pair
BSA	bovine serum albumin
CAM	cell adhesion molecule
CBC	complete blood count
CD	cluster of differentiation
CFC	colony-forming cell
CFU	colony-forming unit
CFU-E	Colony Forming Unit Erythrocyte
CFU-S	spleen-colony units
ChIP	Chromatin immunoprecipitation
CLOUD-HSPC	continuum of low-primed undifferentiated hematopoietic stem and progenitor cell
CLP	common lymphoid progenitor
CM	central memory T-cell
CMJ	corticomedullary junction
CMP	common myeloid progenitor
CRC	colorectal cancer
Cre	Cre recombinase
CSC	cancer stem cell
CTL	cytotoxic T-cell
CXCR	CXC chemokine receptors
DAPI	4′,6-diamidino-2-phenylindole
DC	dendritic cell
DDR	DNA damage response
DEG	differentially expressed genes
DN	double negative
DP	double positive

Early-E	early erythroblasts
EC	endothelial cell
ECM	Extra Cellular Matrix
ECSCRI	European Cancer Stem Cell Research Institute
EDTA	ethylenediaminetetraacetic acid
EHT	endothlial to haematopoietic transition
EM	effector memory T-cell
EMT	epithelial to mesenchymal transition
Eng	Endoglin
EpCAM	epithelial cell adhesion molecule
EPCR	endothelial protein C receptor
EpEX	EpCAM extracellular domain
EpICD	EpCAM intracellular domain
EPO	erythropoietin
EryP	erythroid progenitor
ES	embryonic stem
ETP	early T-cell progenitor
FACS	fluorescence activated cell sorting
FBN1	fibrillin 1
FBS	foetal bovine serum
FDR	False Discovery Rate
FMO	fluorescence minus one control
FSC	forward scatter
GMP	granulocyte-macrophage progenitor
GO	gene ontology
GSEA	Gene Set Enrichment Analysis
HCT	hematocrit
HGB	haemoglobin concentration
HPC	haematopoietic progenitor cell
HSC	haematopoietic stem cell
HSPC	hematopoietic stem and progenitor cell
iCre	codon-improved Cre
IKB	IPA knowledgebase
IL	interleukin
ILC	innate lymphoid cell
ILCP	innate lymphoid cell group2
IMDM	Iscoves modified Dulbecco's medium

IMID	immune-mediated inflammatory disease
IPA	ingenuity pathways analysis
IRF	interferon regulatory factor
Itga2b	Integrin alpha 2b
KEGG	Kyoto Encyclopaedia of Genes and Genomes
KO	knockout
KRT8	keratin 8
Late-E	late erythroblasts
LDL	low-density lipoproteins
LDLR	low-density lipoprotein receptor
LIF	leukemia inhibitory factor
Lin	lineage
LK	Lin-Kit+ Sca-1- cell
LMPP	lymphoid-primed multipotent progenitor
lncRNA	long non-coding RNA
LSC	Leukaemic Stem Cell
LSK	c-Kit+Lin-Sca-1+
LT-HSC	long-term haematopoietic stem cell
MACS	magnetic-activated cell sorting
MAPK13	mitogen-activated protein kinase 13
MCU	mitochondrial calcium uniporter
MCV	mean corpuscular volume
MDS	Myelodysplastic Syndrome
ME	Mds1-Evi1
MegE	megakaryocyte/erythroid
MEP	megakaryocyte-erythroid progenitor
MET	mesenchymal to epithelial transition
MFI	median fluorescence intensity
MK	megakaryocyte
MkP	megakaryocyte progenitor
MLC	mouse large cholangiocyte
MPP	multipotent progenitor
MSC	mesenchymal stem cell
mTOR	mechanistic target of rapamycin
NH4Cl	Ammonium Chloride
NK	natural killer cell
NKT	natural killer T cell

ns	not significant
OPGL	osteoprotegrin ligand
ORA	over-representation analysis
PB	peripheral blood
PBS	phosphate-buffered saline
PCR	polymerase chain reaction
PD-L1	programmed death-ligand 1
PERP	TP53 apoptosis effector related to PMP-22
PFA	paraformaldehyde
PI	propidium iodide
pIpC	polyinosinic–polycytidylic acid
PLT	platelets
PLWH	people infected with human immunodeficiency virus
Pre GM	pre-granulocyte-macrophage progenitor
Pro-E	proerythroblases
PS	phosphatidylserine
PS-2	presenilin-2
PTEN	phosphatase and tensin homolog
RBC	red blood cell
RNA-seq	RNA sequencing
rRNA	ribosomal RNA
RT	room temperaature
SAS	systemic autoimmune syndrome
SCF	stem cell factor
SCID	severe combined immunodefeciency
SCZ	subscapular zone
SDF-1	stromal cell derived factor 1
SEM	standard error of the mean
SLAM	Signalling Lymphocyte Activation Molecule
Slamf1	cell-surface expression of lymphocytic activation molecule family member 1
SP	single positive
SSC	single scatter
ST-HSC	short-term haematopoietic stem cell
T-ALL	t-cell acute lymphoblastic leukaemia
TACE	TNF-alpha-converting enzyme

TCR	T-cell receptors
TF	transcription factor
TGF	transforming growth factor
TNFR	tumour necrosis factor receptor
TROP1	trophoblast cell-surface antigen 1
VSMC	vascular smooth muscle cells
WBC	white blood cell
WT	wild-type
ZEB	zinc-finger E-box-binding homeobox

CHAPTER 1: Introduction

1.1 Haematopoiesis: General Introduction

The mammalian bone marrow contains haematopoietic stem cells (HSCs), which are rare cells that dwell at the top of a hierarchy of progenitors that eventually, on further differentiation, become limited to a few or just one specialised blood or immune cells (Orkin 2000). Functional research on animal models in the last several decades has gradually revealed a cell at the highest level of haematopoietic hierarchy, which is, ultimately, responsible for generation of all blood and immune cells. Firstly, in initial studies led by Jacobson et al. in 1951 the authors were able to completely recover haematopoiesis in mice whose blood system was destroyed by irradiation by intravenously transplanting normal adult BM cells (Jacobson et al. 1951). In further seminal investigations led by Till and McCulloch, after BM transplantation it was discovered that there were clusters of haematopoietic cells, termed colonies, on the spleens of irradiated mice. The potential of a single hematopoietic cell to give rise to a single colony of differentiated blood cells in the spleen of radio-treated mice was termed a spleen-colony unit (CFU-S) (TILL and McCULLOCH 1961). The existence of multiple types of specialised blood cells was shown in the CFU-S assay, revealing the presence of multipotent cells within the bone marrow that may give rise to these differentiated blood cells. This finding opened the door for additional research into the characteristics and identity of the multipotent hematopoietic stem cell (HSC) (TILL and McCULLOCH 1961; Becker et al. 1963; Siminovitch et al. 1963). In the intervening decades, the development of flow cytometry technologies together with transplantation assays has allowed for the identification and refinement of HSC populations and their downstream progenitors, which are responsible for blood cell reconstitution following transplantation.

Haematopoietic stem cells (HSCs) are able to execute a wide range of cellular pathways, including self-renewal, quiescence, proliferation and differentiation through intermediate progenitors into different mature blood lineages (Ema et al. 2014). Since the lifespan of blood cells is short, replenishment of multi-lineage progenitors and the precursors committed to individual haematopoietic lineages are required from HSCs. The self-renewing nature of HSCs allows for a constant pool of HSCs to be maintained while being able to produce specific, non-

renewable lineages of progenitor cells (Benz et al. 2012). According to this paradigm, HSCs continue to self-renew while also producing progenitors that are dedicated to specific blood lineages and have limited lineage potential.

There are multiple classes of HSCs. On one hand, the cells termed long-term haematopoietic stem cells (referred to as LT-HSCs) the classical model, can sustain life-long capacity for self-renewal and multilineage differentiation. These LT-HSCs produce short-term HSCs (ST-HSCs) another classical model, a group of cells that lack the same level of self-renewal potential as their parental cells. In turn, these ST-HSCs can develop multipotent progenitors (MPPs), with further reduced self-renewal potential. There is a significant bifurcation between the myeloid and lymphatic branches which leads to the production of common myeloid progenitor cells (CMP) and common lymphoid progenitor (CLP) cells. The oligo-lineage progenitors CMPs also experience another division into two groups: one being referred to as granulocyte-macrophage progenitor (GMP) and the other as megakaryocyte-erythroid progenitor cells (MEP) (Yu and Cantor 2012; Woolthuis and Park 2016a) (Figure 1.1). MEPs subsequently split into erythroid progenitor (EryP) and unipotent megakaryocyte progenitor (MkP) cells (Yu and Cantor 2012; Woolthuis and Park 2016a). Terminally differentiated adult blood cells produced by these lineage-restricted progenitors include platelets, red blood cells, granulocytes, and antigen-presenting cells such as dendritic cells (DCs), mastocytes, natural killer cells (NKs), monocytes, macrophages, B cells, and T cells (Figure 1.1) (Orkin and Zon 2008a; Doulatov et al. 2012; Yamamoto et al. 2013; Sawai et al. 2016).
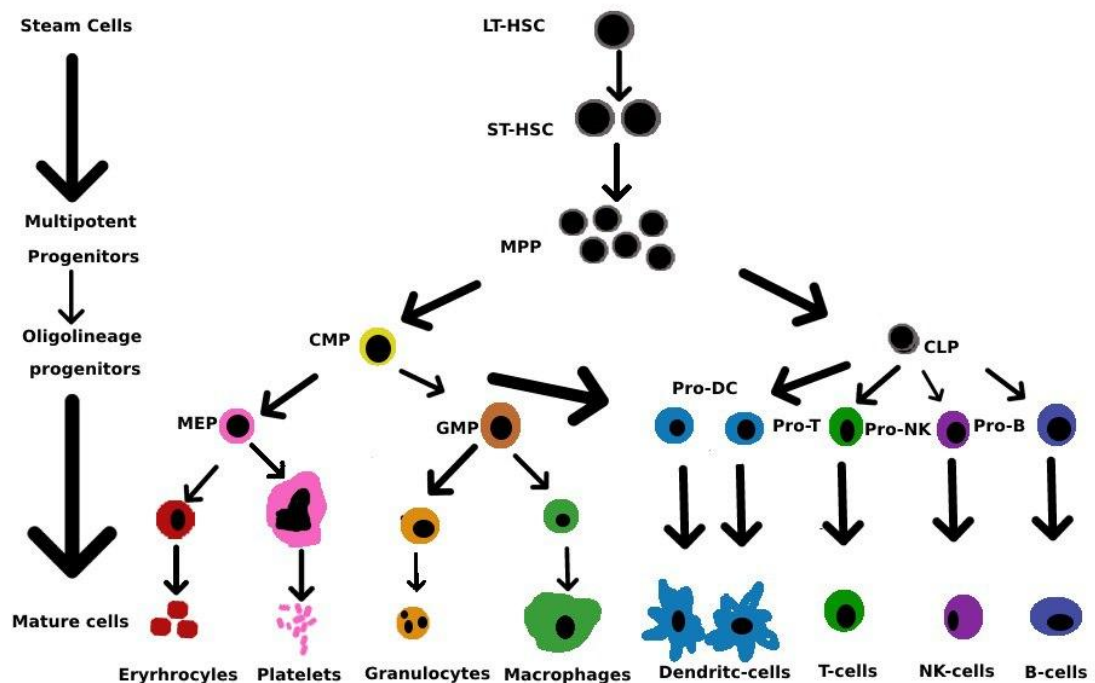
Figure 1.1 The haematopoietic hierarchy. It is possible to distinguish between LT-HSCs, which are highly self-renewing cells that reconstruct an animal throughout its existence, and ST-HSCs, which reconstitute the blood system in the animal for only a short time. The ability of ST-HSCs to further develop into oligo-lineage-restricted progenitors allows a maturation process that ends in the differentiation to MPPs. The lineage of CLPs produces lymphocytes such as T, B, and natural killer (NK) cells are produced by the CLPs. The CMPs generate GMPs, which give rise to fundamental mature cells such as into monocytes, macrophages, and granulocytes Finally, MEPs generate megakaryocytes, platelets, and erythrocytes. Dendritic cells can develop from both CMPs and CLPs. Adapted from Passegué et al. 2003

According to the traditional binary hierarchical model of haematopoiesis, committed precursors that develop after necessary intermediary stages give rise to all megakaryocytes (MKs) (Woolthuis and Park 2016b). Recent data on megakaryocytopoiesis, however, challenges the notion of the traditional binary hierarchical developmental paradigm by suggesting that MKs may be produced directly from HSCs (Yang et al. 2019). MKs and HSCs have similar receptor expression and gene expression profiles, among similar signalling pathways and transcriptional profiles (Yang et al. 2019). Due to these similarities, it is now possible that under the traditional stepwise differentiation paradigm, the megakaryocytic lineage specification takes place earlier than previously believed (Yang et al. 2019). Studies have shown that MKs can develop from HSCs by direct differentiation without the intermediary steps of lineage commitment, providing evidence in favour of this concept (Yang et al. 2019). Additionally, the overlapping involvement of HSCs and MKs in lineage commitment and

differentiation is supported by the expression of several important transcription factors and signalling molecules, including GATA-2 and TPO (Yang et al. 2019). Along the same lines, according to the standard binary developmental paradigm of HSCs, the lymphoid and myeloid lineages are the two main lineages that are produced by HSCs. Recent research in mice has refuted this theory by revealing a group of cells known as lymphoid-primed multipotent progenitors (LMPPs), which differ from traditional HSCs, yet contain the ability to develop into lymphoid or myeloid cells. This research implies that lineage specification may not be as rigidly binary as previously believed and that the early phases of hematopoietic development may be more complex (Yang et al. 2019). These findings have been termed the "two-tier" model. According to this model HSCs can be separated into two different populations, each with a different capacity for self-renewal and differentiation. The HSCs that can generate all different types of blood cells, multipotency and megakaryocytic/erythroid activity are found in the top tier. This means that the megakaryocytic/erythroid lineage bifurcation can occur at any cellular hierarchy prenatally. ST-HSCs, which can only produce a portion of the blood cell types and have a more constrained capacity for self-renewal and differentiation, and uni-lineage progenitors make up the second tier. There are no oligopotent intermediates in between. The functional and molecular investigations of HSCs and their offspring served as the foundation for the two-tier concept. It implies that the degree of self-renewal potential as well as the level of differentiation contribute to the variety of HSCs (Notta et al. 2016; Yang et al. 2019). In other models, researchers suggest that unilineage-restricted cells emerge without passing through discrete hierarchically organised progenitor populations (Velten et al. 2017). In this paradigm, there is no obvious difference between multipotent and lineage-restricted progenitors where haematopoiesis is an ongoing process (Velten et al. 2017). Importantly, in these new models, the HSC compartment directly generates the megakaryocytic lineage (Yang et al. 2019) (Figure 1.2). These HSCs that are biased towards producing megakaryocytes and platelets may have an important physiological function and a function in disease processes, such as biological ageing and stress-induced inflammation (Yang et al. 2019).
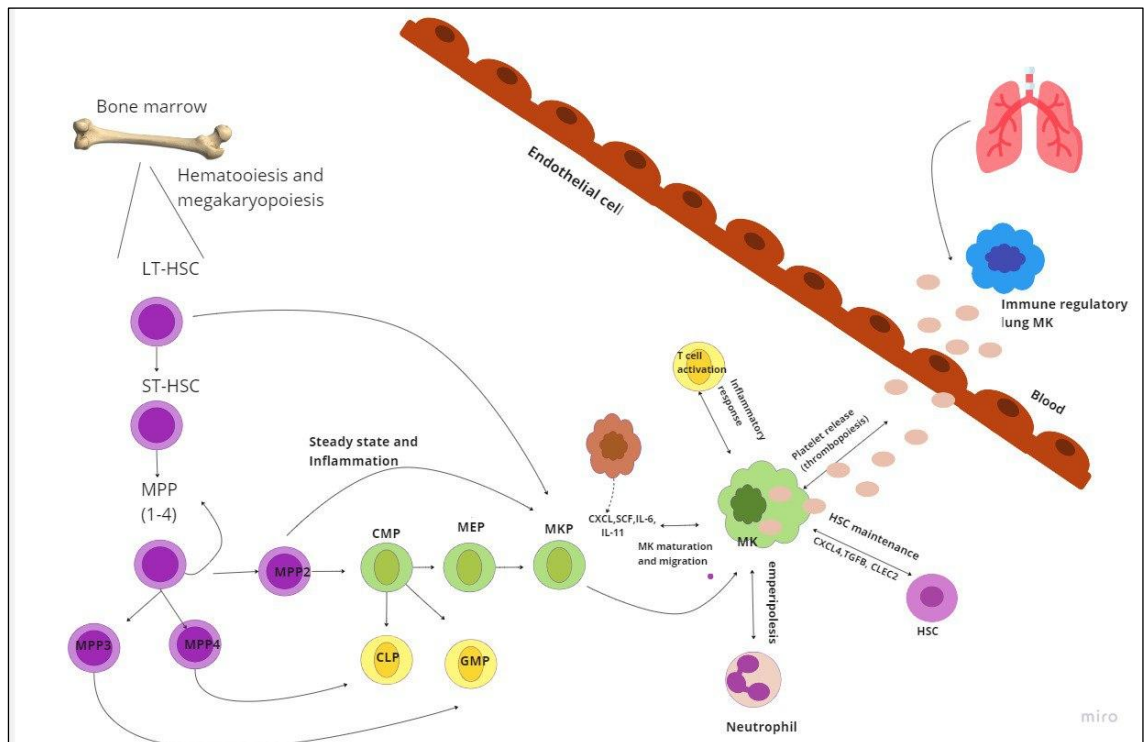
Figure 1.2 Heterogeneity in the growth and operations of megakaryocytes. The process of megakaryopoiesis involves the differentiation of various progenitor cells in the bone marrow, including long-term (LT-HSCs) and short-term HSCs (ST-HSCs or MPP1), multipotent progenitor (MPP2) cells, common myeloid progenitor (CMP) cells, Mk-erythroid progenitor (MEP) cells, and Mk progenitor cells, resulting in the maturation of megakaryocytes (MKs). The process of MK maturation involves enlargement, proplatelet extension, and the release of platelets into circulation (thrombopoiesis). The differentiation of MPP2, MPP4, and MPP3 into MEP, CLP, and GMP, respectively, occurs via separate mechanisms. Although this process is observed under steady-state conditions, it typically occurs in response to stress, such as inflammation. Recent research suggests that besides producing and releasing platelets, MKs also support HSC niche cells, engage in cellular engulfment of other BM cells, control neutrophil movement and activation, and boost CD4^{+} T cell activation and function. Additionally, mesenchymal stem cells (MSCs) regulate the maturation and migration of Mks by producing cytokines, chemokines, and soluble factors. Through adhesion molecules, Mks can interact directly with MSCs. Adapted from: https://www.frontiersin.org/articles/10.3389/fonc.2022.840044/full

1.2 Haematopoietic hierarchy under steady state conditions

HSCs are critical for maintaining the haematopoietic system and, due to their tremendous therapeutic potential, are a target in both clinical and fundamental haematology research. The kinetics of haematopoiesis under steady-state and stress conditions, as well as the role of HSCs in steady-state haematopoiesis, are, however, still debatable, and unclear.

Steady-state differentiation of HSCs allows for the production of an adequate number of differentiated blood cells while preserving the HSC pool for future use (Manfredini et al. 2005; Upadhaya et al. 2018; Olariu and Peterson 2019; Cheng et al. 2020). The study of how HSCs clones and their progeny contribute to blood production over time is known as clonal dynamics in haematopoiesis and it is a field where work is still needed in order to comprehend the observed functional heterogeneity within HSPC populations. A clone refers to a group of cells with a common ancestor (Sun et al. 2014). The analysis of clonal dynamics can provide insights into the diversity, competition, stability, and evolution of HSCs and their descendants. Methods like lineage tracing, single-cell sequencing, and mathematical modelling can be used to measure clonal dynamics (Fabre et al. 2021; Mitchell et al. 2022).

While it is possible to characterise cell populations based on their specific cell-surface markers, the ideal method for assessing the biological activity of HSCs is *in vivo* transplantation (Orkin and Zon 2008b). It entails transferring donor cells into a mouse which does not have its own hematopoietic cells. After integrating into the recipient's bone marrow niche, the donor cells begin to produce blood cells. Researchers can assess the transplanted cells' capacity to reconstruct the hematopoietic system, as well as their capacity for differentiation and self-renewal, by examining the makeup of the blood cells produced over time. This allowed for assessing the role of HSCs in long-term multilineage haematopoiesis (Notta et al. 2011). These transplantation studies are conducted in hosts that have been lethally irradiated and therefore allowed supported the concept that a small population of HSCs is responsible for the production of various types of blood cells through a stable hierarchy of short-lived progenitor cells.

In 2014, this prevailing idea was challenged with a novel transposon-based labelling method to mark individual cells and their descendants in vivo (Sun et al. 2014). The authors of the study discovered that the traditional view of a small number of long-lived haematopoietic stem cells producing a hierarchy of short-lived progenitors was not accurate during native non-transplant haematopoiesis. The study revealed that the primary contributors to steady state haematopoiesis during most of adulthood are multipotent progenitors (MPPs), rather than the traditional definition of HSCs, which contribute minimally to adult unperturbed, steady-state haematopoiesis (Sun et al. 2014; Busch et al. 2015). Following this controversial study, steady-state haematopoiesis during adulthood was shown to be primarily driven by a large number of long-lived progenitors or short-term HSCs, instead of the traditionally defined long-term HSCs, through experiments utilizing inducible Cre recombinase to trace their lineages (Busch et al. 2015). It should be noted that their labelling approach may underestimate the contribution of HSCs because the group of labelled cells include not only LT-HSC or MPPs but also other cells (Sun et al. 2014; Busch et al. 2015; Ito and Frenette 2016).

In contrast, recent reviews focusing on research applying genetic lineage tracing in mice suggest that during native adult haematopoiesis HSCs may indeed be the primary contributors to blood production (Pucella et al. 2020). These findings were pioneered by the work of Sawai and colleagues (Sawai et al. 2016). The researchers found a way to identify and track HSCs in mice by using *Pdzk1ip1* as a genetic marker and track these stem cells' activity over several months (Sawai et al. 2016). They found that these HSCs had the ability to produce different types of blood cells and could also give rise to other HSCs. They were also able to confirm that this marker could identify HSCs properly and that a majority of them were labelled efficiently, in contrast to the underestimation observed in Sun et al. (2014) Busch et al. (2015) and Ito & Frenette (2016). These findings were further confirmed by two separate CreER drivers, *Krt18*-CreERT2 and *Fgd5*-CreER, utilised to trace the lineage of HSCs. Here, it was discovered that adult HSCs significantly contribute to steady-state haematopoiesis and that myeloid cells and B cells followed the platelet lineage in terms of speed and robustness of contribution from HSCs (Chapple et al. 2018).

It is clear how Cre-based labelling is a potent method for lineage tracing and how it can be utilised to identify particular cell populations, such as HSCs or multipotent progenitors. However, the choice of promoter driving Cre expression will probably determine the specificity of the technique and is also one of the sources for the differential, opposing findings across groups (McRae et al. 2019).

1.3 HSC functional definition and immunophenotypic markers

Since haematopoietic cells can be studied by flow cytometry/cell sorting methods, cell surface markers that characterise each type of haematopoietic cell need to be defined. These cell markers allow for the identification of differentiated cells from stem cells and progenitors and, also, detect the stages of differentiation, commitment, or maturation. In humans and mice, the cell surface markers for each cellular type differ. Generally, it is the absence of lineage-specific marker expression that is a critical characteristic of HSCs (Wognum et al. 2003; Pouzolles et al. 2016; Dong et al. 2020; Rix et al. 2022).

In C57/BL6 mice, the co-expression of the cell surface proteins c-Kit and Sca1, as well as the non-expression of Lin (lineage) markers, which are regularly found on committed cells like T-cells and B-cells, NK cells, granulocytes, monocytes, macrophages, and erythrocytes, enriches for HSPC populations. Sca-1, also known as Ly6A, modifies receptor tyrosine kinases and Src family kinases to control cell signalling and adherence (Holmes and Stanford 2007). When the cell surface receptor c-Kit (also known as CD117) is activated by its ligand stem cell factor (SCF), it can control various cellular processes, including apoptosis, differentiation, and proliferation of HSCs (Miettinen and Lasota 2005).

Since these findings, more specific cell surface markers have been found to generate greater purity when isolating HSC populations. Although the Lin-Sca-1+c-Kit+ (LSK) phenotype strongly favours haematopoietic reconstituting activity, progenitor cells also exist in this compartment alongside long-term HSCs, with approximately only 10% of KLS cells containing genuine long-term HSCs (Challen et al. 2009). The Hoechst-effluxing side population (SP), LSKCD150+CD48- cells, LSKCD34-Flk-2- cells have all been identified as populations with LT-HSC reconstituting potential (Goodell et al. 1996; Adolfsson

et al. 2001; Balazs et al. 2006; Dykstra et al. 2006; Kiel et al. 2007). Although cell surface markers EPCR, rhodamine, and SLAM markers CD229 and CD244, and CD41 can be used to isolate dormant and/or functionally distinct subsets, HSCs in the mouse are now typically defined as LSKCD150+CD48- (Wilson et al. 2008; Kent et al. 2009; Oguro et al. 2013; Yamamoto et al. 2013; Miyawaki et al. 2015). HSCs can display lineage bias and lineage biased HSC composition can be evaluated by examining CD150hi (myeloid biased), CD150int (balanced), and CD150lo (lymphoid biased) expression within the HSC compartment (Beerman et al. 2010; Morita et al. 2010; Young et al. 2016).

In contrast to mouse HSCs, mouse MPPs include cells that reside in the LSK fraction with little to no self-renewal potential as evidenced by transplantation experiments. CD135+ (Flk2+) LSK cells, which are the most common and best-characterised MPP subtype, are currently thought to be a completely multipotent but lineage-biased population with low potential for megakaryocyte/erythroid (MegE) lineages and high lymphoid potential(Akashi et al. 2000). One such population of cells can mature into T, B, and natural killer (NK) cells are known as the common lymphoid progenitors (CLPs)(Kondo et al. 1997). In contrast, the myeloid lineage is composed of common myeloid progenitors that can differentiate into granulocyte-macrophage progenitors and megakaryocyte-erythroid progenitors (Akashi et al. 2000). The initial CMP/GMP/MEP paradigm, however, may not adequately depict the true nature of these cells as they may comprise mixed populations of cells with various lineage potentials, according to current investigations(Akashi et al. 2000). The Pronk dissection, a new classification scheme that enables the more exact purification of the myeloid/erythroid compartment, has been offered as a solution to this problem(Pronk et al. 2007). In order to identify more precise progenitor cell subpopulations, this method discriminates bone marrow cells according to the expression of several surface markers (Pronk et al. 2007). Prospective identification of myeloid progenitor subsets with developmentally restricted lineage potentials can be identified through the cell-surface expression of lymphocytic activation molecule family member 1 (Slamf1/CD150), Endoglin (Eng/CD105), and Integrin alpha 2b (Itga2b/CD41) (Pronk et al. 2007). In particular, the Pronk model includes separating the common myeloid progenitors

and granulocyte-macrophage progenitors from the more differentiated megakaryocyte-erythroid progenitors. These subsets include early precursors for the lineages of granulocyte/macrophage, erythroid, and megakaryocytic. Distinct and ordered expression profiles of multiple transcription factors and growth factor receptors were identified through genome-wide expression analyses of these subsets (Pronk et al. 2007). In the following table (Table 1.1), the mouse HSPC populations used in this thesis are highlighted.

Table 1.1 Cell surface markers used to identify the different subtypes of HSCs.

Population	Cell surface markers
LT-HSC (Cabezas-Wallscheid et al. 2014)	Lin- Sca-1+ c-Kit+ CD150+ CD48- CD135- CD34-
MPP1 (short-term self-renewal, multipotent) (Cabezas-Wallscheid et al. 2014)	Lin- Sca-1+ c-Kit+ CD150+ CD48- CD135- CD34+
MPP2 (multipotent) (Cabezas-Wallscheid et al. 2014)	Lin- Sca-1+ c-Kit+ CD150+ CD48+ CD135- CD34+
MPP3 (myeloid biased) (Cabezas-Wallscheid et al. 2014)	Lin- Sca-1+ c-Kit+ CD150- CD48+ CD135- CD34+
MPP4 (lymphoid biased) (Cabezas-Wallscheid et al. 2014)	Lin- Sca-1+ c-Kit+ CD150- CD48+ CD135+ CD34+
CLP	Lin- c-kitlow Sca1low CD127+ CD135+
LMPP conventional	Lin- Sca-1+ c-Kit+ CD150- CD135+ CD34+
LMPP+s	Lin- Sca-1+ c-Kit+ CD135+CD127+
LMPP-s	Lin- Sca-1+ c-Kit+ CD135+CD127-
ILCPs	Lin- Sca-1+ c-Kit-/lo CD135- CD127+
Pre-GM	Lin- c-kit+ Sca1- CD150- CD41- CD16/32- CD105-
GMP	Lin- c-kit+ Sca1- CD34+ CD16/32+
MEP	Lin- c-kit+ Sca1- CD34- CD16/32-
CMP	Lin- c-kit+ Sca1- CD34+ CD16/32-
Pre-MegE	Lin- c-kit+ Sca1- CD150+ CD41- CD16/32- CD105-
MkP	Lin- c-kit+ Sca1- CD150+ CD41+
Pre-CFU-E	Lin- c-kit+ Sca1- CD150+ CD41- CD16/32- CD105+
CFU-E + Pro-Ery	Lin- c-kit+ Sca1- CD150- CD41- CD16/32- CD105+
Myeloid lineage (monocytes, macrophages and granulocyte precursors, immature myeloid cells)	Mac1+ Gr1-
Myeloid lineage (myeloid cells and granulocytes, mature myeloid cells)	Mac1+ Gr1+
Erythoid compartments (Pro-E, Early-E, Late-E)	CD71/Ter119
proerythroblasts (Pro-E)	CD71+ Ter119-/low
Early-erythroblasts (Early-E)	CD71+ Ter119+
late erythroblasts (Late-E)	CD71- Ter119+
T-cells	Gr- Mac- B220- CD4+ or CD8+
B-cells	Mac1- Gr1- B220+ CD4- CD8-

1.4 Role of EMT processes in HSCs

Given the properties of HSCs alluded to above, it is worth mentioning that these characteristics are not 'innate' to all types of HSCs. For instance, developing and adult HSCs can be distinguished by their proliferative capacity – in contrast to developing HSCs, which are highly proliferative, adult HSCs, in contrast, are relatively quiescent (Hamidi and Sheng 2018). How do these adult HSCs acquire these properties? The answer lies, in part, in a developmental process called the epithelial to mesenchymal transition (EMT) (Hamidi and Sheng 2018).

In a multicellular organism, cells can be classified as either epithelial or mesenchymal. In the former, the cells organise themselves with a uniform and consistent apicoplast polarity (Huang et al. 2012; Hamidi and Sheng 2018; Pei et al. 2019; Persa and Niessen 2019). In the Epithelial to Mesenchymal Transition (EMT), polarised epithelial cells become misshapen and acquire motile and migratory properties of mesenchymal cells (Kavanagh et al. 2014; Chen et al. 2017). This process, along with the opposite known as Mesenchymal to Epithelial Transition, involve changes in cellular shape and adhesion regulated by a small group of master pleiotropic transcription factors, including ZEB, SNAI and TWIST gene families (Thiery and Sleeman 2006).

Additional complexity arises from the fact that most EMT/MET processes can be seen to include three independent states: in the two extremes, the epithelial or mesenchymal identities, both extensively studied and defined. A third, 'transitional' state conceptually corresponds to the continuum of interconnected and overlapping transitional states, also known as intermediate states(Hamidi and Sheng 2018). In EMT, the thermodynamic term 'metastable' is used to define this transient state that varies between being completely epithelial to completely mesenchymal. The molecular markers for complete epithelial and full mesenchymal cells are relatively well defined (Zeisberg and Neilson 2009) (Figure 1.3). On the other hand, the metastable condition expresses both epithelial and mesenchymal markers and thus is more difficult to be defined in an EMT/MET continuum (Bakir et al. 2020).
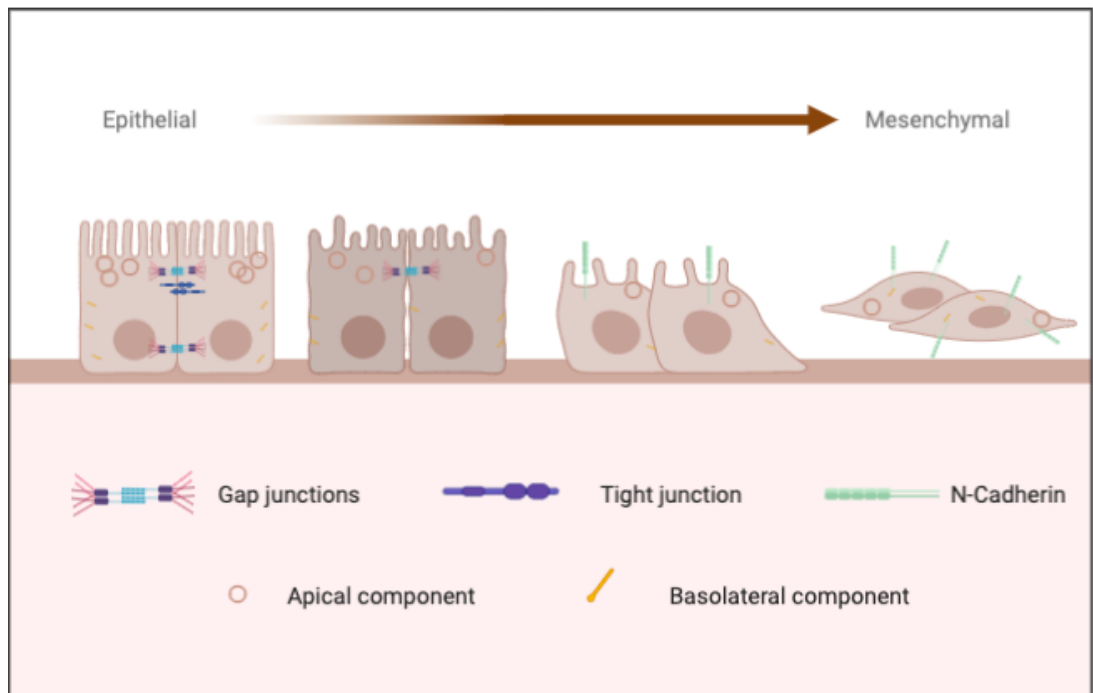
Figure 1.3 Epithelial to Mesenchymal Transition. This illustration shows the modifications to the cellular elements that take place during the epithelial to mesenchymal transition (EMT). Gap junctions closely join cells in the normal epithelial state, and N-cadherin, tight junctions, and apical components are highly expressed. The cells go through several alterations during EMT, including the loss of gap junctions, decreased expression of N-cadherin, and adjustments to the tight junctions. The basolateral components become more noticeable, and the apical components become disordered. In the end, these modifications result in the development of mesenchymal cells, which have a more migratory phenotype. Created in BioRender.com

During mammalian embryogenesis, HSCs undergo a special type of EMT process known as an endothelial-to-haematopoietic transition (EHT) (Kissa and Herbomel 2010). In this dynamic developmental process, HSCs sequentially migrate to many anatomical locations, including the yolk sac, aorta-gonad-mesonephros (AGM) area, placenta, foetal liver and finally the adult bone marrow (Kumaravelu et al. 2002; Ottersbach and Dzierzak 2005; Robin et al. 2009; Ivanovs et al. 2011; Li et al. 2012; Ivanovs et al. 2017). At embryonic day 10.5 (E10.5), the first definitive adult-type HSCs in the mouse are produced from hemogenic endothelial cells in the ventral wall of the dorsal aorta and are part of the haematopoietic clusters closely associated with the endothelium (Ema et al. 2006; Medvinsky et al. 2011; Yokomizo et al. 2011). They have the typical cell–cell junctions, organised cytoskeleton, and apicobasal polarity. In the posterior stages of development, these cells are influenced by a signalling cascade involving the Notch1/Jagged1 pathway, which is thought to be the main EHT driver (Vasquez et al. 2021). Haematopoietic clusters are formed by changing the cell shape and loss of adhesion from the hemogenic endothelium, gaining a

spindle-shaped morphology and increasing cell motility (Antas et al. 2013). This signalling cascade is thought to be triggered by the transforming growth factor (TGF)-B, which in turn can trigger other forms of EMT, by controlling *Jagged1*, *Hey1* and *Twist1* expression(Zavadil et al. 2004). In animal models knocking out these genes, the phenotypes observed are similar and a decrease of *Gata2*, *Runx1* and *Myb* is observed (Kulkeaw et al. 2017). The EMT process during embryogenesis sets the stage for the integration of HSCs into the adult BM niche, where they undergo further interactions with the endosteal and vascular niches to maintain their balance between self-renewal and differentiation(Hamidi and Sheng 2018).

When the organism reaches adulthood, the HSCs move to a specific microenvironment in the bone marrow called the bone marrow cavity. Here, balanced signals control whether HSCs remain in quiescence, self-renew or differentiate into one of the several lineages (Pinho and Frenette 2019). The different interactions with the microenvironments alter the epithelial and mesenchymal characteristics of HSCs. The endosteal niche, part of the bone marrow cavity, is full of spindle-shaped N-cadherin-positive osteoblasts (Lévesque et al. 2010). These interact with HSCs and inhibit the cell cycle of HSCs. The other component of the bone marrow cavity, the vascular niche, helps with the HSCs proliferation by controlling oxygen concentration and metabolic state (Pinho and Frenette 2019). Haematopoietic stem cells HSCs coexist with endothelial, stromal, and other supportive cells in the perivascular niche within the bone marrow, a microenvironment made up of two types of blood vessels called arterioles and sinusoids (Morrison and Scadden 2014). With the provision of signalling cues like Notch ligands and angiopoietin-1 that encourage HSC quiescence and hinder their differentiation, arterioles and sinusoids play a crucial role in controlling HSC fate (Pinho and Frenette 2019). Specifically, HSCs in close proximity to the perivascular niche have a propensity to remain quiescent, whilst those located further away are more likely to differentiate or self-renew (Pinho and Frenette 2019). Balancing HSC self-renewal and differentiation is necessary for the proper functioning of the hematopoietic system and, is likewise, maintained by the perivascular niche (Oh and Nör 2015; Pinho and Frenette 2019). Given that EMT is a highly complex yet reversible process, it seems

plausible that epigenetic mechanisms such as methylation of DNA, gene expression regulation or chromatin modifiers could be involved in finely tuning EMT control in the bone marrow niche.

1.5 Molecular mechanisms in migration and adhesion of HSCs

I previously defined the fundamental role of transplantation in defining whether a subset of cells are indeed HSCs. We could now pose the question: how do these cells migrate and exert their final function? In transplantation, haematopoietic stem cells undergo a journey where they need to actively enter the bone marrow to replenish the body with new blood cells. To do so, they need to attach, roll and then migrate through the endothelial cells of blood vessels (Kanz et al. 2016; Caocci et al. 2017).
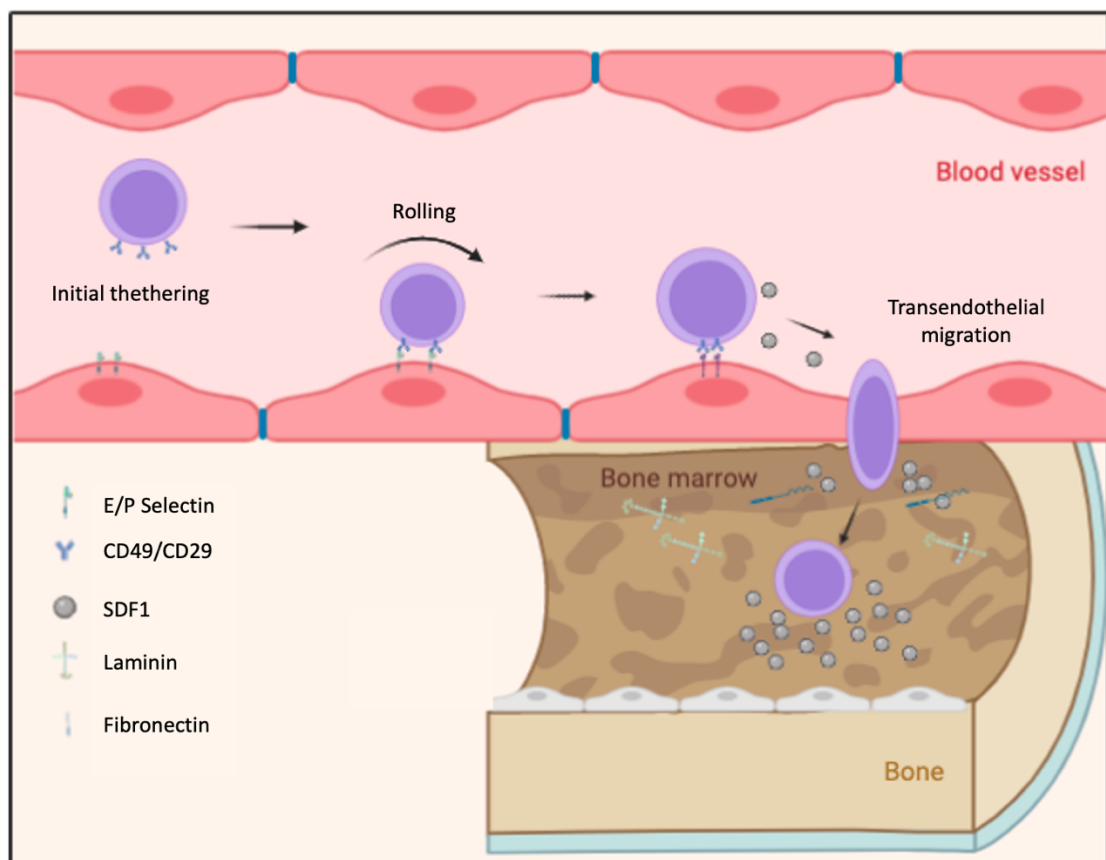
Figure 1.4 Homing of hematopoietic stem cells (HSCs) from the bloodstream to the bone marrow niche. HSCs go through a series of steps to target the endothelial niche. As E- and P-selectin receptors on ECs attach to their ligands on the HSCs, rolling is triggered, acting as a molecular brake to limit HSC migration out of the bone marrow. The adhesion molecules VCAM and ICAM are then activated by the chemokine CXCL12, promoting the strong adherence of HSCs to vascular ECs. HSC extravasation is caused by polarised migration across the endothelium, which is facilitated by chemokines and adhesion molecules. After that, HSCs disperse and engage in interactions with the bone marrow microenvironment to control whether they will proliferate or go into quiescence. Created in BioRender.com

Cell adhesion molecules (CAMs) are proteins that are prominently expressed on the surface of immune cells (such as leukocytes, lymphocytes, macrophages) and on cells that interact with the extracellular matrix (such as endothelial cells, epithelial cells, platelets and fibroblasts) (Harjunpää et al. 2019). CAMs have a significant role in facilitating cell adhesion, migration, and signaling, fostering interactions between cells and their surrounding environment. This particular role, and the fact that cells can bind with one another or the extracellular matrix, shows the importance of CAMs in homing and adhesion (Sam-Yellowe 2021). In homing, for instance, the attachment of cells to the endothelial cells lining blood vessels is expedited by CAMs, which help guide cells to specific tissues or organs. There are several classes of CAMs such as selectins, integrins, cadherins, inmunoglobuli-superfamily CAMs, integrin-related CAMs and mucins. Here, for the purpose of this thesis, we will describe the most relevant to migration and adhesion of HSCs (Harjunpää et al. 2019; Sam-Yellowe 2021).

Selectins are involved in the initial tethering and mediate the rolling of haematopoietic stem and progenitor cells in bone marrow (Xia et al. 2004). Coating a surface with immobilised P- or E-selectin was sufficient enough to induce the rolling of cells under flow conditions (Xia et al. 2004). In contrast, adhesion of CD34+ HPCs to bone marrow-derived endothelial cells was not dependent upon E-selectin in static conditions. In a study of P- and E-selectin deficient mice, the recruitment of HPCs to bone marrow was found to necessitate selectins. To allow trans-endothelial migration to occur, firm adhesion of haematopoietic stem and progenitor cells to endothelial cells is mandatory (Figure 1.4). Therefore, bone marrow homing is a coordinated multistep process (Sahin and Buitenhuis 2012).

Another group of important molecules for HSC adhesion and trans-endothelial migration is the integrins (Voermans et al. 2000). Integrins have been implicated in the regulation of bone marrow homing as well. *In vitro* studies utilizing blocking antibodies showed that both CD49d/CD29 and CD11/CD18 play a distinct part in the adhesion of haematopoietic stem cells and progenitors to endothelial cells and the trans-endothelial migration that subsequently occurs (Voermans et al. 2000). Transplantation following the pre-treatment of HPCs with an antibody

directed against CD49a/CD18 was able to partly decrease their homing to the bone marrow (Carstanjen et al. 2005; Sahin and Buitenhuis 2012).

The third group of molecules that may be involved in bone marrow homing regulation is the cadherins. For example, VE-cadherin inhibition has been shown to improve UCB-derived CD34+ HPC trans-endothelial migration (van Buul et al. 2002; Sahin and Buitenhuis 2012). However, very low levels or sometimes absent levels of N-cadherin mRNA and protein are measured in HSCs. The role of cadherins in the migration is still controversial and requires further investigation (Hosokawa et al. 2007; Haug et al. 2008; Hosokawa et al. 2010).

While the epithelial cell adhesion molecule EpCAM has been identified as a cell adhesion molecule (CAMs), it is not structurally similar to any of the four major CAMs, which include the integrins (e.g., CD41), cadherins (e.g., V - cadherin), selectins (e.g., P - selectin), and Ig superfamily members (e.g., ICAM) (Dollé et al. 2015).

Most CAMs occur ubiquitously across normal cells, as opposed to EpCAM, which is limited to mature simple squamous epithelia and certain adenomatous epithelial cells (Dollé et al. 2015). Cells require the ability to move about each other and repel and communicate with each other so that the proper organisation of multicellular animals can be maintained. By communicating across their plasma membranes, individual cells fulfil these tasks. Interactions regulated by CAMs provide the adhesive forces needed for cell aggregation and tissue formation during morphogenesis. CAM-mediated interactions are highly dynamic in cellular development, providing the fluidity required for morphogenesis-driven cellular movements (Dollé et al. 2015).

Certain CAMs concurrently function as both adhesive bonds and sensors, while others have been driven evolutionarily to predominantly act as only an adhesive molecule or a signal-transmitting sensor. The exact function of EpCAM is still being uncovered, but EpCAM seems to have several actions, two being cell to cell adhesion and signalling, which are mediated by the spatial and temporal expression pattern of EpCAM (Dollé et al. 2015).

Bone marrow homing of haematopoietic stem and progenitor cells requires a chemokine gradient (Wright et al. 2002; Liesveld et al. 2004). Chemo-attractants have also been revealed as molecules that can mediate the migration of haematopoietic stem and progenitor cells to the bone marrow. The chemokine demonstrated most capable of inducing migration was the Stromal Cell Derived Factor 1 (SDF-1) (Wright et al. 2002; Liesveld et al. 2004). Although SDF-1 is currently the most well-studied chemokine involved in bone marrow homing, proteolysis resistant bioactive lipids have recently been revealed as HSC chemo-attractants (Kim et al. 2011; Sahin and Buitenhuis 2012).

1.6 Regulatory dynamics in haematopoiesis

In haematopoiesis, gene regulatory networks are primarily composed of transcription factor proteins, which control the rate at which DNA sequences are transcribed by binding to specific regulatory motifs (Wilson et al. 2011). To be considered a transcription factor, a protein should contain, at least, a DNA binding domain which will be used to then group the proteins into classes depending on this domain (Lee and Young 2013). At the same time, they can also possess other domains which include protein-protein interaction domain and transcriptional activation/repression domains, which co-ordinately recruit the basal transcriptional machinery and allow for the assembly of other complexes (Lee and Young 2013).

In haematopoiesis, almost all families of transcription factors are present. These families include transcription factors with binding domains such as the various zinc-finger classes, bHLH, ets, paired box, and myb families. Of relevance to haematological malignancies, deregulation of haematopoietic transcription factors occurs in the context of chromosomal rearrangements or somatic mutations. This leads to inhibition of function of other downstream pathways or the recruitment of alternative enzymes that modify chromatin, which in turn leads to an inappropriate activation or repression of early myeloid or lymphoid progenitors and subsequent transformation (Look 1997).

In general development, normal transcription factor functions are a key determinant of how HSCs restrict their differentiation during embryogenesis and

in adults (Orkin 2000). Combinatorial interactions of transcription factors, rather than each regulator acting alone, are essential to determine cell identity. For instance, during HSC specification, 3 proteins (FLI1, Gata2, and SCL/TAL1) have been demonstrated to develop into a densely interconnected transcriptional network in the aorta-gonad-mesonephros (AGM), which is first site of HSC emergence (Pimanda et al. 2007). Nonetheless, not all transcription factors that are required for stemness during developmental specification are then essential for maintenance in adults afterwards (Ichikawa et al. 2004). Examples of families of transcription factors required for HSC formation are: MLL, Runx1, TEL/ETV6, SCL/tal1, and LMO2, whereas SCL/Tal1 is expendable for HSC function in the adult (Mikkola et al. 2003). The combinatorial interactions of seven transcription factors (FLI1, ERG, Gata2, RUNX1, SCL/TAL1, LYL1, and LMO2) have been identified as essential to maintain stemness (Wilson et al. 2010) (Figure 1.5).
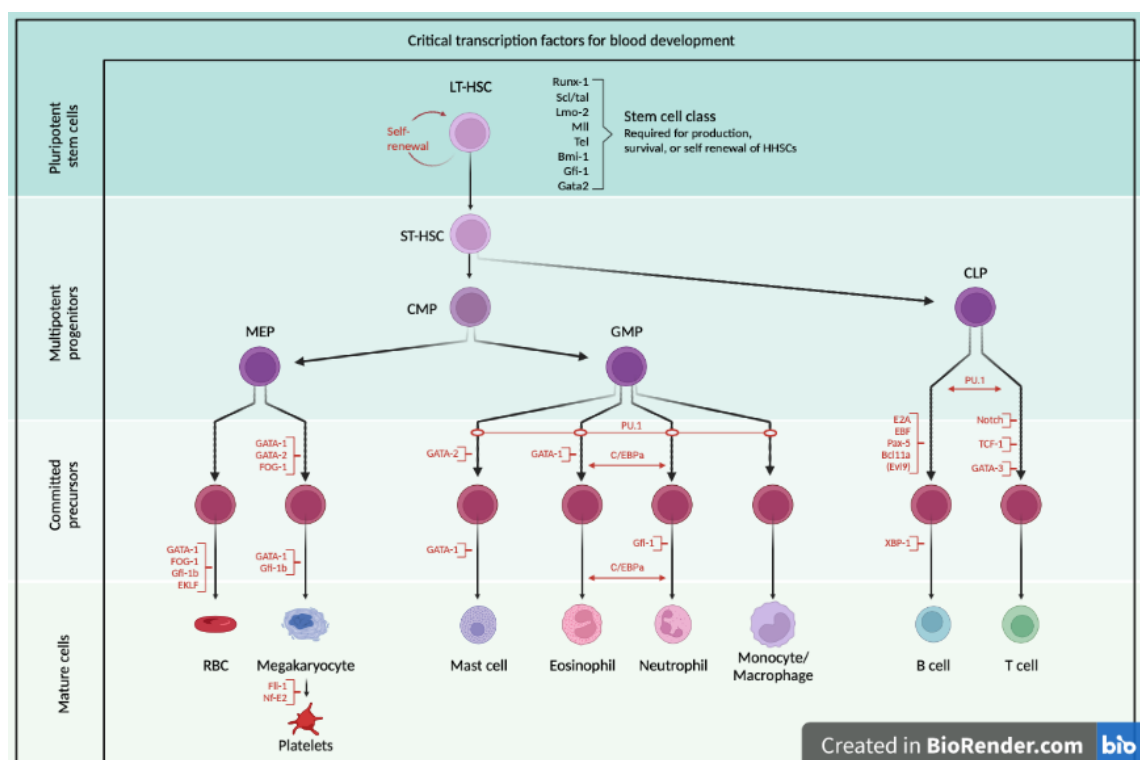
Figure 1.5 Transcriptional regulation of hematopoietic hierarchy. The hierarchy of hematopoietic cells is depicted in this image, along with the transcription factors active at each step, starting with long-term hematopoietic stem cells (LT-HSCs) and progressing through multipotent progenitors, committed progenitors, and differentiated cells. The relationship between transcription factors and the hierarchical arrangement of hematopoietic cells is highlighted in the figure. The specification of HSCs and the transition to multipotent progenitors depend heavily on transcription factors such Runx1, Gata2, and Scl/Tal1. Lineage commitment and differentiation of progenitor cells towards the erythroid, myeloid, and lymphoid lineages depend on transcription factors such as Gata1, Pu.1, and C/EBP.

Upstream of transcription factors, growth factors and cytokines are essential in controlling lineage commitment during cellular development. They give cells the messages and stimuli they require in order to differentiate into particular lineages and gain specialised abilities. During wound healing, for instance, which involves the migration, infiltration, proliferation, and differentiation of different groups of cells will culminate in an inflammatory response with the culmination of the formation of new tissue (Barrientos et al. 2008). This process is executed and regulated by an equally complex signalling network involving numerous growth factors, cytokines and chemokines. These substances are biologically active polypeptides that affect a target cell's metabolism, growth, and differentiation. They can influence cell behaviour as a result of their binding to particular cell surface receptors or ECM proteins, and they can do so through paracrine, autocrine, juxtracrine, or endocrine pathways. These receptors' binding sets off a series of molecular activities. The binding of transcription factors to gene promoters that control the production of proteins governing the cell cycle, motility, or differentiation patterns is the endpoint of this signalling (Barrientos et al. 2008; Bertoli et al. 2013). In haematopoiesis, these signalling molecules regulate cell proliferation, survival, and lineage specification.

The proliferation and differentiation of hematopoietic progenitors produced from hematopoietic stem cells in hematopoietic lineages can be encouraged by one group of signalling molecules, namely hematopoietic growth factors (Kato 2021). The majority of hematopoietic growth factor receptors are type I cytokine receptors, which lack tyrosine kinase activity and have similar characteristics. In order to promote survival, proliferation, and differentiation, the ligand-receptor interaction causes changes in the intracellular conformation of the receptor complex and starts a number of signalling cascades (Kato 2021). Intermediate-acting lineage-nonspecific factors and late-acting lineage-specific factors are the two categories into which hematopoietic growth factors are divided (Kato 2021).

The TGF-family is one of these growth factors with a role in controlling lineage commitment. They function by binding a heteromeric receptor complex made up of one type I and one type II receptor, both of which are serine-threonine kinases,

and are generated by macrophages, fibroblasts, keratinocytes, and platelets (Lee Hyung-Suk et al. 1997). They also bind to a type III non-signalling receptor, which is responsible for delivering TGF- to the type II receptor. The Smad family of transcription factors' downstream signalling molecules are activated once the receptors have undergone autophosphorylation (Liu et al. 2005).

Other growth factors include EGF (epidermal growth factor), FGF (fibroblast growth factor), GDF (growth differentiation factor), IGF (insulin-like growth factor), which generally promote the expansion of hematopoietic progenitors and enhance their survival and PDGF (platelet-derived growth factor), and VEGF (vascular endothelial growth factor) which are involved in angiogenesis and vascular development (Carpenter and Cohen 1990; Dunn et al. 2000).

Another group of signalling molecules are cytokines, in particular, those that belong to the Common gamma chain family such as IL-2, IL-4, IL-7, IL-9, IL-15, and IL-21. They play critical roles in lymphoid cell development, including T cell, B cell, and natural killer (NK) cell differentiation (Akdis et al. 2011; Rashighi and Harris 2017).

1.7 *Zeb1* in haematopoiesis

ZEB1 (also known as TCF8, δ EF1, Zfhx1A or Zfhep) is a protein that is classified among the zinc-finger class of homeodomain transcription factors as it possesses 7 zinc-finger domains, which form two clusters and are responsible for DNA-binding, surrounding one homeodomain (Postigo et al. 2003). During embryonic development, ZEB transcription factors are crucial for the migration of neural crest cells and for the development of structures in the vertebrate embryo. In this process, the epithelial-to-mesenchymal transition (EMT), involves a loss of cell adhesion and invasion into surrounding tissues, which are necessary to provide plasticity during embryogenesis. ZEB transcription factors can both activate transcription by interacting with co-activators p300 and P/CAF and repress transcription by its interaction with the coBP co-repressor because they contain other protein binding domains such as the Smad interaction domain (SID), CtBP interaction domain (CID) and the p300-P/CAF binding domain (CBD) (Postigo et al. 2003; Drápela et al. 2020).

Zeb1 is a transcription factor and zinc-finger E-box-binding homeobox family member that recognizes E2-box DNA sequences. *Zeb1* is involved in several cellular processes, such as differentiation, proliferation, and apoptosis (Zhang et al. 2015a). *Zeb1* is an important regulator of EMT (Zhang et al. 2015a). and helps manage stem cell properties, including self-renewal and quiescence. *Zeb1* is expressed throughout the haematopoietic system, including haematopoietic stem cells (HSCs) and progenitor cells (Higashi et al. 1997; Takagi et al. 1998a). It is also found in many different mature blood cell types, including erythrocytes, granulocytes, monocytes, B cells, and T cells (Higashi et al. 1997; Takagi et al. 1998a). *Zeb1* expression is highly regulated in the haematopoietic system, more generally upregulated in HSCs and downregulated in more differentiated blood cell types (Almotiri et al. 2021; Wang et al. 2021a; Zhang et al. 2022a). The downregulation of *Zeb1* expression in HSCs is required to produce mature blood cells (Almotiri et al. 2021).

Acute conditional deletion of *Zeb1* in HSCs results in the depletion of HSC quiescence, self-renewal, and differentiation (Almotiri et al. 2021). The loss of HSC quiescence in the absence of Zeb1 is accompanied by the activation of the Wnt signalling pathway(Fleming et al. 2008), where *Zeb1* directly represses the expression of the Wnt receptor Fzd7. *Zeb1* also directly represses the expression of miR-200a, which inhibits the translation of Fzd7. The conditional deletion of *Zeb1* in HSCs results in the loss of HSC self-renewal, potentially through repression of Numb expression, which is an important regulator of HSC self-renewal (Almotiri et al. 2021). The downregulation of *Zeb1* expression results in the upregulation of Numb expression, which results in the loss of HSC self-renewal (Almotiri et al. 2021).

1.8 EpCAM structure and regulation

The epithelial cell adhesion molecule (EpCAM, also known as cluster of differentiation 326 (CD326), tumour-associated calcium signal transducer 1, or trophoblast cell-surface antigen 1 (TROP1) is a homophilic molecule causing cell to cell adhesion consisting of 314 amino acids (aa), expressed in many human epithelial tissues (Schnell et al. 2013a). It is a type of transmembrane glycoprotein that co-localises with E-cadherin and claudins at basolateral membranes and

tight-junctions in healthy epithelia (Dollé et al. 2015). EpCAM has a large extracellular domain (N-terminal) of 242 aa, a 23 aa single-spanning transmembrane domain, and a short 26 aa cytoplasmic domain, which is typically overexpressed in tissue progenitors, embryonic stem cells, cancer-initiating cells, and carcinomas (Schnell et al. 2013a).

The extracellular domain (EpEX) and intracellular domain (EpICD) of EpCAM can be released from the membrane-bound form of the protein following cleavage by TNF-α-converting enzyme (TACE) and presenilin-2 (PS-2), and these domains have been shown to act as ligands for signal transduction receptors and as transcriptional cofactors (Schnell et al. 2013a). Experimentally, three N-linked glycosylation sites have been confirmed within the EpEx of the EpCAM molecule sequence (Schnell et al. 2013a). EpCAM glycosylation shows some degree of specificity of the tissue and has been enhanced in tumours versus normal tissue (Schnell et al. 2013a). A potential explanation for upregulated EpCAM glycosylation found in cancers could be related to the benefits of glycosylation to the molecule's membrane retention duration (Dollé et al. 2015). These molecular mechanisms add to the complexity of the functions of EpCAM and complicate its role in cancer progression (Liu et al. 2022a).

EpCAM is associated with enhanced epithelial proliferation and transmits signals into the nucleus through intramembrane proteolysis to release and promote nucleus translocation of its intracellular domain EpICD (Dollé et al. 2015). Aside from its cell adhesion function, EpCAM functions as a tumour-promoting signalling molecule (Schnell et al. 2013a). Therefore, EpCAM is a member of the oncogenic receptor network which may be investigated for its potential as a therapeutic target in cancer.

1.9 Role of EpCAM in normal development

While EpCAM has been identified as a cell adhesion molecule (CAMs), it is not structurally similar to any of the four major CAMs, which include the integrins (e.g., CD41), cadherins (e.g., V - cadherin), selectins (e.g., P - selectin), and Ig superfamily members (e.g., ICAM) (Dollé et al. 2015).

Most CAMs occur ubiquitously across normal cells, as opposed to EpCAM, which is limited to mature simple squamous epithelia and certain adenomatous epithelial cells (Dollé et al. 2015). Cells require the ability to move about each other and repel and communicate with each other so that the proper organisation of multicellular animals can be maintained. By communicating across their plasma membranes, individual cells fulfil these tasks. Interactions regulated by CAMs provide the adhesive forces needed for cell aggregation and tissue formation during morphogenesis. CAM-mediated interactions are highly dynamic in cellular development, providing the fluidity required for morphogenesis-driven cellular movements (Dollé et al. 2015).

Certain CAMs concurrently function as both adhesive bonds and sensors, while others have been driven evolutionarily to predominantly act as only an adhesive molecule or a signal-transmitting sensor. The exact function of EpCAM is still being uncovered, but EpCAM seems to have several actions, two being cell to cell adhesion and signalling, which are mediated by the spatial and temporal expression pattern of EpCAM (Dollé et al. 2015).

In normal adult tissues, EpCAM is expressed in different gastrointestinal tract, reproductive system, and respiratory tract tissues on the basolateral surface of simple, pseudostratified, and transitional epithelial cells (Tissue expression of EPCAM - Summary - The Human Protein Atlas. [2023]). The pattern of tissue expression of EpCAM mRNA is similar to EpCAM protein expression, being high in the intestine with low levels in the lungs, kidneys, pancreas, genitals, and mammary glands, which is consistent with the distribution in epithelial cells (Tissue expression of EPCAM - Summary - The Human Protein Atlas. [2023]). The most normal, nonpathological, epithelial tissue is EpCam positive, excluding epidermal myoepithelial cells, keratinocytes, gastric parietal cells, thymic cortical epithelial cells, and hepatocytes(Dollé et al. 2015). Intriguingly, EpCAM expression was also found to be correlated with many progenitor cell populations during organ development. EpCAM expression is not limited to epithelial precursor cells in this early developmental window, but can also be found in undifferentiated stem cells that have yet to commit to a particular cell lineage (Ng et al. 2010).

EpCAM was identified as a receptor and cell adhesion molecule involved in the fate of embryonic stem (ES) cells in mice (González et al. 2009a). EpCAM is highly expressed in ES cells under self-renewal and pluripotency conditions but is rapidly downregulated during incipient differentiation (González et al. 2009a). The inhibition of EpCAM expression in the presence of LIF (leukaemia inhibitory factor) induced features of differentiating ES cells, including decreased proliferation, diminished AP (alkaline phosphatase) activity, and diminished Oct3/4, c-Myc, and SSEA-1 protein expression. On the other hand, enforced expression of EpCAM in the absence of LIF partly counteracted differentiation, including the expression of Oct3/4 and increased proliferation of cells, proposing a role for EpCAM in regulating ES cell fate (González et al. 2009a). The researchers also found that the expression pattern of EpCAM in murine ES cells was like that of human hepatic progenitor cells and that EpCAM is highly expressed in cancer stem cells of various types of cancer (González et al. 2009a). They suggest that EpCAM may play a role in signalling processes that govern cell proliferation and dedifferentiation, particularly in rapidly growing ES or precursor cells, and that further investigation of the signalling pathways upstream and downstream of EpCAM in ES cells may help to clarify this issue (González et al. 2009a).

EpCAM has been hypothesised to have a broader role in stemness beyond ES cells, which like all stem cells are capable of differentiating into numerous different cell types (Wang et al. 2018c; Mal et al. 2021). Some research has suggested that EpCAM may help modulate stemness in cancer cells and that it may be able to promote the self-renewal properties and proliferation of cancer stem cells (Munz et al. 2009; Li et al. 2016). For example, studies have shown that EpCAM expression is elevated in cancer stem cells in breast cancer and pancreatic cancer and that targeting EpCAM may be able to reduce the stemness of these cells and inhibit their growth (Salnikov et al. 2009; Hiraga et al. 2016). In summary, the expression of EpCAM regulates normal and cancer stem cells and then fades during differentiation. This suggests that the amount of cell differentiation and specialisation depends, at least in part, on EpCAM expression levels.

1.10 Association of Zeb1 and EpCAM proteins in vertebrate models

Vannier and collaborators used a zebrafish model to investigate zeb1a and zeb1b knockdown and overexpression, which led to the detection of gastrulation impairments, such as severe epiboly retardation(Vannier et al. 2013). The authors detected the amount of mRNA in these fish by performing a RT-qPCR and whole mount in situ hybridization. They found that both *zeb1* paralogs had a role in modulating the adhesion of deep cells (the inner layer of cells in the developing zebrafish embryo) through repression of *cdh1* and *epcam* expression. zeb1b overexpression induced some mosaic embryos where a subpopulation of cells had lower *epcam* expression, severely compromised EVL integrity, and deficiencies in convergence movement. More interestingly, when both *zeb1* paralogs were depleted, ectopic *epcam* expression was abnormally seen in the deep cells. Hence, zeb1a/b represses the expression of *epcam* in deep cells throughout normal development.

1.11 Association of Zeb1 and EpCAM in cancer models and disease models

Typically, EpCAM is not seen in mesodermal or ectodermal tumours but can be found in the majority of, or possibly all, carcinomas. Elevated EpCAM expression in primary tumours seems to promote proliferation and a more severe phenotype characterized by metastasis appearance and decreased survival (Spizzo et al. 2011). Reduced EpCAM expression was alternatively found to be associated with the epithelial-to-mesenchymal transition. CTCs were recently found to lack EpCAM and, thus, could provide a cellular mechanism to escape the strict tumour architecture (Dollé et al. 2015).

The H19 gene encodes for a long non-coding RNA (lncRNA). LcnRNAs can function as chromatin remodellers, transcriptional regulators and protein orchestrators (Fang and Fullwood 2016). *H19* has been recognized in multiple physiological and pathological processes with a wide range of functions. In chronic liver disease, there is a clinically relevant role of h19 as a multifunctional regulator, including the orchestration of EMT to promote tumour growth. In a study by Song and colleagues (2017) a critical function of *H19* in cholestatic liver

diseases was elucidated. Obstructive cholestatic liver fibrosis was exacerbated by *H19* hepatic overexpression but improved by deficiency of *H19* (Song et al. 2017). The mechanism underpinning this observation was down-regulation of *Zeb1* and an up-regulation of EpCAM. ZEB1 mechanistically suppressed the activity of the EpCAM promoter and the transcription of genes. H19RNA impeded the inhibitory action of ZEB1 by interacting with the protein ZEB1, which prevented the binding to the promoter EpCAM. ZEB1 or EpCAM knockdown hepatic overexpression decreased *H19*-induced fibrosis; H192/2 mice also prevented the latter (Song et al. 2017). When the authors over-expressed ZEB1 in human HepG2 cells, they observed a decrease in EpCAM mRNA (Song et al. 2017).

The authors used mouse Hepa1 and human Huh7 cells for knockdown experiments because the transfection efficiency of HepG2 cells was low. In Hepa1 and Huh7 cells transfected with *shZEB1* compared to controls, EpCAM protein and mRNA were significantly induced, and a more striking effect was observed in Huh7 cells. These findings suggest that EpCAM was inhibited by ZEB1. Interestingly, H19 significantly reduces ZEB1 in mouse small cholangiocytes which express high EPCAM levels but have no effect on down-regulating ZEB1 in mouse large cholangiocytes (MLCs) containing low EPCAM levels. This implies a selective regulatory mechanism for *Zeb1* in the promoter of *Epcam* (Song et al. 2017).

In human pancreatic and breast cancer cell lines, repression of *EPCAM* expression was demonstrated to be facilitated by ZEB1 directly binding the *EPCAM* promoter (Vannier et al. 2013).

1.12 Regulation of EpCAM by Zeb1

In a comprehensive study of the knockdown of zeb1 in zebrafish and cancer cell lines, Vannier et al (2013) performed chromatin immunoprecipitation (ChIP) with MDA-MB231 breast cancer cell chromatin. Here, they demonstrated that endogenous ZEB1 binds to the native promoter region of *EPCAM*, which has five known sites that ZEB1 can potentially bind (Z-Box-1 and E-boxes 1–4). One of these binding sights is specific only for ZEB factors. The four remaining sites are

the E-boxes that can bind ZEB factors or other activators of EMT such as Snail. Thus, the transcriptional repressor, ZEB1, can bind its promotor to directly prevent *EPCAM* expression (Vannier et al. 2013).

In a similar study in Huh7 cells, Song et al (2017) analysed the *EPCAM* promoter was thoroughly and identified two putative ZEB1 binding sites within the proximal promoter region. The ChIP assays revealed marked enrichment of ZEB1 protein to both site 1 and site 2 in the endogenous *EPCAM* promoter in Huh7 cells. The most remarkable result was that the overexpression of H19 inhibited ZEB1 binding to site 1 without affecting its binding to site 2, suggesting a site-dependent selectivity (Song et al. 2017). The authors subsequently examined *EPCAM* promoter activity in two additional cell lines 293T and Hep3B cells and observed an inhibition by ZEB1 overexpression and activation by knockdown of ZEB1.

1.13 Strategies for knocking-out haematological-related genes

Because many of the genes that are essential for haematopoiesis have critical functions in other tissues, gene targeting in mice can result in a lethal phenotype during embryonic development that precludes the analysis of haematopoietic cell function in adult humans. Therefore, building conditional mouse knockout models in which genes can be deleted by recombination mediated by Cre-lox or Flp-frt in a time-and cell type-specified way can overcome this problem (Rossi et al. 2012; Parker and Peterson 2018). Conditional knockout mice are typically used in haematopoiesis to test the role of specific genes. Different promoters that drive Cre expression have been used in experimental haematology, with the interferon-inducible *Mx1*-Cre still being highly used (Velasco-Hernandez et al. 2016). *Mx1* is a vital part of the mechanism of viral defence and its expression in response to interferon can be imitated. In these mice, Cre recombinase expression is controlled by the closely controlled *Mx1* inducible interferon promoter that can be activated by polyinosinic–polycytidylic acid (pIpC) treatments; therefore, Cre recombinase regulated by the *Mx1* promoter can be triggered by imitating viral infection (Joseph et al. 2013).

Nonetheless, in practical studies, different pitfalls associated with this process can result in misinterpretation of results (Velasco-Hernandez et al. 2016). On one

hand, a high rate of spontaneous recombination when applying commonly used techniques in experimental haematology, and on the other hand, unwanted short-term effects of using polyinosinic: polycytidylic acid, including biological and cellular changes. Other problems that can potentially be associated with the *Mx1*-Cre system include HSC cycling caused by pIpC administration, similar to interferon itself (Velasco-Hernandez et al. 2016). Since the *Mx1* promoter is also active in stromal cells of the bone marrow, in addition to the LT-HSCs, pIpC injection will induce gene deletion in the microenvironment of the bone marrow (e.g. BM MSCs, nestin-positive cells, perivascular cells) as well as LT-HSC and their downstream progeny (Ambrogini et al. 2010; Park et al. 2012; Dishowitz et al. 2013).

There are several alternatives to using the *Mx1*-Cre model (Lewandoski 2001; Kemp et al. 2004; Rossi et al. 2012; Joseph et al. 2013), including the *Vav*-Cre model. The guanine nucleotide exchange factor called Vav is regulated by the Rho/Rac family of small G proteins (Lazer and Katzav 2011). In the haematopoietic system, the constitutively active *Vav*-Cre mice have been commonly used to achieve gene deletion. Two *Vav*-Cre strains with only slightly different specificities have been produced (Georgiades et al. 2002; de Boer et al. 2003; Croker et al. 2004). The mice were generated in one strain (*Vav*-Cre) by Cre expression mediated by elements of the murine *Vav* gene (Georgiades et al. 2002; de Boer et al. 2003; Croker et al. 2004). With the codon improved Cre (iCre), the targeting vector (Ogilvy et al. 1999) was updated. Vav is a protein that is expressed in haematopoietic and endothelial cells(Siegemund et al. 2015). *Vav*-iCre is typically used to alter genes in HSCs and their progeny to provide conditional disruption of floxed genes in mice (Joseph et al. 2013; Siegemund et al. 2015). Even though this system is not entirely specific to HSC, its non-specific targets are fewer than *Mx1*-Cre: namely, endothelial cells and cells in the testes. As a further difference to *Mx1*-Cre mediated gene deletion, where gene deletion is induced in the adult, *Vav*-iCre mediated deletion occurs during HSC development in the embryo, at E.11 (Siegemund et al. 2015).

1.14 Mouse models for studying Zeb1 function

To better understand the role of *Zeb1*, several *Zeb1* knockout mouse models have been generated with different strategies. The mutations of the *Zeb1* gene generally aim to target the deletion of the DNA-binding domain or the deletion of the C-terminal transcriptional repression domain.

In one of the first mouse models developed, the *Zeb1* locus was targeted using a lacZ reporter (Takagi et al. 1998a). This allowed researchers to monitor *Zeb1* expression during development. The deltaEF1null(lacZ) was a targeted null reporter insertion that caused an intragenic deletion. Exon 1 was replaced by a lacZ-neo cassette with termination signals. The DNA-binding and homeodomains necessary for endogenous protein functionality were absent from the fusion protein encoded by the targeted allele (Takagi et al. 1998a). The homozygous deltaEF1null(lacZ) animals grew to term but did not survive after birth. The deltaEF1null(lacZ) homozygotes also had severe T cell insufficiency in the thymus and a variety of skeletal abnormalities (Takagi et al. 1998a).

In addition to the complete *Zeb1* knockout, which is perinatally lethal because of skeletal defects (Takagi et al. 1998a), other *Zeb1* knockout models have been developed showing truncated C-terminal ZEB1 deletion without the CZF domain. A similar strategy, involving a targeted insertion to generate a knockout, was applied to the deltaEF1deltaC727 mouse model. In this case, the crucial zinc finger DNA-binding domain cannot be translated because of a stop codon that was induced by the insertion of a neomycin selection cassette into exon 6 (Higashi et al. 1997). This mutant strain was the first to reveal that *Zeb1* had a direct role in T-cell development. The mutant mice showed a decreased number of cells, atypical T cell differentiation, and irregular thymus development. Furthermore, it was later stated that these mice have deep thymus atrophy and CD4 T cell lymphoma is spontaneously developed at an elderly age (Hidaka et al. 2008). Their hypocellular thymi show an enhanced percentage of double negative cells CD4/CD8 and a dramatic decrease in double positive cells, which suggests that the later parts of the T cell development tend to be partially blocked and the few thymocytes that can differentiate are biased towards the CD4$^+$ T cell lineage (Hidaka et al. 2008). In addition, it was demonstrated that ZEB1 can

control CD4 activity by competing for an E-box enhancer by interacting with transcription activators E12 and HEB.

Some other *Zeb1* mutant mouse models were obtained via chemically induced mutations. Bulk segregation analysis of F2 inter-crossed progeny, using the mapping strain C57BL/10J, revealed the cellophane mutation, which is now another widely used *Zeb1* mouse model. This mutation has the greatest linkage with the marker on Chromosome 18 at location 15408257 bp (synthetic LOD=7.9). A transversion of T to A on chromosome 18 in the NC 000084 region at base pair 5770552 in exon 7 of 8 was seen through whole-genome SOLiD sequencing. This location corresponds to Zeb1 transcript base pair 2725 in exon 7. The mutation causes a tyrosine codon at position 902 to convert into a premature stop codon. The *Zeb*-cellophane shows an early T-cell differentiation block and hypocellular thymi (Arnold et al. 2012). A detailed assessment of other lineages indicated defects in B-cell and NK-cell maturation in the spleen. *Zeb1* was also determined to be integral for T cell growth, the formation of germinal centres, memory B-cell responses, and peritoneal and marginal zone B-1 B-cells (Arnold et al. 2012)

Moreover, haematopoietic specific conditional *Zeb1* knockout mouse models have been generated, where generally *Zeb1* knockout mice were crossed with a variety of tissue specific Cre expressing mice. A conditional *Zeb1*$^{flox/flox}$ mouse has allowed for further inquiry into the role of Zeb1 by intercrossing it with *Sox2*:Cre mice to achieve a complete removal of gene activity specifically in the epiblast (Hayashi et al. 2002; Brabletz et al. 2017a). While homozygous *Zeb1*$^{flox/flox}$ and *Zeb1*$^{del/flox}$ mice are not distinguished from their wild-type littermates, *Zeb1*$^{del/del}$ embryos showed multiple developmental deficiencies. In specific, until mid-gestation, embryos were not impacted. The first phenotype manifested in the head of E11.5 embryos was the appearance of tiny haemorrhages or malformed blood vessels. Deficiencies became more evident at E15.5 and P0 by identifying overall growth retardation, oedema and haemorrhages at multiple locations, curly tail, one-eye shortage and problems with their legs. Pups either died at birth or died shortly after because they were not able to breathe (Brabletz et al. 2017a). The curly tail phenotype was not noted in all mutant embryos in accordance with the standard *Zeb1* knockout mice

(Takagi et al. 1998a). The appearance of oedema and haemorrhages occurred with variable penetrance.

The inducible haematopoietic specific deletion mouse model, *Zeb1 Mx1*-Cre, was used in the laboratory of Dr Neil Rodrigues to examine *Zeb1*-mediated regulation of haematopoietic stem cells in adults (Almotiri et al. 2021). Here, polyinosinic-polycytidylic acid (pIpC) was administered in adults to delete *Zeb1* expression in HSCs and their progeny (Almotiri et al. 2021). We were able to demonstrate that *Zeb1* is critical for regulating T cell maturation and differentiation in adults and is an important transcriptional repressor that balances the global, multi-lineage differentiation destinies of HSCs (Almotiri et al. 2021). A smaller thymus in $Zeb1^{KO}$ mice in comparison to WT mice and there was an absence of T-cells in $Zeb1^{KO}$ mice in primary transplantation. Moreover, while there was no change in HSC number in $Zeb1^{KO}$ mice, we observed that there was a differentiation defect of HSCs after transplantation and decreased self-renewal.

1.15 The role of the thymus in the adaptive immune system and thymocyte differentiation into distinct T cell populations.

The thymus has a crucial and unique function in the immune system facilitating the development of thymocytes into T cells (Takahama 2006; Dzhagalov and Phee 2012; Zhao et al. 2012). The thymus is divided into two lobes, having histologically and functionally distinct sections within each one (Takahama 2006; Love and Bhandoola 2011; Dzhagalov and Phee 2012). The two main parts, the core medulla and the peripheral cortex are separated by an outer capsule (Fig. 1.6) (Dzhagalov and Phee 2012). The two main cell types that make up the thymus are those that originate from non-hematopoietic lineages (epithelial, mesenchymal and endothelial) and hematopoietic stem/progenitor cells in the bone marrow (Love and Bhandoola 2011; Dzhagalov and Phee 2012; Zhao et al. 2012). T lymphocytes (thymocytes), dendritic cells, some B cells, macrophages, and natural killer cells are examples of hematopoietic lineages that are resident in the thymus (Dzhagalov and Phee 2012).
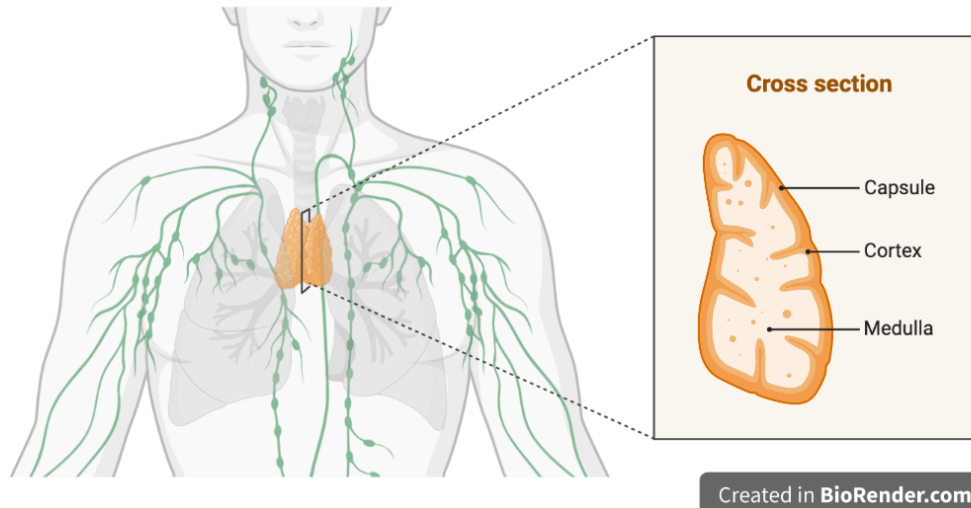
Figure 1.6 Anatomy of the human thymus. The diagram shows a cross section of the human thymus, indicating the microanatomy of one of the lobes. The lobe consists of an outer cortex (rich in thymocytes and epithelial cells) and a central inner medulla. Both are surrounded by a capsule that extends blood vessels into the interior. Between the cortex and capsule there is a subcapsular zone (not shown in diagram). Created in BioRender.com

Immature T cells that compose the thymus are known as thymocytes, which are guided throughout maturation with the aid of epithelial cells (Charles A Janeway et al. 2001). These epithelial thymocytes are identified by the presence of EpCAM (Nelson et al. 1996), a transmembrane glycoprotein that mediates homotypic cell-cell adhesion in epithelia (Keller et al. 2019; Chakrabarti et al. 2022).

There is a highly dynamic pattern of thymocyte development in the thymus, and BM progenitors constantly supply the thymus to ensure long-term T cell production and growth (Charles A Janeway et al. 2001; Famili et al. 2017). Early progenitor cells, referred to as early thymic progenitors / early T cell progenitors; (ETPs), originate as hematopoietic precursors in the BM and migrate to the thymus along capillaries in the corticomedullary junction (CMJ) (Ceredig and Rolink 2002). Once inside the thymus, thymocytes constantly interact with existing stromal cells and mature until cells react to external antigens but not to their own antigens (self-antigens) (Dzhagalov and Phee 2012). The ability of thymocytes to migrate between anatomically distinct microenvironments is one of the essential properties of these cells, which in turn will determine the T cell developmental state with distinct compartmentalisation (Dzhagalov and Phee 2012).
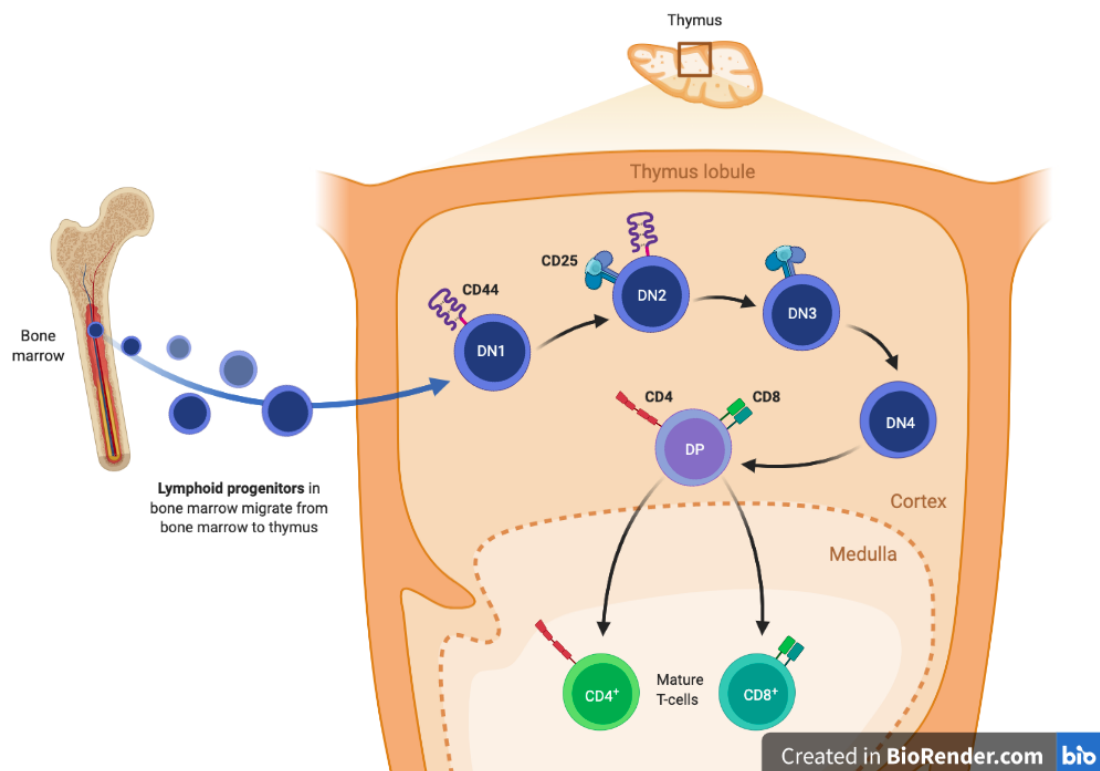
Figure 1.7 Migration of early progenitors to the thymus and maturation of T cells. The diagram shows how early progenitors migrate from bone marrow to the thymus and the developmental process that occurs in the cortex and medulla. The cells undergo a series of negative and positive selection events until they become mature T-cells. Depending on the markers present in the process the cells will be identified as double negative (DN) or double positive (DP). Created in BioRender.com

A typical, simplified, T cell development flow would include early thymic progenitors (ETPs) entering the CMJ from the blood (Cano and Lopera 2013) During this migration, ETPs go through a series of developmental phases in the CD4- CD8- double-negative (DN) stage. As they travel through the cortex, the DN cells progress to the CD4+ CD8+ double-positive (DP) cells (Figure 1.7). Positive selection is a crucial developmental stage in the cortex that selects DP thymocytes that express a functioning TCR (Barthlott et al. 1997; Nakayama et al. 2002; Dzhagalov and Phee 2012). Positively selected thymocytes go to the medulla and differentiate into CD4+ or CD8+ single-positive (SP) thymocytes. Once they reach the subcapsular zone (SCZ), a zone delimited by the cortex and the capsule, they commit to the T cell lineage (Figure 1.7) (Nakayama et al. 2002; Takahama 2006; Love and Bhandoola 2011; Dzhagalov and Phee 2012).

1.16 Thymocyte maturational stages and its defining cell surface markers.

Thymocytes are divided into many maturational phases depending on the expression of specific cell surface molecules. Here, I will focus on maturational stages and markers of T cell development in mice. The first thymocyte stage, which includes the earliest developing immature thymocytes, is the double negative stage (Figure 1.8), where there is a lack of expression of the co-receptors CD4 and CD8 (Ceredig et al. 1983). In this process, T cells that react against the body's own proteins and respond aggressively to self-antigens perish by apoptosis. This initial stage may be further subdivided into four stages. The expression of CD44 and CD25, which are adhesion molecules and the interleukin-2 receptor chain, respectively, might further split the DN population (Table 1.2) (Figure 1.8) (Godfrey et al. 1993). Cells that have committed to the T cell lineage and undergone beta-selection are marked by the absence of CD44 but the presence of CD25 expression (DN3), changing the T cell receptor (TCR). (Capone et al. 1998) (Table 1.2). For passage through DN4, cells that have successfully changed their TCR-chain locus are chosen. (Dudley et al. 1994; Michie and Zúñiga-Pflücker 2002; Bhandoola and Sambandam 2006; Krueger et al. 2017). The TCR beta chain and the pre-T cell receptor alpha (pT alpha) chain, which are joined by a disulfide bond, make up the pre-T cell receptor. The pre-T cell receptor and the signal-transmitting CD3 molecules come together to create a complex (Von Boehmer and Fehling 1997).

Table 1.2 Surface markers typically used to classify T-cells at different developmental stages.

Stage	Defining surface markers
ETP (Early T lineage Progenitor)	Lineage$^-$CD44$^+$CD25$^-$CD117$^+$
DN1 (Double negative 1) or	Lineage$^-$CD44$^+$CD25$^-$
Double negative 2	Lineage$^-$CD44$^+$CD25$^+$
Double negative 3	Lineage$^-$CD44$^-$CD25$^+$
Double negative 4	Lineage$^-$CD44$^-$CD25$^-$
Double positive	CD4$^+$CD8$^+$
Single positive	CD4$^+$CD8$^-$ or CD4$^-$CD8$^+$
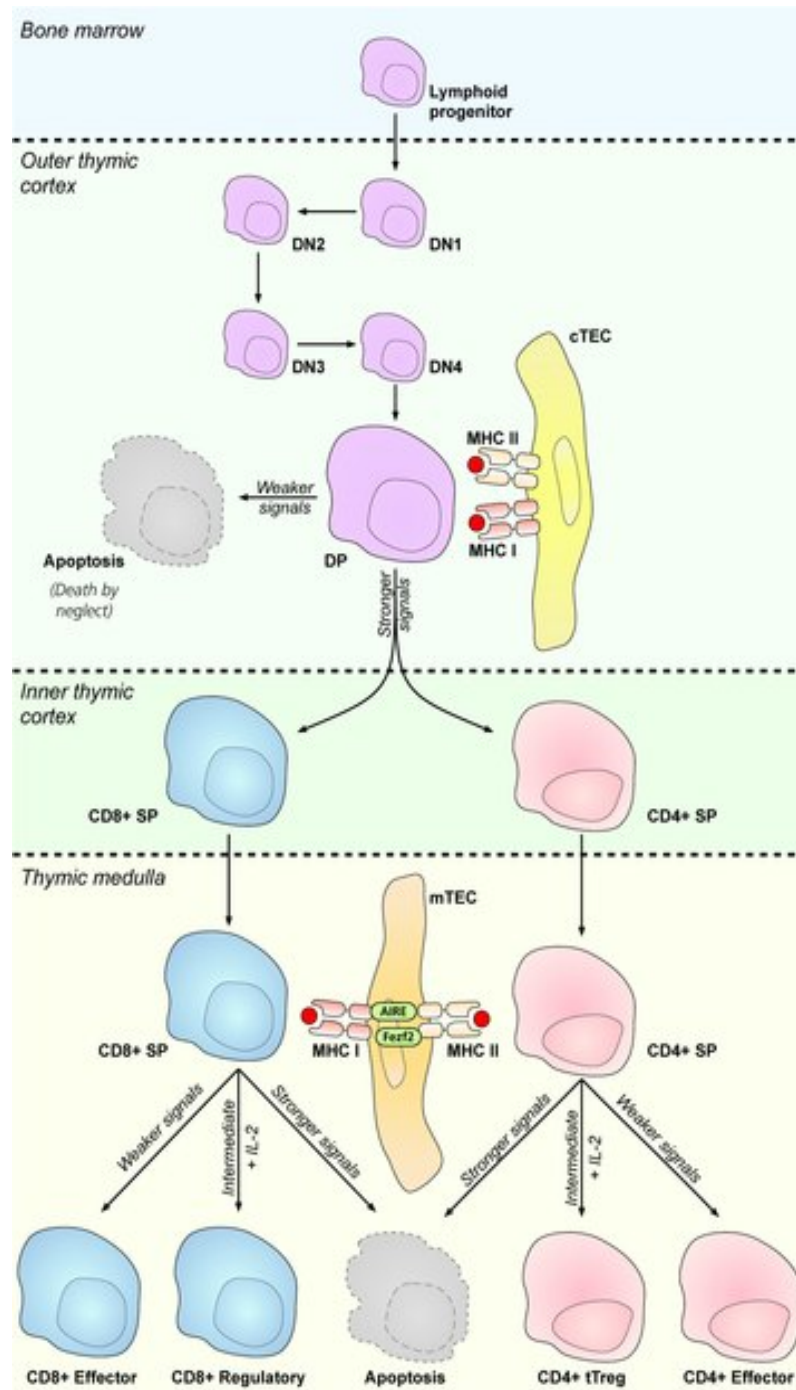
Figure 1.8 Overview of T-cell development across the thymus. The diagram shows a detailed development and maturation process of T-cells inside the thymus. The main stages of thymocyte development are depicted. The thymic architecture is divided into several cortical and medullary sections, each of which is distinguished by the presence of certain stromal cell types and thymocyte precursors at specific maturation stages. Thymocyte differentiation is characterised by the expression of well-defined cell-surface markers such as CD4, CD8, and the T-cell receptor status (TCR). Most juvenile thymocytes in the subcapsular cortical area lack CD4 and CD8 accessory molecules, as well as TCR, and are referred to as double negative (DN, for CD4 and CD8) cells. As they differentiate, they begin to express TCR as well as CD4 and CD8, resulting in double-positive (DP) thymocytes that occupy the majority of the cortical area. These cells are subsequently subjected to negative and positive selection, eventually migrating to the medulla and becoming single positive (SP) cells for either CD4 or CD8, both of which express high densities of TCR. References: cTEC, cortical thymic epithelial cell; DN, double negative; DP, double positive; mTEC, medullary thymic epithelial cell; SP, single positive.

This pre-TCR/CD3 complex causes survival, proliferation, and arrest in further chain loci rearrangement, as well as additional differentiation by positive regulation and expression of CD4 and CD8(Bhandoola & Sambandam, 2006; Dutta et al., 2021; Krueger et al., 2017). Apoptosis occurs in cells that do not undergo beta-selection. Beta-selection is an important checkpoint in mammalian T cell development mediated by the expression of the pre-TCR where CD4$^-$CD8$^-$ (double negative; DN)) c-kit$^-$ CD25$^+$ CD27$^+$ DN3a cells get survival signals from the pre-TCR and differentiate into DN c-kit$^-$ CD25$^+$ CD27$^-$ DN3b cells. Failure of this pathway can result in a developmental halt and/or a proclivity for malignant transformation. Lineage commitment is enforced through beta selection (Bhandoola and Sambandam 2006; Krueger et al. 2017; Dutta et al. 2021) TCR diversity during beta-selection can be increased by triggering pre-TCR signals independently or by ligand activation (Dutta et al. 2021). Then, the next significant stage occurs, which is known as double positive selection (positive for both CD4$^+$ and CD8). Following that, T lymphocytes differentiate into single-positive (SP) CD4$^+$ or SP CD8$^+$ cells upon leaving the thymus and entering the peripheral circulation (Hale and Fink 2009).

1.17 Markers of apoptosis, proliferation, and cell cycle

Cell death is an essential phase in the life cycle of cells and one of the mechanisms responsible for this process is apoptosis (also known as programmed cell death)(Elmore 2007). Apoptosis proceeds through distinct stages, which are marked by specific alterations in cell morphology and can lead to the uptake of apoptotic cells by macrophages (Elmore 2007). T cell selection and development rely heavily on apoptosis. As mentioned earlier, it is part of essential functions during development where thymocytes containing non-functional autoreactive TCRs are destroyed (Zhang et al. 2005a) Immunological tolerance and lymphocyte proliferation must be kept under control for both host defence and resistance against self-directed immune attack (Zhang et al. 2005a)

The intrinsic pathway, which is initiated by internal signals and is mediated by mitochondria, and the extrinsic pathway, which is controlled by death receptor signaling, are the two main forms of apoptosis (Zhang et al. 2005a; Elmore 2007). The intrinsic apoptotic process entails cytochrome c release from the

mitochondria, which activates caspases and causes the disintegration of cellular components and finally cell death. T-cell survival and homeostasis are significantly regulated by the intrinsic apoptotic pathway. T-cell receptor (TCR) signalling can induce the expression of pro-apoptotic proteins such Bim, Puma, and Noxa, which can then activate this pathway. The anti-apoptotic protein Bcl-2 is bound by and inhibited by these proteins, causing the release of cytochrome c from the mitochondria and the activation of caspases, which initiate apoptosis. Immune deficits or autoimmune disorders can arise as a result of dysregulation of the intrinsic apoptotic pathway in T-cells (Zhang et al. 2005b; Elmore 2007). A ligand-binding process activates the extrinsic apoptotic pathway, which is one of the markers used in this study.The FAS receptor, which belongs to the TNFR superfamily, is often involved in regulating immune response and preventing self-attack by the immune system (Lenardo et al. 1999). In the immune system, Fas-FasL interactions are primarily responsible for *in vitro* activation-induced cell death (AICD) in T cells (Lenardo 1996; Lenardo et al. 1999; Zhang et al. 2005b). If the Fas receptor is present and contacts its ligand, Fas ligand, it causes apoptosis. Additionally, Fas-mediated cell death is a key mechanism used by cytotoxic T cells (Nagata and Suda 1995).

Cell proliferation refers to the rapid expansion of a cell population because of cell growth and division. During this process, all biochemical and molecular activity must be controlled tightly because even minor perturbations can result in an uncontrolled rise in cell numbers. Cell expansion is generally counterbalanced by an increase in apoptosis to maintain homeostasis. Cell proliferation may be quantified by measuring the protein levels of important proliferation markers like the nuclear proliferation antigen Ki-67. Of relevance here, T-cell homeostasis requires an adequate balance of proliferation and apoptosis. In addition, the marker Annexin V joins to phosphatidylserine on the membrane's outer surface. The externalisation of phosphatidylserine (PS), a phospholipid present in the inner membrane of healthy cells, is one of the most prevalent hallmarks of apoptosis that can be evaluated by flow cytometry. Annexin V binds to phosphatidylserine, hence annexin V tagged with fluorophores can be used to assess apoptosis. Propidium Iodide (PI) is a dye that binds to DNA; however, it can only enter cells with damaged membranes, and live cells with intact

membranes cannot be labelled with PI. If cells are positive for both Annexin V and PI, they are considered dead, but if they are only positive for Annexin V, they are believed to be undergoing apoptosis (Geske et al. 2001; van der Mark et al. 2013). This statement explains how labelling cells with both Annexin V and PI enables distinguishing two separate cell populations that cannot be distinguished otherwise, highlighting the importance of differentiating between apoptotic and dead cells.

1.18 Definition and characteristics of immunological ageing, T -cell exhaustion and immune senescence

Immunosenescence refers to the alterations that occur with ageing in the immune system, affecting both innate and adaptive immunity (Goronzy and Weyand 2013; Swain and Blomberg 2013). In particular, immunosenescence is defined by reduced ability to fight against newly invasive infectious pathogens, inadequate memory T cell responsiveness, increased susceptibility to autoimmune diseases, and ongoing low-grade inflammation (also known as "inflammaging") (Goronzy and Weyand 2013; Swain and Blomberg 2013). For instance, reduced immune responses causes accelerated biological ageing, evidenced recently by studies showing that people infected with human immunodeficiency virus (PLWH) have a significantly higher risk of cardiovascular disease, owing to heightened inflammation and immunological dysregulation(Bick et al. 2022).

Age-related changes have been widely studied in T cell populations. In particular, given their ongoing contact with different stressors from the internal and external surroundings, these cells undergo continuous remodelling (Rodriguez et al. 2021). Given the necessity to maintain the naive T cell repertoire, these cells are very sensitive and react to chronic or latent infections as well as novel pathogens via clonal proliferation and differentiation to effector subpopulations (Nikolich-Žugich 2017).

Thymic involution occurs during ageing; the thymus gradually recedes and degenerates with age, and this is one of the principal age-related events that happen in the immune system, resulting in differences in the number of naive T cells, with a significant decline in CD8$^+$ T cells rather than CD4$^+$ T cells

(Rodriguez et al. 2021; Liang et al. 2022). The decline in the number of T cells is linked to a decrease in the variety of TCR clones and a rise in the memory subpopulation. Additionally, there is an accumulation of T cells that are either exhausted or dysfunctional and have reached their end stage of differentiation (Goronzy and Weyand 2019; Quinn et al. 2019a). A memory immune cell is an immune cell that has the ability to detect a previously encountered foreign particle and generate a quicker and stronger immune response (Ratajczak et al. 2018). T and B lymphocytes, as well as natural killer (NK) cells, have the ability to determine a speedy and effective response to a second contact with the same antigen (Ratajczak et al. 2018). Of clinical relevance, senescence, anergy, and exhaustion are three key dysfunction states of T lymphocytes in cancer that differ significantly in terms of molecular regulation throughout tumour growth (Lian et al. 2020; Zhao et al. 2020; Zhang et al. 2021). Anergy describes a lack of response by the immune system to external stimulus, it is caused by direct induction of peripheral lymphocyte tolerance. The immune system is unable to develop a normal immunological response to a specific antigen, typically a self-antigen (Schwartz 2003).

Several investigations have shown that terminally differentiated CD8$^+$ T cells are less reliant on TCR activation and more receptive to innate signals (Pereira et al. 2020). CD8$^+$ T cells showcase senescence characteristics such as low proliferative activity, telomere shortening, decreased telomerase activity, and expression of senescence-associated markers (e.g. CD57, CD62L and KLRG1) and intracellular molecules during ageing. In particular, the cell adhesion molecule L-selectin, commonly known as CD62L, is present in leukocytes (Ager 2012; Ivetic et al. 2019). CD62L is a cell surface component that belongs to the adhesion/homing receptor family and plays a crucial role in lymphocyte-endothelial cell contacts, particularly to promote homing of naive lymphocytes and lymphocyte trafficking (Carman and Martinelli 2015; Ivetic et al. 2019). A significant alteration noticed in ageing is the composition and functioning of CD4$^+$ T cells. In normal conditions, CD4$^+$ T cells have a high frequency of naive cells, showing the immune system's capacity to meet new antigens, respond to them efficiently, and develop immunological memory (Goronzy and Weyand 2017; Nikolich-Žugich 2018; Alpert et al. 2019; Elyahu et al. 2019). The naive subset

declines with age, coupled with the growth of highly differentiated memory cells, which frequently exhibit dysregulated capacities. These altered properties include decreased proliferation, decreased release of the cytokine interleukin-2 (IL-2), accumulation of metabolic abnormalities, increased production of pro-inflammatory mediators, and decreased CD62L levels. This results in CD62L being a good marker for ageing naïve CD4^{+} T cells (Goronzy and Weyand 2017; Nikolich-Žugich 2018; Alpert et al. 2019; Elyahu et al. 2019) The expression of L-selectin can indicate the activation of T cells. Research has shown that in mice, T cells with a CD62L+ phenotype that is naive or central memory are more effective at controlling the growth of solid tumors compared to CD62L− cytotoxic T cells (CTLs) (Ager 2012; Watson et al. 2019).

1.19 Thesis aims.

ZEB1 is understood to have a crucial function in the EMT process. ZEB1 has also been found to be involved in other tissue maintenance/developmental processes such as myogenesis, post-gastrulation embryogenesis, neuronal and T-cell development, and neuronal differentiation (Postigo et al. 1997; Postigo and Dean 1999; Clark and Chiu 2003; Zhang et al. 2015a; Singh et al. 2016a; Zhou et al. 2017; Jiang et al. 2018; Wang et al. 2019a). On the other hand, *Bmi1*, *Klf4*, and *Sox2* are transcription factors associated with stem cell function and have been shown to have oncogenic potential and *Zeb1* has been found to regulate the expression of these transcription factors (Wellner et al. 2009; Singh et al. 2017). Although our laboratory and other researchers have previously published on *Zeb1's role* in stem-cell-function maintenance and differentiation in the haematopoietic system (Almotiri et al. 2021; Wang et al. 2021a; Zhang et al. 2022a) and prostate epithelial cells (Wang et al. 2020), the cellular and molecular mechanisms underlying *Zeb1* mediated regulation of HSC function is still ill-defined. In addition to the *Mx1*-Cre model, these questions can be addressed with mouse models more specific to HSCs, such as *Vav*-iCre, where sustained gene deletion is better maintained than with *Mx1*-Cre mediated gene deletion (Georgiades et al. 2002; Siegemund et al. 2015), facilitating a more precise examination of long-term HSC function. Our aims are:

- To explore the molecular mechanisms mediating *Zeb1* function in adult hematopoietic stem cells by performing RNA-seq experiments using *Mx1*-Cre mouse model.

- To use genetically modified mice using the *Vav*-iCre strategy to uncover the functional role of *Zeb1* in long-term haematopoietic stem cell maintenance.

- To investigate the role of the EMT transcription factor *Zeb1* in T-cell differentiation from hematopoietic stem cells during ontogeny.

CHAPTER 2: Methods and Materials

2.1 Mouse models, breeding and tissue collection.

All experiments using animals were performed following all ethical committee guidelines according with the Animals Scientific Procedures Act (1986) and were authorised by the UK Home Office (Project licence: P6D863C95, Personal licence: ICEAE35D0). This study used C57BL/6 mice bought from The Jackson Laboratory (Bar Harbor, ME USA). Zeb1$^{fl/fl}$ mice (Brabletz et al. 2017a) were a generous gift given by Dr. Florian Siebzehnrubl of the Cardiff University European Cancer Stem Cell Research Institute (ECSCRI). Dr. Kamil Kranc of the University of Edinburgh (now Barts Cancer Institute, Queen Mary University) generously donated the Mx1-Cre and Vav-iCre mice.

2.2 Mouse models

The Cre-Lox system is a widely used technique to introduce targeted genetic changes into specific tissues or cell types (Nagy 2000; Kim et al. 2018). This system employs the Cre recombinase enzyme, which is a protein that belongs to the λ integrase family and recognizes specific sequences called LoxP sites (Nagy 2000; Kim et al. 2018). The Cre enzyme cuts the DNA between the LoxP sites, resulting in changes such as gene deletion, inversion or translocation (Nagy 2000; Kim et al. 2018). The specific changes that occur depend on the orientation and location of the LoxP sites (Nagy 2000; Kim et al. 2018). To direct the recombination to specific cell types or tissues, the Cre gene can be linked to a specific promoter. In the field of haematopoiesis, researchers have used the Cre-Lox system to study the role of specific genes in the development and maintenance of haematopoietic stem cells. Two commonly used promoters in haematopoiesis are the *Mx1* and *Vav* promoters, which drive haematopoietic cell-specific Cre-mediated recombination (Joseph et al. 2013; Siegemund et al. 2015).

The *Mx1*-Cre system is activated by administration of synthetic Polyinosinic-Polycytidylic acid (pIpC) double-stranded RNA. This triggers the Cre recombinase enzyme expression controlled by the *Mx1* promoter (Kühn et al. 1995). The *Vav* gene is normally activated around day E11.5, the middle stage

of embryonic development, in haematopoietic cells (Shimshek et al. 2002; Stadtfeld and Graf 2005).

Exon 6 is a specific region of the *Zeb1* gene that codes for a significant portion of the protein. In both *Mx1*-Cre and *Vav*-iCre models, exon 6 is surrounded by LoxP sites and is controlled by a tissue-specific promoter (*Mx1* or *Vav* promoters) that initiates the removal of the LoxP flanked exon 6 by the Cre recombinase enzyme. This allows for the conditional inactivation of *Zeb1* during development. Exon 6 deletion causes exons 5-7 splicing, leading to the translation of a premature stop codon (Figure 2.1) (Brabletz et al. 2017a). The *Mx1*-Cre system offers the ability to control the timing of gene deletion (Kühn et al. 1995; Almotiri et al. 2021). while the *Vav*-iCre system offers the ability to study the role of a gene of interest in the early stages of haematopoiesis (Shimshek et al. 2002; Stadtfeld and Graf 2005).
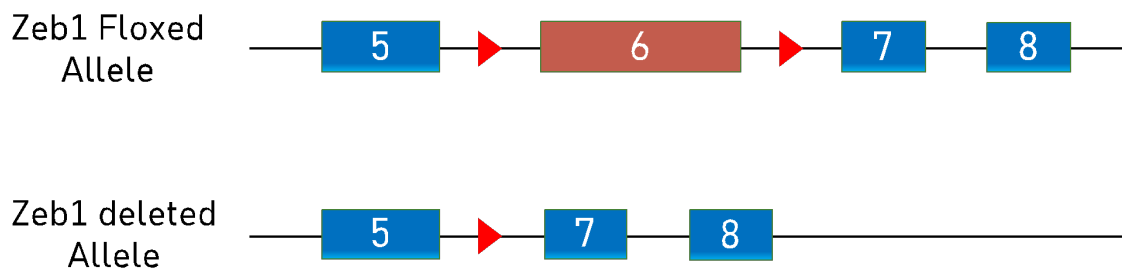
Figure 2.1 Generating a conditional knockout of the Zeb1 model Cre recombinase activation leads to the splicing of exon 5-7 after the floxed exon 6 is deleted. The triangles (red) represent the loxP sites and the rectangles represent the exons.

2.3 Breeding strategies

To generate the $Zeb1^{fl/fl}$ *Vav*-iCre+ mouse model, we first bred $Zeb1^{fl/fl}$ mice (Brabletz et al., 2017) with *Vav*-iCre+ mice, producing 50% $Zeb1^{fl/+}$ and 50% $Zeb1^{fl/+}$; *Vav*-iCre+ mice. Then, $Zeb1^{fl/fl}$ male mice were bred with $Zeb1^{fl/+}$; *Vav*-iCre+ female mice, generating 25% $Zeb1^{fl/fl}$; *Vav*-iCre+ mice (*Zeb1* KO), and 50% of the mice from the cross can be used as experimental controls as they are *Vav*-iCre negative, except for the 25% $Zeb1^{fl/+}$; *Vav*-iCre+ mice (Shimshek et al. 2002; Stadtfeld and Graf 2005).

To generate the *Zeb1*^{fl/fl} *Mx1*-Cre+ mouse model, we bred *Zeb1*^{fl/fl} *Mx1*-Cre+ mice with *Zeb1*^{fl/fl} *Mx1*-Cre mice, producing 50% *Zeb1*^{fl/fl}; *Mx1*-Cre+ mice where the *Mx1* promoter can be activated by administering pIpC, which activates the expression of Cre recombinase and conditionally deletes *Zeb1*, and 50% *Zeb1*^{fl/fl}; *Mx1*-Cre- mice, which can be used as experimental controls (Kühn et al. 1995; Almotiri et al. 2021).

2.4 Mice identification methods

Right ear units.	Left ear units.
Top = 1 Down = 3	Top = 10 Down = 30
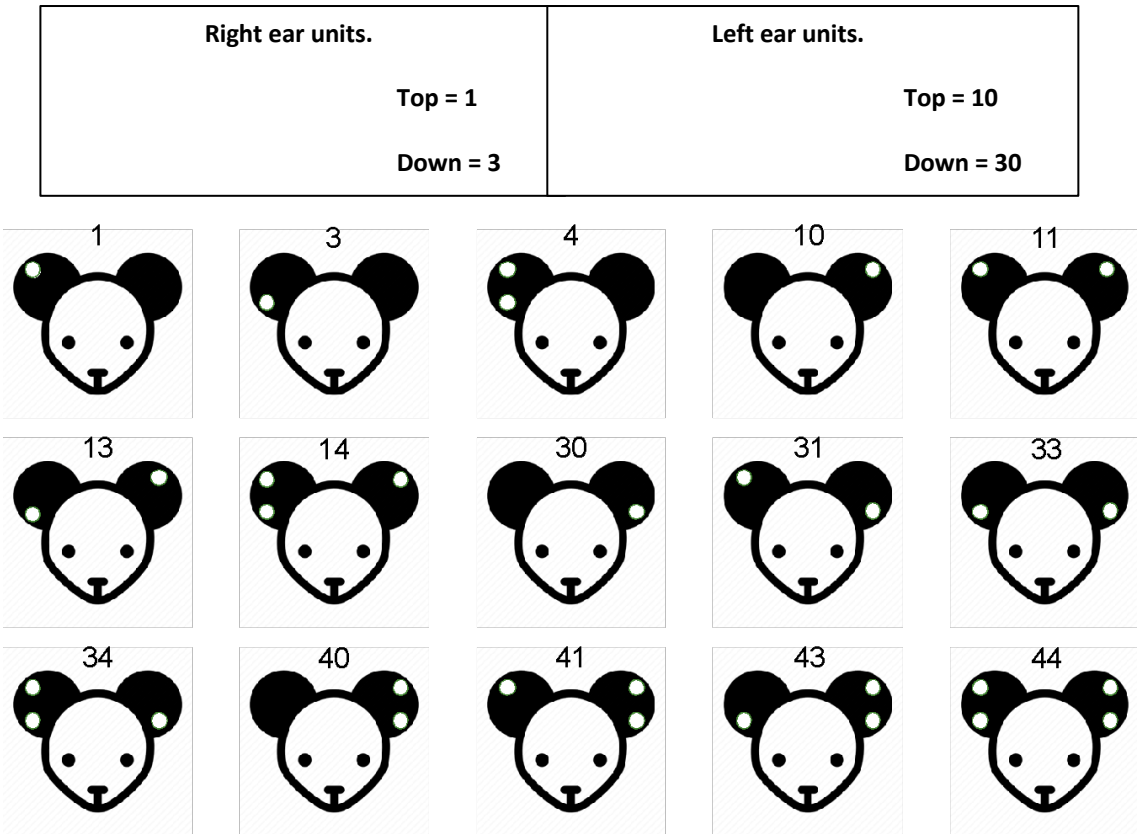
Figure 2.2 Mice ear-notch identification strategy.

2.5 Genotyping

We used ear-notches from the mouse identification strategy illustrated above to perform the genotyping (Figure 2.2). Genomic DNA was purified using the ISOLATE II Genomic DNA Kit Protocol from Bioline. For this process, 25 mg of animal ear-notch tissue was transported into a 1.5 mL microcentrifuge tube. Subsequently, the sample was completely covered in solution by adding 180 µL of Lysis Buffer GL and 25 µL of Proteinase K solution to the tube, and the mixture

was vortexed. The sample was then incubated for 1-3 hours at 56°C until lysed completely, with occasional shaking or vortexing. Next, 200 µL of Lysis Buffer G3 was added, and the tube was vortexed vigorously followed by incubation at 70°C for 10 min. Afterward, 210 µL of ethanol (96-100%) was added and vortexed vigorously. Once placed into a 2 mL Collection Tube, the sample was loaded onto the ISOLATE II Genomic DNA Spin Column (green). The column was then centrifuged for 1 minute at 11,000 x g, and the flow-through was disposed of. 500 µL of Wash Buffer GW1 was used to wash the silica membranes twice, then once with 600 µL of Wash Buffer GW2. After each wash, the flow-through was discarded, and the Collection Tube was reused. To remove residual ethanol, the silica membrane was centrifuged at 11,000 x g for 1 min, and the column was placed in a 1.5 mL microcentrifuge tube. The Elution Buffer was preheated at 70°C and then 100 µL were added onto the centre of the silica membrane, the mixture was incubated at room temperature (RT) for 1 min. Finally, DNA was eluted by centrifugation of the column for 1 min at 11,000 x g. Using a Nanodrop-2000 spectrophotometer, the DNA concentration, aiming for a final concentration within the range of 20-35 ng/L, and purity with the DNA absorbance ratio at 260 nm and 280 nm within the range of 1.7-1.9, were measured (ThermoFisher Scientific). We stored the isolating DNA sample at -20 °C.

2.6 DNA amplification and Gel electrophoresis

To amplify genomic DNA isolated from mouse tissue, we performed the polymerase chain reaction (PCR) using the T100TM Thermal Cycler (Bio-Rad). A 25 µl mix was prepared for each sample, containing 12.5 µl of Mango *Mix* (Bioline), 8.3 µl of nuclease-free water, 4 µl of the DNA sample that had a final DNA concentration ranging from 20-80 ng/µL, and 0.1 µl of the forward and reverse primers (Sigma-Aldrich) (Table 2.1). We used the T100TM Thermal Cycler for the three conditions we studied: *Zeb1*^fl/fl, *Mx1*-Cre, and *Vav*-iCre (Table 2.1).

To confirm the PCR product by molecular size, we conducted agarose gel electrophoresis. First, we created a 2% agarose gel by mixing 3 g of agarose (Bioline) and 150 mL of 1xTAE buffer (ThermoFisher Scientific) and microwaving the mixture at 900 W for 3 min to reach polymerization. Then, we added 7 µl of

SafeView nucleic acid stain (NBS Biologicals) and added it to a gel tray for solidification at RT. We transferred the gel tray into the electrophoresis chamber and covered the 2% agarose gel with a 1xTAE buffer. We then loaded a molecular weight ladder (100 bp, BioLabs) into the first lane and, subsequently, the individual amplified DNA samples into the agarose gel (10 µl of each sample), running the gel for 45 min at 95 Volts. Finally, we visualised the DNA fragments using a device with UV light and imaged with the ChemiDocTMMP imaging system (Bio-Rad). The image was viewed and annotated the results using the ImageLab Software program.

Table 2.1 PCR thermal conditions and primers

Primer Name		primer sequences	PCR thermal conditions
Zeb1	forward	5'-CGTGATGGAGCCAGAATCTGACCCC-3'	Denaturation: 95°C,30 sec Annealing: 54°C, 45 sec
	reverse	5'-GCCCTGTCTTTCTCAGCAGTGTGG-3'	Extension: 72°C, 1 min Repeat 39 cycles
	excised reverse	5'-GCCATCTCACCAGCCCTTACTGTGC-3'	Final cycle: 72°C, 5 min Cooling: 10°C
Mx1-Cre	forward	5'-TGACCGTACACCAAAATTTG-3'	Denaturation: 94°C,30 sec Annealing: 55°C, 30 sec Extension: 72°C, 1 min Repeat 30 cycles
	reverse	5'-ATTGGCCCTGTTTCACTATC-3'	Final cycle: 72°C, 5 min Cooling: 10°C
Vav-iCre	forward	5' CCGAGGGGCCAAGTGAGAGG 3'	Denaturation: 94°C,40 sec Annealing: 64°C, 40 sec Extension: 72°C, 30 sec Repeat 30 cycles
	reverse	5' GGAGGGCAGGCAGGTTTTGGTC 3'	Final cycle: 72°C, 5 min Cooling: 10°C

2.7 Tissue collection and processing

2.7.1 Dissection and tissue collection

This study utilised mice which were humanely culled through cervical dislocation. The femur, tibia, hip bone, spleen, and thymus were carefully collected and covered in phosphate-buffered saline (PBS) that was supplemented with 2% foetal bovine serum (FBS).

2.7.2 Peripheral blood (PB)

To obtain peripheral blood (PB), approximately 30-50 µL was collected from each animal via tail vein using an EDTA-coated bleeding tube (Starstedt). To eliminate red blood cells (RBCs), ammonium chloride solution (NH4Cl) (Stem Cell Technologies) was used. Specifically, 12 µL of blood was mixed with 600 µL of NH_4Cl and gently mixed after 6 minutes. The mixture was then allowed to stand for an additional 6 minutes, followed by centrifugation at 370 g for 10 minutes at RT. The white blood cell (WBC) pellet was isolated and utilized for PB lineage investigation.

2.7.3 Bone marrow

To isolate bone marrow (BM) cells, femurs, tibias, and hip bones were removed from mouse legs. The bones cleaned of muscle and skin tissues were immersed in 10 mL of PBS with 2% FBS (2% PBSFBS) solution. Subsequently, mortar and pestle were used to crush bones, with the process repeated twice. The resulting suspension was transferred to a 50 mL sterile conical tube through a 70 µm cell strainer (Miltenyi Biotec), yielding a total suspension volume of 30 mL. The total cell count of the BM was then performed.

2.7.4 Spleen and Thymus

The isolation of splenic and thymic cells involved placing the organs on a 70 µm cell strainer in a sterile 60-mm Petri dish, adding 2 mL of 2% PBSFBS. Tissue was then gently mashed using a sterile 2 mL syringe, with the process repeated twice. The resulting cell suspension was transferred to a 15 mL sterile tube, with

a total suspension volume of 7 mL for the spleen and 4 mL for the thymus. The total cell count of both organs was subsequently performed.

2.8 Flow cytometric analysis

Flow cytometric analysis was conducted to analyse the immune cells from the PB, BM, spleen, and thymus. The antibodies used for flow cytometry analysis in this thesis are detailed in Table 2.2, apart from B220-FITC, CD48-FITC, and CD34-FITC, which have stock concentrations of 0.5 mg/mL and 4 g/mL. All other antibodies have a starting concentration of 0.2 mg/mL, and the recommended dilution for staining of each antibody is provided in Table 2.2.

BD LSRFortessaTM (BD Biosciences) was used to analyse the samples, while BD FACSAriaTM Fusion (BD Biosciences) was used for cell sorting. The spectrum overlap was corrected after carrying out single staining for each fluorochrome, and the software algorithms were used to acquire each tube containing a single stain.

Negative controls, including unstained samples and the fluorescence minus one control (FMO), were used to establish population gates. All fluorochromes except the one tested in FMO were included in a tube. Further information on the staining procedure and the quantity of stained and acquired cells can be found in the relevant sections below.

After the samples were processed and compensation was applied, files were exported into and analysed with the FlowJo software (FlowJo™ v10.8).

Table 2.2 The antibodies list used for FACS.

Target cells	Cellular marker	Clone	Reactivity	Conjugate	Marker dilution	Company
Lineage+ Cocktail	CD3ε	17A2	Mouse	Biotin	1/40	Biolegend
	CD4	GK1.5	Mouse	Biotin	1/80	Biolegend
	CD8a	53-6.7	Mouse	Biotin	1/40	Biolegend
	CD45R/B220	RA3-6B2	Mouse/Human	Biotin	1/20	Biolegend
	CD11b (Mac1)	M1/70	Mouse/Human	Biotin	1/10	Biolegend
	Gr1	RB6-8C5	Mouse	Biotin	1/20	Biolegend
	Ter119	TER-119	Mouse	Biotin	1/5	Biolegend
Haematopoitic stem cells and committed progenitors	c-kit	2B8	Mouse	PE / APC	1/100	Biolegend
	Sca-1	D7	Mouse	APC-Cy7 / PE	1/25	Biolegend
	CD150	TC15-12F12.2	Mouse	PE-Cy7	1/100	Biolegend
	CD48	HM48-1	Mouse	BV510 / FITC	1/50	Biolegend
	CD34	RAM34	Mouse	FITC / PE	1/25	Biolegend
	CD127 (IL-7ra)	A7R34	Mouse	BV650	1/50	Biolegend
	CD16/32	93	Mouse	PE-Cy7 / FITC / PE	1/25	Biolegend
	CD135 (Flt3)	A2F10	Mouse	PE	1/50	Biolegend
	CD105	MJ7/18	Mouse	PE	1/50	Biolegend
	CD41	MWreg30	Mouse	BV510 / FITC	1/1000	Biolegend
	Streptavidin	NA	Mouse	PB / PerCP	1/100	Biolegend
	FC block	93	Mouse	---	1/50	Biolegend
Competitive tarasplant	CD45.1	A20	Mouse	APC / FITC / BV510	1/1000	Biolegend
	CD45.2	104	Mouse	FITC / PE / BV650	1/1000	Biolegend
Myeloid Cells	CD11b (Mac1)	M1/70	Mouse/Human	APC / PE	1/1000	Biolegend
	Gr1	RB6-8C5	Mouse	FITC / PE-Cy7	1/1000	Biolegend
Erythroid Cells	Ter119	TER-119	Mouse	APC-Cy7	1/1000	Biolegend
	CD71	RI7217	Mouse	PE	1/1000	Biolegend
T Cells	TCRb	H57-597	Mouse	FITC	1/1000	Biolegend
	CD69	H1.2F3	Mouse	PE	1/1000	Biolegend
	CD3ε	17A2	Mouse	FITC	1/1000	Biolegend
	CD4	GK1.5	Mouse	PE-Cy7 / PE / PerCP	1/1000	Biolegend
	CD8a	53-6.7	Mouse	APC-Cy7 / PE	1/1000	Biolegend
	CD25	PC61	Mouse	PerCP	1/1000	Biolegend
	CD44	IM7	Mouse/Human	APC	1/1000	Biolegend
	CD62L	MEL-14	Mouse	PE-Cy7	1/1000	Biolegend
B Cells	CD45R/B220	RA3-6B2	Mouse/Human	FITC / APC	1/1000	Biolegend
	CD19	1D3/CD19	Mouse	APC-Cy7	1/1000	Biolegend
	IGm	RMM-1	Mouse	PE-Cy7	1/1000	Biolegend
	CD249 (BP1)	2D3/APA	Mouse	PE	1/1000	BD Biosciences
	CD43	S11	Mouse	APC	1/1000	Biolegend
Apoptosis / Tolerance	CD95 (Fas)	SA367H8	Mouse	FITC	1/1000	Biolegend
	CD279 (PD-1)	29F.1A12	Mouse	BV711	1/1000	Biolegend
	Annexin V	NA	All mammalian	PE	1/25	Biolegend
	BCL-xL	54H6	Mouse	PE	1/100	Biolegend
proliferation	Ki-67	16A8	Mouse	PE	1/25	Biolegend
Isotype	Isotype PE	REA293	Mouse	PE	1/100	Biolegend
	Isotype APC	MOPC-21	Mouse	APC	1/100	Biolegend
Adhesion Molecules	CD324 (CDH1)	DECMA-1	Mouse	PE	1/50	Biolegend
	EpCAM	G8.8	Mouse	BV711 / FITC	1/50	Biolegend
	CD104 (Itgb4)	346-11A	Mouse	PE	1/50	Biolegend
Migration	CXCR4	L276F12	Mouse	BV711	1/50	Biolegend

2.8.1 Immunophenotypic analysis of HSPCs and committed progenitors in BM and spleen

The analysis of spleen cells and haematopoietic stem and progenitor cells (HSPCs) in BM was carried out using a lineage negative (Lin-) mixture prepared by pooling biotinylated antibodies targeting differentiated cell markers in 2%PBSFBS. The Lin- cocktail was composed of Ter119 for erythroid lineage, Mac1 and Gr1 for myeloid cells, B220 for B cells, and CD3e, CD4, and CD8a for T-cells. The Lin- cocktail was utilised to stain 10×10^6 bone marrow (BM) and spleen cells. For the analysis of HSPCs (LSK SLAM), the Lin- cocktail was supplemented with Sca-1, c-Kit, CD150, CD48, CD127, CD34, and CD135 (Flt3) for identifying HSC, MPPs, LMPP, HPC1, and HPC2. To identify CMP, GMP, MEP, and CLP for committed progenitor (LK) analysis, the Lin- cocktail, Sca-1, c-Kit, CD34, CD16/32, CD127, and Flt3 were utilized (figure 2.1).

The HSPCs (LSK SLAM) staining tube was incubated with 50 ul of Fc block (anti CD16/CD32) for 2 minutes before staining. Then, 50 ul of the antibody mixture was added to the HSPCs (LSK SLAM) staining tube and 100 ul to the committed progenitor (LK) staining tube, and the tubes were incubated in the dark at 4°C for 30 minutes. After incubation, the cells were washed with 1 ml of 2%PBSFBS. Subsequently, 100 μl of streptavidin was added to detect the biotinylated antibodies in the Lin- cocktail and incubated at 4°C in the dark for 30 minutes. After this, the cells were washed with 1 ml of PBS 2% FBS. Finally, 600 ul of 2%PBSFBS were added to the sample tube, making it ready for analysis. Prior to analysis of the samples on the BD LSRFortessaTM (BD Biosciences), DAPI (4',6-diamidino-2-phenylindole) was added at a 0.2 μg/mL final concentration to exclude dead cells.

In transplantation experiments, two markers, CD45.1 and CD45.2, were added to differentiate between donor and competitor cells. Additionally, EpCAM antibody was used to analyse its expression in HSPCs. An FSC-A vs SCC-A gate containing all mononuclear cells was used for sample acquisition, excluding dead cells and debris. A minimum of 2.5×10^6 events were acquired for HSPC analysis in BM and 4×10^6 in spleen, while 1.5×10^6 events were acquired for committed

progenitor analysis in both BM and spleen. The BD LSRFortessaTM (BD Biosciences) was used for cell analysis.
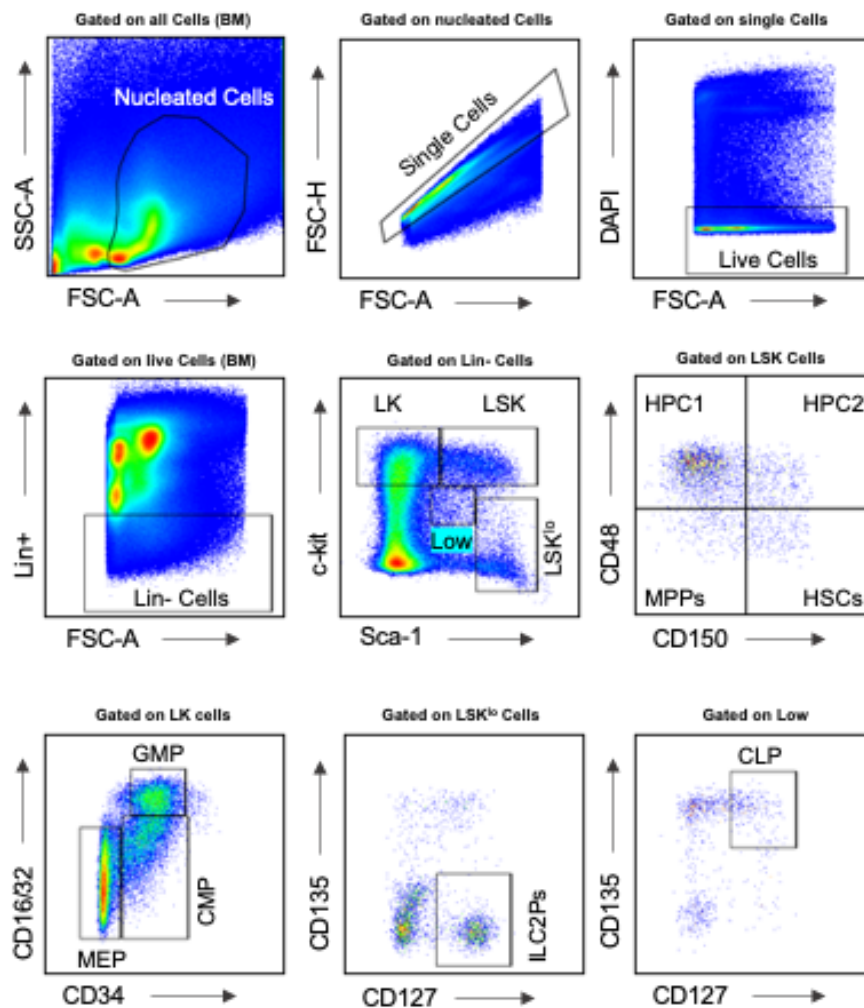
Figure 2.3 Gating strategies of HSPCs and restricted progenitor cells**.**

2.8.2 Lineage positive cells staining

A fluorochrome cocktail was prepared for the following cell surface markers: Ter119 for erythroid lineage, Gr-1 and Mac-1 for myeloid cells, CD3, CD4, and CD8 for T-cells, and B220 for B-cells. Lineage positive cells were analysed using 250,000 PB, BM, and spleen cells. To detect thymocytes, 500,000 cells were used, staining for c-Kit, CD4, CD8, CD25, and CD44. To analyse naive, central memory, and effector memory T-cells in various T-cell subsets in PB, thymus, BM, and spleen, CD62L and CD44 were used together with CD3, CD4, and CD8. To distinguish between donor and competitor cells in transplantation experiments, staining of CD45.1 and CD45.2 was also performed. Prior to sample

analysis, a 0.2 µg/mL final concentration of DAPI was added for the exclusion of dead cells.

2.8.3 Apoptosis analysis

Annexin V is a phosphatidylserine (PS)-binding protein normally present in the inner leaflet of the plasma membrane. PS is involved in apoptosis where it is translocated to the outer leaflet of the plasma membrane and can be detected by annexin V (Köhler et al. 1997). Annexin V staining is a commonly used technique to detect early apoptosis in cells (Reutelingsperger and Van Heerde 1997; Crowley et al. 2016; Wallberg et al. 2016).

After staining the cells with the previously reported cell surface markers, the cells were incubated in 100 µL of annexin V buffer (Biolegend), which contained the annexin V antibody (Biolegend) in the dark at RT for 30 minutes. The reaction was stopped by adding 600 µL of Annexin V buffer. Before analysing the samples, 0.2 µg/mL of DAPI was added to exclude dead cells.

2.8.4 Intracellular staining and Cell cycle analysis

Intracellular staining was conducted for stem and progenitor cells in BM and thymocytes to analyse the intracellular proteins, KI-67 and BCL-xL, after staining for cell surface markers as previously described. BCL-xl (B-cell lymphoma-extra large) is a BCL-2 protein family member that regulates the intrinsic pathway of apoptosis by acting as an anti-apoptotic protein (Adams and Cory 2007). The proliferation assay was carried out to determine the cell cycle phases present in a specific population at a certain time point. High expression of the nuclear Ki-67 antigen can be found in the G1/G2/M phases of proliferating cells compared to the G0 phase, the quiescent cell phase (Gerdes et al. 1984).

Intracellular staining was performed by fixing surface-stained cells with 1% paraformaldehyde (PFA) (ThermoFisher) for 20 minutes and washing them with cold PBS at 4°C for 5 min at 500 xg. The cells were kept on ice and permeabilized with PBS containing 1% paraformaldehyde, then PBS containing 0.1% saponin and 2% bovine serum albumin (BSA), for 15 min at 4°C. Subsequently, PBS with 0.1% saponin was used to wash the cells for 5 min at 4°C at 500 xg . Next, the

cells were stained intracellularly with 100 µL of Ki-67 antibody in 0.1% saponin and 2% BSA, incubated for 30 min in the dark, and then washed using PBS with 2% BSA. The cells were resuspended in 600 µL of PBS containing 2% BSA with 6 µL of 500 µg/mL and filtered through a 30 µm Nylon filter. For cell cycle analysis, 5 µg/mL concentration of DAPI was added 5 minutes prior to running the sample on the BD LSRFortessaTM (BD Biosciences).

2.9 c-kit+ cell enrichment and HSC isolation by FACS

Following the isolation of bone marrow cells as detailed in section 2.7.3, the cell suspension was lysed with 1 mL of NH_4Cl lysis buffer for 2 minutes. Next, 10 mL of 2% PBSFBS was added, and the mixture was centrifuged for 5 minutes at 500 xg to separate and remove the supernatant. The cells were then resuspended in a 300 µL solution of 2% PBSFBS containing 25 µL of anti c-kit MicroBeads (Miltenyi Biotec). The sample was then incubated in the dark for 20 minutes at 4°C on a rotating shaker. After incubation, the cells were washed with 1 mL of 2% PBSFBS and centrifuged at 500 xg for 5 minutes. Cells enriched for c-Kit using magnetic-activated cell sorting (MACS) (MACS®, Miltenyi Biotec) were stained as described earlier in section 2.8.1 and sorted using the BD FACSAriaTM Fusion (BD Biosciences) to obtain HSCs.

2.10 Colony forming cell assay

The manufacturer's protocols were used for BM colony-forming cell (CFC) assays. Briefly, $3x10^3$ BM cells were suspended in 250 µL of Iscoves Modified Dulbecco's Medium (IMDM) (StemCellTM Technologies). The complete cell suspension was then added to 2250 µL of the methylcellulose medium M3434 for the colony forming unit assay (CFC). The methylcellulose medium M3434 contained BSA, FBS, recombinant mouse SCF, recombinant mouse IL-3, recombinant human IL-6, recombinant human insulin, human transferrin (iron-saturated), recombinant human erythropoietin (EPO), and 2-Mercaptoethanol (Stem Cell Technologies). The cell suspension was plated in two wells of a 6-well plate (with approximately 1ml M3434/cell suspension per well). For ten days, the cultures were incubated at 37°C, after which, colonies were identified by light microscopy.

2.11 HSC transplant assay

To investigate the actions of haematopoietic stem cells (HSCs) in haematopoiesis and blood cell development, as well as to elucidate the mechanisms of HSC engraftment, a transplantation experiment was performed. The primary transplant experiment involved the use of two strains of mice: C57BL/6 SJL mice (CD45.1) as recipients and C57BL/6 (CD45.2) mice as donors. Specifically, 100 HSCs sorted from $Zeb1^{-/-}$ and control mice aged 10 to 12 weeks were transferred to lethally irradiated recipients along with 200,000 supporting CD45.1+ total bone marrow cells. Engraftment was assessed by regular analysis of peripheral blood (PB), which was collected every 4 weeks after the transplant and processed according to the protocol described in section 2.7.2.

2.12 RNA-seq analysis

2.12.1 Sample Preparation and Sequencing

Fourteen days after the final injection of Poly I:C, RNA was extracted from haematopoietic stem cells (HSCs) of four control and four $Zeb1^{-/-}$ mice using the RNAeasy Micro Kit (Qiagen). The Agilent 2100 Bioanalyzer and RNA Nano 6000 kit (Agilent Technologies) was used to determine the total RNA quality and quantity. cDNA libraries from 0.5-6 ng of total RNA with a RIN value greater than 8 were created using the NEBNext® Single Cell/Low Input RNA Library Prep Kit for Illumina®. These libraries were then fragmented, end-repaired, 5' phosphorylated, dA-tailed, adaptor-ligated, and PCR enriched using the NEBNext® kit. The resulting libraries were cleaned up with Agencourt Ampure® XP beads (Beckman Coulter®) and indexed using Illumina® Dual Index primers set 2: NEB E7780. Library quality was verified with the Agilent 2100 Bioanalyzer and high-sensitivity kit (Agilent Technologies) and quantified with Qubit® (Life Technologies). Using a 75-base paired-end (2x75bp PE) dual index read format, the libraries were normalised to 4 nM, pooled, and sequenced on the Illumina® HiSeq4000.

2.12.2 Raw Data Processing and Analysis Trimming

Trimming and QC on the trimmed reads were carried out through a wrapper tool that employs cutadapt and FastQC to eliminate adaptor sequencer and low-quality read ends called Trim Galore.

2.12.3 Mapping

STAR was used to map trimmed reads to the GRCm38.p6 mouse genome, with the MultimapNMax=1 flag utilised to treat reads mapping to multiple positions as unmapped.

2.12.4 Expression Summarization

Exon and transcript expression counts were determined by Subread feature Counts Version 1.6.2, which allocated sequence reads to genomic features. The gene model GENCODE M18 was used for specifying the exon and transcript positions and read summarization at the gene level was performed for paired end read fragments. Reads overlapping multiple features were excluded from the count summary to provide strict and reliable statistics.

2.12.5 Differential Gene Expression

The DEseq2 Bioconductor package analysis identified differentially expressed genes on normalised count data. The FDR method was used to adjust for multiple testing and false discovery in the resulting p-values.

2.12.6 Gene Ontology Over-Representation Analysis

The GOstats Bioconductor package was employed to conduct Gene ontology over-representation analysis (GO ORA), with FDR correction for multiple testing and false discovery. The top 200 ranking genes, ordered by p-value, were analysed for cellular components, biological processes, and molecular activities.

2.12.7 Data Visualization

Ingenuity Pathways analysis (IPA) was used to generate the canonical pathways. The heatmap was produced with https://software.broadinstitute.org/morpheus, and an FDR of 0.05 was used for DEGs. Top enriched pathways were identified using the Kyoto Encyclopaedia of Genes and Genomes database (KEGG), and Prism was used to generate the graph (GraphPad Software version 9.4.1).

2.13 Statistical analysis

The statistical analysis and graphs were generated with the GraphPad Prism software (GraphPad Software version 9.4.1). The data presented in the graphs represent the mean and standard error of the mean (SEM). The unpaired 2-tailed t-test, Mann-Whitney U test, or One-Way ANOVA with Tukey's multiple comparisons were used to determine statistical significance. All tests used a level of significance set at $p < 0.05$, with increasing numbers of asterisks indicating higher levels of significance. Specifically, *, **, ***, and **** represent $p < 0.05$, $p < 0.01$, $p < 0.001$, and $p < 0.0001$, respectively.

CHAPTER 3: Exploring the molecular mechanisms mediating *Zeb1* function in adult hematopoietic stem cells (HSCs).

3.1 Introduction

Epithelial-mesenchymal transition (EMT) promotes cellular plasticity and migration through cell fate and phenotypic changes that are often associated with cell polarity and adhesion loss (Kalluri and Weinberg 2009; Nieto et al. 2016). Transcription factors (TFs), of the ZEB, SNAI, and TWIST families help regulate EMT. Specifically, Zinc finger E-box binding homeobox 1 (ZEB1), a zinc finger TF that binds to E-box motifs, is known to be involved in the EMT process and several other processes, including myogenesis, postgastrulation embryogenesis, neuronal and T-cell development, and neuronal differentiation (Postigo et al. 1997; Postigo and Dean 1999; Clark and Chiu 2003; Zhang et al. 2015a; Singh et al. 2016a; Zhou et al. 2017; Jiang et al. 2018; Wang et al. 2019a). ZEB1 has been found to regulate the expression of multiple TFs associated with stem cells, such as BMI1, KLF4, and SOX2, which have oncogenic potential (Wellner et al. 2009; Singh et al. 2017).

Zeb1 has also been established as important in the regulation of EpCAM (epithelial cell adhesion molecule) and E-cadherin expression, two genes that play a role in cell adhesion and signalling. Aside from knowing *Zeb1* plays a role in regulating cell differentiation, its overall wider role in normal stem cell fate decisions is not fully understood. Previous research conducted by our laboratory has suggested that *Zeb1* is a critical regulator of haematopoietic stem cell (HSC) differentiation and adult haematopoiesis. Transplanted *Zeb1*$^{-/-}$ HSCs showed reduced engraftment capacity and poorer contribution to mature blood cells and BM progenitors (Almotiri et al. 2021).

In this chapter, we investigated potential ZEB1 target genes by RNA-seq of HSCs after *Mx1*-Cre mediated deletion of *Zeb1* by RNA-seq and identified *Epcam* as a key target. We then analysed the impact of *Zeb1* mediated regulation of *Epcam* expression on the transcriptional programming and molecular fate of HSCs.

3.2 Aims

3.2.1 Aim 1: Identify the molecular mechanisms behind *Zeb1* function in *Zeb1*$^{-/-}$ and wild-type mice using RNA-seq experiments.

To further study the role of *Zeb1* in HSCs and its regulation of HSC fate, RNA-seq experiments were conducted using a mouse model. These mice had Zeb1 conditional alleles and inducible Mx-cre (*Zeb1*$^{fl/fl}$; *Mx1*-Cre+), where *Zeb1* can be depleted in HSCs and their progeny by the administration of polyinosinic-polycytidylic acid (pIpC) (Almotiri et al. 2021). Our target goal was to identify the molecular mechanisms underscoring Zeb1 function in *Zeb1*$^{-/-}$ and wild-type mice of HSC fate.

3.2.2 Aim 2: Investigate the role of *Zeb1* in regulating EpCAM expression in HSCs and its potential implications for understanding the role of *Zeb1* in normal haematopoiesis.

In the RNA-seq experiments described in Aim 3.2.1, the *Epcam* gene was found to be a key target of the *Zeb1* gene. EpCAM is characterized as a homophilic, Ca2+-independent adhesion molecule that plays critical functions in intercellular adhesion, cell signalling, proliferation, differentiation, and development and maintenance of organ morphology (Schnell et al. 2013a). EpCAM has also been shown to control the epithelial-mesenchymal transition (EMT), stemness, and metastasis of cancer cells via the phosphatase and tensin homolog /AKT/mechanistic target of rapamycin kinase (PTEN/AKR/mTOR) pathway (Wang et al. 2018c).

Previous studies demonstrated that *Zeb1* is capable of negatively regulating EpCAM expression in several cell types; however, its action in HSCs has not been fully explored. In this aim, we therefore examined the actions of *Zeb1* in regulating EpCAM expression in HSCs. We used the genetically engineered *Zeb1* Mx1-Cre mouse model to knockout *Zeb1* specifically in adult HSCs, and then analysed gene expression profiles of EpCAM^{+} and EpCAM^{-} HSCs by RNA-seq.

3.3 Results

3.3.1 Transcriptional markers of haematological differentiation and cell polarity are both dysregulated in *Zeb1*$^{-/-}$ HSCs.

Following the final dose of pIpC (section 2.2), on day 14 we conducted RNA-Seq of isolated highly enriched HSCs (LSK CD150+CD48-) from *Zeb1*$^{-/-}$ or control animals to identify the transcriptional signature underlying *Zeb1*-mediated regulation in HSCs. For the experiment, we used a range of 10,000 to 18,500 cells. To obtain a higher number of hematopoietic stem cells (HSCs), we pooled together some of the samples. 47 (21%) of the 222 differentially expressed genes (DEG) from *Zeb1*$^{-/-}$ HSCs were upregulated, while 175 (79%) were downregulated (Figure 3.1 A). The elevated and most enriched pathways according to the biological pathway analysis included immune system, tight junction, cell junction organisation, cell adhesion, and endocytosis pathways (Figure 3.1 B).

We used heatmaps to visualise the results of RNA-seq experiments comparing control mice and *Zeb1*$^{-/-}$ animals (Figure 3.1 C) and found deregulated transcriptional activity related to HSC and other haematopoietic gene signatures (e.g. T-cells, B-cells and myeloid cells) and cell adhesion, lipid metabolism and cytoskeleton. For example, for HSC genes, we observed several upregulated genes, including *Spint2, Spint1, Fzd6, Ahr, and Cfc1*. Spint1 and Spint2 are members of the Kunitz family of serine protease inhibitors, which are characterised by their ability to inhibit the activity of serine proteases (Wu et al. 2021). We also observed several downregulated genes related to HSCs, including *Foxp2, Gfi1, Id1, Emxn, Serpina3f,* and *Gfi1b*. For T cell related genes, we observed several upregulated genes involved in immune response including *Cdcp1, Lat, H2-Ob, Lck, Lat2,* and *Cd7*. We also observed several downregulated genes in T cells, including *Lmo1, Ncam1,* and *Lgals1*. Overall, the heatmaps provided a comprehensive overview of the changes in gene expression that occurred in HSCs from *Zeb1*$^{-/-}$ mice and allowed us to identify key pathways and processes that were affected by the absence of *Zeb1*.
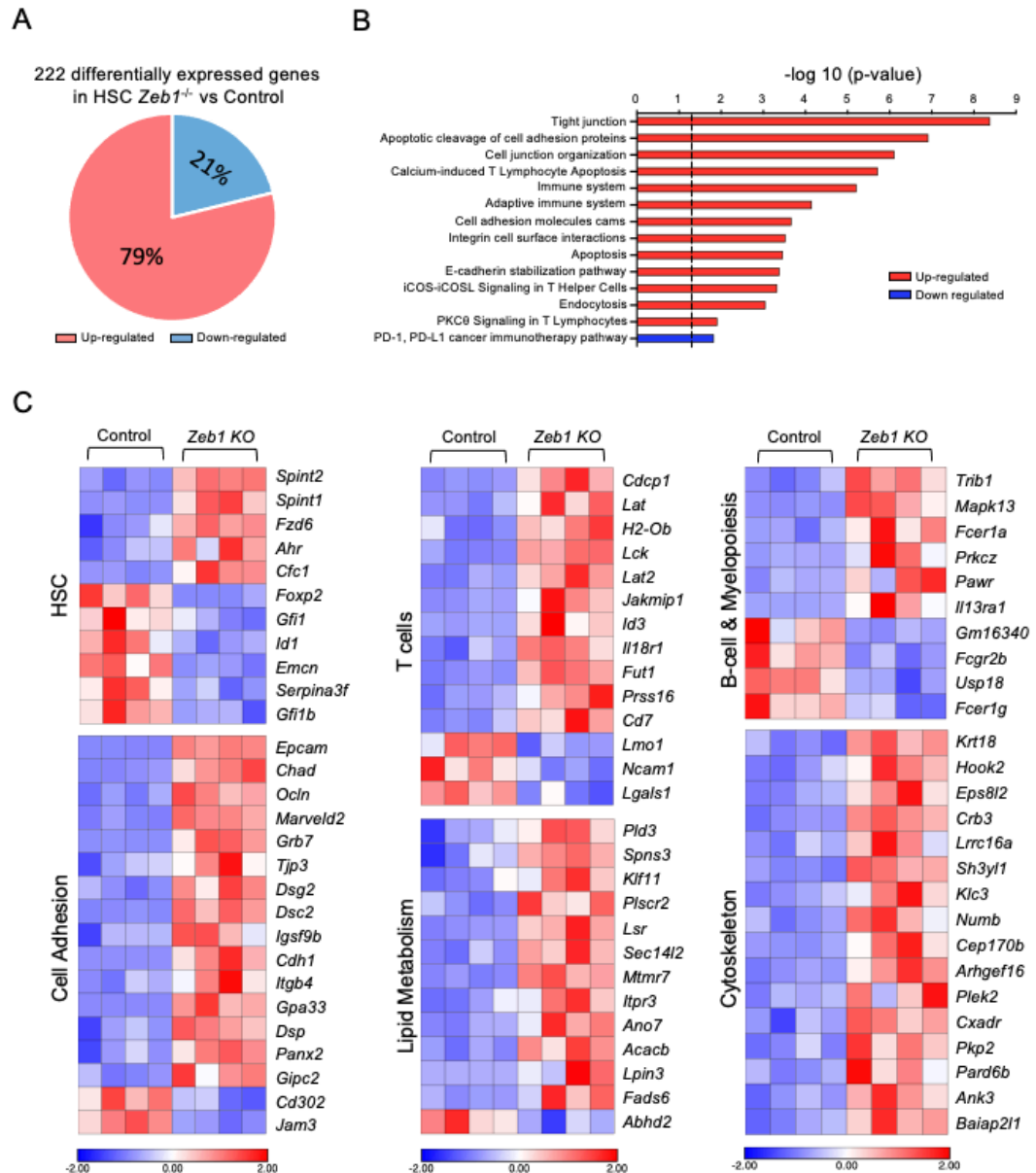
Figure 3.1 Heatmaps displaying deregulation of haematopoietic stem cell function and cell adhesion and polarity transcriptional programming in *Zeb1*^{-/-} HSCs. 14 days post last pIpC dose, HSCs (LSK CD48-CD150) were sorted from both *Zeb1*^{-/-} and control (n = 4 for each group) for RNA-Seq analysis. (A) The pie diagram portrays the number of differentially expressed genes from HSCs of *Zeb1*^{-/-} compared with the control. (B) The analysis of biological pathways displays the most enriched pathways in HSCs from *Zeb1*^{-/-} compared with control animals. Data are presented as –log10 (P value). The dashed black line denotes a 0.05 P value. (C) Heatmaps of the Zeb1 deleted DEGs showed relation to T-cells, B-cells, HSC function, cytoskeleton, lipid metabolism, and cell adhesion. The heatmap scale represents a z score. (This experiment was a collaboration with Dr. Almotiri. Cells were sorted by both Dr. Almotiri and myself. The RNA extraction was performed by Dr. Almotiri, and we sent the extracted RNA samples to Wales Gene Park. I conducted the bioinformatics analysis and data visualization, with the assistance of Dr. Almotiri, specifically in categorising the gene list in Category C.)

3.3.2 *Zeb1* deletion results in Inhibiting apoptosis pathway: Insights from IPA analysis

Since previous studies in our laboratory demonstrated that long-term *Zeb1* loss affected cell survival of HSPCs (data not shown) and the classical apoptosis pathway in panel B (GSEA) of figure 3.1, we decided to explore apoptotic pathways in our RNA-seq dataset. The Ingenuity Pathway Analysis (IPA) was used to identify genes related to apoptosis in the DEG list of *Zeb1*$^{-/-}$ HSCs. Only genes with a log2 fold change greater than 1.5 were included in the analysis to prioritize those showing substantial expression changes and potentially significant involvement in apoptosis in *Zeb1*$^{-/-}$ HSCs. Figure 3.2 A illustrates the top 10 upregulated apoptotic genes in the *Zeb1*$^{-/-}$ HSCs DEG list, as identified by IPA, with EpCAM being one of them. Figure 3.2 B is a heatmap showing the upregulated genes in the *Zeb1* KO HSCs DEG list, and the IPA was used to predict the potential impact of these genes on apoptosis.

Of the upregulated genes identified, a group of genes (*Cdh1, Dscd2, Epcam, Spnt1, Sfn, Mpz, Ggt1*) were found to lead to the inhibition of apoptosis (Figure 3.2 B). DSCD2, or desmocollin 2, is a protein involved in the formation of desmosomes, which are structures that help to anchor cells to one another (Hansford et al. 2015). SPNT1, or spermatogenesis-associated protein 1, is a protein involved in spermatogenesis and cell proliferation (Uhlén et al. 2015). SFN, or stratifin, is a protein found to regulate cell growth and differentiation (Leffers et al. 1993). MPZ, or myelin protein zero, is a protein involved in the formation of the myelin sheath around nerve fibres (Mandich et al. 2009). GGT1, or gamma-glutamyltransferase 1, is an enzyme involved in the degradation of proteins and the detoxification of drugs (Heisterkamp et al. 2008).

In contrast, another smaller group of genes (*Perp, Mapk13, Krt8*) were found to lead to the activation of apoptosis. PERP (TP53 apoptosis effector related to PMP-22) is a protein involved in the regulation of apoptosis and cell cycle progression. MAPK13, or mitogen-activated protein kinase 13, is a protein involved in signalling pathways that regulate cell growth, differentiation, and apoptosis (Roberts and Paraoan 2020). KRT8, or keratin 8, is a protein involved in the structure and function of epithelial cells (Werner et al. 2020). These findings

suggest that there are both inhibitory and activating influences on apoptosis in the *Zeb1⁻/⁻* HSCs DEG list but, overall, the data suggest a dominant anti-apoptotic gene signature in *Zeb1⁻/⁻* HSCs. It is worth noting that the IPA results in Figure 3.4 B show inhibition of the apoptosis pathway. However, this analysis does not show whether the inhibited apoptotic pathways are anti- or pro-apoptotic. Overall, this analysis suggests that the loss of *Zeb1* may cause cell survival advantages to HSCs, which has now been confirmed in long-term *Zeb1* deletion experiments from our laboratory (data not shown). Additionally, using the Ingenuity Pathway Analysis software (IPA), a gene-interaction network was created including a regulatory node that involves *Epcam*, *Crb3, Pard6b, Itgb4, Cdh1, Krt18,* and *Ocln* genes (Figure 3.2 C). Based on IPA, *ZEB1* plays a normal role in suppressing *CXADR, ITBGB4, CRB3, EPCAM, CDH1, PARD6B* and *KRT18.* The absence of *Zeb1* expression leads to the upregulation of these genes. Furthermore, *CDH1* was upregulated not only because there was an absence of its repressor *Zeb1* but also because the upregulation of *EPCAM* could leads to upregulation of *CDH1*(Fan et al. 2022). Finally, these results suggest that the upregulation of *CDH1* leads to the upregulation of *KRT18* and *OCLN*. This network could demonstrate Zeb*1*-specific regulation of target genes relating to cell adhesion, cell polarity, and the cytoskeleton, confirming our initial observations in Figure 3.1 C.
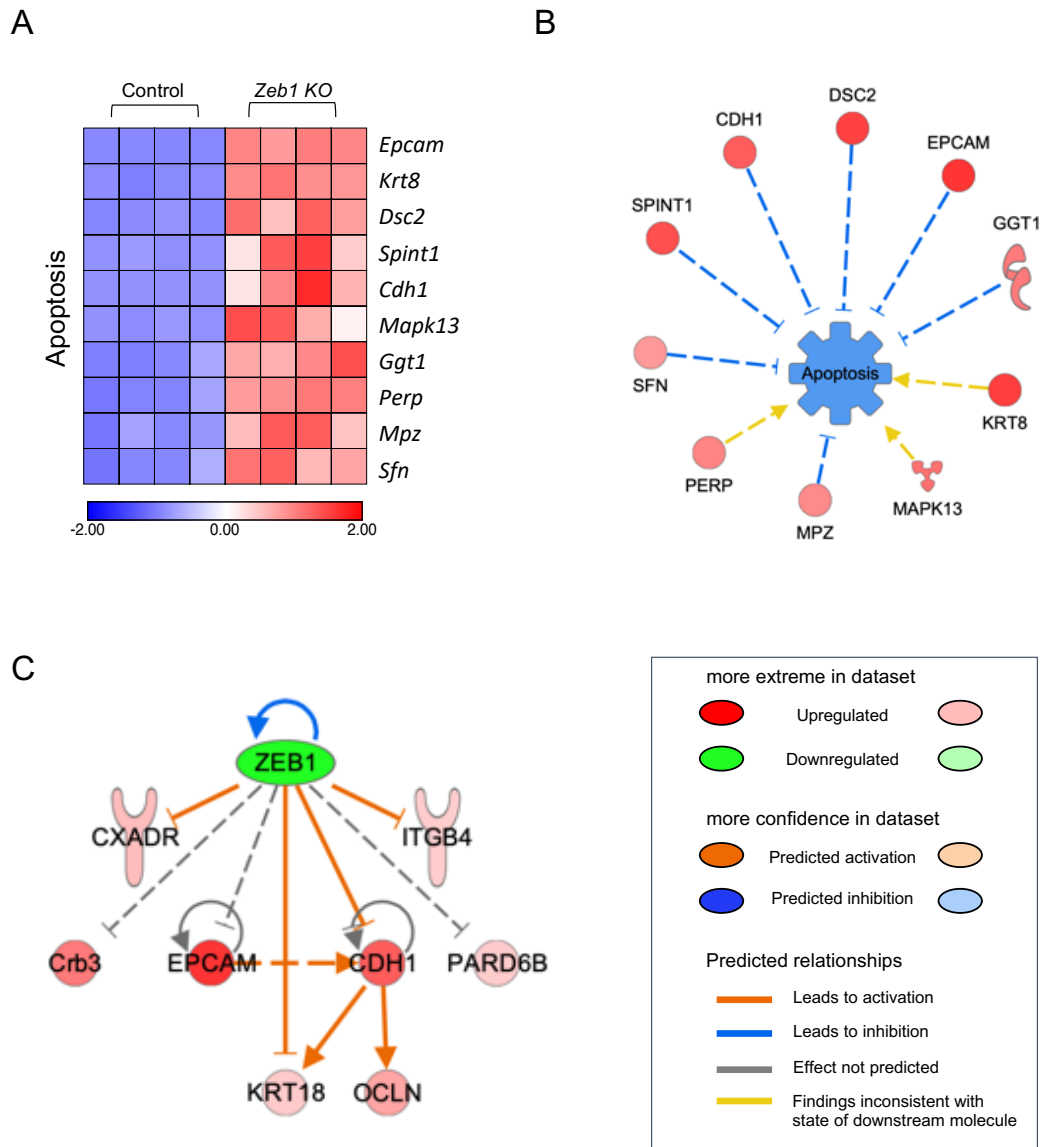
Figure 3.2 _Zeb1⁻ᐟ⁻_ HSCs display deregulation of Apoptosis related genes and inhibit the apoptosis pathway. Heatmaps of the DEGs (>1.5 log2 fold change only) within _Zeb1⁻ᐟ⁻_ HSCs and control after Zeb1 deletion related to apoptosis using the Ingenuity Pathway Analysis (IPA) software (A). Interactomic analysis in apoptosis by Ingenuity Pathway Analysis (IPA) software (B). Ingenuity Pathway Analysis (IPA) software rendition of a network of Zeb1 interaction with several target genes. Epcam, Pard6b, and Crb3 were added manually because of their confirmed binding to ZEB1 from literature (C). Networks displayed as nodes represent genes and edges represent their biological relationships. Nodes are indicated by symbols of different colours: green refers to downregulation in our DEGs, and red is upregulation. Coloured arrows represent biological relationships between nodes and the other significant genes (the molecule affects expression of the other). The orange colour indicates activation. The grey arrow indicates there are no known interactions between the molecules of which the IPA can predict. Blue coloured lines indicate inhibition. The yellow-coloured lines indicate inconsistencies between the regulation of the molecule and the role in the pathway.

3.3.3 *Zeb1* deletion results in increased EpCAM expression results in a cell-survival advantage of HSCs

The most differentially expressed gene in $Zeb1^{-/-}$ HSCs was *Epcam*, a glycoprotein that mediates cell attachment in epithelia (Schnell et al. 2013a) (Figure 3.1 C). Since *Epcam* is a key regulator of stem cell maintenance and differentiation in various types of stem cells (González et al. 2009a), we decided to investigate the role of *Epcam* expression during *Zeb1*-mediated control of HSC fate. Flow cytometry on various haematopoietic cell populations in $Zeb1^{-/-}$ mice was able to validate protein-level enhancement of *Epcam* expression across the entire haematopoietic differentiation hierarchy, with the exception of CMP, GMP, and MEP committed progenitors (Figure 3.3 A).

We also validated the expression of bioinformatics identified components of the *Zeb1-Epcam* gene axis in HSPCs identified in Figure 3.2. E-cadherin, and ITGB4, which are both cell adhesion molecules (Van Roy and Berx 2008; Xiong et al. 2021), were overexpressed at the protein level in $Zeb1^{-/-}$ HSPCs, as assessed by flow cytometry (Figure 3.3 B-E). Our results showed that the percentage of E-cadherin-positive cells in $Zeb1^{+/+}$ mice was significantly lower compared to $Zeb1^{-/-}$ mice, with an approximate 90 to 678-fold change (Figure 3.3 B-C). Specifically, we observed an increase of at least 60% in the percentage of E-cadherin-positive cells in $Zeb1^{-/-}$ mice, with the highest increase of almost 80% being observed in MPP cells. There was also an observed increase in the ITGB4-positive cell percentage in $Zeb1^{-/-}$ mice compared to $Zeb1^{+/+}$ mice (Figure 3.3 D-E). The percentage of ITGB4-positive cells increased by at least 30% in $Zeb1^{-/-}$ mice, with the highest increase being observed in MPP cells.
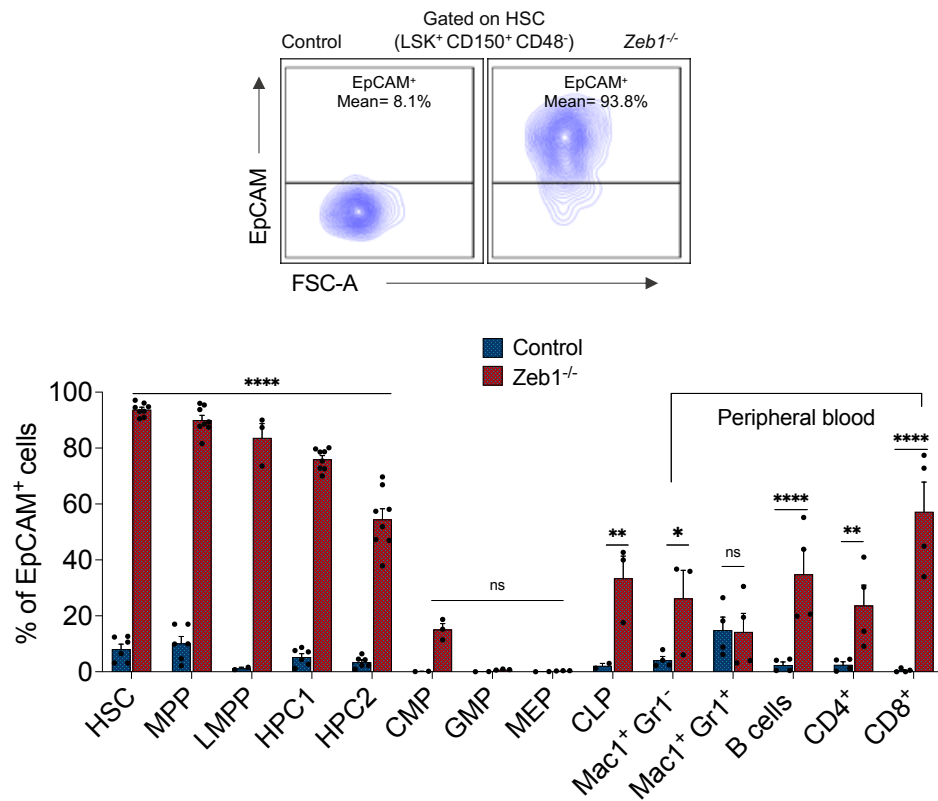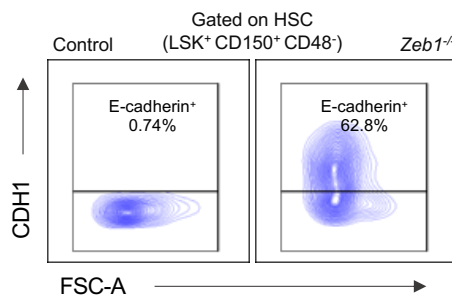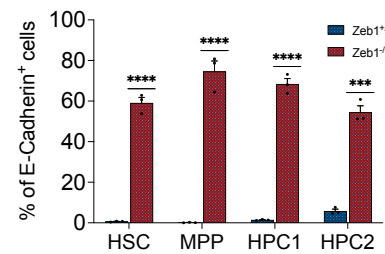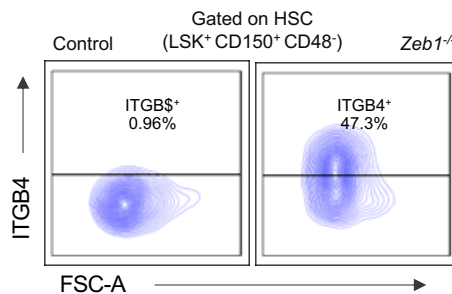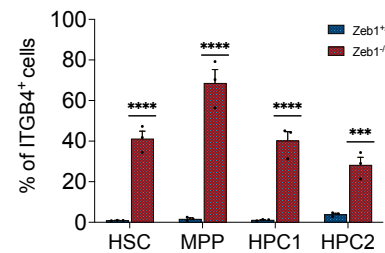
Figure 3.3 Flow cytometry results validating the EpCAM, E-cadherin and ITGB4 expression is mediated by *Zeb1*. (A) top plot: Representative flow cytometry plots in HSCs of EpCAM expression 14 days post pIpC injection for both Zeb1$^{-/-}$ and control. bottom, 14 days post pIpC injection analysis of EpCAM expression in BM subpopulations and PB mature cells. (B, D) Representative plots from flow cytometry analysis for E-cadherin and ITGB4 expression in HSCs. The expression of E-cadherin (C) and ITGB4 (E) in BM HSPCs from control and Zeb1$^{-/-}$ (n=3 for each) 14 days post pIpC injection. Error bars show mean ± SEM. Holm-Šídák's multiple comparisons test was used to calculate significance as follows: *P < .05, **P < .01, ***P < .001, ****P <0.0001.

Since we found that the loss of Zeb1 suggested survival advantages and given that EpCAM has a role in apoptosis (Bremer and Helfrich 2008; Herreros-Pomares et al. 2018; Aiman Mohtar et al. 2020) and is the most significant DEG identified (Figure 3.2), we decided to explore the relationship between regulators of apoptosis further. First, we used the IPA to explore the relationship between *Zeb1*, EpCAM and apoptosis regulators. In Figure 3.4 A the prediction analysis results show normal Zeb1 expression represses EpCAM, and that leads to activation of apoptosis, and that losing Zeb1 leads to upregulation of the EpCAM that, in turn, leads to inhibition of apoptosis pathways. This prediction is consistent with the known role EpCAM plays in inhibiting apoptosis (Bremer and Helfrich 2008; Herreros-Pomares et al. 2018; Aiman Mohtar et al. 2020).

We next tested this predicted relationship experimentally *in vitro*. Figure 3.4 B shows the total cell number after culturing 2500 Lin-Sca-1+c-Kit+ (LSK) cells from *Zeb1 KO* EpCAM-negative (n = 6) and EpCAM-positive (n = 6) mice from three separate experiments, revealing a significantly higher number of *Zeb1 KO* EpCAM-positive ($Zeb1^{-/-}$ $EpCAM^+$) cultured LSK cells compared to ZEB1 KO EpCAM-negative ($Zeb1^{-/-}$ $EpCAM^-$) cells. Thus, EpCAM expression appears to confer a cell-survival signal in $Zeb1^{-/-}$ HSCs. This is suggested by the fact that $Zeb1^{-/-}$ LSK EpCAM-positive HSPCs grew more *in vitro* than the EpCAM-negative HSPCs (Figure 3.4 B). To confirm this, we performed Annexin V analysis in LSK cells from *Zeb1 KO* EpCAM-negative (n = 6) and EpCAM-positive (n = 6) mice as before, which showed a significant decrease in the Annexin V+ cell percentage in $Zeb1^{-/-}$ $EpCAM^+$ LSK cells compared to $Zeb1^{-/-}$ $EpCAM^-$ LSK cells. Therefore, in $Zeb1^{-/-}$ $EpCAM^+$ subsets, we found lower apoptosis *in vitro*, directly confirming our bioinformatic prediction that EpCAM expression promotes cell survival in $Zeb1^{-/-}$ HSPCs (Figure 3.4 C).

To confirm this observation *in vivo*, the analysis of apoptosis in fresh bone marrow HSPCs was carried out in *Zeb1 KO* EpCAM-negative (n = 4) and EpCAM-*positive* (n = 4) mice from two separate experiments. Data from these experiments showed a significant decrease in the Annexin V+ cell percentage in $Zeb1^{-/-}$ $EpCAM^+$ HSCs, multipotent progenitors (MPPs), haematopoietic progenitor cells 1 (HPC1), and haematopoietic progenitor cells 2 (HPC2) compared to $Zeb1^{-/-}$ $EpCAM^-$ cells with approximate fold changes of 2.3, 4.8, 1.9, and 1.4,

respectively (Figure 3.4D). However, *Zeb1*^{-/-} HSCs showed no change in the cell cycle state as measured by Ki67 expression (Figure 3.5E-F). These results indicate that increased *Zeb1* mediated EpCAM expression produces an anti-apoptotic advantage in the absence of changes to cell cycle status.
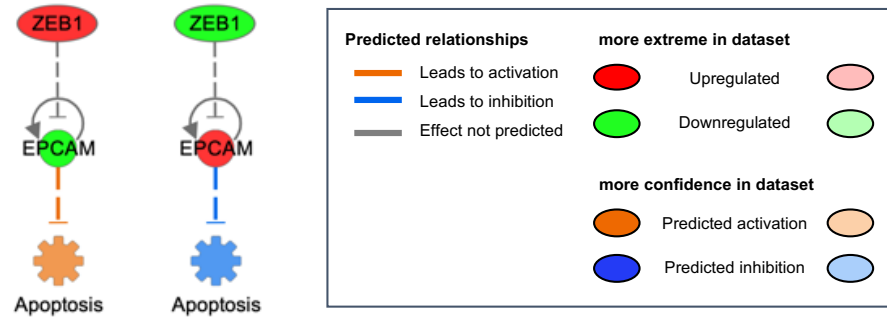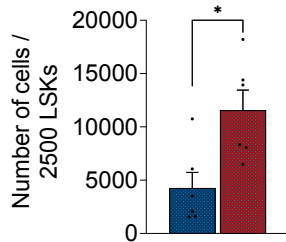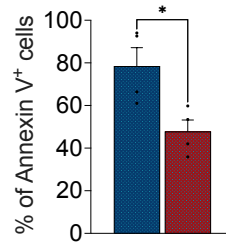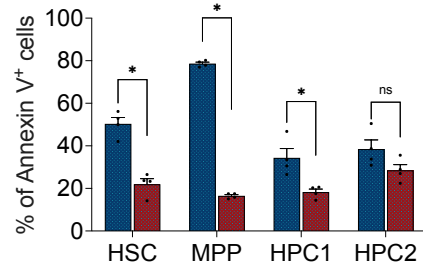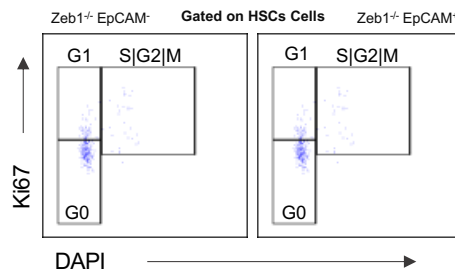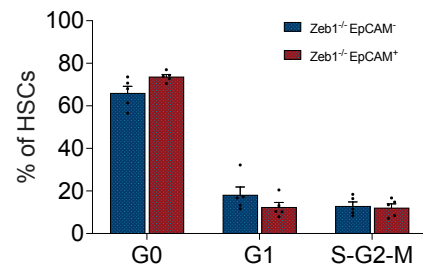
Figure 3.4 Increased expression of EpCAM expression in *Zeb1*^{-/-} HSCs confers cell survival advantage. (A) The prediction analysis results between Zeb1, EpCAM and apoptosis pathway. Column one, Exist of Zeb1 (red) leads to downregulation of EpCAM (green) which leads to activation of the apoptosis (orange). Column two, absent of Zeb1 (green) leads to upregulation of EpCAM (red) which leads to inhibition of apoptosis (blue). (B) The result of total cell counts after culturing 2500 of sorted LSKs from both Zeb1^{-/-} EpCAM[-] and Zeb1^{-/-} EpCAM[+] (n = 6 each from 3 separate experiments). (C) Frequency analysis of Annexin V (Apoptosis) in LSKs from both Zeb1^{-/-} EpCAM[-] and Zeb1^{-/-} EpCAM[+] after culture (n = 6 each from 3 separate experiments). (D) Frequency analysis of Annexin V (Apoptosis) in BM HSPCs from both Zeb1^{-/-} EpCAM[-] and Zeb1^{-/-} EpCAM[+] 14 days post pIpC injection (n = 4 each from 2 separate experiments). (E) Representative plots from flow cytometry analysis for proliferation in HSCs along with summary graph (D) from both Zeb1^{-/-} EpCAM[-] and Zeb1^{-/-} EpCAM[+] 14 days post pIpC injection via Ki67 and DAPI staining (n = 5 each from 1 experiment). Error bars represent mean ± SEM. Mann-Whitney U test used for significance testing. *P < 0.05; **P < 0.01.

3.3.4 *Zeb1⁻ᐟ⁻* EpCAM⁺ HSPCs exhibit increased cell survival and decreased transcriptional markers for mitochondrial metabolism, RNA synthesis, and differentiation.

After we found that an increase in EpCAM expression confers survival advantages, we elected to use *Zeb1⁻ᐟ⁻* EpCAM⁺ LSK cells or *Zeb1⁻ᐟ⁻* EpCAM⁻ LSK cells for RNA-seq analysis to broadly assess the transcriptomic signature underscoring EpCAM expression in *Zeb1⁻ᐟ⁻* HSPCs.

Figure 3.5 shows the transcriptomic signature of *Zeb1 KO* HSPCs isolated by EPCAM expression. In panel A, the volcano plot demonstrates the connection between the magnitude of the change in gene expression (log2 of fold-change; x-axis) and statistical significance of the change (–log10 of adjusted P value; y-axis) in a comparison of *Zeb1⁻ᐟ⁻* EpCAM⁺ with *Zeb1⁻ᐟ⁻* EpCAM⁻ LSK cells. 3263 genes were found to be upregulated and 3153 genes were downregulated in *Zeb1⁻ᐟ⁻* EpCAM⁺ HSPCs (Figure 3.5 A).

GSEA analysis shows the apoptotic regulation, p53 stabilisation, p53 targeted phosphorylation, and HSC differentiation in *Zeb1⁻ᐟ⁻* EpCAM⁺ HSPCs. Supporting enhanced cell survival and blocked differentiation in *Zeb1⁻ᐟ⁻* EpCAM⁺ HSCs (Figure 3.4 B) and (Almotiri et al. 2021), the biological pathway analysis identified signatures for p53-mediated pro-survival and anti-haematopoietic differentiation in *Zeb1⁻ᐟ⁻* EpCAM⁺ HSPCs (Figure 3.5 B).

In Figure 3.5 panel C, the top canonical pathways found to be robust in *Zeb1⁻ᐟ⁻* EpCAM⁺ LSK cells are shown, as found in the IPA (IPA, retrieved 2023 from Ingenuity Pathway Analysis | QIAGEN Digital Insights), KEGG (Kanehisa and Goto 2000), PID (Schaefer et al. 2009), and Reactome (Croft et al. 2014) pathway databases. These results show that ribosome biogenesis and ribosome-associated processes, such as rRNA processing, whose downregulation has previously been linked to conferring stress tolerance in preleukemic HPSCs (Cai et al. 2015), were similarly downregulated in *Zeb1⁻ᐟ⁻* EpCAM⁺ HSPCs, underscoring the relatively low bioenergetic status of this cell population (Figure 3.5). In addition, lower mitochondrial gene expression, transport, translation, and protein import were seen in *Zeb1⁻ᐟ⁻* EpCAM⁺ HSPCs, as well as reduced activity

in related mitochondrial metabolic pathways important for HSC fate (for example, pyruvate metabolism and TCA cycle) (Filippi and Ghaffari 2019).
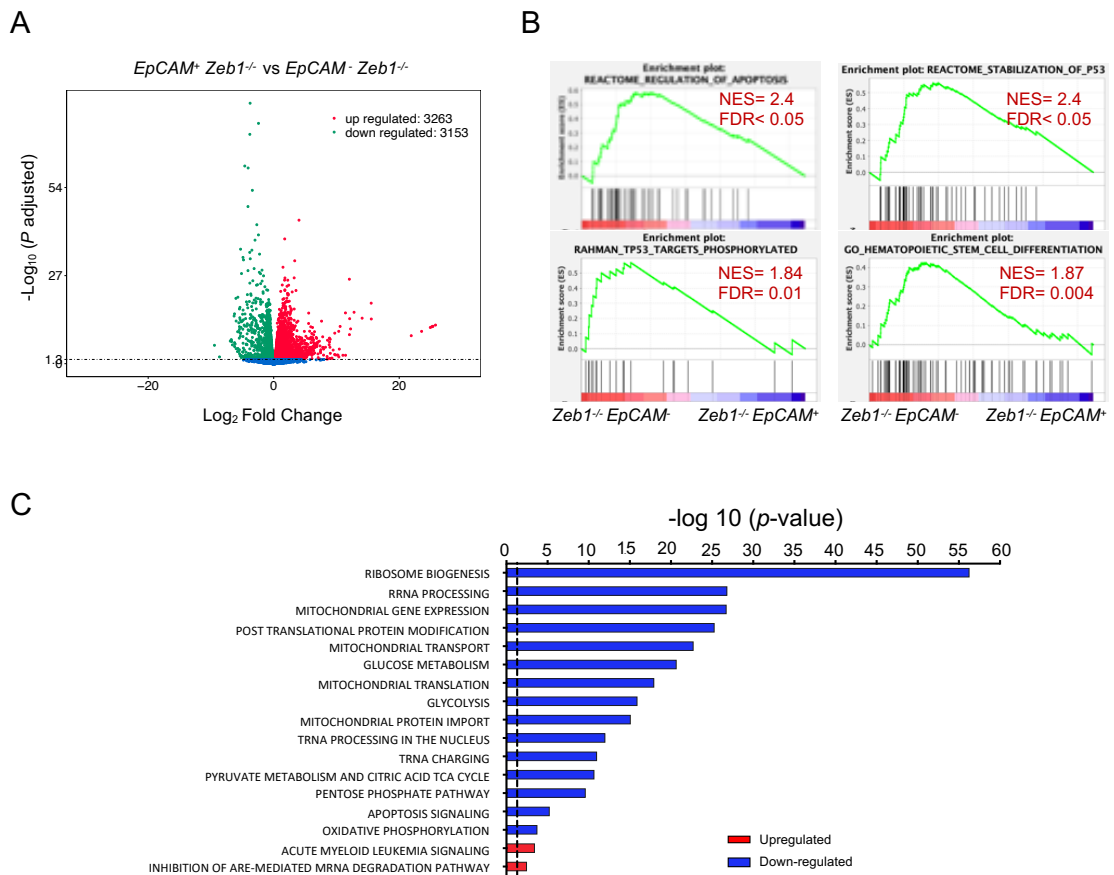
Figure 3.5 Differential transcriptional signatures for *Zeb1*^{-/-} EpCAM[+] HSPCs. (A) Volcano plot showing an association between magnitude of gene expression change (log2 of fold-change; x axis) and the change's statistical significance (–log10 of adjusted P value; y axis) for EpCAM[+] to EpCAM[-] in Zeb1-deficient LSK cells. Coloured points signify DEGs (cut-off FDR < 0.05) that are either upregulated (red) or downregulated (green) in *Zeb1*^{-/-} EpCAM[+] compared with *Zeb1*^{-/-} EpCAM[-]. (B) GSEA plots organised as follows; top left, regulation of apoptosis pathways, top right, stabilisation of P53 pathways, TP53 targets phosphorylated pathways, and lower right HSC differentiation pathways. (C) Canonical pathways highly enriched in *Zeb1*^{-/-} EpCAM^{+} LSK cells. Data are displayed as –log10 (P value) with a dashed black line indicating a 0.05 P value. We performed the analysis with GSEA software and IPA (n=4 per genotype).

In Figure 3.6 we further explored enhanced in cell survival signature in *Zeb1⁻/⁻ EpCAM⁺* HSPCs. In panel A, a heatmap shows the differentially expressed genes (DEGs) within EpCAM⁺ Lin-Sca-1+c-Kit+ (LSK) cells after *Zeb1* deletion that are related to anti-apoptosis pathways and pro-apoptosis. Figure 3.6 Panel B shows an interactomic analysis of apoptosis in LSK and haematopoietic cells, as well as an EpCAM interaction network and several differentially expressed genes related to apoptosis in *Zeb1⁻/⁻* EpCAM⁺ versus *Zeb1⁻/⁻* EpCAM⁻ HSPCs. The network displays the genes graphically as nodes and the edges indicate their biological relationships. Nodes are indicated by symbols of different colours: green refers to downregulation in our DEGs, and red is upregulation. Coloured arrows indicate the biological relationships between nodes and other significant genes whereas the molecule affects the expression of the other. Blue indicates inhibition, and orange colour indicates activation. IPA predicts that the apoptosis in both the LSK and haematopoietic cells is inhibited (blue). Interestingly, we identified an EpCAM⁻p53-BCL-XL (BCL2L1) network of interacting genes indicating that apoptotic regulation in *Zeb1⁻/⁻* HSPCs EpCAM leads to the inhibition of TP53, and the role of TP53 is to inhibit BCL2L1; however, since TP53 is inhibited by EpCAM, it leads to upregulation of the BCL2L1. This, in turn, leads to the inhibition of apoptosis in haematopoiesis.

Finally, by intracellular flow cytometry, we experimentally tested whether anti-apoptotic BCL-XL was upregulated *Zeb1⁻/⁻* EpCAM⁺ LKS cells with an approximate 1.34-fold change, as predicted above. Consistent with our bioinformatic predictions in Figure 3.6, we observed enhanced anti-apoptotic protein BCL-XL expression in *Zeb1⁻/⁻* EpCAM⁺ HSPCs (Figure 3.6 C, D). Overall, these data suggest that *Zeb1⁻/⁻* EpCAM⁺ HSPCs display enhanced cell survival that is mediated, in part, by BCL-XL.
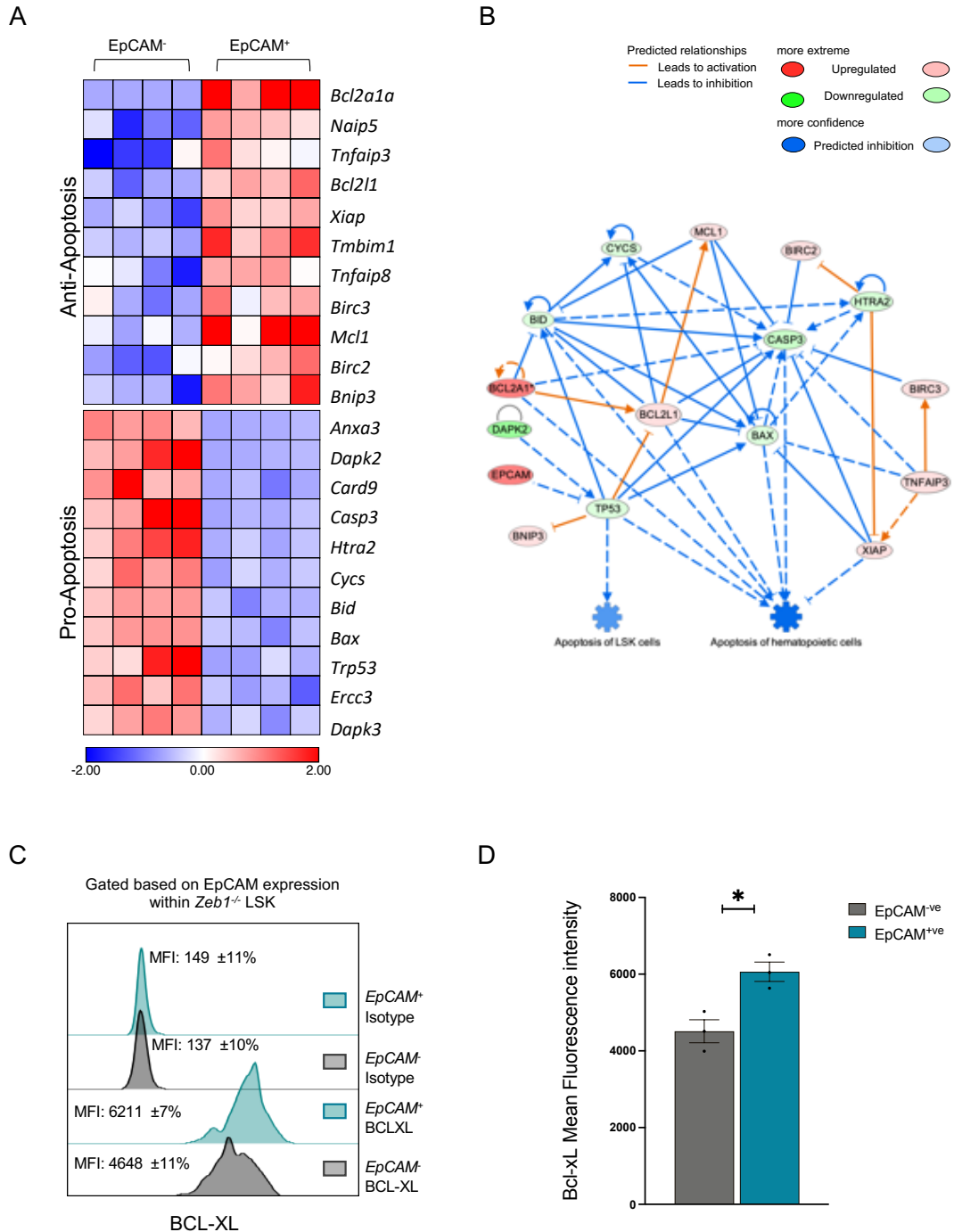
Figure 3.6 Differential gene expression in apoptotic pathways display enhanced cell survival for *Zeb1*^{-/-} EpCAM mediated by BCL-XL. (A) Heatmaps of the DEGs from EpCAM[+] and EpCAM[-] LSKs post *Zeb1* deletion relating to antiapoptosis. (B) Heatmaps of the DEGs from EpCAM[+] and EpCAM[-] LSKs post Zeb1 deletion relating to proapoptosis. (C) Interactomic analysis of apoptosis of LSK and haematopoietic cells and interaction network of EpCAM of differentially expressed apoptotic genes in *Zeb1*^{-/-} EpCAM[+] compared to *Zeb1*^{-/-} EpCAM[-]. Apoptotic process in HSCPs by Ingenuity Pathway Analysis (IPA). The network is displayed graphically as nodes (genes) and edges (the biological relationships). Nodes that are green = downregulation in DEGs, and nodes that are red = upregulation. The biological relationships between nodes and other significant genes are represented as coloured arrows (the molecule affects expression other) with blue indicating inhibition and orange indicating activation. (C) histogram representing EpCAM fraction BCL-XL levels in *Zeb1*^{-/-} LSK along with summary graph (D) (n=3 per genotype). Error bars display the mean and SEM. Whitney U test was used to establish statistical significance according to the following: *P < .05, **P < .01, ***P < .001, ****P <0.0001

3.4 Discussion

Zeb1 governs a variety of embryonic developmental processes and in adult tissue-specific stem cells, it functions as a crucial modulator of tissue homeostasis (Brabletz and Brabletz 2010; Kahlert et al. 2015; Gupta et al. 2021). Previous research carried out in the laboratory by Alhomidi Almotiri has thoroughly characterised the role of *Zeb1* in normal haematopoiesis and a differentiation defect of HSC after transplantation, and engraftment failure in secondary recipients. These initial results imply that *Zeb1* acts as a critical modulator for adult HSC self-renewal and differentiation in haematopoiesis (Almotiri et al. 2021). Yet, a gap in knowledge still exists for the cellular and molecular processes underscoring control of stem cell self-renewal, lineage selection, and differentiation by *Zeb1* in HSCs. This chapter aimed to further investigate the role of *Zeb1* in adult HSCs, employing a murine model with conditional alleles of *Zeb1* through an inducible *Mx*-cre system.

In collaboration with Dr Almotiri, by deleting *Zeb1* specifically in adult mice using the *Mx1*-Cre system, we were able to identify the molecular mechanisms behind Zeb1 function in HSCs using RNA-seq experiments. Our results showed that the deletion of *Zeb1* leads to significant changes in gene expression in HSCs, including upregulation of cell adhesion and cytoskeletal organization related genes and downregulation of lipid metabolism related genes.

Notably, we discovered that the deletion of *Zeb1* led to increased expression of cell adhesion molecule EpCAM in HSCs, indicating that *Zeb1* is a transcriptional repressor of EpCAM. How *Zeb1* achieves this in our mouse model of haematopoiesis is unclear but there is evidence to suggest that ZEB1 mechanistically directly suppresses the activity of the *EpCAM* promoter in both zebrafish and cell line models (Vannier et al. 2013; Song et al. 2017). IPA analysis also revealed an EpCAM mediated gene interaction network involving *Crb3, Pard6b, Itgb4, Cdh1, Krt18, and Ocln* genes, all of which are related to cell polarity, cytoskeleton, and cell adhesion properties. Interestingly, EpCAM is typically upregulated in embryonic stem cells, tissue progenitors, cancer-initiating cells, and carcinomas, acting as a signalling molecule with tumour-promoting functions (Schnell et al. 2013b). Furthermore, *ZEB1* represses human *EPCAM*

expression in pancreatic and breast cancer cell lines (Vannier et al. 2013). Given the overlap in molecular characteristics between embryonic stem cells and cancer stem cells and the known role of Zeb1 in mediating AML stem cell (LSC) transformation, it will be interesting to analyse the specific role of EpCAM during *Zeb1*-mediated modulation of AML LSCs. Of relevance here, EpCAM has an involvement in influencing cell survival, wherein upregulating cancer cell EpCAM expression confers survival, and, conversely, silencing cancer cell EpCAM expression causes apoptosis (Gao et al. 2014). We found that EpCAM may be able to promote cell survival by activating signalling pathways that inhibit cell death, such as anti-apoptotic BCL-XL (Athyala et al. 2019; Li et al. 2020; Loo et al. 2020). This is consistent with studies in other cancers which have shown that EpCAM may be able to upregulate the expression of Bcl-2, another anti-apoptotic BCL family member, in cancer cells (Gao et al. 2014). Of possible therapeutic relevance to AML (Wei et al. 2020), it was found in other cancers that targeting *EPCAM* may be able to reduce Bcl-2 expression and induce cell death (Hussain et al. 2006).

On a related note, RNA-sequencing of *Zeb1*$^{-/-}$ HSCs our data suggests that *Zeb1* mediates a survival advantage in HSCs through other molecular regulators associated with an *Epcam* gene network. This inference was made as we noted upregulation of a large group of *Epcam* related genes (*Cdh1, Dscd2, Epcam, Spnt1, Sfn, Mpz, Ggt1*) hypothesised to inhibit apoptosis while another, smaller gene set (*Perp, Mapk13, Krt8*) leads to the activation of the apoptosis pathway. What this means for the integrity of the HSC pool in the absence of *Zeb1* is that the dominant anti-apoptotic tone likely supports the growth of dysplastic or neoplastic HSCs. Such a hypothesis is consistent with the lower expression of *Zeb1* in AML and AML LSCs and an enhanced AML signature in EpCAM[+] HSCs from *Zeb1*$^{-/-}$ mice (unpublished data) (Almotiri et al. 2021). This postulate is also supported by the finding of EpCAM derepression in *Zeb1*$^{-/-}$ *HSCs* is associated with improved HSC survival and blocked differentiation during homeostasis and the proliferative stress of transplantation – notably, both enhanced cell survival and blocked differentiation are hallmarks of AML development (Olsson et al. 1996).

In $Zeb1^{-/-}$ mice, EpCAM is highly expressed in HSCs, while in $Zeb1^{+/+}$ mice, EpCAM expression is low, suggesting that the expression of EpCAM in (HSCs) is regulated by $Zeb1$. Currently we have only explored the correlation between EpCAM expression in the context of $Zeb1$ deletion. The RNA-seq was performed on EpCAM-positive and EpCAM-negative Zeb1-deficient HSCs to identify potential downstream targets of EpCAM in this setting, but there is no clear functional relevance at this point. To better elucidate the function of EpCAM under these conditions, an RNAi mediated knockdown experiment of EpCAM should be conducted to investigate whether EpCAM is directly involved in the observed phenotype in $Zeb1^{-/-}$ mice, and whether it plays a role in normal haematopoiesis was proposed. Specifically, we should examine the effect of EpCAM knockdown in HSCs from both $Zeb1^{-/-}$ and $Zeb1^{+/+}$ mice followed by functional analysis *in vitro* and in vivo, as judged by transplantation. We hypothesise that the phenotype observed in $Zeb1^{-/-}$ mice could be rescued in these EpCAM knockdown experiments. Additionally, by performing EpCAM knockdown experiments in wild-type mice we will be able to determine the requirement for EpCAM in normal HSC function, which is at present unclear.

Our study found that the deletion of $Zeb1$ increased EpCAM expression in HSCs, and subsequent RNA-seq analysis revealed other significant molecular differences between EpCAM-positive and EpCAM-negative cells in $Zeb1$-deficient HSCs. Specifically, we observed that mitochondrial gene expression, transport, translation, and protein import pathways were inhibited in EpCAM-positive $Zeb1$-deficient HSCs compared to EpCAM-negative cells. The observed defect in HSC maintenance, commitment, differentiation, and survival in the $Zeb1$ KO HSCs could be associated with the high expression of EpCAM, which inhibits mitochondria that play a critical role in regulating cellular activities, such as apoptosis, by modulating various signalling pathways, metabolic processes, oxidative stress responses, and energy production. These findings are consistent with a recent study that showed HSCs with high EpCAM expression exhibit reduced mitochondrial activity and cellular metabolism, and that upregulation of EpCAM in HSCs is related to reduced OXPHOS activity and higher glycolytic activity compared to EpCAM-negative HSCs (Zhang et al. 2022b). Furthermore, the study showed that manipulating the metabolic state of EpCAM-positive HSCs

by targeting metabolic pathways could affect their self-renewal and differentiation potential (Zhang et al. 2022b). These findings suggest that *Zeb1* may act as a crucial regulator of mitochondrial function in HSCs by modulating EpCAM expression and may provide new insights into the complex interplay between transcription factors, mitochondrial activity, and stem cell function in HSCs.

HSCs primarily use glycolysis and have a low metabolic rate, but before differentiating, they switch to oxidative phosphorylation in response to haematological stress (Ito et al. 2018; Nakamura-Ishizu et al. 2020). The metabolic status of HSCs is directly associated with their condition and fate, such as cell cycle exit and entry, stemness maintenance, and exhaustion (Ito et al. 2018). Metabolism is extremely important and is connected to stem-cell functions by mitochondria (Khacho et al. 2016) and our research found that *Zeb1*^{-/-} EpCAM[+] HSCs display altered metabolic pathways (Almotiri et al. 2021). For mitochondrial activities and stemness maintenance, balanced mitochondrial morphology, which is governed by mitochondrial fusion and fission, is crucial (Pernas and Scorrano 2016). The mitochondrial dynamics are molecularly controlled to synchronise HSC metabolism and stemness, and it was found that by blocking Mitofusin-2, *Zeb1* links the fractured shape of mitochondria to the stemness of HSCs (Zhang et al. 2022b). Its inhibition keeps the mitochondrial structure immature and the mitochondrial metabolism at a low level and so it could be hypothesised how the dysregulated metabolic pathway in our mouse model could be controlled by a Zeb1/Mitofusin-2/fragmented mitochondrial pathway influencing the status of mitochondria and properties of long-term self-renewal in HSCs (Zhang et al. 2022b).

Overall, our results expand upon previous research indicating that *Zeb1* is a critical regulator of adult HSC function by identifying critical targets molecular target genes and pathways under the control of *Zeb1* in HSC self-renewal, apoptosis and differentiation.

CHAPTER 4: Genetically modified mice using the *Vav-iCre* strategy uncovers the role of *Zeb1* during development

4.1 Introduction

Gene expression is a fundamental process in biology that allows cells to produce the proteins and other molecules needed for their function and development (Alberts et al. 2002). Haematopoiesis, for example, is a complex process that involves the generation of various blood cell lineages from hematopoietic stem cells. Each blood cell type has a specific function, and the expression of different genes is required to give rise to these different cell types(Eaves 2015). However, the regulation of gene expression is complex and involves multiple layers of control, including tissue-specific factors. The exploration of gene expression specifically in each tissue is crucial for understanding the molecular mechanisms underlying various biological processes and diseases (Sonawane et al. 2017).

Transcription factors can either activate or repress gene expression, depending on their specific function. When a transcription factor binds to a response element, it can either recruit other proteins that help to initiate the transcription of the gene into RNA, or it can block the binding of other proteins that are needed for transcription to occur (Latchman 2001; Lambert et al. 2018). *Zeb1(*zinc finger E-box-binding homeobox 1 or TCF8/DeltaEF1), is a transcription factor part of the zinc finger E-box-binding (ZEB) family of proteins (Vandewalle et al. 2009; Gheldof et al. 2012; Zhang et al. 2015b; Stemmler et al. 2019). It plays a key role in regulating the expression of various genes, particularly in the context of epithelial-mesenchymal transition (EMT), a process in which epithelial cells lose their epithelial phenotype to become more mesenchymal-like (Vandewalle et al. 2009; Zhang et al. 2015b; Stemmler et al. 2019).

Since many transcription factors, including *Zeb1*, have critical functions in other organs, constitutive gene targeting in mice can result in a deadly phenotype during embryonic development that prevents the analysis of hematopoietic cell function (Takagi et al. 1998a). Therefore, conditional mouse knockout models in which *Zeb1* can be deleted by recombination mediated by Cre-lox in a time-and cell type-specific way have been developed (Almotiri et al., 2021; Brabletz et al., 2017; Wang et al., 2021).

Our laboratory and recent studies by colleagues have reported the role of *Zeb1* in maintaining stem cell activity and promoting differentiation into multiple lineages in the hematopoietic system (Almotiri et al. 2021; Wang et al. 2021b; Zhang et al. 2022a). Our laboratory used an inducible conditional mouse model (*Zeb1 Mx1*-Cre) to examine *Zeb1*-mediated regulation of somatic stem cells (Almotiri et al. 2021). Here, *Zeb1* expression was deleted in hematopoietic stem cells and their descendant cells by the administration of polyinosinic polycytidylic acid (pIpC) (Almotiri et al. 2021) that activates *Mx1*-Cre to induce *Zeb1* deletion. We demonstrated *Zeb1* was a critical, essential regulator of adult T cell maturation and differentiation and as an important transcriptional repressor required for HSC self-renewal and multi-lineage differentiation in the adult haematopoietic system (Almotiri et al. 2021). We also concluded that *Zeb1* functions as a tumour suppressor in the development of AML, as evidenced by *Zeb1* deletion causing an increase in how quickly AML develops in mouse models of AML and the lower expression of *Zeb1* in AML patients.

Wang et al., (2021) focused their study on the cooperative functions of *Zeb1* and *Zeb2* in preserving the integrity of hematopoietic lineages. In their study, they combined different conditional mouse models using *Tie2*-Cre and *Vav*-Cre. The *Tie2*-Cre system is a mouse model that is commonly used to study the role of specific genes in the vasculature. The *Tie2* promoter is active in cells of the endothelium, the inner lining of blood vessels (Kisanuki et al. 2001; Payne et al. 2018). Therefore, when the Cre recombinase is expressed in these cells, it can be used to selectively inactivate or activate genes of interest in the vasculature. The *Vav*-iCre system is commonly used for the disruption of genes in HSCs and their progeny, starting at day E11.5 (Siegemund et al. 2015). Wang et al., (2021) observed that mice engineered to be deficient in *Zeb1* (*Tie2*-Cre x *Vav*-iCre *Zeb1* KO) during embryonic haematopoiesis Zeb1 does not lead to evident embryo mortality or head haemorrhage, but it induces slightly diminished Mendelian ratios that may be related to Zeb1 loss in either hematopoietic or endothelial cells. The authors concluded that *Zeb1* is crucial for adult haematopoiesis using a double knock-out for *Zeb1* and *Zeb2*, for monocyte formation and the upkeep of ST-HSC and MPP populations. In addition, they observed that deletion of *Zeb1* affects the ability of all hematopoietic lineages to self-renew and differentiate

using both methylcellulose replating assays and competitive BM reconstitution studies in long-term reconstitution trials using an R26-Cre-ERT2; *Zeb1* *fl/fl* mutant line. The Rosa26-Cre-ERT2 mouse is generated by expressing the Cre recombinase enzyme under the control of the promoter for the Rosa26 gene (Payne et al. 2018). Notably, this promoter is active in many cell types and tissues (Irion et al. 2007). In addition, the Cre recombinase is fused to the oestrogen receptor, which allows it to be activated by the administration of the drug tamoxifen (Indra et al. 1999). This latter experiment showed some similarities with Almotiri et al., (2021), in the fact that monocyte abnormalities and a reduced ability of Zeb1-null HSPCs to regenerate are seen in mice with Zeb1 depletion. While Wang et al., (2021) study has comprehensively compared the role of *Zeb1* and *Zeb2* deficiency in mice, the use of distinct mutant lines (each of them carrying its own pitfalls) and combinatorial knockout of *Zeb1* and *Zeb2* make it difficult to interpret the haematopoietic specific effects of *Zeb1*.

Our analysis of *Zeb1* in HSCs using the *Mx1*-Cre system was limited by the fact that analysis was undertaken 14 days after gene deletion, which does not address how *Zeb1* regulates the long-term maintenance of HSCs and the haematopoietic system. In addition, in the *Mx1*-Cre system, HSC cycling may be altered by pIpC administration, similar to interferon itself (Sato et al. 2009; Velasco-Hernandez et al. 2016). Furthermore, *Mx1*-Cre mediated gene deletion occurs in a wide variety of non-haematopoietic cell types (Kühn et al. 1995; Joseph et al. 2013). The literature contains several alternatives to the Mx1-Cre model, including the *Vav*-iCre model alluded to above (Lewandoski 2001; Rossi et al. 2012; Joseph et al. 2013). Even while the *Vav*-iCre is not entirely specific to HSCs, its non-specific target tissues are far fewer than *Mx1*-Cre: namely, endothelial cells and cells in the testes(Joseph et al. 2013).

In this chapter, we therefore generated a haematopoietic stem cell specific deletion of *Zeb1* using only the *Vav*-iCre system. Our model allows tissue specific *Zeb1* function to be studied more specifically within the hematopoietic system and, in particular, permits assessment of the function of Zeb1 in the maintenance of HSCs and haematopoiesis over an extended period under normal conditions and under the stress of transplantation.

4.2 Aims

4.2.1 Aim 1: Disrupt *Zeb1* in HSCs at murine embryonic developmental stage E11.5 using Vav-iCre and determine the effect of Vav-iCre mediated *Zeb1* deletion on mouse survival.

Previous studies have shown that *Zeb1* plays critical roles in other organs, and constitutive gene targeting in mice can result in a lethal phenotype during embryonic development, thereby hindering the analysis of hematopoietic cell function (Takagi et al. 1998a). However, it remains unknown whether specific disruption of *Zeb1* in HSCs using Vav-iCre at the E11.5 stage would lead to a similar lethal phenotype and affect mouse survival. Therefore, this aim aims to investigate the effect of *Vav*-iCre mediated *Zeb1* deletion on mouse survival at E11.5, providing valuable insights into the function of *Zeb1* in mouse survival.

4.2.2 Aim 2: Assess the effect of Vav-iCre mediated *Zeb1* deletion on various cell types in the BM, SP, PB and thymus.

To achieve this aim, we will perform a detailed analysis of the bone marrow (BM), spleen (SP), peripheral blood (PB) and thymus from *Zeb1* knockout (KO) mice. Specifically, we will investigate the impact of *Zeb1* deletion on erythroid development by examining the gross appearance and overall characteristics of the BM and spleen. This analysis is crucial in providing valuable insight into the role of *Zeb1* in haematopoiesis and will contribute to our understanding of the immunophenotypic impact of *Zeb1* deletion in different cell types in the haematopoietic system.

4.2.3 Aim 3: Elucidate the transcriptional signature underlying *Zeb1*-mediated long-term maintenance of HSC function.

To further study the role of *Zeb1* in HSCs and its regulation of HSC fate, RNA-seq experiments were conducted using a mouse model. We employed the *Vav*-iCre system to disrupt *Zeb1* in murine embryonic development at stage E11.5. We aim to comprehend the transcriptional signature underlying *Zeb1*-mediated regulation of HSC function of HSC fate.

4.3 Results

4.3.1 A conditional genetic approach using the Vav-iCre system successfully disrupts *Zeb1* gene expression in HSCs at E11.5 of embryonic development.

In order to more accurately study the role of *Zeb1* in HSC maintenance, we utilised the *Zeb1*^{fl/fl} *Vav*-iCre+ mouse model. We generated the *Zeb1*^{fl/fl} *Vav*-iCre+ mouse model by first breeding *Zeb1*^{fl/fl} mice (Brabletz et al. 2017a) with *Vav*-iCre⁺ mice producing 50 % *Zeb1*^{fl/+} mice and 50 % *Zeb1*^{fl/+}; *Vav*-iCre⁺ mice. Then *Zeb1*^{fl/fl} male mice were bred with the *Zeb1*^{fl/+}; *Vav*-iCre⁺ female mice, generating 25% *Zeb1*^{fl/fl}; Vav-iCre⁺ mice (*Zeb1* KO), 25% *Zeb1*^{fl/+}; *Vav*-iCre⁺ mice and 50% of *Zeb1* genotype combinations that can be generated from this cross are *Vav*-iCre negative and can be utilised as controls (Figure 4.1 A).

In order to verify *Zeb1* deletion in *Zeb1*^{fl/fl} *Vav*-iCre+ (referred to from now on as *Zeb1*⁻/⁻ or *Zeb1* KO), we performed genotyping on *Zeb1*⁻/⁻ and control mice using genomic DNA PCR from sorted c-kit+ cells, a tyrosine kinase receptor involved in signalling on HSCs and progenitors (Okada et al. 1992). Floxed homozygous mice (*Zeb1*^{fl/fl}) amplified a 295 bp mutant *Zeb1* fragment. Normal WT mice (*Zeb1*^{+/+}), with no floxed allele inserted, amplified a 230 bp *Zeb1* fragment. In heterozygotes (*Zeb1*^{fl/+}) two fragments of DNA were amplified: a 295 bp mutant fragment and a 230 bp wild-type fragment (Brabletz et al. 2017a). In homozygous (*Zeb1*^{fl/fl}) or heterozygous (*Zeb1*^{fl/+}) floxed mice different primer sets were used to detect *Vav*-iCre positivity. In this case, *Vav*-iCre+ mice carrying amplify a 367 bp target region (Figure 4.1 B) (Brabletz et al. 2017a). In Figure 4.1 B, a representative agarose gel electrophoresis image of mouse PCR-genotyping shows the complete deletion of *Zeb1* only in c-kit+ cells in *Zeb1*⁻/⁻ mice (Figure 4.1 B). Thus, we were able to confirm that *Vav*-iCre mediated deletion of *Zeb1* from an enriched HSPC (c-kit+) population.

After 8-12 weeks, peripheral blood, bone marrow, spleen and thymus were harvested from *Zeb1*^{fl/fl} or *Zeb1*^{fl/+} *Vav*-iCre- (control) and *Zeb1*⁻/⁻ mice were harvested for further immunophenotypic and functional analysis of their haematopoietic potential (Figure 4.1 C).
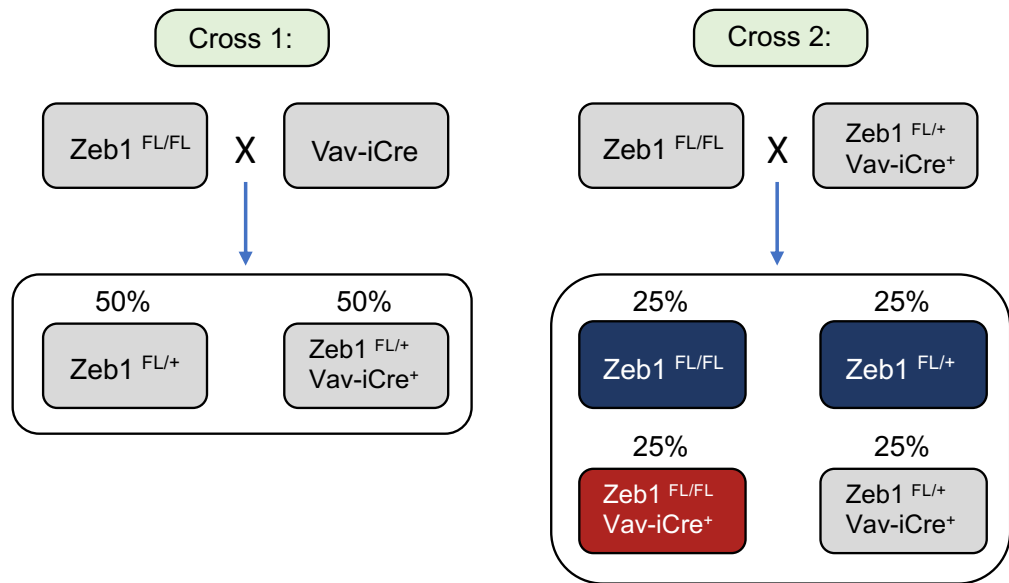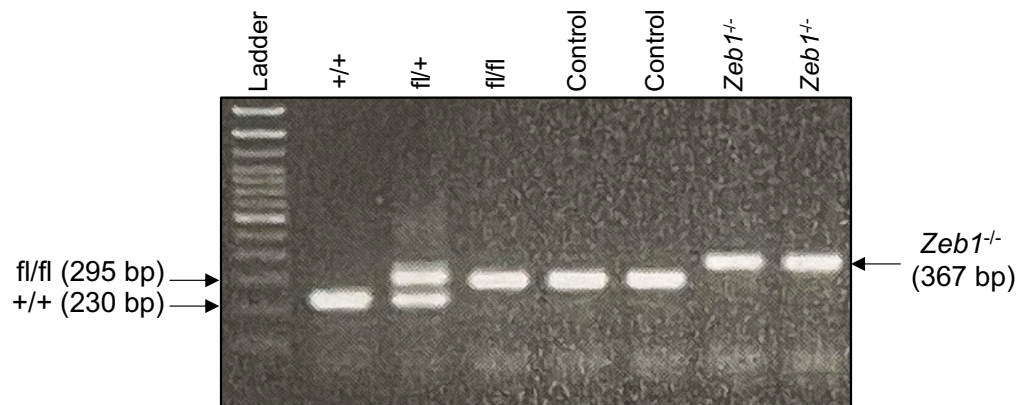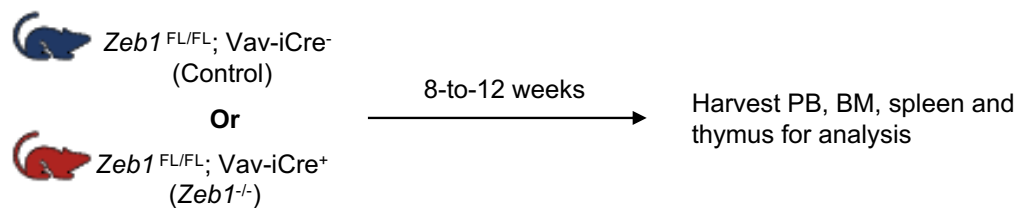
Figure 4.1 *Zeb1*^{fl/fl}; *Vav-iCre+* **mice show complete *Zeb1* deletion in HSPCs.** (A) A breeding scheme to generate Zeb1[FL/FL], *Vav*-iCre[+] and control mice. In the first cross *Zeb1*[FL/FL] mice are bred with *Vav*-iCre[+] mice producing 50 % *Zeb1*[FL/+] mice and 50 % *Zeb1*[FL/+]; *Vav*-iCre[+] mice. The *Zeb1*[FL/FL] male mice are then bred with the *Zeb1*[FL/+]; *Vav*-iCre[+] female mice generating 25 % *Zeb1*[FL/FL]; *Vav*-iCre[+] mice. The other mice from the cross can be used as experimental controls except the 25% *Zeb1*[FL/+]; *Vav*-iCre[+] mice. (B) Gel electrophoresis analysis confirms the deletion of *Zeb1* in C-Kit^{+} cells for both Control and *Zeb1*^{-/-}. (C) A scheme describes the experimental design, PB, BM, spleen and thymus from 8-to-10 weeks old *Zeb1*[f/f]; *Vav*-iCre[+] (Knockout) and *Zeb1*[f/f]; *Vav*-iCre[-] mouse (Control) were used for analysis.

4.3.2 *Vav*-iCre-mediated *Zeb1* deletion resulted in partial lethality.

Using the breeding strategy shown in Figure 4.1, we successfully generated the mouse model needed and confirmed the *Zeb1* deletion. However, we observed that some pups died before weaning and we asked if these pups were *Zeb1* KO mice. Notably, *Vav*-iCre mediated gene deletion can cause partial lethality if it disrupts a gene that is essential for the development or function in haematopoiesis (Joseph et al. 2013).

Based on the breeding strategy, we can predict the Mendelian ratio of offspring and their genotypes, which are the expected ratios of different genotypes that occur in the offspring of a cross between two parents with different genotypes. The ratio is calculated by dividing the number of offspring with a particular genotype by the total number of offspring. Table 4.1 shows that the experimental percentage of *Zeb1* KO mice after weaning is less than the expected Mendelian ratio, suggesting *Zeb1* deletion in haematopoietic stem cells during embryonic development impacts the survival of these mice.

Table 4.1 *Vav-iCre* mediated *Zeb1* deletion resulted in partial lethality.

Survival at weaning (209 mice from 14 breading cages)		
	Mutents*		Controls†
Ratio	Vav-iCre⁺;Zeb1^flox/flox	Vav-iCre⁺;Zeb1^flox/+	Vav-iCre⁻;Zeb1^flox/flox or Zeb1^flox/+
Expected‡	25%	25%	50%
Experimental§	8%	37%	54%

*Mutants include Vav-iCre+;Zeb1^flox/flox or Vav-iCre+;Zeb1^flox/+. †Controls include Vav-iCre-;Zeb1^flox/flox and Vav-iCre-;Zeb1^flox/+.
‡Expected indicates the expected Mendelian genetic ratio of genotypes. §Experimental indicates genotypes from surviving animals.

Like their control littermates, *Zeb1* KO mice that survived as neonates showed normal development, activity, and behaviour from birth through weaning and puberty to adulthood (data not shown). The body weight gain, however, was smaller in *Zeb1*-Vav iCre mice, and these mice were weaker and presented with skin manifestations (data not shown). These findings indicate that the loss of Zeb*1* in haematopoietic cells has no direct impact on behavioural development but rather on physiological parameters.

4.3.3 *Vav*-iCre mediated *Zeb1* deletion causes hypochromic normocytic anaemia

To examine *Zeb1's* impact on the hematopoietic system's immune cell properties., the peripheral blood of 8–12-week-old *Zeb1* KO and control mice were collected, and a complete blood count (CBC) was performed. A variety of indices were assessed, including white blood cells (WBCs), haemoglobin concentration (HGB), mean corpuscular volume (MCV), hematocrit (HCT), platelets (PLT), and erythrocyte number (RBC).

A statistically insignificant reduction was noted in WBCs with an approximate 1.3-fold change from *Zeb1* KO mice compared to *Zeb1* controls with MCV and PLT counts unchanged. Notably, *Zeb1* KO mice had lower RBC, HGB, and HCT with approximate fold changes of 2, 2.2, and 2.1, respectively, indicating an impairment in erythropoiesis in the context of *Zeb1* deficiency (Figure 4.2 A-F). Red blood cells (RBCs) in circulation are typically red in colour (normochromic, observable via HGB) and have the same size (normocytic, observable by the MCV) (O'Connell et al. 2015). In this case, we observed that the *Vav*-iCre-mediated *Zeb1* deletion causes a reduction in total red blood cell count (via the haematocrit) and a change in the colour of RBCs (via HGB), termed hypochromic. In particular, haemoglobin, a pigment that gives RBCs its distinctive red colour, significantly decreased. In the case of our hypochromic normocytic anaemia mouse model, acanthocytes were observed in peripheral blood smears (Figure 4.2 G). Acanthocytes, also referred to as spur cells, are erythrocytes with surface irregularities with spikes on the outside that can be observed in hypochromic normocytic anaemia (Redman et al. 1989; Lanzkowsky 2016; Baeza et al. 2019; Peikert et al. 2022). A lower-than-normal haematocrit is also indicative of anaemia(BRILL and BAUMGARDNER 2000; Raabe et al. 2011). Thus, our results are consistent with conditional *Zeb1* deletion in haematopoietic stem cells causing anaemia. (Figure 4.2 A–F).
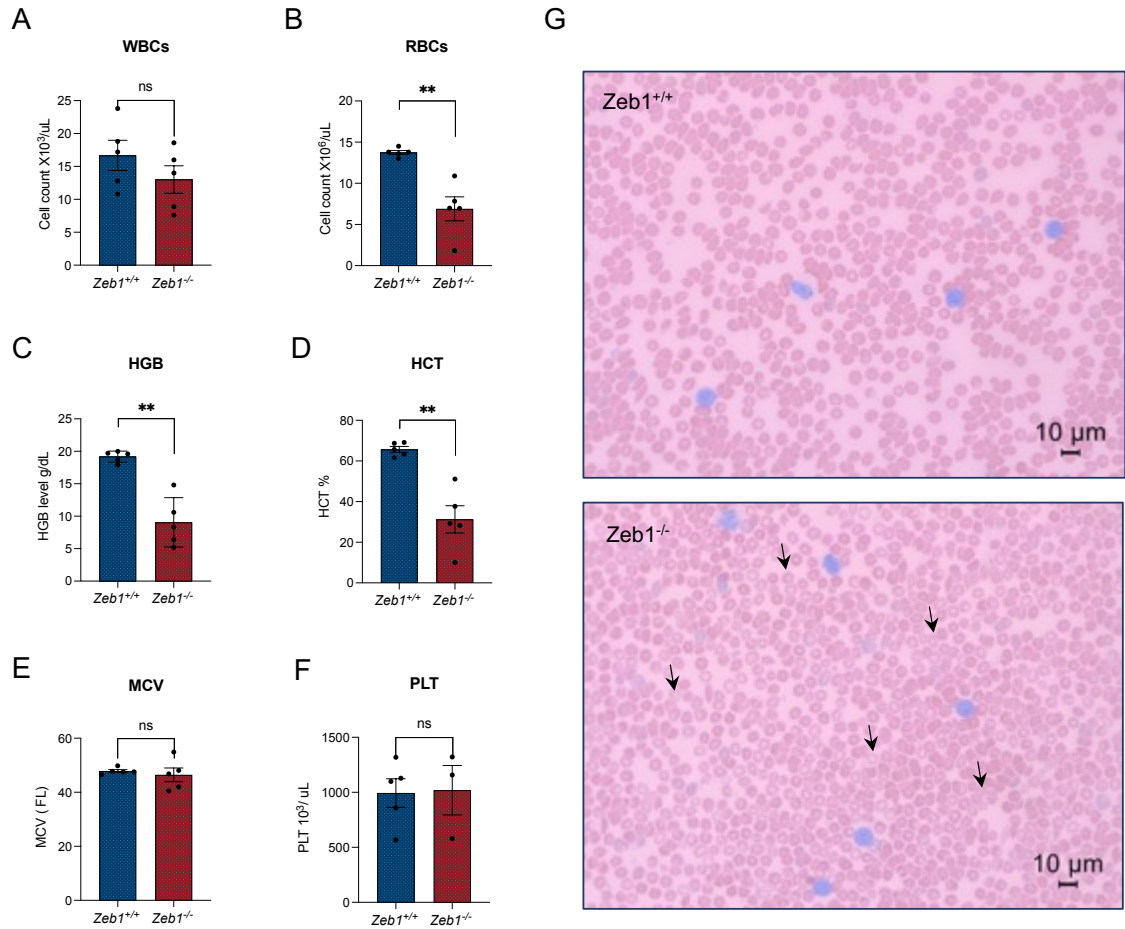
Figure 4.2 *Vav*-iCre mediated *Zeb1* deletion causes hypochromic normocytic anaemia. CBC analysis has been performed for both control and *Zeb1*-/- (KO) 8-to-10 weeks old mice, WBCs count (A), RBCs count (B), haemoglobin level (C), haematocrit % (D), MCV (E), platelets (F) and Peripheral blood smear image for the control and the Zeb1 KO, black arrows indicate of acanthocytes (G). N= 5 in each genotype. Error bars display the mean and SEM. Whitney U test was used to determine statistical significance in the following manner: *P < .05, **P < .01, ***P < .001, ****P <0.0001

90

4.3.4 Vav-iCre-mediated *Zeb1* deletion leads to a reduction in the bone marrow and spleen cellularity

The observed reduction in red blood cell (RBC) count, haemoglobin (HGB), and haematocrit (HCT) in *Zeb1* knockout (KO) mice suggests a potential impairment in erythropoiesis. The bone marrow (BM) and spleen are crucial sites for erythropoiesis, with the BM being the primary site for adult erythropoiesis, while the spleen can serve as a compensatory site in response to stress or injury (Chen et al. 2021). Therefore, the analysis of BM and spleen could provide valuable insight into the impact of *Zeb1* deletion on erythroid development. Initially, we examined the gross appearance and overall characteristics of BM and spleen from *Zeb1* KO mice.

The bones of *Zeb1* KO mice were brittle (unpublished observation), and bones (Figure 4.8 A) and BM cells in suspension (Figure 4.3 B) were also observed to be less red in hue in mice lacking *Zeb1*. Further, overall BM cellularity was significantly reduced in *Zeb1* KO mice with an approximate 1.2-fold change (Figure 4.3 C).

Macroscopic examination of the spleen was also carried out, with a recording of pathological changes in 8–12-week-old mice in *Zeb1* KO mice compared to controls. The spleen of *Zeb1* KO mice was noticeably smaller, paler, more rigid, hypocellular and weighed with an approximate 1.7-fold change less than those of control mice (Figure 4.3 D, E, F). The spleen was also sectioned, fixed and processed for microscopic examination by H&E staining which revealed that the architecture of the spleens from *Zeb1* KO mice was significantly altered; notably, the white pulp was significantly altered, and the red pulp appeared to be absent (Figure 4.3 G). Overall, these findings support the idea that mice lacking *Zeb1* have an increased propensity to develop anaemia.
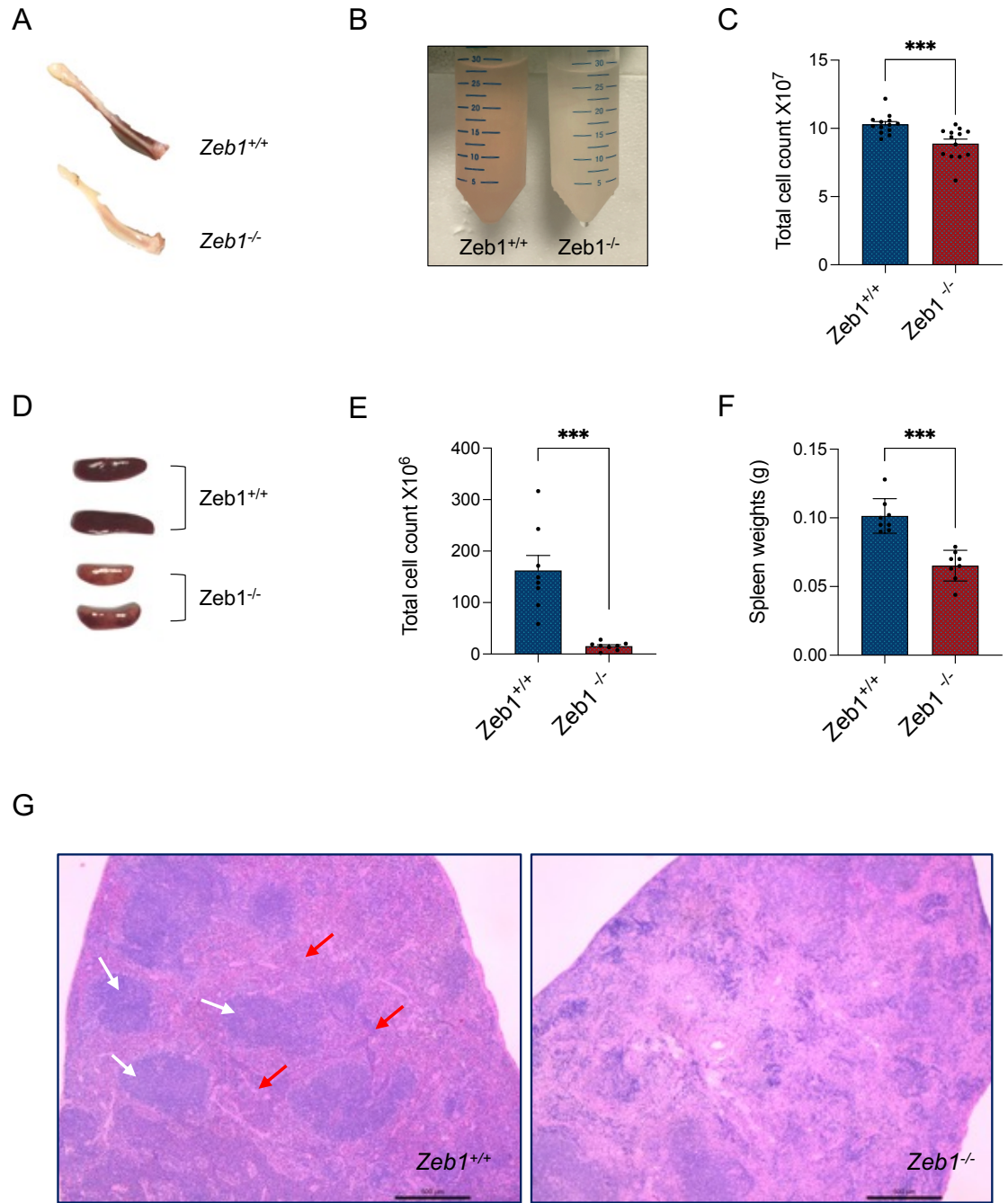
Figure 4.3 *Vav*-iCre mediated *Zeb1* deletion causes decrease in BM cellularity and a dramatic decrease in spleen cellularity and weight and spleen atrophy. Image of mouse tibia (A), Picture showing representative BM cell suspension (B), Total BM cellularity(C), Spleen size (D), Total spleen cellularity(E), and weight (F). Spleen tissue section stained by H&E staining, white arrow for white pulp and a red arrow for red pulp(G). BM n=13 and SP n=8 in each genotype. Error bars display the mean and SEM. Whitney U test was used to determine statistical significance in the following manner: *P < .05, **P < .01, ***P < .001, ****P <0.00.

4.3.5 *Vav*-iCre-mediated *Zeb1* deletion causes a reduction of erythroid cell development

The observed low haemoglobin count (RBCs) in *Zeb1*$^{-/-}$ mice can be associated with conditions that cause the body to generate few red blood cells. This can occur if, for example, there is decreased production of erythrocytes or increased destruction of red blood cells faster than they are being produced (O'Connell et al. 2015). Therefore, in order to understand the origin of this defect in *Zeb1*$^{-/-}$ mice, we carried out further analysis in erythroid compartments by using Ter119 and CD71 markers in flow cytometry(Koulnis et al. 2011a). In *Zeb1*$^{-/-}$ mice, we observed a significant reduction in the frequency of the pan-erythroid marker Ter119 in BM with an approximate 1.4-fold change and a trend toward a reduction in the frequency of SP (Figure 4.4 B, C), and a significant reduction of absolute numbers of Ter119+ cells in both SP and BM (Figure 4.4 B, C).

Adult bone marrow or spleen co-stained with CD71 and Ter119 allows for the discrimination of developmental subgroups of developing erythrocytes (Koulnis et al. 2011a). We therefore further categorised erythroid cells into three different subgroups were identified based on the expression of CD71 and TER119: proerythroblasts (CD71-positive, TER119-negative or low), early-erythroblasts (CD71-positive, TER119-positive), and late-erythroblasts (CD71-negative, TER119-positive) (Koulnis et al. 2011b; Chao et al. 2015; Shim et al. 2020). We noticed a substantial decline in the frequency of in the frequency of early (CD71+, Ter119+) and late (CD71-, Ter119+) erythroblasts and a non-statistically significant reduction in the frequency of proerythroblasts (CD71+, Ter119-/low) (Figure 4.4 D) from the BM of *Zeb1*$^{-/-}$ mice. We also observed a non-statistically significant reduction in the frequency of proerythroblasts in SP and early- and late- erythroblasts in SP of *Zeb1*$^{-/-}$ mice (Figure 4.4 F). Overall, the overall cellularity of pro-, early-, and late-erythroblasts was shown to have significantly decreased in both SP with approximate fold changes of 5.8, 8.2 and 6.7, respectively and BM with approximate fold changes of 1.5, 1.5 and 8.4, respectively in *Zeb1*$^{-/-}$ mice (Figure 4.4 E, G). These data indicate a hitherto unrecognized requirement for *Zeb1* in erythroid maturation.
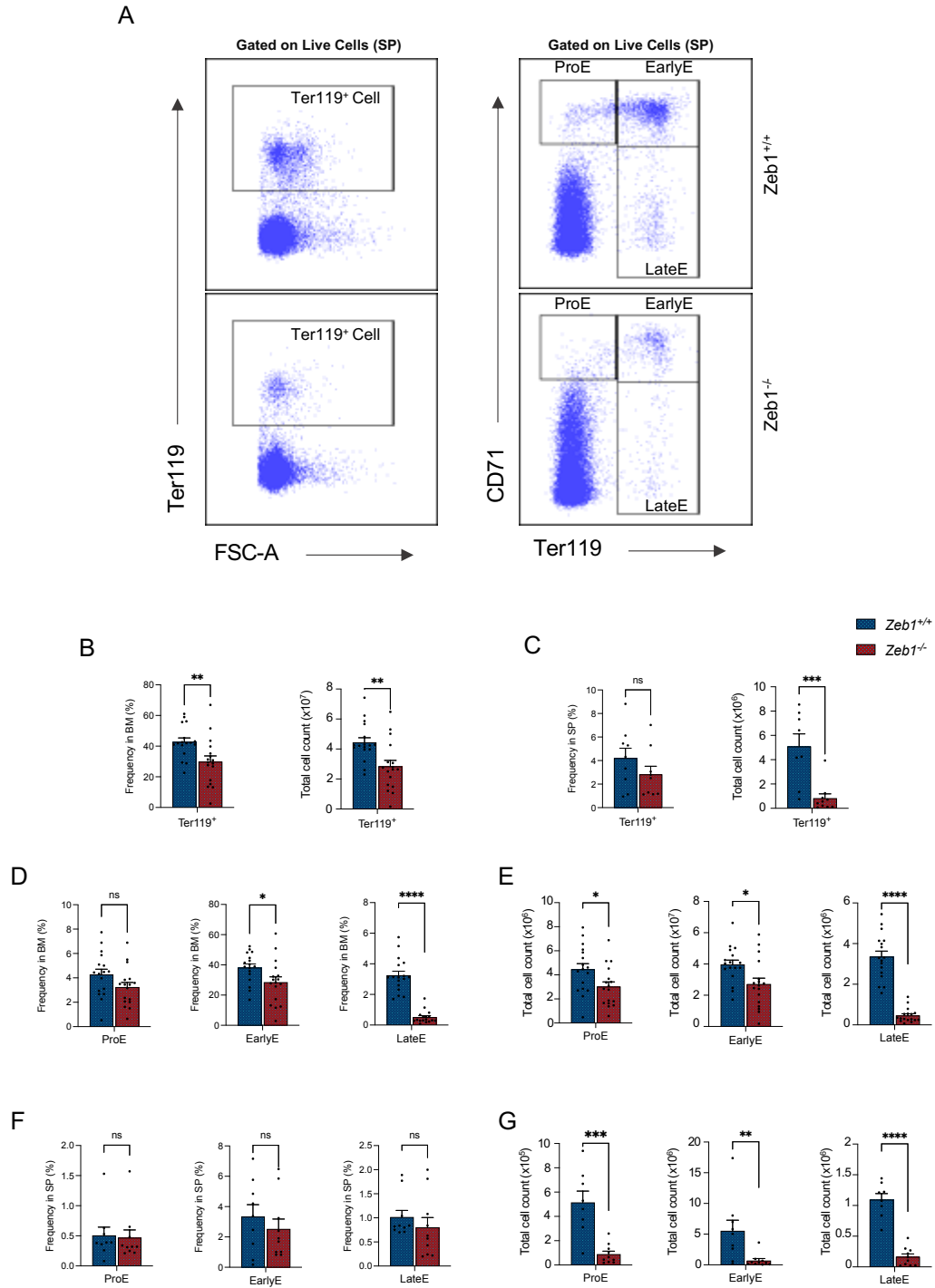
Figure 4.4 *Vav*-iCre mediated *Zeb1* deletion causes a reduction in maturing erythroid cells. SP and MB tissues were collected from 8-to-12 weeks old mice for both control and *Zeb1*$^{-/-}$ (KO). Representative FACS plots of SP analysis of erythroid cells (Ter119+) gated from DAPI negative cells (live cells in SP) and Early-E denotes early erythroblasts (CD71+ Ter119+); Late-E denotes late erythroblasts (CD71- Ter119+); Pro-E denotes proerythroblasts (CD71+ Ter119 -/low).(A), the same gating strategy was used to analyse the BM. The frequencies and the total cell count of erythroid cells (Ter119+) in BM (B) and in SP (C). The frequencies and the total cell count of Pro-E indicate proerythroblasts (CD71+ Ter119 -/low); Early-E, early-erythroblasts (CD71+ Ter119+); Late-E, late erythroblasts (CD71- Ter119+) in BM (D,E) and in SP (F,G). BM n=17 and SP N=10 in each genotype. Error bars display the mean and SEM. Whitney U test was used to determine statistical significance in the following manner: *P < .05, **P < .01, ***P < .001, ****P <0.00.

4.3.6 *Vav*-iCre-mediated *Zeb1* deletion causes a reduction in Gr1-Mac1+ cells in PB and SP.

Having observed variable WBC counts in the peripheral blood (PB) of *Zeb1 KO* mice, we next conducted a more detailed immunophenotypic analysis of the myeloid lineage to assess Mac1+ Gr1- cells (monocytes, macrophages, and granulocyte precursors, immature myeloid cells) (Lagasse and Weissman 1996; Sunderkötter et al. 2004) and Mac1+ Gr1+ (myeloid cells and granulocytes, mature myeloid cells) (Lagasse and Weissman 1996; Sunderkötter et al. 2004) in PB, bone marrow (BM), and spleen (SP) tissues. This analysis uncovered a reduction in Mac1+ cell frequency in PB with an approximate 2.4-fold change (Figure 4.5 A, B) and SP (Figure 4.5E), and a reduction in absolute numbers of Mac1+ Gr1- cellularity in the SP of *Zeb1$^{-/-}$* mice (Figure 4.5 F) but no alterations were observed in BM of *Zeb1$^{-/-}$* mice (Figure 4.5 C-D). Also, we saw a substantial drop in frequency and cellularity of Mac1+ Gr1+ cells in SP of *Zeb1$^{-/-}$* mice with an approximate 2.7-fold change (Figure 4.5 F) without significant alterations in PB or BM (Figure 4.5 B, D). These data indicate that *Zeb1* regulates select mature myeloid lineages in the PB and SP.
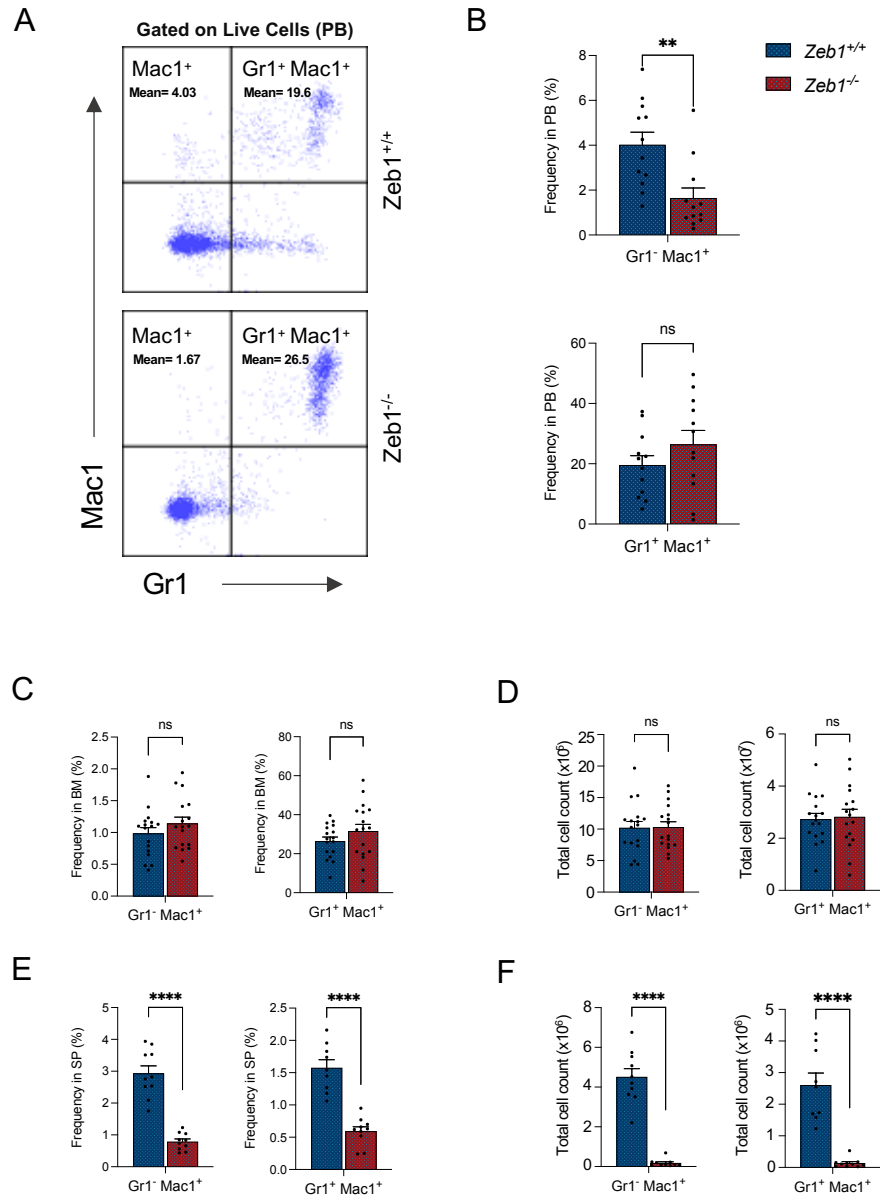
Figure 4.5 *Vav*-iCre mediated *Zeb1* deletion causes a reduction in Gr1- Mac1+ cells in PB and SP. PB was collected from 8-to-12 weeks old mice for both control and *Zeb1⁻/⁻* (KO). Representative FACS plots of PB analysis of myeloid cells gated from DAPI negative cells (live cells) (A). The same gating strategy was used to analyse the myeloid cells in BM (C,D) and Myeloid cells in SP (E,F). (B) The frequencies of myeloid (Gr1- Mac1+ and Gr1+ Mac1+) in PB. (C) The frequencies of myeloid (Gr1- Mac1+ and Gr1+ Mac1+) in BM (C), and total cell count results of myeloid (Gr1- Mac1+ and Gr1+ Mac1+) in BM (D). The frequencies of myeloid (Gr1- Mac1+ and Gr1+ Mac1+) in SP (E), and total cell count results of myeloid (Gr1- Mac1+ and Gr1+ Mac1+) in BM (F). BM n=17, SP N=10 and PB n= 11 in each genotype. Error bars display the mean and SEM. Whitney U test was used to determine statistical significance in the following manner: *P < .05, **P < .01, ***P < .001, ****P <0.00.

4.3.7 *Vav*-iCre-mediated *Zeb1* deletion impacts on committed myeloid progenitors.

Having observed the defects in both mature myeloid and erythroid cells, we further investigated the role of *Zeb1* in committed myeloid progenitors. Multipotent common myeloid progenitor (CMP) cells are produced from multip-potent progenitors (MPPs). Megakaryocyte-erythrocyte progenitor (MEP), which gives rise to erythrocytes and platelets, can then grow from CMP., or granulocyte-monocyte progenitor (GMP) cells, which generate granulocytes or monocytes (Akashi et al. 2000). To distinguish between three classes of committed myeloid progenitors, we used flow cytometric labelling as follows—common myeloid progenitor (CMP) (CD34+ CD16/32-), granulocyte-monocyte progenitor (GMP)(CD34 + CD16/32 +), and megakaryocytic-erythroid progenitor (MEP) (CD34-CD16/32-) cells (Akashi et al. 2000).

The proportions of CMPs and GMPs in *Zeb1* KO mice were reduced in comparison to those in the control animals, while they remained similar for MEPs (Figure 4.11 B). The absolute cellular quantities of CMPs, GMPs, and MEPs were all decreased in *Zeb1* KO mice (Figure 4.6 B). These results demonstrate that *Zeb1* is required for the development of adult myeloid progenitor CMP, GMP and MEP cells in BM, and suggest an origin for the myeloid and erythroid defect observed in *Zeb1* KO mice.

A

Gated on Lin- Cells

Gated on LK
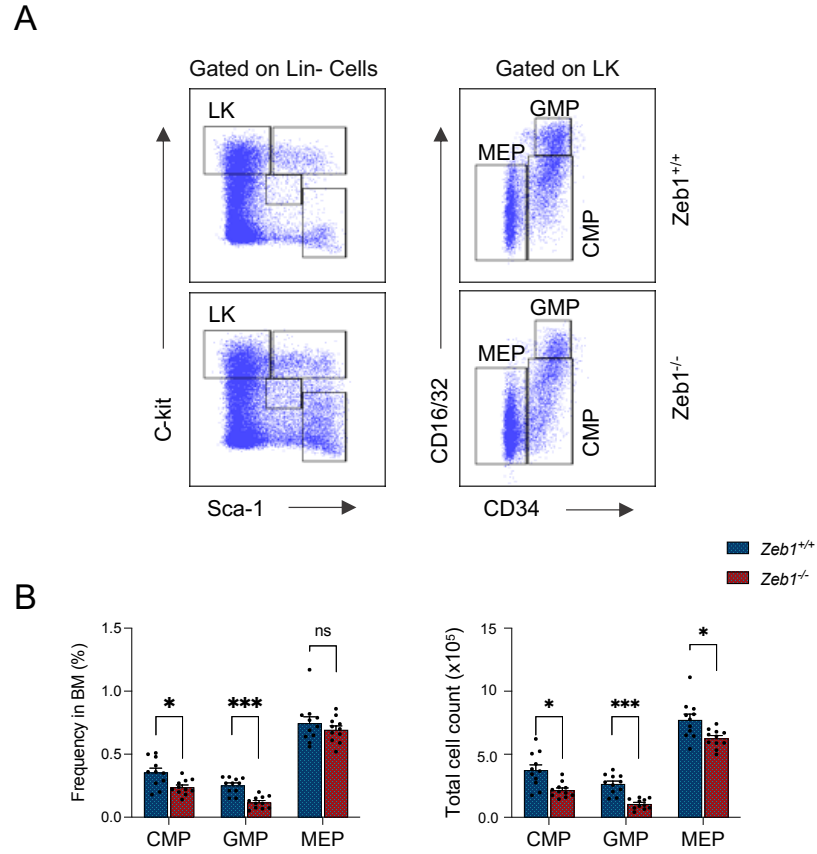
Figure 4.6 *Vav*-**iCre mediated** *Zeb1* **deletion causes defects in lineage-restricted progenitors in the BM.** (A) Representative FACS plots and gating strategy of committed progenitors: CMP, GMP and MEP analysis of 8-12 old mice from control (*Zeb1*$^{+/+}$) and *Zeb1*$^{-/-}$. (B) significant reduction in frequency and total cellularity of CMP (LK CD34+ CD16/32-), GMP (LK CD34+ CD16/32+) and MEP (LK CD34+ CD16/32+). N=11 in each genotype Error bars display the mean and SEM. Whitney U test was used to determine statistical significance in the following manner: *P < .05, **P < .01, ***P < .001, ****P <0.00.

4.3.8 *Vav*-iCre-mediated *Zeb1* deletion does not impact myelo-erythroid progenitors.

We next used the haematopoietic hierarchy devised by Pronk et al to examine early progenitors restricted to the myeloid, erythroid, and megakaryocytic lineages further (Pronk et al. 2007). In this paradigm of haematopoietic differentiation, several subsets of myeloid progenitors with limited lineage potential can be identified, including at the incipient stages of lineage-restriction to the granulocyte/macrophage, erythroid, and megakaryocytic lineages respectively, by comparing the cell-surface expression of Slamf1, endoglin (Eng/CD105), and integrin alpha 2b (Itga2b/CD41). Within the LK myeloid progenitor compartment, six resolvable cell populations can be identified (Pronk et al. 2007). These unique populations are Pre-MegE, Pre CFU-E, CFU-E, MkP, Pre GM, and GMP as shown in Figure 4.7A.

We found no differences in the frequency and total cell count for all subsets analysed (Pre GM, Pre MegE, Pre CFU-E, GMP and MkP) (Figure 4.7 B). This suggests that *Zeb1* does not have a specific role in early restriction to myelo-erythroid progenitors and that myeloid and erythroid defects observed in *Zeb1* KO mice are independent of these progenitor subsets.
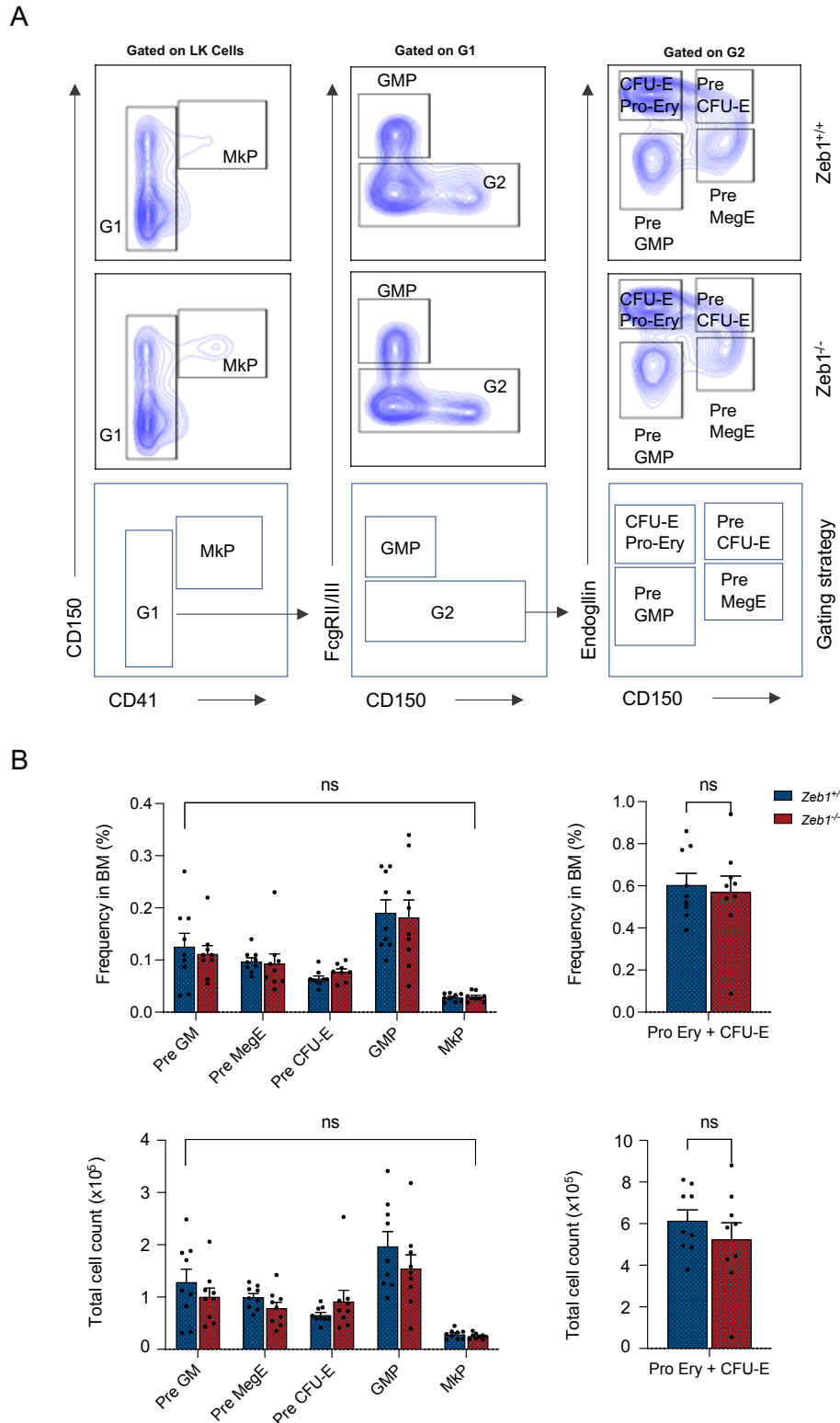
Figure 4.7 *Vav*-iCre mediated *Zeb1* deletion causes no defects in early myeloid precursors. (A) Representative FACS plots and gating strategy of Pre-GM and GMP (Myeloid), Pre-MegE and Pre-CFU-E (Erythroid), Pre-MegE and MkP (Megakaryocyte progenitors). The results show no differences between Zeb1 KO and control (B). N=9 in each genotype. Error bars show mean ± SEM. Mann-Whitney U test was used to calculate significance as follows: *P < .05, **P < .01, ***P < .001, ****P <0.0001.

4.3.9 *Vav*-iCre-mediated *Zeb1* deletion causes a decrease in T-cells, NK cells, NKT cells and an expansion of B-cells.

Given the known role of *Zeb1* in lymphopoiesis, and in particular in T-cells (Takagi et al. 1998a; Wang et al. 2009; Guan et al. 2018a; Zhang et al. 2020) (See Chapter 5), we next conducted flow cytometric analysis for lymphoid lineage-specific haematopoietic cells - CD4, CD8 (T-cells), B220 (B cells), NK1.1 CD3-ve (NK cells), and NK1.1 CD3+ve (NK T cells) - in the PB, BM, and SP in control and $Zeb1^{-/-}$ mice.

We observed a decrease in CD4, CD8, NK1.1, and NKT frequency in SP with approximate fold changes of 182, 467, 41 and 9, respectively, BM with approximate fold changes of 2.4, 16, 2 and 6.4, respectively, and PB with approximate fold changes of 107, 140, 8 and 0.3, respectively of $Zeb1^{-/-}$ mice (Figure 4.8 A, B, and D). CD4, CD8, NK1.1, and NKT significantly decrease in cellularity in SP and BM of $Zeb1^{-/-}$ mice. (Figure 4.8 C, E). In striking contrast, there is an expansion in B-cell frequency in PB (Figure 4.8 A, first column), BM (Figure 4.8 B, first column), and SP (Figure 4.8 D, first column) of $Zeb1^{-/-}$ mice, while we observe a non-significant tendency of B cells to increase in cellularity in the BM (Figure 4.8 C, first column) and a significant reduction in B cells cellularity in SP of $Zeb1^{-/-}$ mice (Figure 4.8 E, first column).
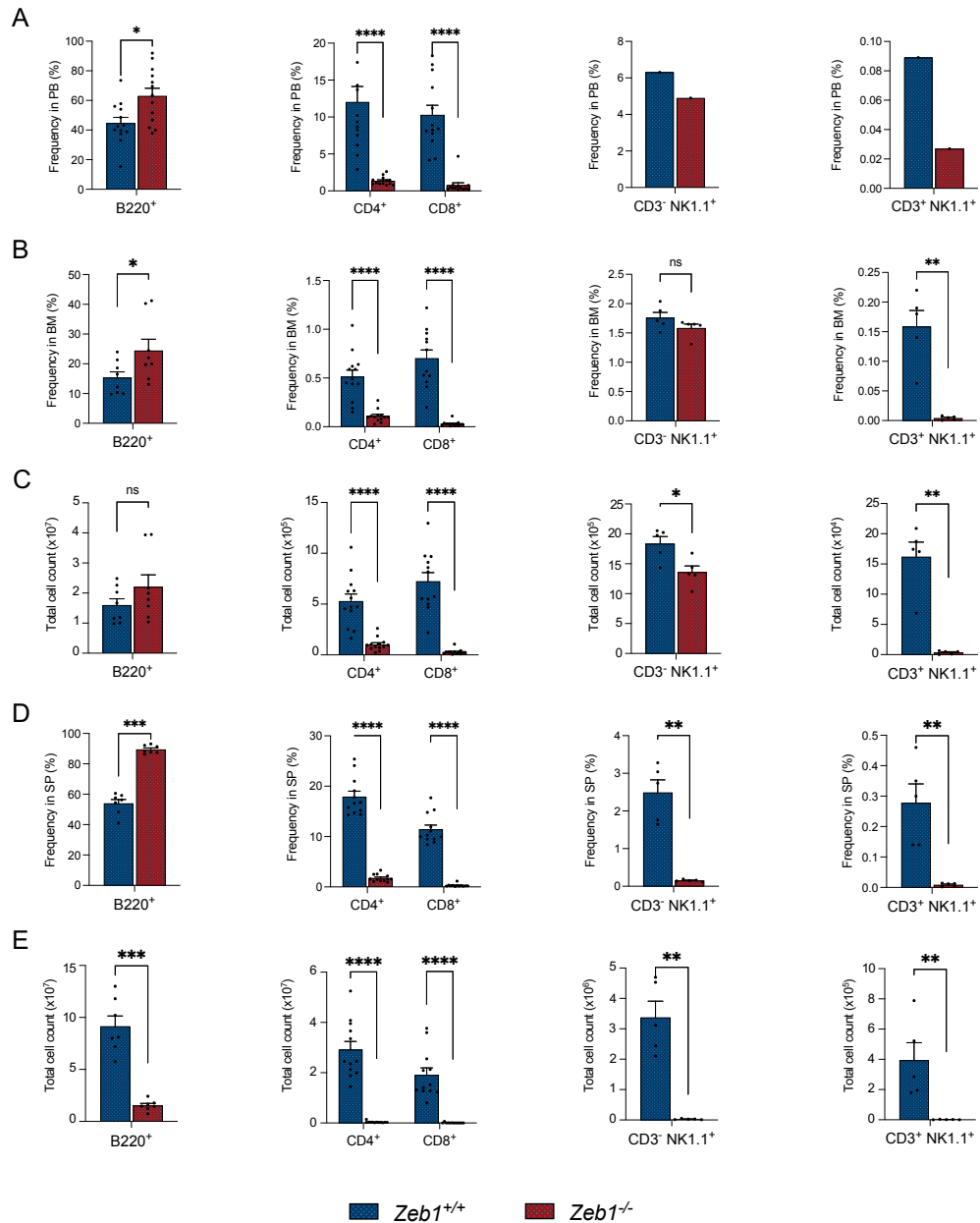
Figure 4.8 *Vav*-iCre mediated *Zeb1* deletion causes depletion of T cells and increases B cells frequencies in PB, MB and SP. The frequency results of B220+, CD4+, CD8+, CD3-NK1.1+ and CD3+ NK1.1+ in PB (A), in BM (B) and in SP (D). The total cell count results of B220+, CD4+, CD8+, CD3- NK1.1+ and CD3+ NK1.1+ in BM (C) and SP (E). BM n=13, SP n=12 and PB n=13 in each genotype. Error bars display the mean and SEM. Whitney U test was used to determine statistical significance in the following manner: *P < .05, **P < .01, ***P < .001, ****P <0.00.

4.3.10 *Vav*-iCre-mediated *Zeb1* deletion impairs B-cell differentiation.

To investigate the differentiation specific mechanism of expanded B-lymphopoiesis in *Zeb1* KO mice, It was determined how pre-pro-B, pro-B, pre-B, and immature B-cells were distributed in the bone marrow. B220 expression shows common lymphoid progenitors' commitment to the B-cell lineage, which is followed by differentiation into pre-pro-B, pro-B, and pre-B cells during B-lymphopoiesis, and eventually immature B-cells (Patton et al. 2014; Michael N. Hall 2018). Following their final phases of maturation in secondary lymphoid organs, like the spleen, these immature B-cells exit the bone marrow to mature into fully differentiated plasma cells that produce antibodies. Upon activation by antigen presentation, these plasma cells migrate back to and colonise the bone marrow (Hardy et al. 1991; Li et al. 1996; Osmond et al. 1998; Ogawa et al. 2000; Nagasawa 2006).

In *Zeb1* KO mice or their control counterparts, within B220+cells, we measured early B-cell precursors (IgM−CD43+), which were sub-divided into pre–pro-B (CD19−BP1−), pro-B (CD19+BP1−) and early pre-B cells (CD19+BP1+) cells (Figure 4A, B). Late pre-B cells (IgM−CD43−), and immature B cells (IgM+CD43−) were distinguished based on CD19+ expression (Figure 4A, B).

Analysis of the early precursor IgM-CD43+ cell compartment revealed, as shown in Fig. 4.9 C-D, that the percentage and total cell number of Pre-pro-B cells showed a significant reduction in the bone marrow of $Zeb1^{-/-}$ mice with an approximate 2.7-fold change, suggesting *Zeb1* regulates pre-pro-B-cell development in BM. In striking contrast, the frequency and total cell number of pre-B cells were significantly increased in the BM of $Zeb1^{-/-}$ mice with an approximate 1.7-fold change (Figure 4.9 E–F). Immature B cells, however, were unimpaired in $Zeb1^{-/-}$ mice (Figure 4.9 G–H). These data indicate that *Zeb1* selectively regulates the Prepro B and Pre-B stages of B-cell development in the BM.
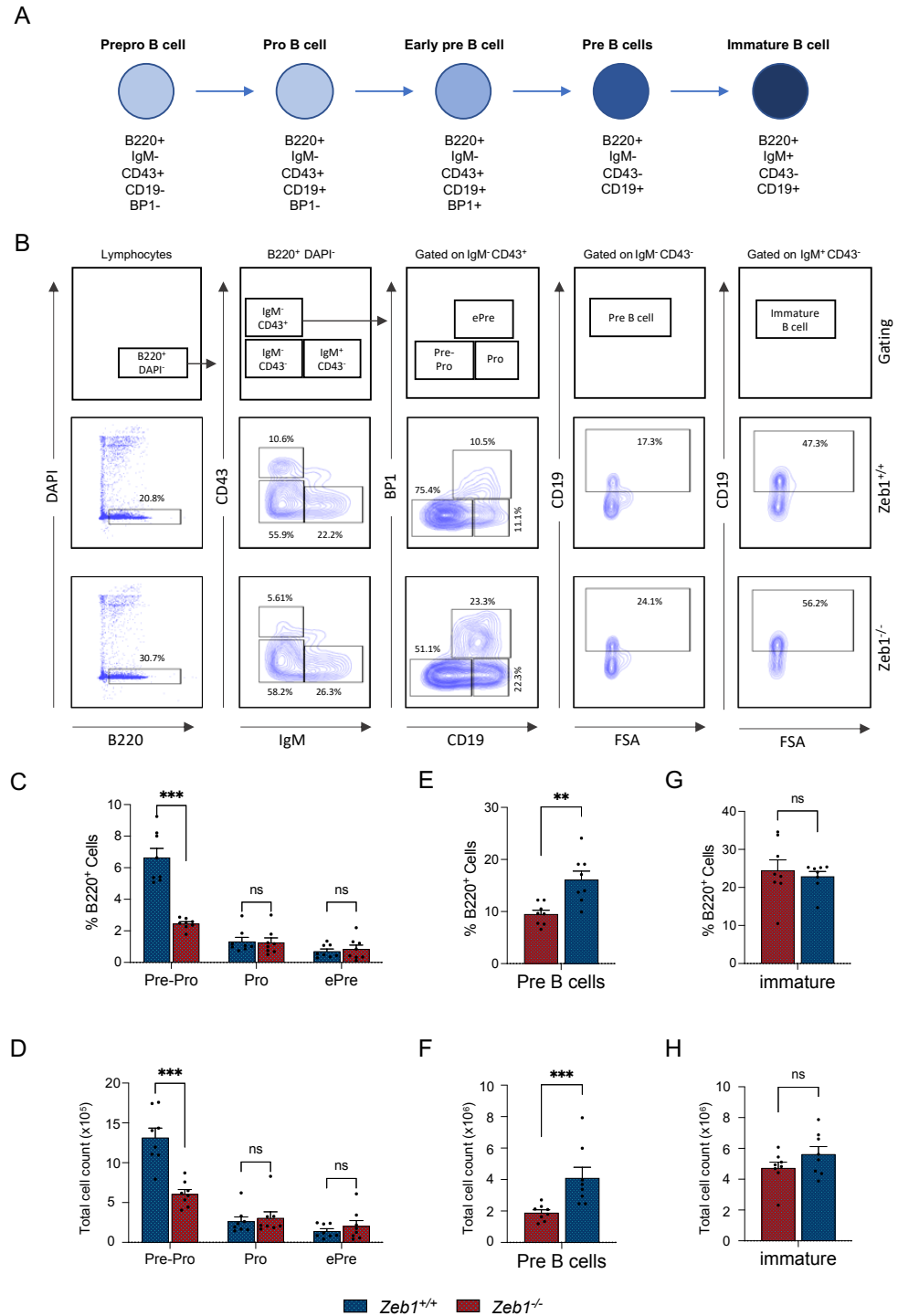
Figure 4.9 *Vav*-iCre mediated *Zeb1* deletion causes a decrease in Prepro B cells and an increase of pre-B cells frequency and cellularity in BM. (A) Representative FACS plots and gating strategy, bone marrow from WT (*Zeb1*+/+), and KO (*Zeb1*-/-) mice were examined by flow cytometry to examine live B cells (DAP- B220+), then early precursors (IgM- CD43+), late pro- and pre-B cells (IgM-CD43-), and immature and mature B cells (IgM+ CD43-). The IgM- CD43+ population was then divided into pre–pro-B (CD19- BP1-), pro-B (CD19+ BP1-), and early pre-B cells (CD19+ BP1+) cells. Then the Pre B cells (IgM-CD43- CD19+) and immature B cells (IgM+ CD43- CD19+) (A,B). The result shows a significant reduction in pre-pro B cells (B220+ IgM-CD43+ CD19- BP1-) and an increase in the Pre B cells (C,D), and no change was observed in the Pro, ePre and immature B cells. N=8 in each genotype. Error bars show mean ± SEM. Mann-Whitney U test was used to calculate significance as follows: *P < .05, **P < .01, ***P < .001, ****P <0.0001

As B-cells mature in the spleen, we next investigated whether impaired B-cell development was also observed in the spleen of *Zeb1*$^{-/-}$ mice.–There was a statistically significant decrease in the frequency at Pre-pro B cell stages in the spleen of *Zeb1*$^{-/-}$ mice with an approximate 13-fold change, mirroring results from the BM (Figure 4.9). Similarly, no defects were seen in Pro and e-Pre fractions in the spleen of *Zeb1*$^{-/-}$ mice (Figure 4.10 A). Akin to what was observed in the BM (Figure 4.9), in the spleen of *Zeb1*$^{-/-}$ mice the proportion of pre-B cells was dramatically increased with an approximate 2.4-fold change. However, in striking contrast to BM, immature B-cells from the spleen of *Zeb1*$^{-/-}$ mice were noticeably decreased with an approximate 1.4-fold change. Altogether, the increase of the Pre-B cells in both SP and BM suggests a specific role of *Zeb1* in Pre-proB and pre-B cell proliferation. The spleen data point to an additional role for *Zeb1* in the maturation of immature B-cells.

A
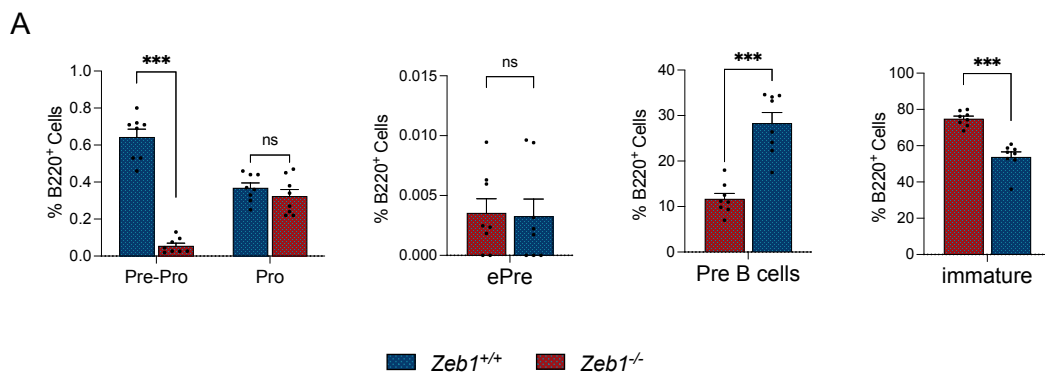
Figure 4.10 *Vav*-iCre mediated *Zeb1* deletion causes an increase of pre-B cells frequency and cellularity in SP. The result shows a significant reduction in the frequency of pre-pro B cells (B220+ IgM- CD43+ CD19- BP1-), increase in the Pre-B cells and reduction in immature B cells (B). No changes found in ePre and Pre-B cells (B). N=8 in each genotype. Error bars show mean ± SEM. Mann-Whitney U test was used to calculate significance as follows: *P < .05, **P < .01, ***P < .001, ****P <0.0001.

4.3.11 *Vav*-iCre-mediated *Zeb1* deletion impact on committed lymphoid progenitors in BM.

Given the broad impact of *Zeb1* on B-cells, T-cells and innate lymphoid cells in *Zeb1*$^{-/-}$ mice, we next assessed (i) subsets of early lymphoid committed populations, as assessed by evaluation of lymphoid-primed multipotent progenitors (LMPPs), (ii) progenitor commitment exclusively to the lymphoid lineage, as assessed by the common lymphoid progenitor (CLP) and (iii) progenitor commitment exclusively to NK cells and innate lymphoid cells (ILCs). It is believed LMPPs, which have limited self-renewal potential and both myeloid and lymphoid potential, give rise to CLPs (Adolfsson et al. 2005). Cytotoxic NK cells and ILCs are members of the innate lymphocyte family (Diefenbach et al. 2014; Artis and Spits 2015). The three subsets of cytokine-producing ILCs— group 1 (ILC1), group 2 (ILC2), and group 3 (ILC3)— share a similar precursor that expresses Id2 and is known as CHILP (common progenitor to all helper-like ILCs) (Klose et al. 2014). In our analysis, we also distinguished between the CD127- and CD127+ subsets of LMPPs which are referred to as LMPP-s and LMPP+s, respectively (Ghaedi et al. 2016) . LMPP-s have been found to differentiate more into NK cells and ILCs, whereas LMPP+s give rise to T cells and B cells (Ghaedi et al. 2016). CLPs (Figure 4.11 B), conventional LMPPs (Figure 4.11 D), LMPP+s (Figure 4.11 E), and LMPP-s (Figure 4.11 F) frequency and total cell count were all decreased in *Zeb1* KO mice. In marked contrast, the frequency and cell count of ILC2Ps were increased in *Zeb1* Vav-iCre mice, suggesting a potential mechanism for the reduction in NK cells and ILC production in *Zeb1* KO mice through the reduction of LMPP-s, an accumulation of ILC2Ps and a block in further differentiation of ILC2Ps to innate lymphoid cells (Figure 4.11 C).
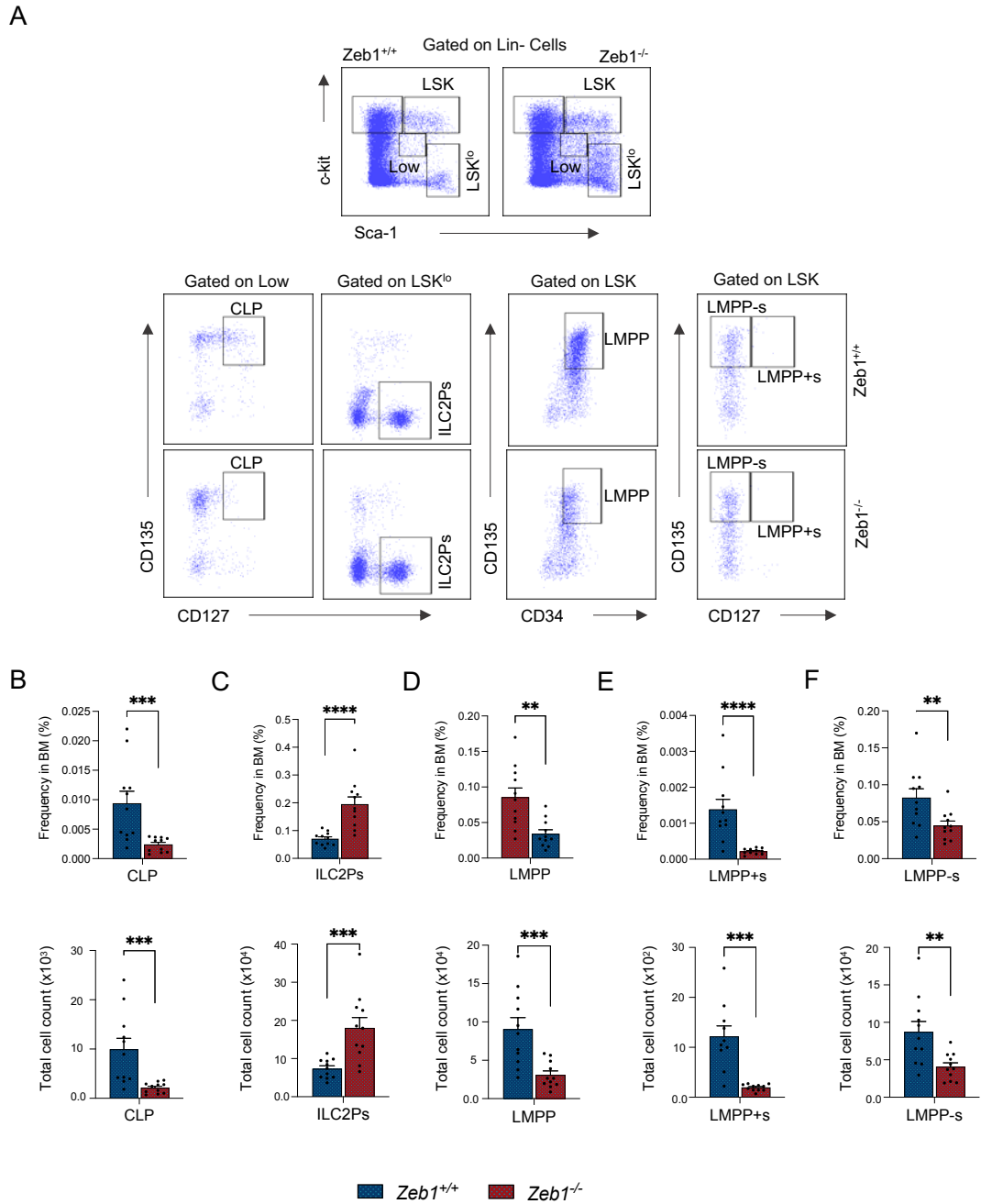
Figure 4.11 *Vav*-iCre mediated *Zeb1* deletion causes defects in lymphoid lineage-restricted progenitors in the BM. (A) Representative FACS plots and gating strategy of committed progenitors: CLP, LMPPs and ILC2Ps analysis of 8-12 old mice from control (*Zeb1*^{+/+}) and *Zeb1*^{-/-}. (B) significant reduction in CLP (c-kitlo sca-1lo CD135+ CD127+). (C) Increase in ILC2Ps (c-kitlo/- sca-1hi CD135- CD127+). (D) Significant reduction in conventional LMPP (c-kit+ sca-1+ CD135+ CD127+). (E, F) significant reduction in LMPP-s (LSK+ Flt3hi CD127-) and LMPP+s (LSK+ Flt3hi CD127+). N=11 in each genotype. Error bars display the mean and SEM. Whitney U test was used to determine statistical significance in the following manner: *P < .05, **P < .01, ***P < .001, ****P <0.00.

4.3.12 Vav-iCre-mediated *Zeb1* deletion causes an expansion of the frequency of HSCs and a reduction in lymphoid committed HSPCs in BM.

Given the multi-lineage haematopoietic differentiation defect in *Zeb1*^{-/-} mice under steady state conditions, we next asked whether this defect originated in HSCs/HSPCs, which are the common origin for all haematopoietic lineages. By immunophenotyping, we therefore analysed HSPC numbers in the BM of *Zeb1*^{-/-} mice and control mice at eight to ten weeks old.

We found that the frequency and cellularity of HSC enriched Lin-Kit+ Sca-1+ (LSK) cells (Yang et al. 2005) in the BM of *Zeb1*^{-/-} mice was comparable to that of control mice (Figure 4.9 B). The bone marrow (BM) population of Lin-Kit+ Sca-1- cells (LK) directly precedes the development of committed myeloid cells (Akashi et al. 2000). Contrary to what was observed in the LSK compartment, a significant reduction in LK frequency and cellularity was found in *Zeb1*^{-/-} mice (Figure 4.12 C). These data suggest that *Zeb1* directly regulates lineage commitment to the myeloid lineage.

Further enrichment for HSCs and multipotent progenitors (MPPs) within the LSK fraction is enabled by the SLAM markers CD150 and CD48 (Bryder et al., 2006). The two SLAM family markers, CD150 (Slamf1) and CD48 (Slamf2) subdivide the adult mouse bone marrow LSK cells into functionally-distinct fractions of cells: one that contains HSCs (LSK CD150+ CD48-) that give rise to MPPs (LSK CD150- CD48-), which in turn divide to two restricted hematopoietic progenitor subsets (HPCs; CD150- CD48+ (HPC1), and LSK CD150+ CD48+ (HPC2) (Oguro et al. 2013).

We found an increase in HSC frequency with an approximate 1.5-fold change. (Figure 4.12 D) but no differences in total cellularity in *Zeb1*^{-/-} mice (Figure 4.12 E). A reduction in the frequency with an approximate 1.34-fold change and absolute cell count was found for the HPC1, which is a lymphoid biased progenitor subset (Oguro et al. 2013; Mooney et al. 2017) (Figure 4.12 D, E) yet no alterations were found in MPP or HPC2 in *Zeb1*^{-/-} mice (Figure 4.12 D, E).

These data suggest that *Zeb1* directly regulates lineage commitment to the lymphoid cell compartment from MPPs.
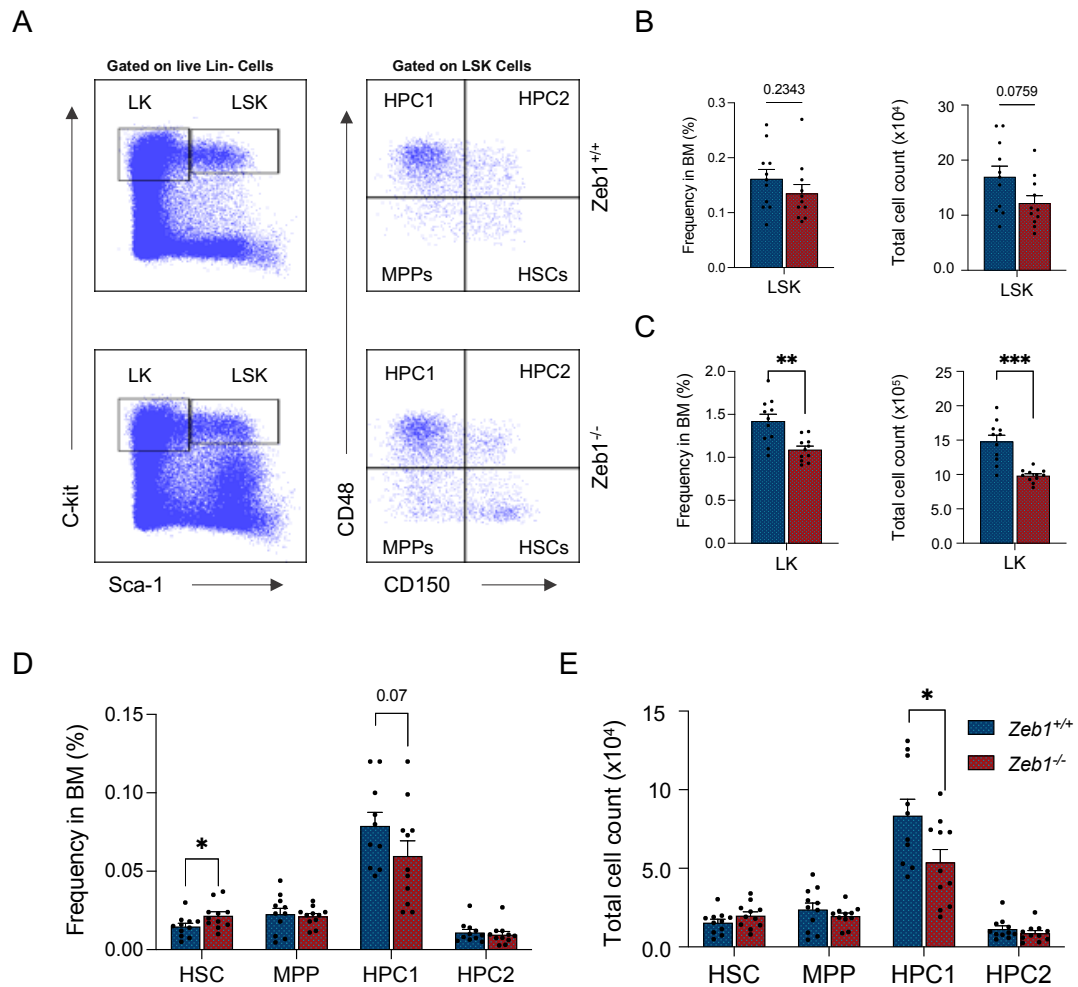
Figure 4.12 *Vav*-iCre mediated *Zeb1* deletion causes expansion in HSC frequency and reduction in BM lymphoid restricted progenitors. (A) Representative immunophenotypic analysis and gating strategy of control (*Zeb1*^+/+^) and Zeb1^-/-^ hematopoietic stem and progenitor populations. (B,C) slight decrease of HSPCs (defined as lineage- cKit+ Sca1+ [LKS]) and a significant decrease in the LK+ Cells (defined as lineage- cKit+ Sca1- [LK]). (D,E) Increase in frequency of HSC (LKS+ CD48- CD150+) and a slight increase in total cellularity in the *Zeb1*^-/-^ compared with control BM, a significant decrease in total cellularity of the restricted progenitors HPC1 (CD150− CD48+ LSK) and no defect observed in the MPP (LKS+ CD48- CD150-) and the restricted progenitors HPC2 (CD150+ CD48+ LSK). N=11 in each genotype. Error bars display the mean and SEM. Whitney U test was used to determine statistical significance in the following manner: *P < .05, **P < .01, ***P < .001, ****P <0.00.

4.3.13 *Vav*-iCre-mediated *Zeb1* deletion causes alterations in the frequency of lineage biased HSCs and loss of lymphoid committed progenitors.

We used an independent hierarchical model that separates myeloid- and lymphoid-biased progenitors to resolve heterogeneity observed within the MPP compartment. Based on a stepwise increase in CD34, CD48, and CD135 expression as well as a loss of CD150 expression, MPPs have been immunophenotypically classified into the MPP1, MPP2, MPP3, and MPP4 populations (Wilson et al. 2008; Cabezas-Wallscheid et al. 2014). We observed that there were no significant changes in most MPP populations, except for MPP4, which is a lymphoid biased progenitor subset that significantly overlaps with LMPP (Wilson et al. 2008; Cabezas-Wallscheid et al. 2014) (Figure 4.13 B, C). The frequency and total cell count of MPP4 were decreased in *Zeb1*$^{-/-}$ mice with an approximate 2.4-fold change. (Figure 4.13 B, C).

We next analysed the lineage-biased HSC composition of *Zeb1*$^{-/-}$ mice (Beerman et al. 2010; Challen et al. 2010; Dykstra et al. 2011) which are classified into three types: CD150hi (myeloid biased), CD150int (balanced), and CD150lo (lymphoid biased) HSCs (Beerman et al. 2010; Morita et al. 2010; Young et al. 2016). As shown previously, we observed an increase in the entire frequency of HSCs in the BM (Figure 4.13 B). This appears to be accounted for by no change in frequency of the CD150hi (myeloid) population, a decrease in the frequency of the CD150int (balanced) population and an increase in the CD150lo (lymphoid biased) population with approximate fold changes of 1.27, and 1.28, respectively (Figure 4.13 D) in *Zeb1*$^{-/-}$ mice. Therefore, *Zeb1* deletion seems to primarily affect lymphoid-primed MPP cells (MPP4) perhaps due to an accumulation and block in differentiation of lymphoid biased HSCs in the BM.
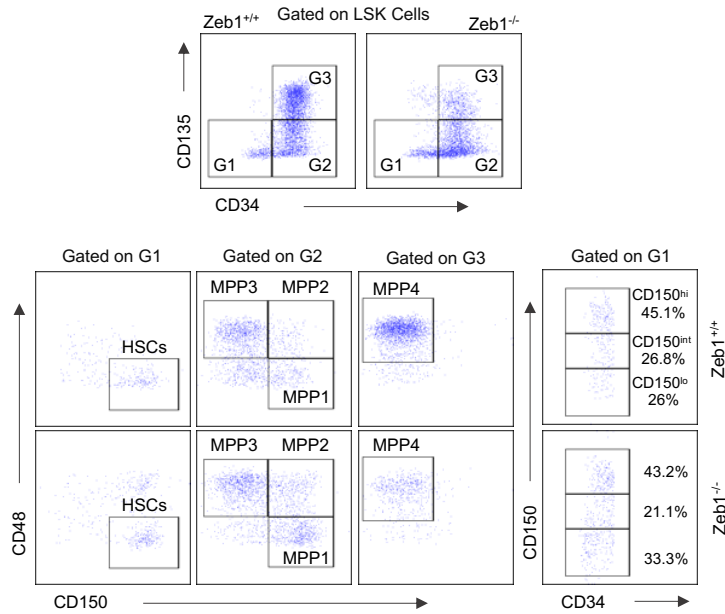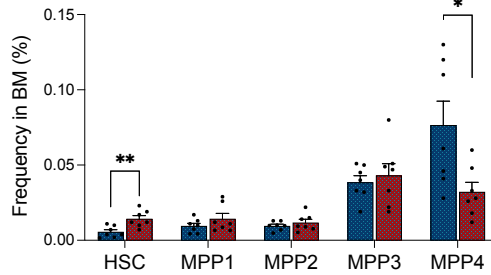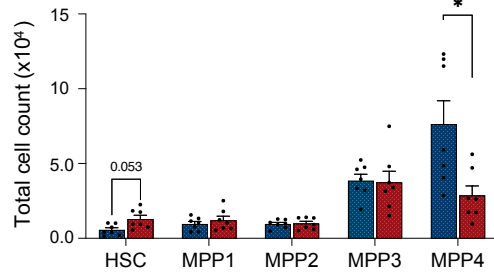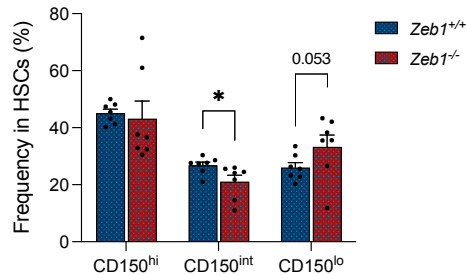
Figure 4.13 *Vav*-iCre mediated *Zeb1* deletion causes alterations in the frequency of lineage biased HSCs and loss of lymphoid committed progenitors. (A) Representative immunophenotypic analysis and gating strategy of control (*Zeb1*^{+/+}) and Zeb1^{-/-} hematopoietic stem and progenitor populations HSC, MPP1, MPP2, MPP3, MPP4 and CD150hi (LSK CD135- CD34- CD150hi) myeloid biased, CD150int (LSK CD135- CD34- CD150int) balanced and CD150lo/- (LSK CD135- CD34- CD150lo/-) lymphoid biased. (B,C) Increase in frequency of HSC (LKS+ CD135- CD34- CD48- CD150+) and trend increase in total cellularity in the *Zeb1*^{-/-} compared with control BM, no defect observed on MPP1 (LKS+ CD135- CD34+ CD48- CD150+), MPP2 (LKS+ CD135- CD34+ CD48+ CD150+), MPP3 (LKS+ CD135- CD34+ CD48+ CD150), ,but a significant decrease in frequency and total cellularity of the MPP4 (LKS+ CD135+ CD34+ CD48+ CD150-). (D) The frequency within HSCs (LSK+ CD135- CD34-), no change in CD150hi (myeloid biased), reduction in CD150int (balanced) and trend increase in CD150lo/- (lymphoid biased. N=7 in each genotype. Error bars show mean ±s SEM. Mann- Whitney U test was used to calculate significance as follows: *P < .05, **P < .01, ***P < .001, ****P <0.00.

111

4.3.14 *Vav*-iCre-mediated *Zeb1* deletion impairs the generation of lymphoid progenitors from HSCs.

We next employed CD34 and CD135 to independently determine whether the accumulation of lymphoid biased HSCs and the associated reduction in lymphoid committed progenitors may result from a differentiation block in *Zeb1* KO mice. There was a significant increase in the frequency of CD34- cells in *Zeb1* KO mice, while the opposite was observed for CD34+ (Figure 4.14 C). The same pattern was observed for CD135- and CD135+ (Figure 4.14 E). In both cases, as expected, the MFI of CD34 showed a decreasing trend (Figure 4.14, D) and FLT3 (Figure 4.14, F) exhibited statistically significant decreases in *Zeb1* KO mice. Notably, CD34- and CD135- both mark LT-HSC function (Cell 1996; Osawa et al. 1996; Adolfsson et al. 2005; Volpe et al. 2015; Sumide et al. 2018), and the increase in both these populations in *Zeb1* KO mice is consistent with the expanded HSC population observed in *Zeb1* KO mice using CD150 and CD48 (Figure 4.13B and 4.13C). Conversely, the decreased expression of CD34+ and CD135+, which marks differentiation to the lymphoid compartment within the LSK pool (Cell 1996; Adolfsson et al. 2005; Volpe et al. 2015), is consistent with block in lymphoid commitment to LMPP found in *Zeb1* KO mice. Consistent with an increase in HSC frequency, CD150- frequency decreases and CD150+ increases for *Zeb1 KO* mice with approximate fold changes of 1.2 and 1.7, respectively (Figure 4.14G). This is correlated to the MFI observed for CD150 in LSK in *Zeb1 Vav*-iCre mice, where there is a significant increase in expression of CD150 (Figure 4.14 H). In contrast, no significant changes were observed in either the frequency of CD48 and CD127 or the MFI for CD48 (Figures 4.14 I-L) between *Zeb1 Vav*-iCre mice and controls. Together, these data suggest that *Zeb1* negatively regulates the differentiation of CD34-, CD135- and CD150+ HSCs into its downstream lymphoid progenitors.
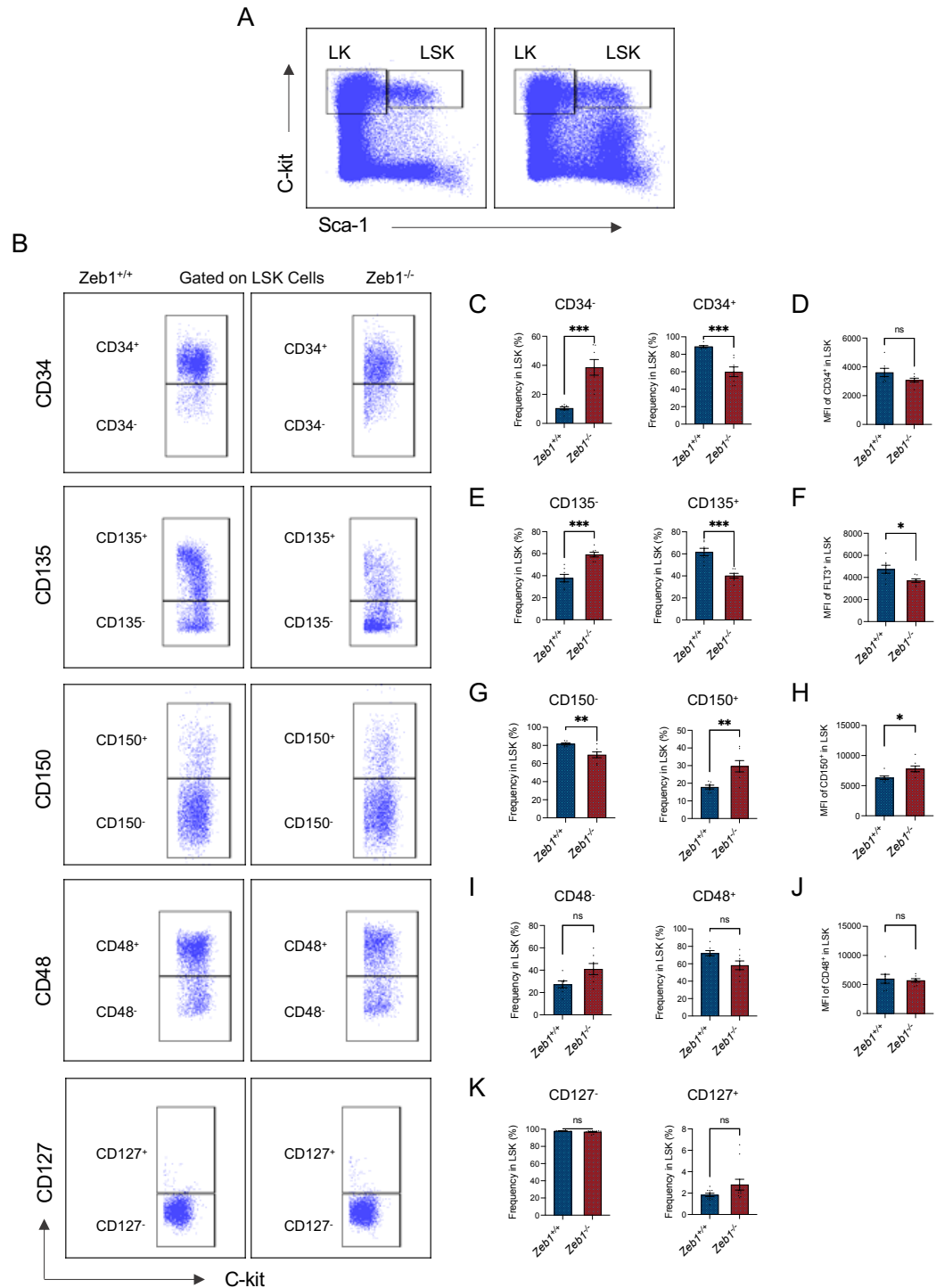
Figure 4.14 *Vav*-iCre mediated *Zeb1* deletion causes alterations in the frequency of lineage biased HSCs and loss of lymphoid committed progenitors. (A) Representative FACS plots of LSK compartment of the bone marrow of the 8-12 weeks old Zeb1 KO and control mice. (B) The LSK cells were further analysed for surface expression of CD34, CD135 (FLT3), CD150, CD48 and CD127. The result shows, an increase in CD34-, CD135- and cd150+ frequency in LSK cells (C,E,G), and decrease in CD34+, CD135+ and cd150- frequency in LSK cells (C,E,G), no differences observed in CD48+, CD48-, CD127+ and CD127- frequency in LSK (I,K). The MFI analysis of CD34, CD135 (FLT3), CD150, CD48 and CD127 in LSK cells using flow cytometry, the results shows a decrease of the MFI of CD34 and CD135 (FLT3) and increase in MFI of CD150 in LSK (D,F,H) and no change found in the MFI of CD48 and CD127 (J,L). N=7 in each genotype. Error bars display the mean and SEM. Whitney U test was used to determine statistical significance in the following manner: *P < .05, **P < .01, ***P < .001, ****P <0.00.

4.3.15 *Vav*-iCre-mediated *Zeb1* deletion causes no defect in HSPCs survival.

Apart from the apparent block in differentiation of HSCs to committed lymphoid progenitors in *Zeb1^-/-* mice, we next sought to examine alternative mechanisms of HSC expansion and HSPC loss in *Zeb1^-/-* mice. We therefore performed Annexin V staining of the BM cells from control and *Zeb1^-/-* mice to assess cell survival of HSCs/HSPCs. There was no significant change in Annexin V+ in LSK and LK cells after the deletion of Zeb (Figure 4.15 B). Total apoptosis was also no different between the HSC, MPP, HPC1 and HPC2 groups in *Zeb−/−* mice (Figure 4.15 C). These results show that *Zeb1* is not essential for the survival of HSCs and HSPCs.
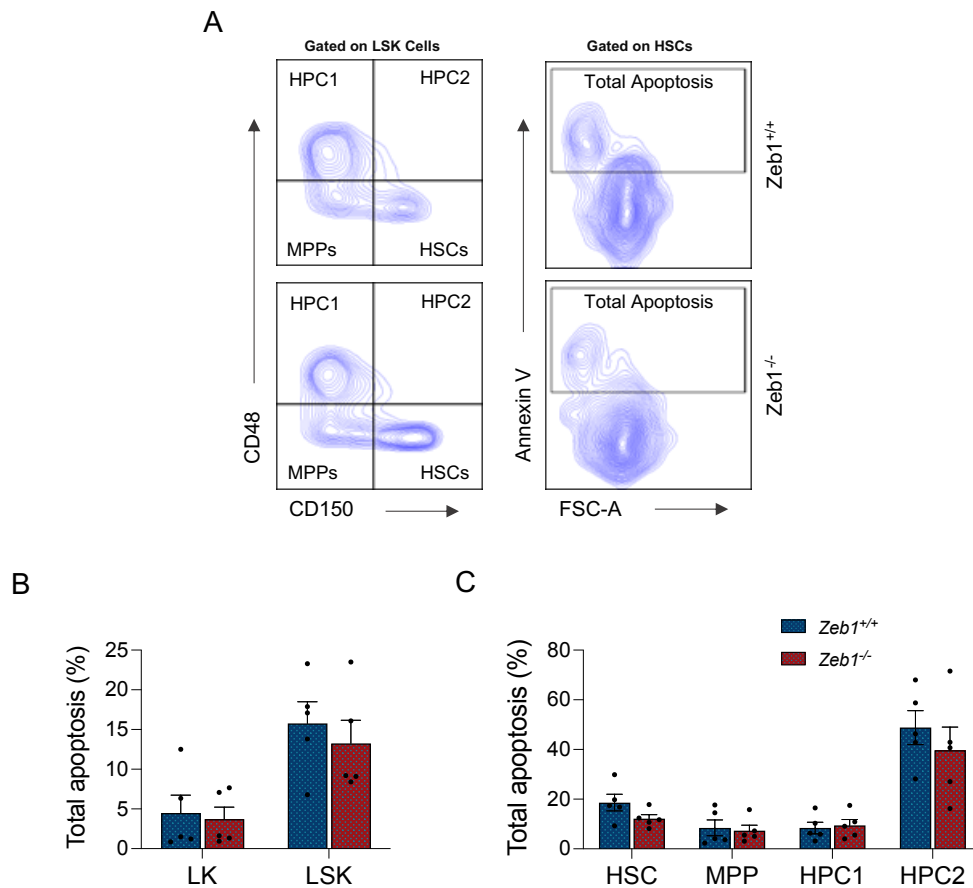
Figure 4.15 *Vav*-iCre mediated *Zeb1* deletion causes no defects in the survival of HSPCs. (A) Representative FACS plots of apoptosis analysis using Annexin V in HSPCs of 8-12 old mice from control (*Zeb1^+/+*) and *Zeb1^-/-* . The results of total apoptosis show no differences in LK (comprises committed progenitors) and LSK (HSPCs) between Zeb1 KO and control (B). (C) The total apoptosis was analysed in HSC, MPP, HPC1 and HPC2 and the results show no difference between Zeb1 KO and control. N=5 in each genotype. Error bars show mean ± SEM. Mann-Whitney U test was used to calculate significance as follows: *P < .05, **P < .01, ***P < .001, ****P <0.0001.

4.3.16 *Vav*-iCre-mediated *Zeb1* deletion does not alter HSC and HSPC quiescence/proliferation.

As another mechanism regulating HSPC behaviour, the proliferation of *Zeb−/−* HSCs and HSPCs was investigated using Ki67 staining. In LSK cells, *Zeb1* depletion did not cause a loss of quiescence as evidenced by the comparable frequency of cells in G0, G1 and S-G2-M stages in both *Zeb1$^{-/-}$* mice and control mice (Figure 4.16 B). Thus, *Zeb1* is not required to preserve HSC, MPP, HPC1 and HPC2 quiescence or proliferation (Figure 4.16 C).
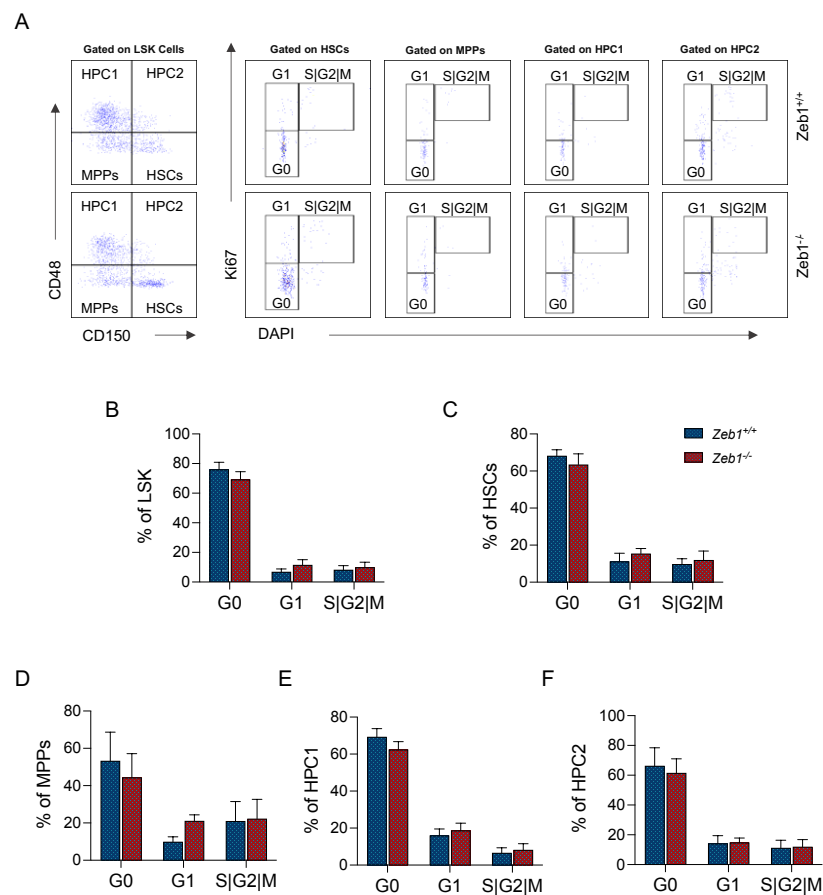
Figure 4.16 *Vav*-iCre mediated *Zeb1* deletion causes no defects in cell cycling of HSPCs. (A) Representative FACS plots of cell cycle analysis using Ki67 in HSPCs of 8-12 old mice from control (*Zeb1$^{+/+}$*) and *Zeb1$^{-/-}$*. The results of G0 (Ki67- DAPI-), G1 (Ki67+ DAPI-), S|G2|M (Ki67+ DAPI+) in LSK and its compartments HSC, MPPs, HPC1 and HPC2 shows no differences between Zeb1 KO and control (B-F). N=4 in each genotype. Error bars show mean ± SEM. Mann-Whitney U test was used to calculate significance as follows: *P < .05, **P < .01, ***P < .001, ****P <0.0001.

4.3.17 *Vav*-iCre-mediated *Zeb1* deletion causes depletion in HSPCs in the spleen.

Given that the HSC frequency was expanded in the BM and the significant reduction of the total cell count of the spleen, we asked whether Vav-iCre mediated *Zeb1* deletion would affect extramedullary HSPC numbers. The immunophenotypic results mirror the hypocellular spleen and a significant reduction in the total cells of the LSK (Lin-Sca-1+ c-Kit+) (Figure 4.17, A). In contrast to the expansion of HSC frequency of $Zeb1^{-/-}$ mice, the preliminary analysis of the spleen of $Zeb1^{-/-}$ mice shows depletion of HSC, MPP, HPC1 and HPC2 (Figure 4.17, B). Similar results of cell depletion were observed in the LK (Lin- c-Kit+ Sca-1-) cells, which directly precede the development of myeloid cells. Within the LK compartment, the results show a significant reduction in the total cellularity of the common myeloid progenitor (CMP) (CD34+ CD16/32-) with an approximate 16-fold change, granulocyte-monocyte progenitor (GMP)(CD34 + CD16/32 +), and megakaryocytic-erythroid progenitor (MEP) (CD34-CD16/32-) in the spleen of $Zeb1^{-/-}$ mice. Furthermore, splenic depletion of CLPs (c-kit^{lo} sca-1^{lo} CD135+ CD127+) and conventional LMPPs (c-kit^{+} Sca-1^{+} CD135+ CD127+) cells was observed in $Zeb1^{-/-}$ mice (Figure 4.17, C).
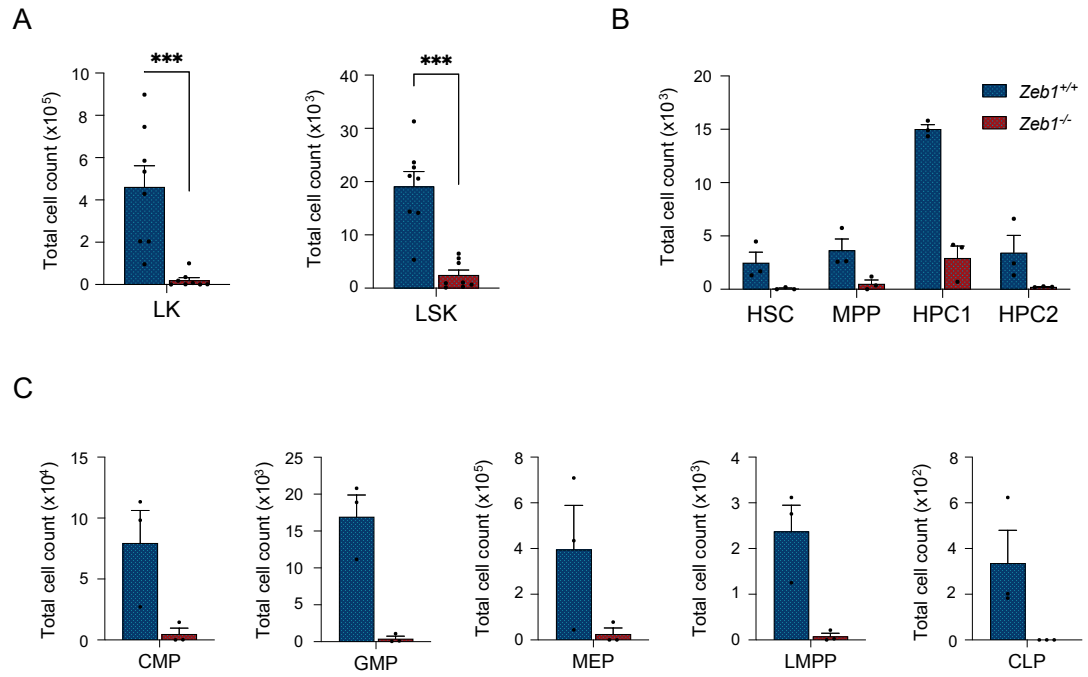
Figure 4.17 *Vav-iCre* mediated *Zeb1* deletion causes a reduction of HSPCs and committed myeloid and lymphoid progenitors in the spleen. (A) the results show a significant reduction in the total cell count of LK and LSK populations. (B) the total cell counts of HSC, MPP, HPC1, and HPC2. (C) The total cell counts of CMP, GMP, MEP, LMPP and CLP. N=3 in each genotype. Error bars show mean ± SEM. Mann-Whitney U test was used to calculate significance as follows: *P < .05, **P < .01, ***P < .001, ****P <0.0001.

4.3.18 HSCs from *Zeb1* KO mice exhibit a multilineage haematopoietic differentiation defect after transplantation.

We applied transplantation experiments with highly purified HSCs *Zeb1*$^{-/-}$ or control mice to decipher the function of *Zeb1* in HSCs. Transplantation experiments can be used to study the mechanisms underlying HSC engraftment and retention in the bone marrow (Mori and Osumi 2022). In these experiments, HSCs are transplanted intravenously into mice that have been lethally irradiated. Transplanted HSCs then home, proliferate, and differentiate into all blood cell types. Here, lethally irradiated animals received HSCs from *Zeb1*$^{-/-}$ and control mice and the ability of *Zeb1*-deficient HSCs to repopulate primary recipients was evaluated by flow cytometry for mature blood cell types.

We purified 100 HSCs from control or *Zeb1*$^{-/-}$ mice (in a CD45.2 background) by FACS, combined these cells with 200,000 BM competitor cells from the congenic CD45.1 mice and transplanted the resulting mixture into CD45.1 recipients who were conditioned with lethal irradiation (Figure 4.18 A). We tracked the engraftment in PB of these recipients (Figure 4.18 B) until week 20 post-transplant. From week 4 onwards, there was a significant drop in engraftment in recipients of *Zeb1* KO donor cells compared to recipients receiving control HSCs. Engraftment in recipients of *Zeb1* KO donor HSCs declined further until week 12 and showed significantly diminished engraftment until week 20 (Figure 4.18 B).

In order to test *Zeb1* KO HSC donor contribution to mature haematopoietic cells, we analysed the engraftment of specific lineages in peripheral blood by evaluating the presence of donor cells (CD45.2) in combination with markers for monocytes (Mac1+), granulocytes (Mac1+ Gr1+), B cells (B220+), and T cells (CD4+/CD8+). Transplantation of *Zeb1*$^{-/-}$ HSCs did not result in the production of engrafted T cells., which is consistent with previous findings (section 4.3.9**)**, showing a substantial decrease in T cells (Figure 4.18 B). Additionally, recipients of *Zeb1*$^{-/-}$ HSCs showed a marked and significant reduction in donor contribution to B cells at all time points (Figure 4.18 B). Donor *Zeb1*$^{-/-}$ HSCs showed variable decreases in myeloid engraftment, reaching significance at 4 and 12 weeks post-transplant in monocytes, and 4 and 20 weeks in granulocytes (Figure 4.18 B).

Therefore, sustained Zeb1 expression is necessary for HSC multi-lineage differentiation *in vivo*.
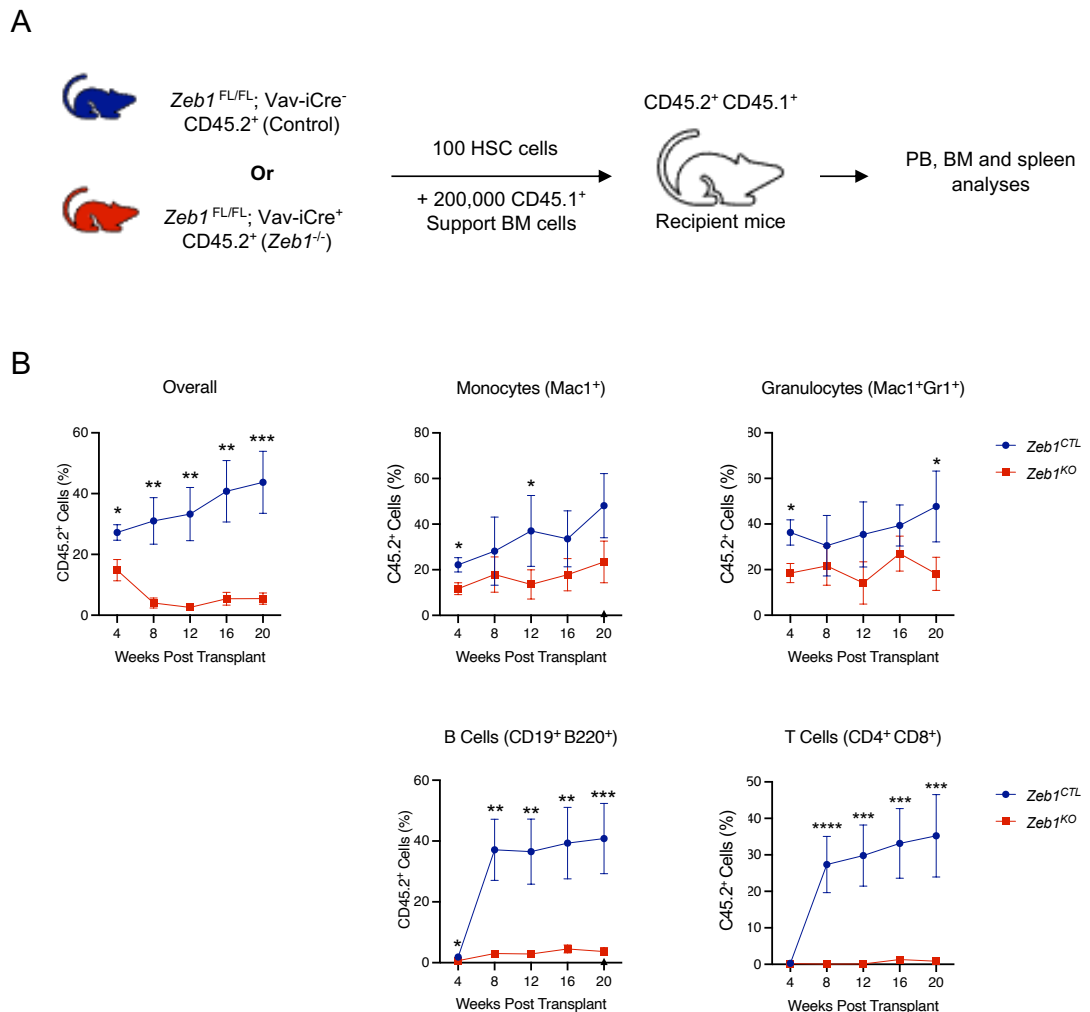
Figure 4.18 HSCs of *Vav-iCre* mediated *Zeb1* exhibit a multilineage haematopoietic differentiation defect after transplantation. (A) A scheme describes the transplantation assay: 100 HSC cells sorted from *Zeb1* KO and Control mice were transplanted into lethally irradiated recipients together with 200,000 support CD45.1+ total BM cells (the number of recipients injected in both the control group (n=8) and the KO group (n=12), sourced from three different donors). The PB analysis was performed every 4 weeks post-transplant, and the results show a reduction in the total percentage of the *Zeb1* KO donor cells in comparison to Control donor cells at different time points post-transplant. Reduction in Mac1+ (Monocytes), and Mac1+ Gr1+ (Granulocytes) cells and a significant reduction in donor contribution to PB T cells (CD4+ CD8+) and B cells (CD19+CD220+) of the *Zeb1* KO donor cells in comparison of Control donor cells at different time points post transplant. Error bars display the mean and SEM. Whitney U test was used to determine statistical significance in the following manner: *P < .05, **P < .01, ***P < .001, ****P <0.0001. (This experiment was a collaboration with Prof. Kamil Kranc (lab based at Barts Cancer Institute). After I prepared the experimental mice, I harvested the tissue and transferred it to Kamil Lab. The entire experiment, including the harvesting and sorting of hematopoietic stem cells (HSCs), as well as the HSCs transplant and the generation of Panel B in Figure 4.18, was conducted by Dr. Hannah Lawson.)

4.3.19 Reduced multi-lineage differentiation potential in the bone marrow and spleen of recipients receiving HSCs from *Zeb1*-/- mice

At 20 weeks post-transplantation, recipient mice were euthanized and total donor cell contribution in the BM (Figure 4.19 A) and spleen (Figure 4.19 B) was assessed, which showed significantly reduced engraftment in the *Zeb1*-/- group of recipients. In a similar manner, we analysed the donor contribution to LSK and LK populations, which was significantly reduced in both compartments in BM for the *Zeb1* genotype (Figure 4.19 C). Each of the HSPCs compartments (HSCs, MPP, HPC-1 and HPC-2) was also significantly reduced in recipients of *Zeb1*-/- HSCs in BM (Figure 4.19 D). Given the multi-lineage defects observed in the PB of recipients, we therefore explored whether the reduction was also observed in differentiated populations in the BM (Figure 4.19 E) and spleen (Figure 4.19 F). For all analysed subsets in the BM (B cells, monocytes and granulocytes) and the spleen (CD4 and CD8 T cells, B cells, monocytes and granulocytes) the donor contribution was dramatically reduced in recipients receiving *Zeb1*-/- HSCs. It is worth noting that for spleen data, the production of donor engrafted T cells from *Zeb1*-/- HSCs was completely absent.

To further examine the multi-lineage defect in HSCs in *Zeb1*-/- mice, in parallel to HSC transplant experiments, we evaluated the ability of *Zeb1* HSPCs and progenitors to differentiate *in vitro* using a colony forming unit assay. Colony forming unit (CFU) assays (CFC) are used to quantify the number of cells that are able to form colonies *in vitro* (Almotiri et al. 2021). We seeded 30,000 bone marrow cells from both control and *Zeb1*-/- mice on methylcellulose and counted the number of colonies formed after a 10-day incubation at 37°C, specifically focusing on colonies of myeloid lineage. We observed that there was a significant reduction in the total number of colonies (Figure 4.19 G) and of cell number with all colonies (Figure 4.19 H) from the BM of *Zeb1*-/- mice in comparison to control mice.
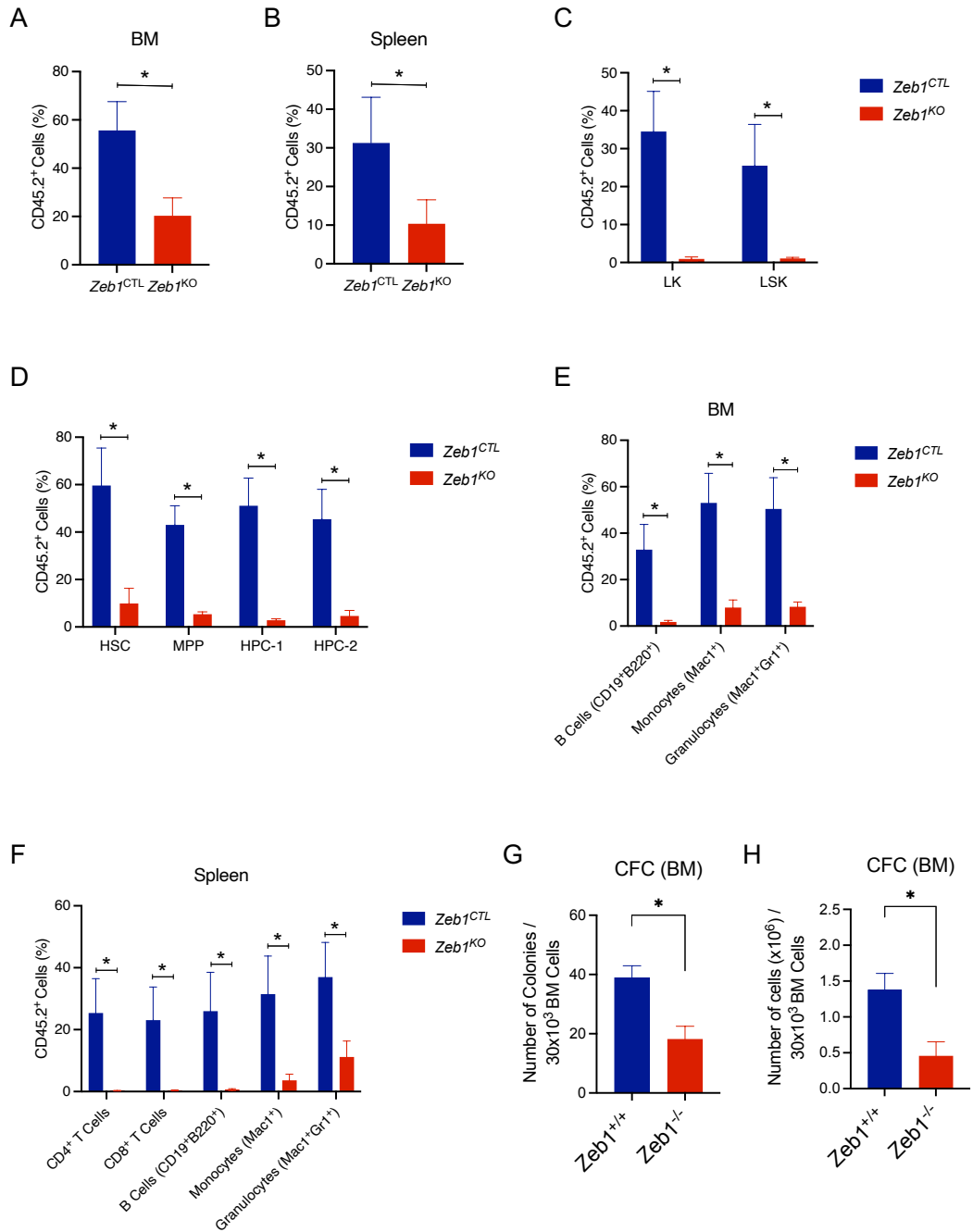
Figure 4.19 HSCs *Zeb1* deficiency showed a reduced donor contribution to HSPC in BM.
For HSCs transplant assay (section 2.11), 20 weeks post transplantation, BM and SP tissues
were harvested and the percentage of total cells donor contribution in BM (A) and SP (B) from
Zeb1 KO and Control were calculated. Analyses the donor contribution to LSK and LK population
(C), and the donor contribution to HSPCs in BM (D). The percentage of total donor contribution
to differentiated cells in BM (E) and spleen (F) from Zeb1 KO and control mice. For colony forming
unit assay (CFC), 30,000 total BM cells from Zeb1 KO and Control were plated in M3434
methylcellulose media supplemented with SCF, IL-3, IL-6 and Epo, the total number of colonies
(G) and the total number of cells (H) were counted after 10 days. n= 5 mice for each genotype
from three independent experiments. Error bars display the mean and SEM. Whitney U test was
used to determine statistical significance in the following manner: *P < .05, **P < .01, ***P < .001,
****P <0.0001.(The HSC transplant experiment was a collaboration with Prof. Kamil Kranc (lab
based at Barts Cancer Institute). After I prepared the experimental mice, I harvested the tissue
and transferred it to Kamil Lab. The entire experiment, including the harvesting and sorting of
hematopoietic stem cells (HSCs), as well as the HSC transplant and the generation of Panels A-
F in Figure 4.19, was conducted by Dr. Hannah Lawson).

4.3.20 HSCs from *Vav*-iCre-mediated *Zeb1 KO* mice display altered transcriptional programming related to erythropoiesis, immunodeficiency, inflammation and HSC maintenance pathways

To explore the molecular mechanisms underlying perturbed HSC function in *Zeb1* KO mice, we used RNA sequencing to look into the transcriptional alterations connected to *Zeb1*-mediated regulation of HSC function in isolated HSCs (LSK CD150+ CD48-) from control and four *Zeb1*$^{-/-}$ mice. 624 differentially expressed genes (DEG) were found in our data (327 downregulated and 297 upregulated; FDR 0.05) (Figure 4.20 A). The top overexpressed genes were *EpCAM, Vldlr, Plscr2, Krt8, Grb7, Lsr, Cdh1* and *Ap1m2*. The most reduced genes in our analysis were *Fcna, Unc45b, Pfkfb4, Gas6, Fhl1, Cpxm1, Zeb1* and Itsn1 (Figure 4.20 C).

We submitted our findings from RNA-seq gene expression to the web-based bioinformatics tool Ingenuity Pathway Analysis (IPA) for functional analysis, integration, and deeper understanding of transcriptional regulation by *Zeb1*. In general, IPA is used to examine lists of genes and it enables the interactive construction of networks to reflect biological systems. We categorised the DEGs based on how they were linked in different pathways and then produced a graphical representation. Many enriched pathways associated with the maintenance of HSC integrity (Akala and Clarke 2006; Cheung and Mak 2006; Naka and Hirao 2011; Ito and Suda 2014) including STAT3 pathway, p53 signalling, PTEN signalling and H1Fa signalling, were found to be upregulated by biological pathway analysis. The downregulated pathway activities were related to acute myeloid leukaemia signalling, NF-kB activation (Fadeev et al. 2015), S100 family signalling pathway which is important in AML (Alanazi et al. 2020), and erythropoietin signalling pathway, which may be linked to anaemia (Figure 4.20, B). We then categorised each of the DEGs into categories available at the IPA knowledgebase, which allowed us to observe the most important regulators in each phenotype by creating a heatmap (Figure 4.20 C). We then used IPA to predict the activity of these dysregulated molecules, in an unbiased manner, on each specific group of genes.
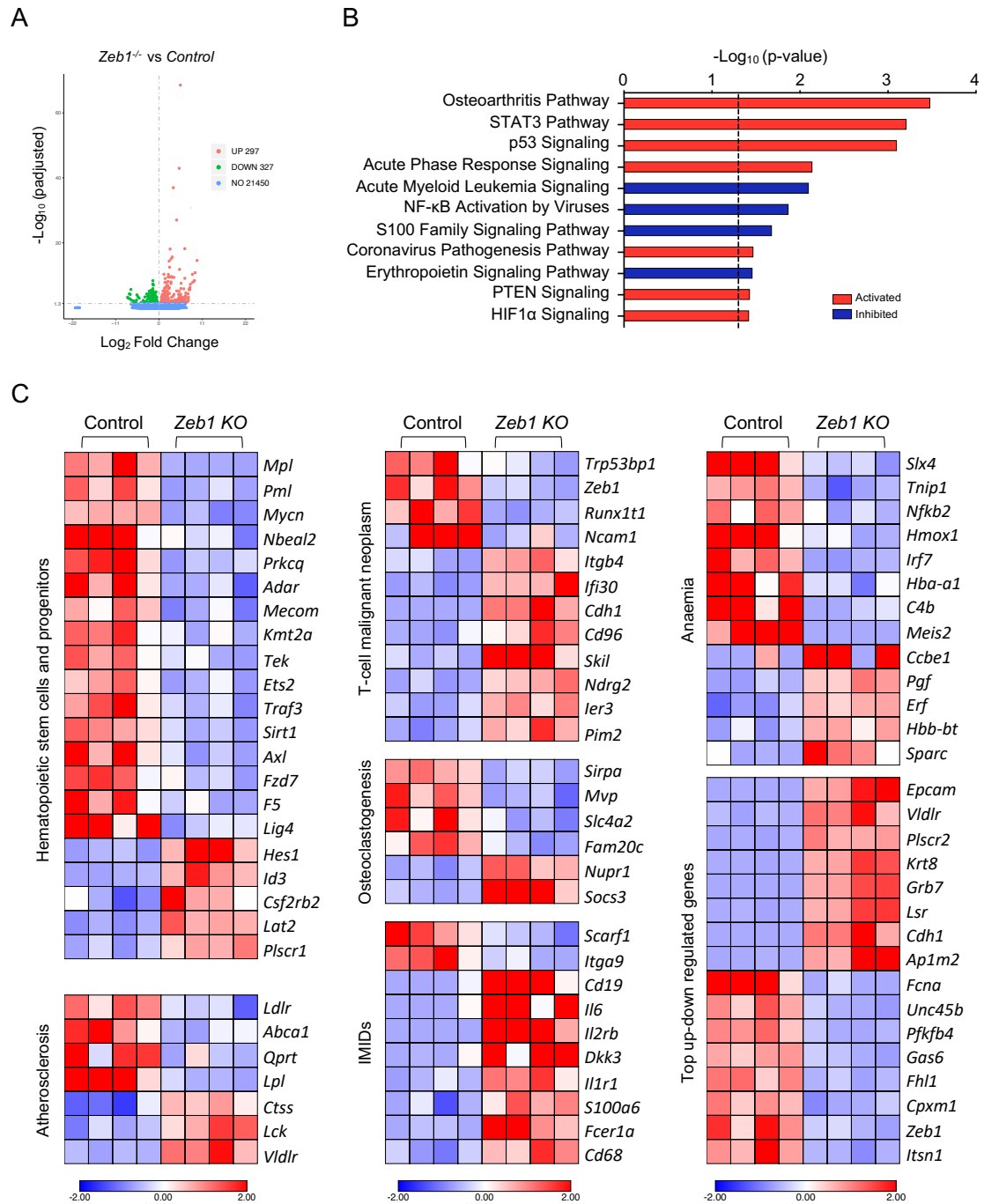
Figure 4.20 *Vav-iCre* mediated *Zeb1* deletion in HSCs shows deregulation of anaemia and IMIDs transcriptional programming. (A) A volcano plot illustrating the relationship between the statistical significance of the change (-log10 of adjusted p-value; y-axis) and the change in gene expression (log2 fold-change; x-axis) in a comparison of Zeb1$^{-/-}$ and *Zeb1*$^{+/+}$ HSC cells. The coloured dots represent differentially expressed genes that are either overexpressed (red) or underexpressed (green) in *Zeb1*$^{-/-}$ compared to *Zeb1*$^{+/+}$ (cut-off FDR 0.05). (B) IPA-derived canonical pathways, comprising activated (red) and inhibited (blue) pathways, that are primarily enriched in Zeb1$^{-/-}$ HSC cells. The black dashed line denotes a p-value of 0.05, and the data are displayed as -log10 (p-value). (C) Heat maps of the genes that expressed differently after Zeb1 was deleted, related to hematopoietic stem cell and progenitors, anaemia, atherosclerosis, osteoclastogenesis, T-cell malignant neoplasm and immune-mediated inflammatory disease (IMIDs) and the top up-down regulated genes. The heatmap scale represents Z-score.

Causal networks were built to define the primary interactions concerning the DEGs. According to the IPA knowledgebase (IKB), all the consistent-with-experiment relationships engaged in anaemia, inflammatory disease, haematopoiesis, and atherosclerosis were identified and these were selected for evaluation. The pathways were identified independently, in an unbiased manner, when the DEGs are used as input in IPA. Analyses are depicted in Figure 4.21 where green elements represent under-expressed molecules, whereas red represents their over-expressed counterparts which are based on the DEGs obtained from the experiment. In the interactome figures, using arrows we represent the role of these genes regarding a particular pathway (e.g. anaemia). The colour of the arrows represents if the results are consistent with the activation (orange) or inhibition (blue) of a pathway. The yellow results indicate that there is an inconsistency with the state of the molecule. In some cases molecules are shown in grey, which means that the specific effect of the molecules is not predicted, but it is possible to use literature to explore more in detail the effect of the regulators on the phenotype. Therefore, using the IKB and the figures generated, we can rapidly get an overview of the role of the up- and down-regulated molecules in several pathways related to *Zeb1* deficiency in HSCs.

In anaemia, We found that *Zeb1* deficiency generally impacted the expression of transcription regulators, resulting in a decrease in the expression of regulators such as *Meis2*, *Irf7*, *Mycn*, and *Nfkb2* and an increase in the expression of *Erf and Csf2rb*. It is noteworthy that most of these regulators act as inhibitors in the development of anaemia. *Erf* and *Irf7* were found to be inconsistent with the state of their downstream molecules. Meis2 expression skews hematopoietic development to megakaryocytic progenitor in mouse embryonic stem cells while decreasing erythroid differentiation (Wang et al. 2018b). Interferon regulatory factor 7 (IRF7) is a member of the IRF family of interferon regulatory transcription factors. It has been demonstrated that IRF7 participates in the transcriptional activation of cellular genes induced by viruses, such as interferon beta chain genes. Notably, IRF7 induced expression is primarily limited to lymphoid tissue (IRF7 protein expression summary - The Human Protein Atlas. [no date]) (https://www.proteinatlas.org/ENSG00000185507-IRF7).
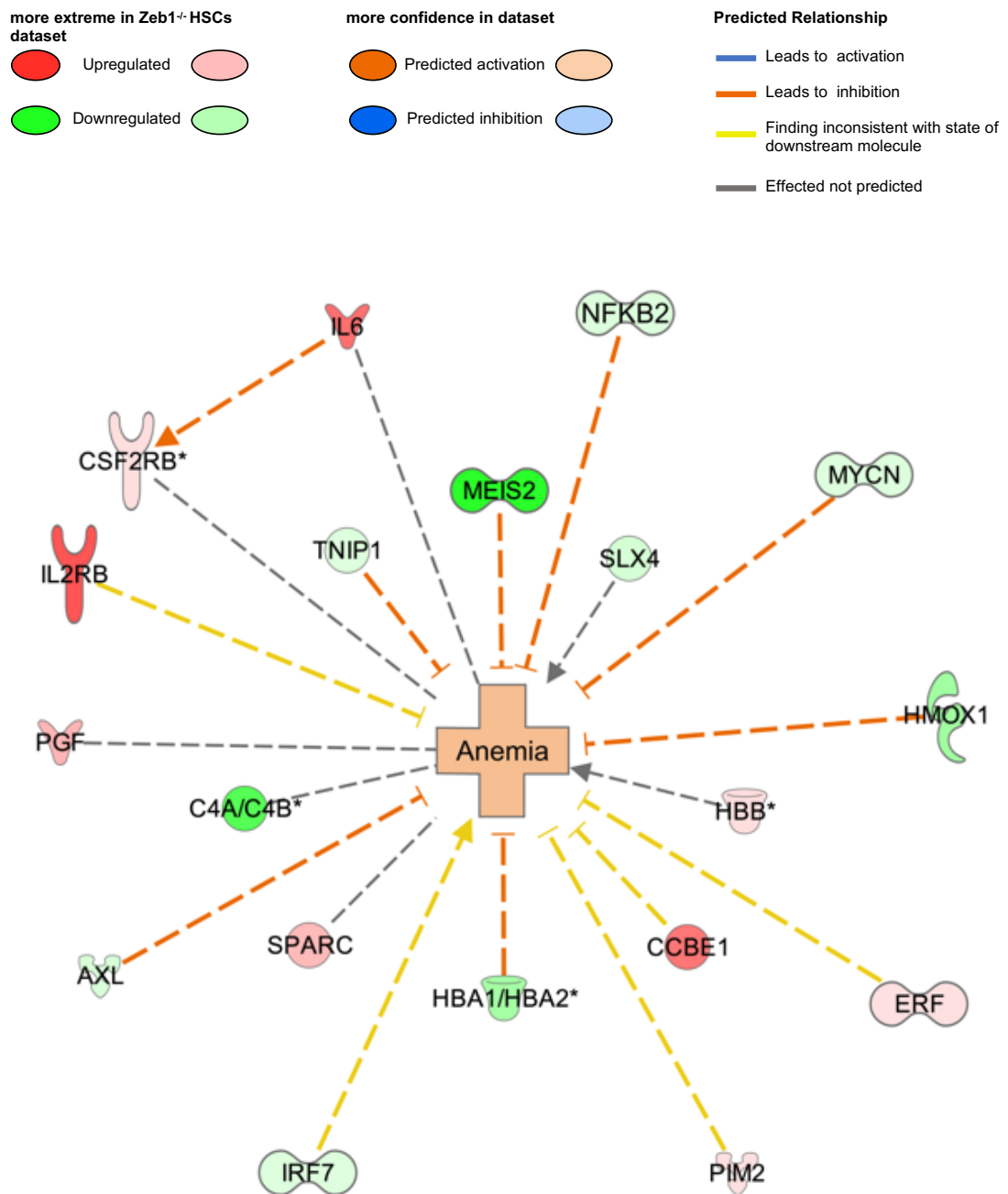
Figure 4.21 Interactome analysis in anaemia by Ingenuity Pathway Analysis (IPA) software. The network is displayed graphically as nodes (genes) and edges (the biological relationships). Nodes are indicated by symbols of different colours: green refers to downregulated and red is upregulated, based on the DEGs. The biological relationships between nodes and the other significant genes are indicated by coloured arrows (indicating that a molecule modulates the expression of another), and the orange colour indicates activation. The yellow colour indicates inconsistencies between the regulation of the molecule and the role in the pathway. The grey arrow indicates there are no known interactions between the molecule and the pathway.

Immune-mediated inflammatory disease (IMID) constitutes a common, clinically varied collection of diseases with similar underlying pathogenetic characteristics (McInnes and Gravallese 2021). IMIDs can affect any organ or tissue in the body and often result in long-term or permanent damage. Systemic autoimmune syndrome (SAS) describes a group of conditions that share many similarities, including chronic inflammation, autoimmunity, and immune system dysregulation. SAS is a broad term that encompasses many different diseases, including lupus, rheumatoid arthritis, and Crohn's disease (Wahren-Herlenius and Dörner 2013). Although IMID and SAS are two different conditions, they are often grouped together because they share many common features: both are chronic, inflammatory, autoimmune diseases that can affect multiple organs and systems in the body.

The pathogenesis of IMID and SAS is not fully understood, but it is believed that these conditions are the result of a dysregulated immune system (Wahren-Herlenius and Dörner 2013; McInnes and Gravallese 2021). This results in the immune system attacking healthy tissue, which leads to chronic inflammation (Aksentijevich et al. 2020).

Our analysis suggests that *Zeb1* could play a role in the development of IMIDs and SAS by dysregulating the immune system via the molecules observed in Figure 4.22. Several receptors, such as *Ilr2b*, *Fcer1a*, *Cd19*, *Il1r1*, and *Scarf1* are upregulated with the exception of *Scarf1*, which is downregulated. CD19 plays a critical role in B cell development, activation, survival and function, and dysregulation of CD19 signalling has been implicated in the development of several autoimmune diseases, including SLE and primary immunodeficiency disorders (Engel et al. 1995; n, Eunsung Mouradian 2008).
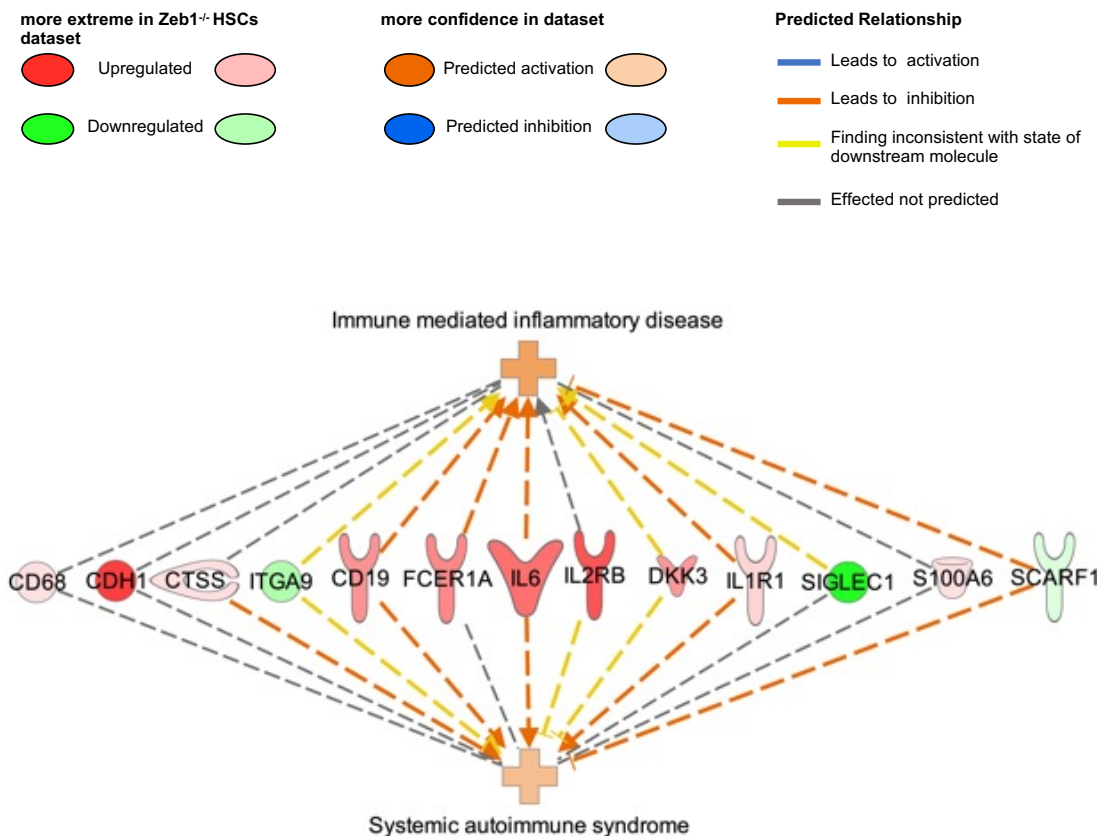
Figure 4.22 Interactomic analysis in immune-mediated inflammatory disease by Ingenuity Pathway Analysis (IPA) software. The gene network is represented visually as nodes (genes) and edges (biological relationships). The nodes are depicted in different colours, with green indicating down-regulated genes in our DEGs and red indicating upregulated genes. The biological relationships between nodes and other significant genes are represented by coloured arrows, with orange indicating activation. The yellow colour indicates inconsistencies between the regulation of the molecule and the role in the pathway. The grey arrow indicates there are no known interactions between the molecule and the pathway.

Given the phenotype observed in knockout mice, we explored how the *Zeb1* Vav-iCre-mediated deletion could be affecting the categories related to hematopoietic cells. Most of the molecules related to the IPA categories "quantity of hematopoietic cells" and "development of hematopoietic system" tend to be down-regulated (figure 4.23). In the IKB network, these downregulated molecules predict with high confidence their function is to inhibit the quantity of hematopoietic cells and the development of the hematopoietic system. The network is mainly composed of a cluster of downregulated transcription factors such as *Mycn*, *Nfkb2*, *Tp53bp1*, *Kmt2a*, *Pml*, *Sirt1*, and *Mecom*, which a few exceptions of upregulated transcription factors such as *Id3* and *Hes1* (Figure 4.23). *Mycn* is a member of the *Myc* family, which encodes transcription factors

that are potent oncogenes and have been implicated in the reprogramming of adult fibroblasts into stem cells(Laurenti et al. 2008) N-Myc is coexpressed with c-Myc in immature HSCs and that the combined deficiency of c-Myc and N-Myc results in pancytopenia and rapid lethality. The Myc activity, including both c-Myc and N-Myc, controls crucial aspects of HSC function including proliferation, differentiation, and survival(Laurenti et al. 2008). Additionally, the lack of both Myc genes leads to apoptosis, and only self-renewing HSCs accumulate a cytotoxic molecule, which reveals another mechanism of stem cell apoptosis (Laurenti et al. 2008). The gene for Mixed Lineage *Leukaemia* 1 (KMT2A) is essential for the growth and upkeep of hematopoietic stem cells (HSCs). Acute myelogenous leukaemia (AML) frequently has chromosomal translocations involving MLL1, which produce oncogenic MLL-fusion proteins (MLL-FPs) (Chen and Ernst 2019). PML is a tumour suppressor that was initially identified as a component of the PML–RARα fusion protein, which is involved in acute promyelocytic leukaemia (Nakahara et al. 2014). PML is involved in regulating various cellular processes, including the DNA damage response, apoptosis, senescence, and angiogenesis. Recent research has identified PML as a regulator of metabolic pathways in stem cell compartments, particularly in the hematopoietic system, with essential roles in stem cell maintenance and differentiation. PML is also critical for the maintenance of leukaemia-initiating cells(Nakahara et al. 2014). It has been reported that the overexpression of HES1 inhibits the development of erythroid and megakaryocytic cells in colony assays (Ishiko et al., 2004). Regarding MECOM, it has been recently suggested that ME deficiency alone leads to decreased HSC number and long-term repopulation capacity (Kataoka et al. 2011). High expression of *ZEB1* characterises a poor prognosis in osteosarcoma, which is regulated by SIRT1-*ZEB1*-positive feedback which promotes EMT (Yu et al. 2019).
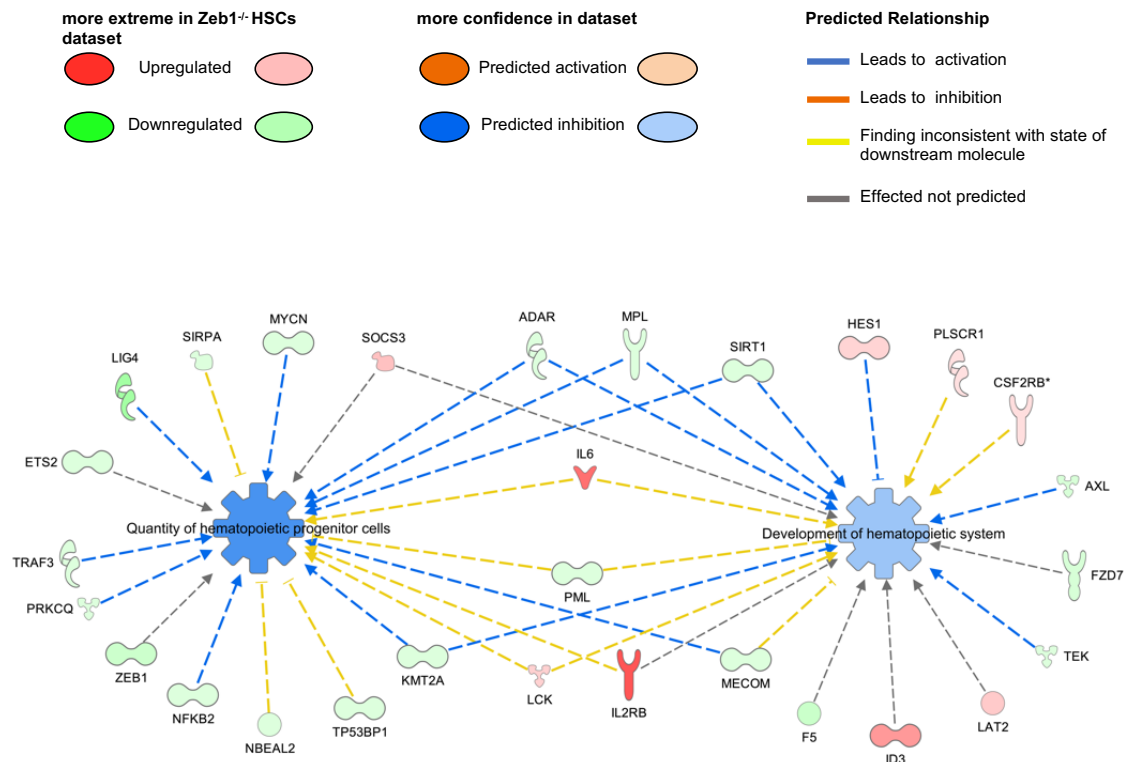
Figure 4.23 Interactomic analysis of hematopoietic pathways regulated *Zeb1* using Ingenuity Pathway Analysis (IPA) software. The gene network is represented visually as nodes (genes) and edges (biological relationships). The nodes are depicted in different colours, with green indicating down-regulated genes in our DEGs and red indicating upregulated genes. The biological relationships between nodes and other significant genes are represented by coloured arrows, with orange indicating activation, and blue colour indicating inhibition. The yellow colour indicates inconsistencies between the regulation of the molecule and the role in the pathway. The grey arrow indicates there are no known interactions between the molecule and the pathway.

As alluded to previously, *Zeb1* Vav-iCre mice showed more fragile bone tissue in comparison to their control littermates. This phenotype, in concert with the fact that the osteoarthritis pathway is one of the most upregulated pathways in the RNA-seq dataset led us to explore the molecular mechanisms altered in osteoclastogenesis mediated by *Zeb1* absence (Figure 4.24). Osteoclastogenesis is the process by which osteoclasts are formed (Yavropoulou and Yovos 2008). Osteoclasts are bone cells that break down bone tissue and are derived directly from myeloid hematopoietic progenitors. Most frequently, bone tissue is broken down by osteoclasts when there is an injury or when the body is trying to repair a fracture (Yavropoulou and Yovos 2008). The differentiation and activation of osteoclasts are regulated by the cytokine osteoprotegerin ligand (*Opgl*) and the transcription factor *Nfatc1*, which integrate

RANKL signalling (Ash et al. 1980; Jacome-Galarza et al. 2019). We observed a high proportion of genes downregulated by *Zeb1 (Ldlr, Mvp, Nfkb2, Pi3k, Sirpa, Slc4a2, Fam20c, Tek)*, which have different roles regarding their activation or inhibition of osteoclastogenesis. The downregulated genes (*Mvp, Nfkb2, Fam20c*) lead to the activation of the osteoclastogenesis pathway (Figure 4.24). Furthermore, the upregulated genes (*Il6, Hes1, Src, Socs3, Nupr1*) in this pathway show more correlation to the activation role these molecules show in osteoclastogenesis.
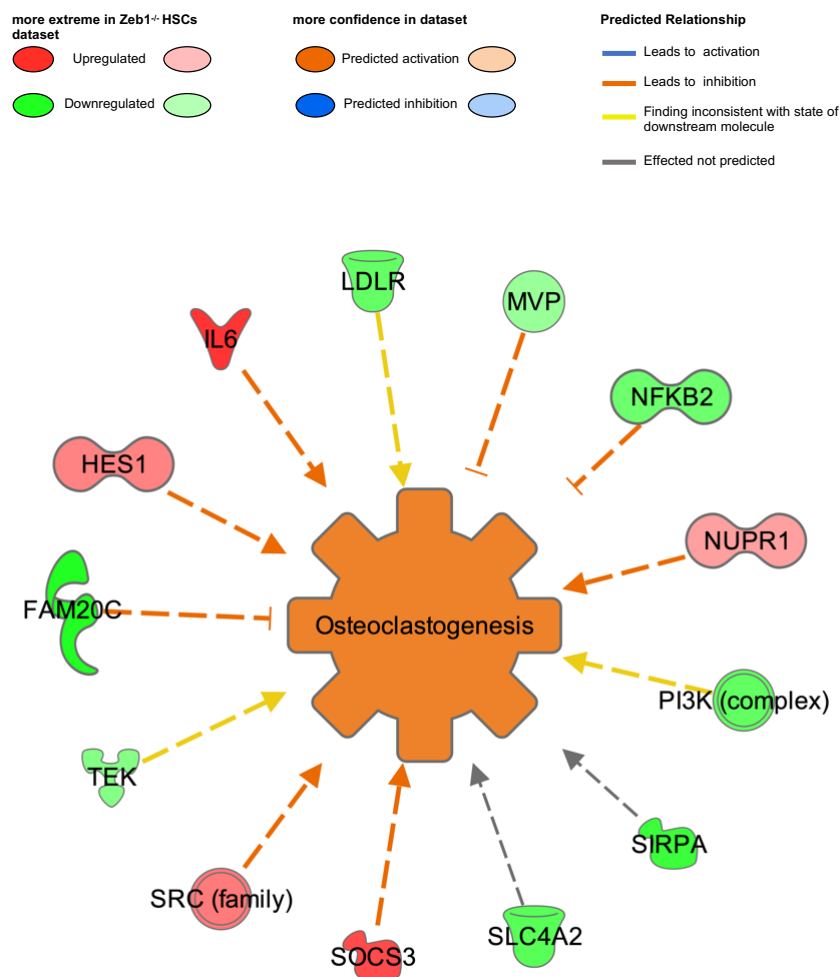
Figure 4.24 Interactomic analysis in osteoclastogenesis neoplasm by Ingenuity Pathway Analysis (IPA) software. The gene network is represented visually as nodes (genes) and edges (biological relationships). The nodes are depicted in different colours, with green indicating down-regulated genes in our DEGs and red indicating upregulated genes. The biological relationships between nodes and other significant genes are represented by coloured arrows, with orange indicating activation. The yellow colour indicates inconsistencies between the regulation of the molecule and the role in the pathway. The grey arrow indicates there are no known interactions between the molecule and the pathway.

Atherosclerosis is a disease in which plaque builds up inside arteries. Over time, plaque hardens and narrows arteries which limit the flow of oxygen-rich blood to the heart and other organs (Ross 1986). Atherosclerosis can lead to heart attack, stroke, or peripheral artery disease. Myeloid cells, such as monocytes and macrophages, have a significant role in the progression of atherosclerosis by accumulating lipids and becoming foam cells (Koltsova et al. 2013; Moore et al. 2013a). In hypercholesterolemia, excess cholesterol in the blood triggers increased uptake of cholesterol by myeloid cells, leading to foam cell formation, which contributes to the development of atherosclerosis (Tall and Yvan-Charvet 2015; Wesseling et al. 2018). We observed upregulated levels of IL6, which is a cytokine that plays a role in inflammation. High levels of IL6 have been associated with an increased risk of atherosclerosis (Hartman and Frishman 2014; Reiss et al. 2017a) (Figure 4.25). LPL is a lipase that is involved in the breakdown of triglycerides. Triglycerides are a type of fat that can build up in the arteries and contribute to atherosclerosis (Talayero and Sacks 2011). LPL helps to break down triglycerides so that they can be cleared from the arteries. LDLR is a receptor that helps to remove LDL cholesterol from the blood. LDL cholesterol can also build up in the arteries and contribute to atherosclerosis (Linton et al. 2019). ABCA1 is a transporter protein that helps to move cholesterol and other lipids out of cells (Phillips 2018). This helps to keep cholesterol levels low and prevents it from building up in the arteries.
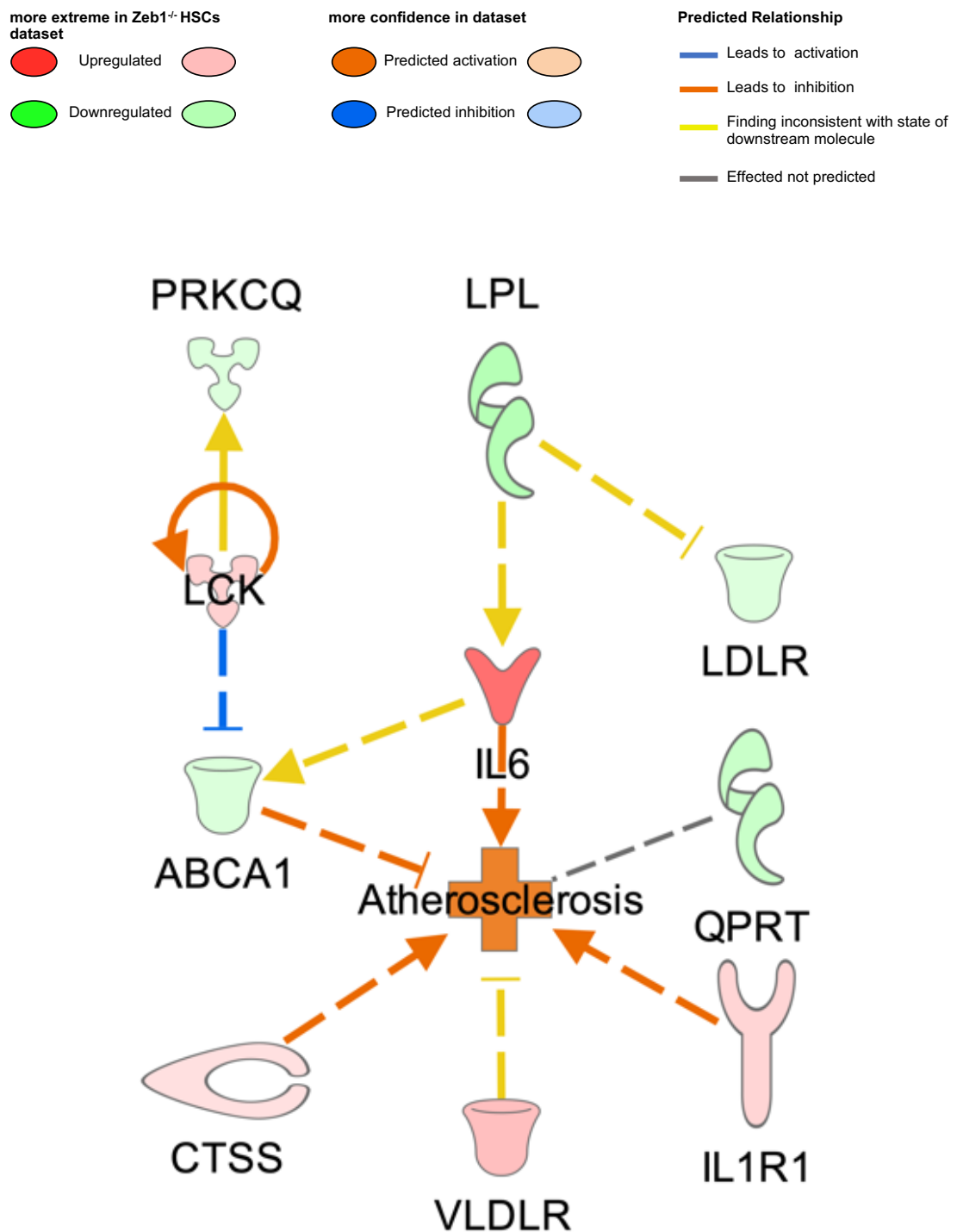
**Figure 4.25 Interactomic analysis in atherosclerosis by Ingenuity Pathway Analysis (IPA) software.** The gene network is represented visually as nodes (genes) and edges (biological relationships). The nodes are depicted in different colours, with green indicating down-regulated genes in our DEGs and red indicating upregulated genes. The biological relationships between nodes and other significant genes are represented by coloured arrows, with orange indicating activation. The yellow colour indicates inconsistencies between the regulation of the molecule and the role in the pathway. The grey arrow indicates there are no known interactions between the molecule and the pathway.

Zeb1 is a transcription factor involved in epithelial-to-mesenchymal transition (EMT), and EMT has been shown to play an important role in vascular development and disease, including atherosclerosis (Wesseling et al. 2018; Kovacic et al. 2019). Our RNA-sequencing (RNA-Seq) data from *Zeb1 Vav-iCre+* and control mice showed a striking upregulation of epithelial markers, such as *Epcam* and *Cdh1*. In addition, there is evidence to suggest that increased levels of pro-inflammatory cytokines such as *Ifn-γ*, *Tnf-α*, and *Il-6* can directly contribute to the development of atherosclerosis (Tousoulis et al. 2016).Therefore, validating the expression of *Epcam* and *Cdh1* by flow cytometry (Figure 4.26 B-C), as well as measuring the levels of *IFN-γ*, *TNF-α*, and *IL-6* by electrochemiluminescence immunoassays (Figure 4.26 D), could provide valuable information about the potential role of these markers in the development of atherosclerosis in the context of ZEB1 deletion-induced immunodeficiency and anaemia.

Using flow cytometry (Figure 4.26 A), the results show a striking increase in the expression of epithelial cell adhesion molecule (*Epcam*) and *E-Cadherin* in *Zeb1$^{-/-}$* hematopoietic stem cells (HSC), multipotent progenitors (MPP), and hematopoietic progenitor cells (HPC1 and HPC2) populations (Figure 4.26 B-C). In addition, pro-inflammatory cytokines *IFN-γ*, *TNF-α*, and *IL-6* were quantified in the whole blood of *Zeb1$^{-/-}$* and control mice, and the results show an elevation of these cytokines in the Zeb1 KO mice compared to controls (Figure 4.26 D).
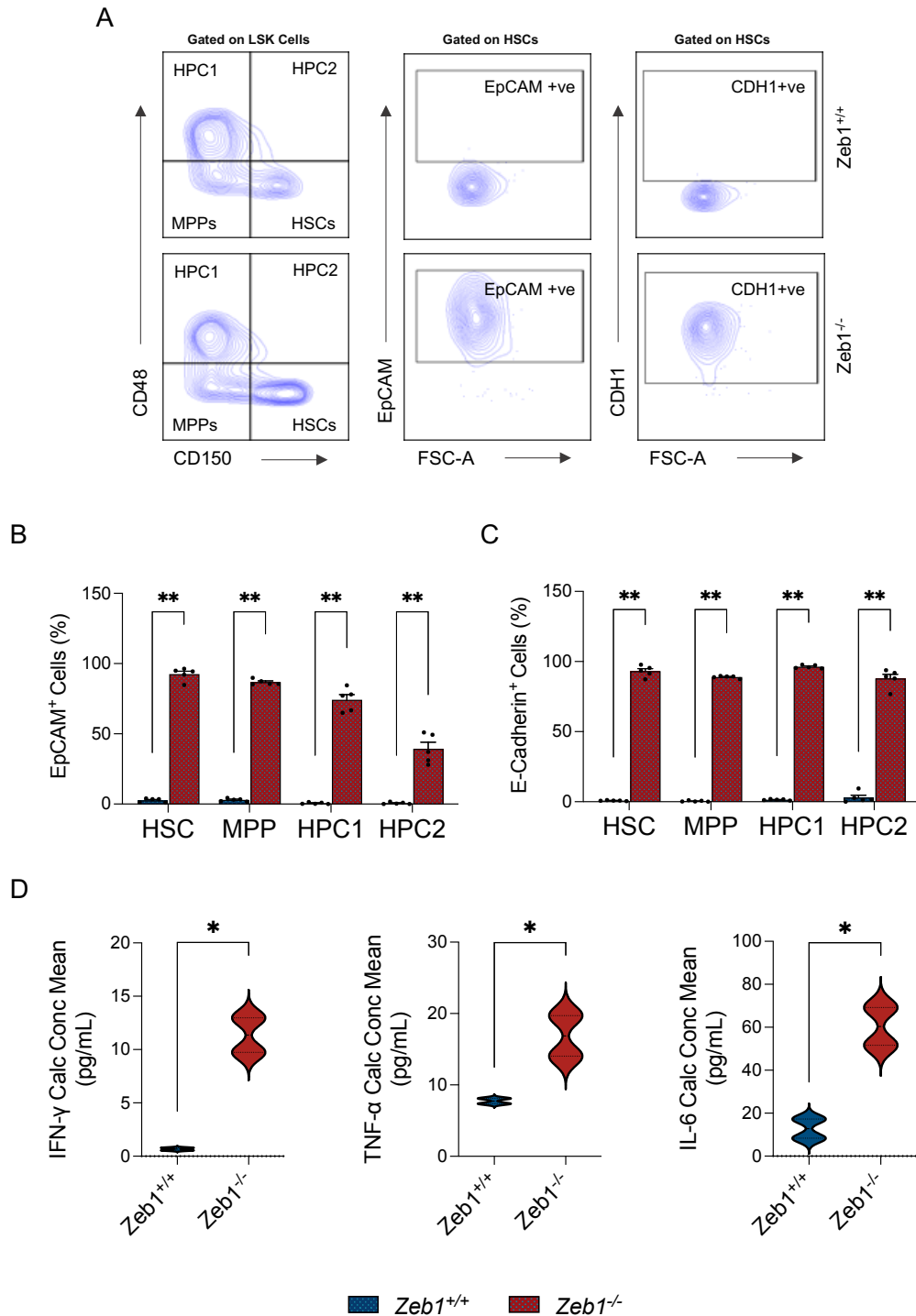
Figure 4.26 *Vav*-iCre mediated *Zeb1* deletion causes an increase of EMT and inflammatory markers in HSPCs. (A) Representative FACS plots of EpCAM and E-cadherin analysis in HSPCs of 8-12 old mice from control (*Zeb1*^{+/+}) and Zeb1^{-/-} . (B, C) The total EpCAM+ and CDH1 were analysed in HSC, MPP, HPC1 and HPC2 and the results show an increase in Zeb1 KO in comparison with the control (n=5 in each genotype). (D) The INF-y, TNF-a and IL-6 Cytokines were quantified in whole blood from cardiac puncture of 8-12 old mice from control (*Zeb1*^{+/+}) and *Zeb1*^{-/-} using electrochemiluminescence immunoassays principle using Meso Scale Discovery QuickPlex SQ120, USA (Han et al. 2021), the result shows *Vav*-iCre mediated *Zeb1* deletion causes increased inflammatory cytokine response (n=4 in each genotype). Data shown are mean ± SEM of calculated concentration mean (pg/mL); the Mann-Whitney U test was used to calculate significance as follows: *P < .05, **P < .01, ***P < .001, ****P <0.0001.

4.3.21 *Vav*-iCre-mediated *Zeb1* deletion impairs HSC self-renewal capacity and reduces survival of *Zeb1* KO mice in ageing

Serial transplantation of HSC is used to test HSC self-renewal capacity, but it is also acknowledged that this experiment mimics the ageing process *in vivo* (Cupit-Link et al. 2018). Given the low level of engraftment after primary HSC transplantation of *Zeb1* KO HSCs (Figures 4.18 and 4.19), we opted instead to assess long-term maintenance and self-renewal of HSCs by ageing *Zeb1*⁻/⁻ and control mice. Mice from each group, *Zeb1* KO and control, were observed in Scantainer cages, which are typically used for research purposes to maintain mice under specific pathogen-free conditions; this is highly relevant given the immune-compromised status of *Zeb1*⁻/⁻ mice described in this Chapter.

We followed the survival *Zeb1* KO and control mice using a Kaplan-Meier survival curve. We observed that over 19 weeks the survival of *Zeb1* KO mice was 16% less than its control littermates (n=31, for each genotype) (Figure 4.27A). When both genotypes were observed for up to 50 weeks, the inferior survival of *Zeb1*⁻/⁻ mice became even more apparent with a 70% lower survival than its control littermates (n=10, for each genotype) (Figure 4.27 B).
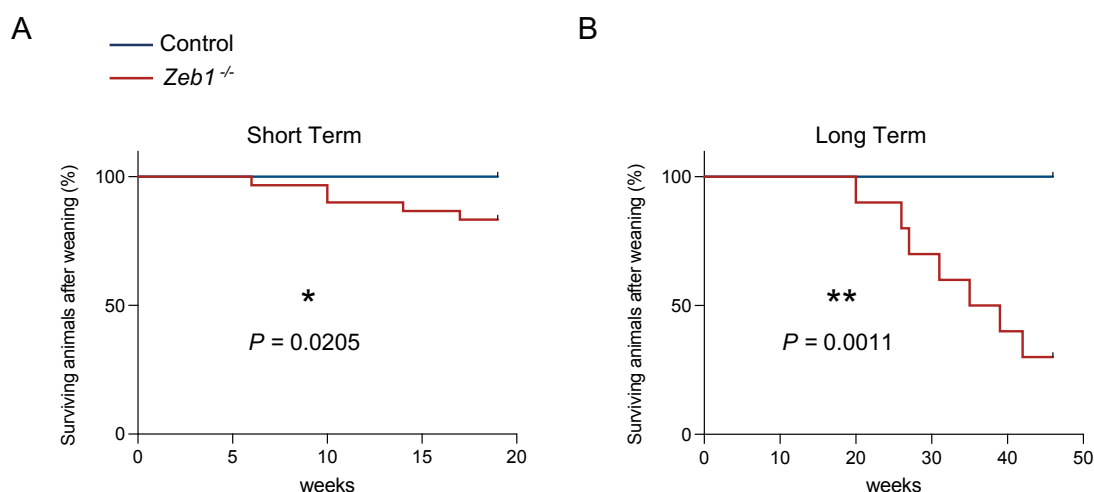
Figure 4.27 Kaplan-Meier survival curve of *Zeb1*⁻/⁻ and control. (A) Short term up until 19 weeks (n = 31) or (B) Long term up until 50 weeks (n = 10). Mantel-Cox test. *P < 0.05.

We used three mice in an initial analysis to investigate the reason behind the illness observed on them. The mice became moribund at different time points, specifically at 31 weeks, 35 weeks, and 59 weeks. These are represented on a bar graph in Figure 4.28. One of the three *Zeb1* KO mice (represented on orange, 31 weeks old) has hypocellular BM, and, surprisingly, exhibited splenomegaly and cell count which was opposite to other two *Zeb1* KO mice (represented in red) and young adult *Zeb1* KO mice, aged 8-12 weeks (previously shown). Moreover, in this single *Zeb1* KO mouse we observed a substantial expansion in CD4+ cells in BM and SP (Figure 4.28 D, E), an increase in myeloid cells Gr1-Mac1+ in BM with an approximate 6.3-fold change (Figure 4.28 F) and no differences in SP when compared to the control and an increase when compared to the other two *Zeb1* KO mice (Figure 4.28 G). In relation to erythroid cells, we observed reduction in Ter119+ cells with an approximate 3.6-fold change in the BM and strikingly increased Ter119+ cells with an approximate 3.5-fold change in SP compared to both the control and other two *Zeb1* KO mice (Figure 4.28 H, I).
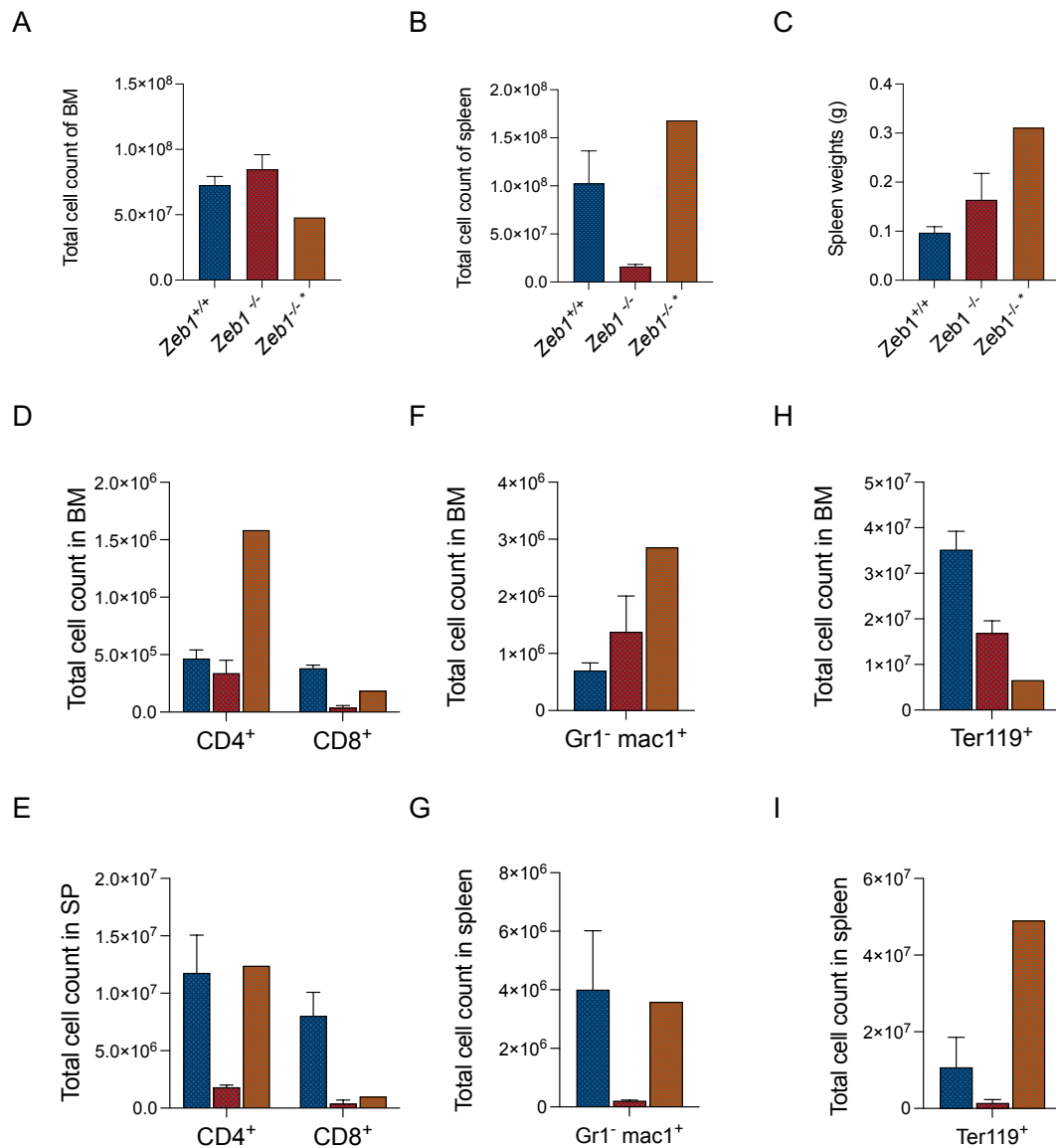
Figure 4.28 Prolonged *Zeb1* deficiency causes an increase in CD4+ cells in BM. Total BM cellularity(A), Total spleen cellularity(B), and weight (C). Total cellulrity of CD4 and CD8 in BM (D) and in SP (E). Total cellularity of myeloid cells Gr1- Mac1+ in BM (F) and in SP (G). Total cellularity of erythroid cells Ter119+ in BM mice(F) and in SP (G). One of the three mice showed increased CD4+ cells (orange bar) in comparison to the other two Zeb1 KO mice (red) and the control (blue).

As the results in Figure 4.28 show, two of the three Zeb1 KO mice (represented in red) mirror the results of the young adult Zeb1 KO mice aged 8-12 weeks, as previously shown at the beginning of this chapter. The third mouse (represented in orange) showed the opposite results. These results lead us to investigate this mouse more in-depth, as in a similar study (Hidaka et al. 2008) , it was found that TCF8 mutant mice (*Zeb1*) frequently developed CD4+ T-cell lymphoma/leukaemia at around half a year (around 25 weeks) after birth, suggesting that *Zeb1* has an important tumour suppressor role in this context.

Therefore, mirroring that study, we wanted to explore the T-cell phenotype of the 31-week old *Zeb1* Vav-iCre, which became moribund. Therefore, we quantified the frequency and cell counts for different compartments in the 31-week old mice in the bone marrow and spleen. While parameters, such as B220 frequency and cell count varied slightly in *Zeb1* KO mice and control in the bone marrow (Figure 4.29 A-B) and spleen (Figure 4.29 C-D), we observed a strikingly high frequency and cell count of CD4+ in the bone marrow of this 31-week old mice (Figure 4.29 A, B). Moreover, a depletion in the frequency and cell counts of CD8+ (Figure 4.29 C, D) in the spleen was observed. These observations are consistent with this mouse developing a CD4+ T-cell lymphoma/leukaemia-like phenotype. For this reason, we decided to follow up our investigations by studying this specific mouse in further detail to gain a better understanding of the *Zeb1* deficiency and its effects (Figures 4.30 to 4.34).
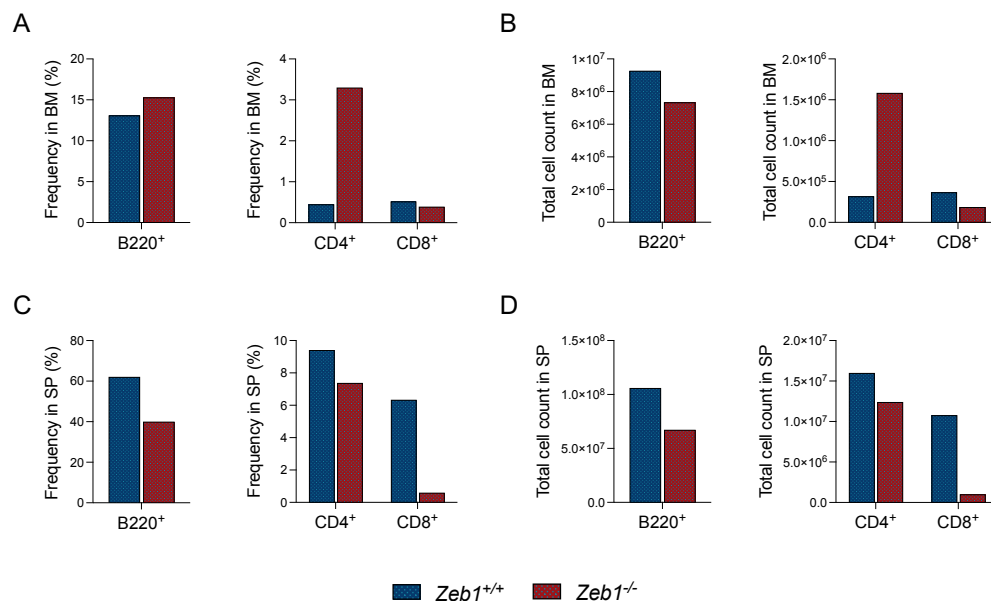
Figure 4.29 Prolonged *Zeb1* deficiency causes an increase of CD4+ cells in BM. The frequency results of B220+, CD4+, and CD8+ in BM (A) and in SP (C). The total cell count results of B220+, and CD4+, CD8+ in BM (B) and SP (D).

In this single *Zeb1* KO mouse, we observed a whiter and more fragile tibia and femur bone than a control mouse of the same age, likely indicative of anaemia (Figure 4.30 A) and an enlargement of spleen size (Figure 4.30 B) and weight (Figure 4.30 E). Notably, splenomegaly is opposite to the result observed in the cohort of young mice analysed (Figure 4.8). Total cellularity was reduced in the

BM (Figure 4.30 C) while, despite the splenomegaly, cellularity remained equivalent to the control in the spleen (Figure 4.30 D).
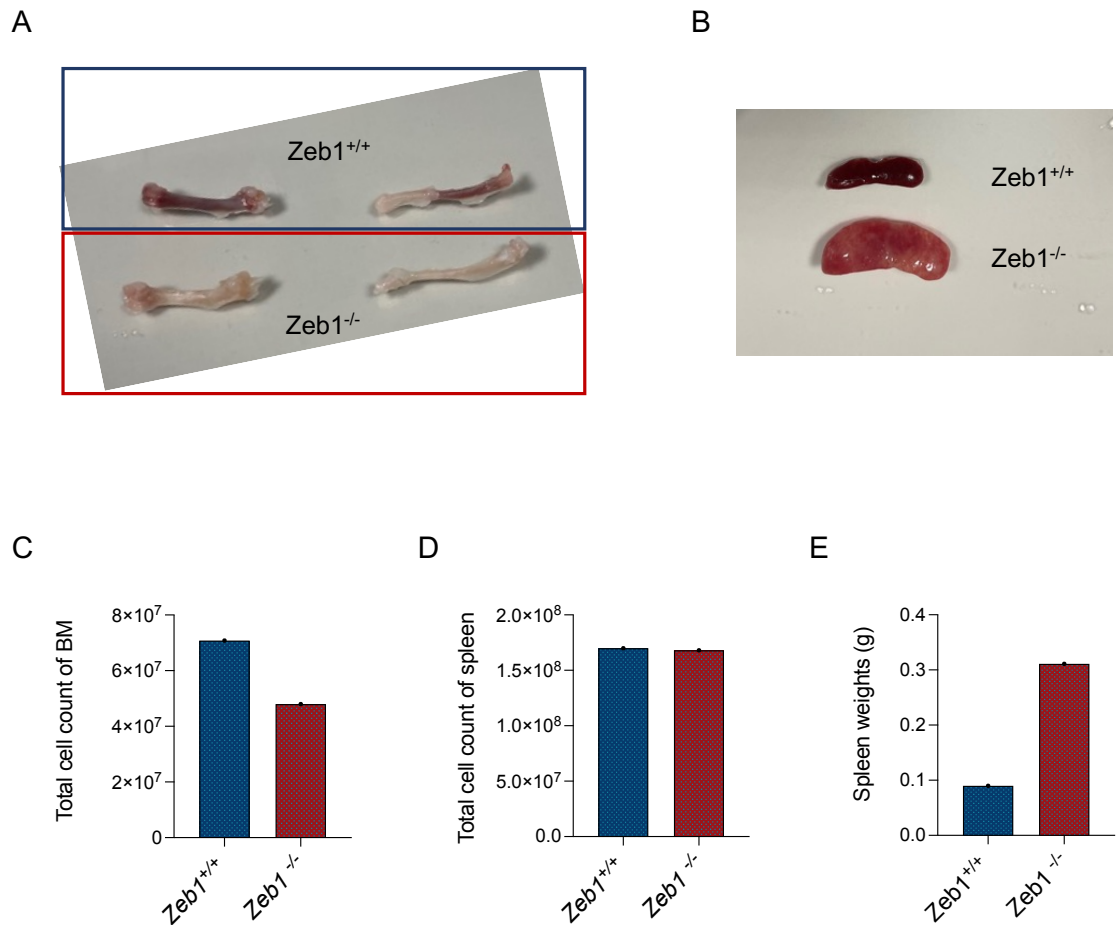
Figure 4.30 Prolonged *Zeb*1 deficiency causes a decrease in BM cellularity and an increase in spleen weight. Image of mouse tibia and femur (A), Spleen size (B), Total BM cellularity (C), Total spleen cellularity(D), and weight (E).

We next quantified the frequency and total cellularity of Gr1- Mac1+ and Gr1+ Mac1+ cells in the BM and spleen. We observed an increase of myeloid cells (Gr1- Mac1+) and Gr1+ mac1+ cells in the BM (Figure 4.31 A-B). In the spleen, Gr1- Mac1+ frequencies and total cellularity decreased, whereas Gr1+ Mac1+ frequencies and total cellularity increased (Figure 4.31 C-D).
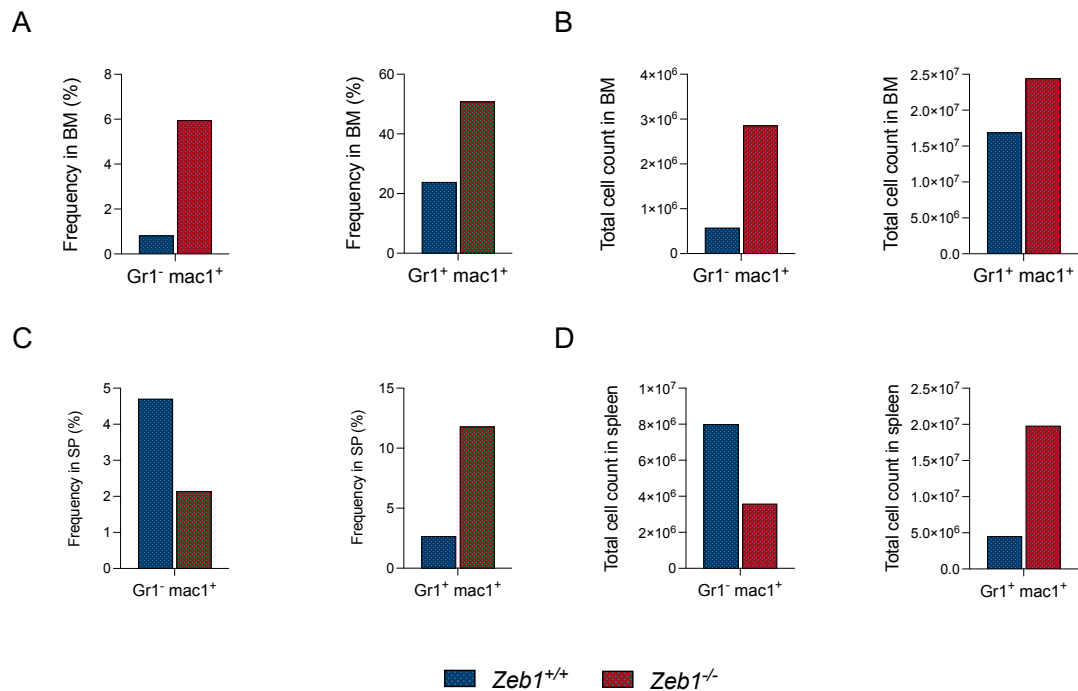
Figure 4.31 Prolonged *Zeb1* deficiency causes an increase in Gr1+ mac1+ cells in BM and SP. BM and SP tissues were collected from 35 weeks old mice for both control and *Zeb1*-/- (KO). The frequencies and total cellularity of myeloid (Gr1- Mac1+ and Gr1+ Mac1+) in BM were increased (A, B). The frequencies and total cellularity of Gr1- Mac1+ in SP were decreased while the frequencies and total cellularity of Gr1+ Mac1+ were increased (C, D).

As we observed whiter tibia and femur bones, suggestive that this mouse has anaemia, we further analysed erythroid cells (Ter119$^+$) in the BM and SP. The frequencies and the total cell count of erythroid cells (Ter119$^+$), Pro-E (CD71+ Ter119 -/low), Early-E (CD71+ Ter119+) and Late-E (CD71- Ter119+) were decreased in BM (Figure 4.32 A-D). However, opposite to the results of the young adult Zeb1 KO mice aged 8-12 weeks, the frequencies, and the total cell count of erythroid cells (Ter119$^+$), Pro-E, and Early-E were increased while the Late-E was decreased in the SP (Figure 4.32 E-H). These results are consistent with anaemic, which may be further driven by a pre-leukaemic/leukaemic state.
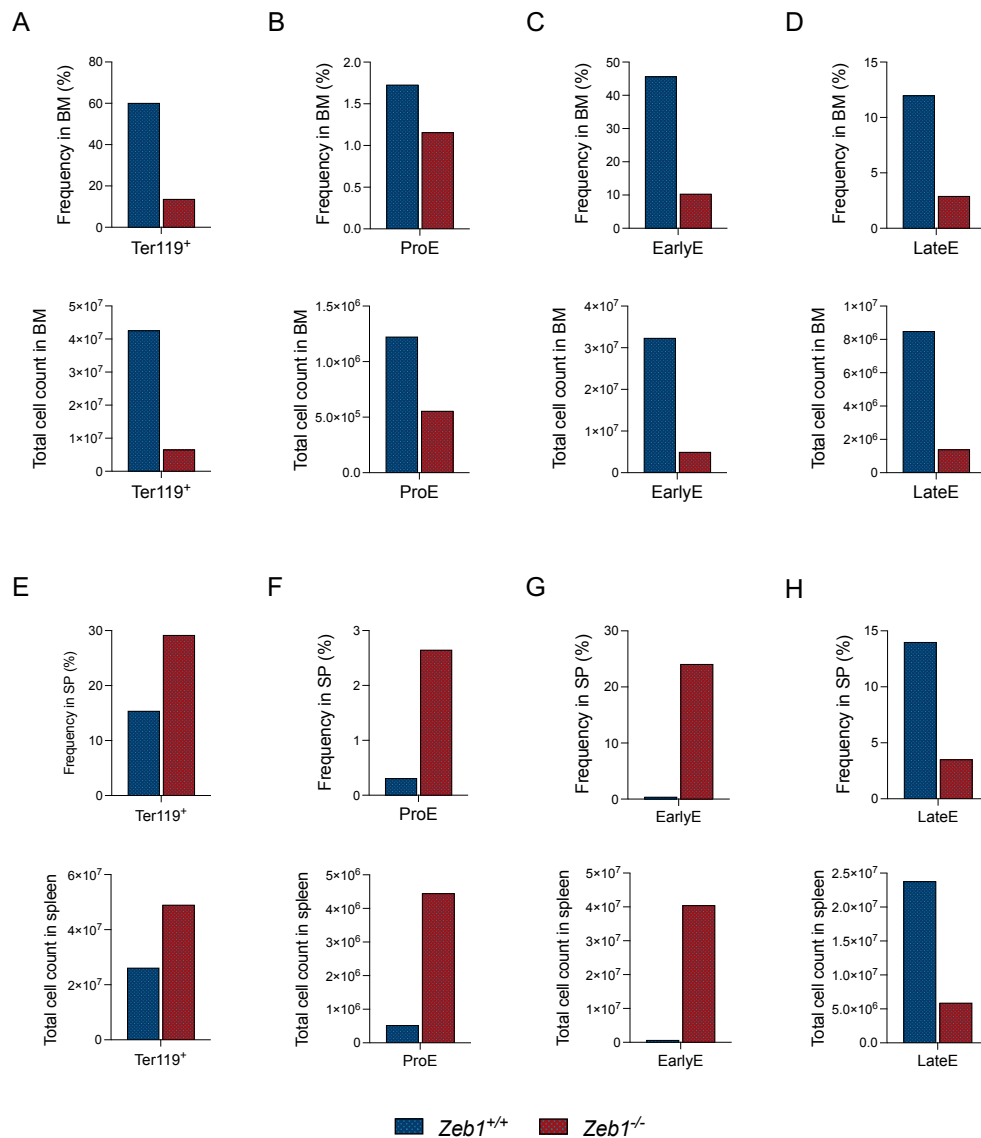
Figure 4.32 Prolonged *Zeb1* deficiency causes a reduction of erythroid cells in BM. SP and MB tissues were collected from 35 weeks old mice for both control and *Zeb1*-/- (KO). BM and SP analysis of erythroid cells (Ter119+) gated from DAPI negative cells (live cells in SP) and Pro-E indicate proerythroblasts (CD71+ Ter119 -/low); Early-E, early-erythroblasts (CD71+ Ter119+); Late-E, late erythroblasts (CD71- Ter119+). The frequencies and the total cell count of erythroid cells (Ter119+), Pro-E, Early-E and Late-E were decreased in BM (A-D). The frequencies and the total cell count of erythroid cells (Ter119+), Pro-E, and Early-E were increased while the Late-E was decreased in SP (E-H).

We investigated the quantity and functionality of hematopoietic stem and progenitor cells between this aged *Zeb1* KO mouse and a control mouse counterpart to determine the impact of sustained *Zeb1* deficiency on long-term HSC maintenance and development. We evaluated the direct impact of *Zeb1* deficiency in hematopoietic stem cells by measuring the LK and LSK fractions in the bone marrow using C-kit and Sca-1 (Figure 4.33 A). In a normal context, LT-

HSCs and multi-potent (LSK) progenitor cells become more prevalent during ageing (Morrison et al. 1996; Pearce et al. 2007; De Haan and Lazare 2018b). However, we observed that the frequency and total cell count of LSK cells were decreased in the bone marrow of the *Zeb1* KO mouse at 31 weeks (Figure 4.33 C) in comparison to control mice of the same age. Moreover, the lower frequency of LSK in the *Zeb1* KO mouse compared to that in the control group indicates that myelosuppression in bone marrow may be induced by *Zeb1* (Figure 4.33 C). Additionally, we saw a drop in the overall number of Lin-c-Kit+ (LK), which is enriched in myelo-erythroid progenitors (Figure 4.33 B). There was also a reduction in frequency and cell count in most MPP populations and LMPP in this *Zeb1* KO mouse (Figure 4.33 D, E). Furthermore, we observed a decrease in the frequency and total cell count of HSCs in the BM (Figure 4.33 D, E). In particular, there was a decrease in the frequency of the CD150hi (myeloid biased) and CD150int (balanced) populations, and, interestingly, an increase in the frequency of the CD150lo (lymphoid biased) population in both HSCs and total BM of *Zeb1* KO mice at 31 weeks old (Figure 4.33 F, G).
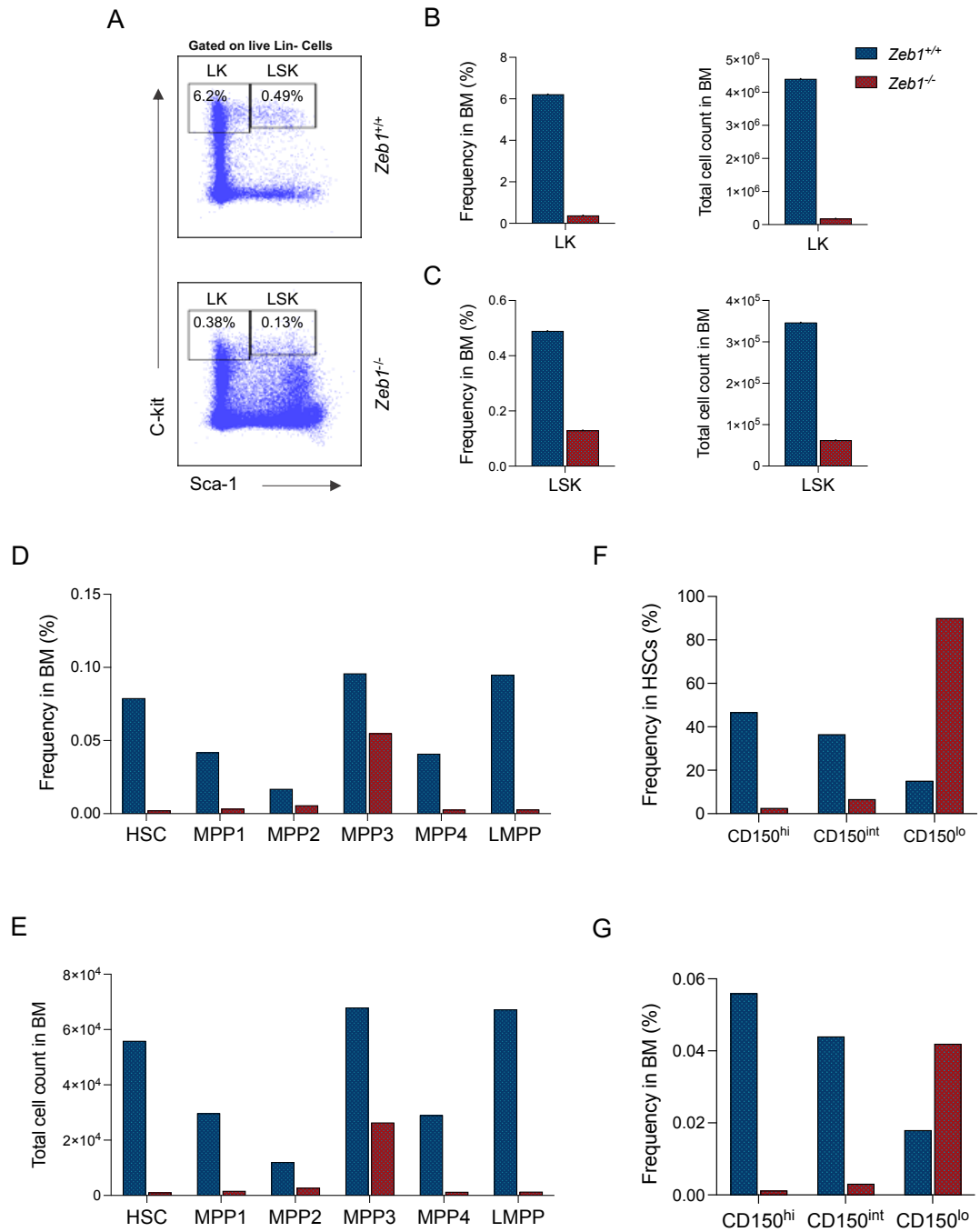
Figure 4.33 Prolonged *Zeb1* deficiency exhausts HSPCs in BM. Representative FACS plots of control (*Zeb1*^{+/+}) and *Zeb1*^{-/-} LK (Lin- c-kit+ sca1-) , LSK (Lin- c-kit+ sca1+) population (A), and decrease in frequency and total cell count of LK and LSK (B, C). Decrease in frequency and total cell count of HSC (LKS+ CD135- CD34- CD48- CD150+), MPP1 (LKS+ CD135- CD34+ CD48- CD150+), MPP2 (LKS+ CD135- CD34+ CD48+ CD150+), MPP3 (LKS+ CD135- CD34+ CD48+ CD150), MPP4 (LKS+ CD135+ CD34+ CD48+ CD150-) and LMPP (LSK CD135+ CD34+ CD150−) (D,E). Decrease the frequency of CD150hi (LSK CD135- CD34- CD150hi) myeloid biased and CD150int (LSK CD135- CD34- CD150int) balanced within HSCs and total BM (F, G) and increase the frequency of CD150lo/- (LSK CD135- CD34- CD150lo/-) lymphoid biased within HSCs and total BM (F, G).

In contrast to the BM, an increased frequency of LSK in the spleen of the *Zeb1* KO mouse was noted, while LK cells in the spleen were reduced (Figure 4.34 A - C). To further characterise this phenotype, we analysed the frequency and total cell count of the compartments HSC, MPP HPC1, HPC2 and LMPP (Figure 4.35 D, F). While we observed a depletion in the frequency and cell count of HSCs and LMPPs (Figure 4.34 D, F), we noted an expansion of MPP, HPC1 and HPC2 in the spleen of *Zeb1* KO mice (Figure 4.34 D, F). This preliminary data indicate extramedullary haematopoiesis is regulated by *Zeb1* during ageing. These data also suggest that during ageing *Zeb1* deficiency causes an accumulation of MPPs in the spleen, including that of lymphoid biased HPC1 that leads to a block in LMPP formation.
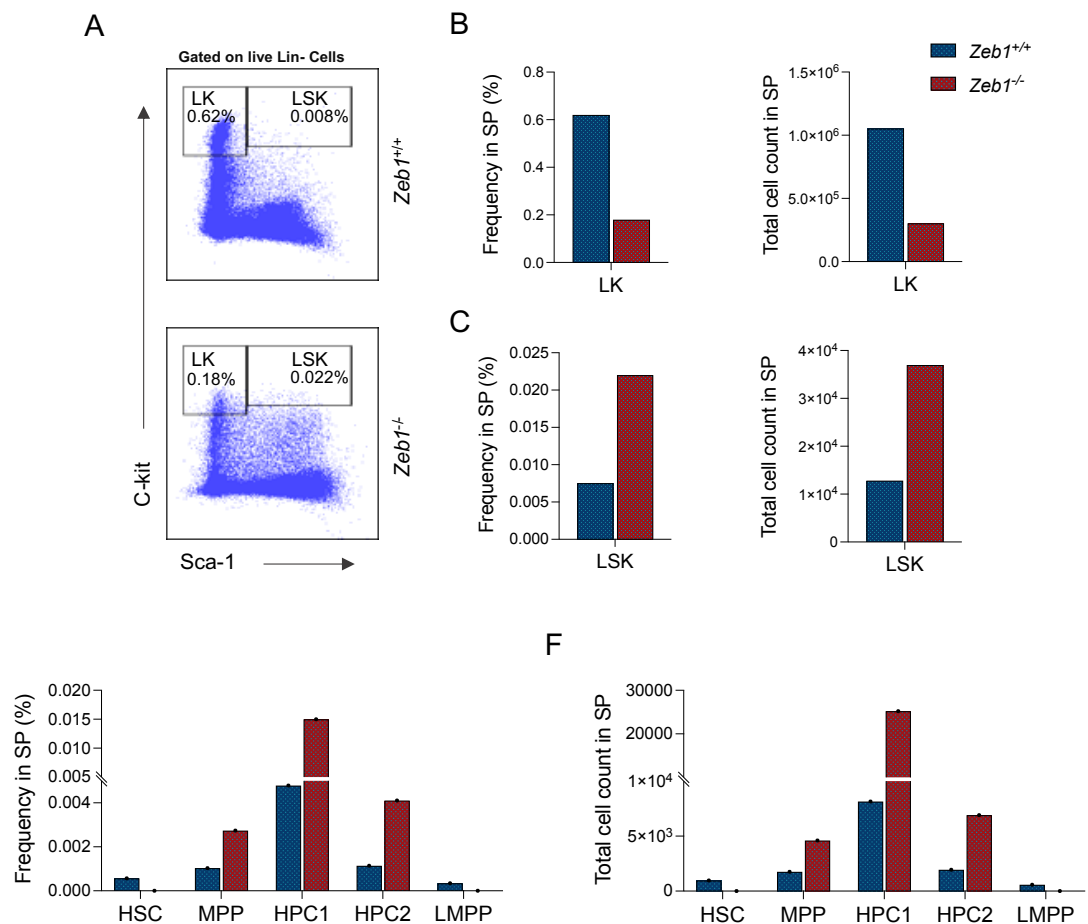
Figure 4.34 Prolonged *Zeb1* deficiency causes an increase in MPP, HPC1 and HPC2 in the spleen. Representative FACS plots of control (*Zeb1*^{+/+}) and *Zeb1*^{-/-} LK (Lin- c-kit+ sca1-), LSK (Lin- c-kit+ sca1+) population (A), the analyses show a reduction in frequency and total cell count of LK and increase LSK populations (B, C). Reduction in frequency and total cell count of HSC and LMPP and increase in frequency and the total cell count of MPP, HPC1 and HPC2 (D, F).

4.4 Discussion

In order to more accurately study the role of *Zeb1* in long-term HSC maintenance, we generated a *Vav*-iCre+ mouse model that deletes *Zeb1* in HSCs at day e11.5 of embryonic development. This model contrasts with our previous studies using *Mx1*-Cre mediated conditional deletion that was used to examine the impact of acute *Zeb1* deletion in adult HSCs. However, the impact of *Zeb1* on HSC functioning is largely consistent between these conditional deletion models, with *Zeb1* regulating HSC function and, in particular, the multi-lineage differentiation capacity of HSPCs, as evidenced by immunophenotyping and functional analysis. The *Vav*-iCre model developed here additionally and specifically revealed haematopoietic specific defects in erythroid and B-cell differentiation and broad immunodeficiency beyond T-cell defects previously associated with *Zeb1* deficiency. Notably, the crucial importance of *Zeb1* to erythroid differentiation from HSCs is illustrated by the development of anaemia in mice lacking *Zeb1* in HSCs, which is one possible cause of the fatality experienced during embryonic development and ageing of *Zeb1*$^{-/-}$ mice.

The cause of the developmental fatality in mice engineered to be deficient in *Zeb1* is unclear and will require further investigation. In another study, sub-Mendelian rates of survival were also observed in intercrossing *Zeb1* conditional mice (*Zeb1*fl/fl) with *Tie2*-Cre and hematopoietic-restricted *Vav*-iCre mouse models on a pure C57Bl/6 inbred background (Wang et al. 2021b), suggesting the cause of embryonic/neonatal fatality was linked to *Zeb1* deletion in either endothelium or HSCs. Given that the *Vav*-iCre system deletes *Zeb1* early in HSC development, our data suggests the specific requirement for *Zeb1* during HSC ontogenesis. Further studies are needed to examine the requirement for *Zeb1* in HSCs from AGM, the initial site of HSC emergence (de Bruijn 2000), and foetal liver, a site of HSC proliferation and expansion prior to migration to BM(Lewis et al. 2021). Given the known role of *Zeb1* regulating cellular migration (Drake et al. 2009; Wang et al. 2019b; Guo et al. 2022; Perez-Oquendo and Gibbons 2022). it will be of interest to further explore the impact of HSC/haematopoietic cell trafficking between these and other sites of haematopoietic development; interestingly,

preliminary evidence suggests *Zeb1* is specifically necessary for hematopoietic cell migration from the dorsal aorta to the foetal liver.

The anaemic phenotype of *Zeb1*$^{-/-}$ mice, observed in mice aged 8-12 weeks, could have its root at any stage of the hematopoietic differentiation, such as with the production of HSCs in the BM with HSCs being unable to mature into progenitor cells, at the committed progenitor cell stage (when the cells are dividing and differentiating into specific blood cell types) or with the maturation of developing red blood cells (erythroblasts) at the final stage of development prior to being released into the bloodstream. By immunophenotyping, we identified differentiation specific effects of *Zeb1* related to maturation of early and late erythroblasts rather than a defect in the incipient lineage commitment of HSCs to the erythroid lineage. However, transcriptional programming of *Zeb1*$^{-/-}$ HSCs showed an altered erythropoietin signalling and a gene signature associated with anaemia. An interpretation of this data is that *Zeb1* is likely required for both erythroid lineages priming in HSCs (Orkin 2003) and the maturation of erythroblasts but it is expendable for the production of committed erythroid progenitors as *Zeb1* loss may be compensated for in erythroid progenitors by other more essential erythroid transcription factors such as GATA1 (Gutiérrez et al. 2020).

Our results using the Akashi analysis show a reduction in the proportion and absolute cellular quantity of MEPs, CMPs, and GMPs in *Zeb1* KO mice, indicating impaired development of myeloid progenitor cells in the bone marrow (BM). In contrast, the Pronk analysis shows no differences in frequency and total cell count for all subsets analysed, including Pre GM, Pre MegE, Pre CFU-E, GMP, and MkP. This suggests that Zeb1 may not have a specific role in early restriction to myelo-erythroid progenitors, and the myeloid and erythroid defects observed in *Zeb1* KO mice are independent of these progenitor subsets. In other words, the Akashi model indicates a specific role for *Zeb1* in the development of MEPs, CMPs, and GMPs, while the Pronk model does not show any specific role for *Zeb1* in these subsets, particularly GMPs. Studies have suggested that the Pronk model may be more specific for analysing the development of myeloid cells than the Akashi model. For example, the common myeloid progenitor (CMP) stage in the Akashi model has been shown to be a mixture of granulocyte-macrophage

progenitor (GMP) cells, and the GMP stage in the Akashi model is not restricted to the granulocyte-macrophage lineage. In contrast, the Pronk model includes the analysis of pre-granulocyte-macrophage progenitor (Pre GM) cells, which are thought to be more specific for the granulocyte-macrophage lineage, and GMP cells, which are restricted to the granulocyte-macrophage lineage. Thus, the Pronk model may provide a more specific and accurate analysis of the regulation and development of myeloid cells (Akashi et al. 2000; Pronk et al. 2007).

While we have pinpointed erythroid specific defects leading to anaemia in $Zeb1^{-/-}$ mice, we cannot completely exclude the possibility anaemia may independently be symptomatic of immunodeficiency that is observed in these animals. Indeed, previous evidence suggested that $Zeb1$ deficiency affected lymphoid lineage commitment and T-cell differentiation in particular (Hidaka et al. 2008; Almotiri et al. 2021). In this chapter, we were able to further explore these alterations by inspecting several lymphoid compartments, where we observed decreases not in only CD4+ and CD8+ T-cell subsets, as described before (Takagi et al. 1998a), but also decreases innate lymphoid cells NK1.1 and NKT frequency in the SP, BM and PB. Interestingly, there was an increase in B cell frequency in PB, SP and BM while we observe a non-significant tendency of B cells to increase in cellularity in the BM, suggesting that $Zeb1$ is a critical regulator of B-cell differentiation. After $Zeb1$ deletion, loss or deregulation of lymphoid-specific hematopoietic cells suggests that this lineage could have alterations in apoptosis or differentiation and/or no new lymphoid-specific cells were derived from the CLPs or LMPPs (MPP4), both of which were reduced in our model. Notably, $Zeb1$ deficient HSCs appear to expand and are more lymphoid biased, suggesting a block in the transition to lymphoid progenitors that is supported by our analysis of CD34 and CD135 expression in LKS showing that these markers are decreased (which enriches for LT-HSCs) as opposed to increased (which selects for LMPP). Overall, the increase in CD34- and CD135- in LSK suggests that $Zeb1$ negatively regulates the differentiation of CD34-CD135- HSCs into its downstream lymphoid progenitors. As both LMPPs and CLPs (which were also reduced in $Zeb1^{-/-}$ mice) express high levels of CD135 and CD127 and we didn't observe a change in the CD127 frequency, we can hypothesise that $Zeb1$ mediated regulation of lymphoid progenitors is likely to be critically regulated

CD135. It is also interesting to note that in comparison to *Zeb2*, prior to committing to further myeloid and lymphoid lineages (MPP2 and MPP4/LMPP respectively), short-term HSC (ST-HSC)/multipotent progenitor (MPP1) cells appear to have higher amounts of *Zeb1* mRNA (Wang et al. 2021b). This suggests that *Zeb1* but not *Zeb2* is required for developmental commitment towards lymphoid lineage and that *Zeb2* is unable to compensate for the loss of *Zeb1*.

ILC2s are a subset of type 2 immune cells that can detect cytokines, lipids, neuropeptides, and hormones in the local environment but do not contain antigen-specific receptors (Moro et al. 2009; Xue et al. 2014; Cardoso et al. 2017; Klose et al. 2017; Laffont et al. 2017; Wallrapp et al. 2017). *Zeb1 Vav*-iCre mice had enhanced ILC2 progenitor numbers and reduced ILC2s. Recently, it was discovered that in the steady state, immature ILC2s in the bone marrow (BM) express elevated levels of RANKL and facilitate the differentiation of osteoclasts (Momiuchi et al. 2021). Since *Zeb1* regulates ILC2Ps and reduced ILC2s, in *Zeb1 Vav*-iCre mice the increase in the number of ILC2Ps could lead to diminished osteoclastogenesis. Mechanistically, this could be happening due to a downregulation in genes involved in this pathway, such as those we observed in our RNA-seq of *Zeb1* deficient HSCs. In turn, this can also translate to the fragile bone we observed in our mouse model. We may also suggest that this mechanism is present in the *Zeb1* Vav-iCre mouse model, as the RNA-seq results point to an increase in pro-inflammatory cytokines related such as IL-6 and TNF-a, which was further validated in the whole blood of these mice. If the regulatory balance of osteoclastogenesis is disrupted, it can lead to osteoporosis or fragile bone, as observed in *Zeb1* KO mice.

In terms of other lymphoid cells regulated by *Zeb1*, we observed that the quantity and proportion of bone marrow B220+ B cells were dramatically increased in *Zeb1* KO mice. When we used flow cytometry to further investigate the role of *Zeb1* in the formation of adult B cells, we found Pre-pro early precursor B cells were significantly reduced in the bone marrow of *Zeb1 Vav*-iCre mice, while no differences were observed in pro or epre B cells. The most interesting finding was the increase in pre-B cells in both the spleen and bone marrow, which may suggests a role for *Zeb1* in pre-B cell proliferation/maturation, as the spleen is a

site for B-cell maturation (Cariappa et al. 2007). Given the overlap between the precursor cells of pre-pro B cells and CLPs(Nutt and Kee 2007), and *Zeb1*'s known role in reducing CLP numbers (Almotiri et al., 2021), it is reasonable to suggest that *Zeb1*'s function extends to the first identifiable B cell-specified progenitors that arise from CLPs, namely the pre-pro B cells(Nutt and Kee 2007), and that the observed reduction of pre-pro B cells in *Zeb1* KO mice is related to the decreased CLP numbers.

In this chapter, we also present evidence that *Zeb1* regulates extramedullary haematopoiesis as evidenced by smaller spleen weight, hypocellularity and altered architecture and structural alignment. Contrasting to the expansion of HSCs observed in *Zeb1* KO BM, depletion of HSCs was noted in the spleen together with depletion of other HPSC subsets. Though the reason for this behaviour is unclear, we may hypothesise that *Zeb1* mediated regulation of extramedullary haematopoiesis may be a consequence of *Zeb1's* known role in EMT and the control of cellular migration (Drake et al. 2009; Wang et al. 2019b; Guo et al. 2022; Perez-Oquendo and Gibbons 2022).

In HSC transplant experiments, we found that long-term *Zeb1* expression is required for HSCs to carry out the multi-lineage differentiation *in vivo* under conditions of stress. Though *Zeb1* KO donor contribution was decreased for all examined subsets in the bone marrow (BM) and the spleen (CD4 and CD8 T cells, B cells, monocytes, and granulocytes), statistical significance was consistently achieved throughout all time points only for lymphoid lineages rather than the myeloid lineages, which contrasts with our previous findings in the *Mx1-Cre* model where *Zeb1* was deleted acutely in HSCs (Almotiri et al. 2021). The duration of *Zeb1* deletion in HSCs in the acute versus chronic setting in this chapter may be the cause of these variations, suggesting that long-term maintenance of HSC differentiation in transplantation mediated by *Zeb1* is more important for lymphoid rather than myeloid differentiation. This may also be a reflection of the different cellular and molecular alterations occurring over time following *Zeb1* deletion.

We conducted RNA-seq on *Zeb1$^{-/-}$* HSCs to explore the transcriptional programming underpinning the HSC immunophenotypic and functional defects.

According to RNA-seq data in HSCs, Zeb*1* deletion resulted in an upregulation of 47.6% of all DEGs, which is consistent with the idea that *Zeb1* primarily functions as a transcriptional repressor (Zhang et al. 2015b). Our findings revealed that several genes involved in cytoskeleton and polarity, as well as cell adhesion (*Epcam*, *Cdh1*, and others), were expressed more frequently. The gene encoding for the Epithelial cell adhesion molecule EpCAM was the most highly elevated in our dataset. EpCAM preserves stemness in mouse embryonic stem cells (ESCs) and controls a number of cellular functions, including proliferation, differentiation, cell cycle, and adhesion. It can also function as an oncogene or a tumour suppressor in epithelial cancer (Schnell et al. 2013a). Our RNA-Seq results support the idea of *Zeb1* playing a crucial role in regulating genes related to cell adhesion and polarity, and its deficiency leads to the development of a unique gene signature in HSCs that may result in an epithelial-like phenotype.

We found a *Zeb1* mediated gene signature in HSCs associated with atherosclerosis. Of relevance to this, *ZEB1* has been implicated in the development and progression of atherosclerotic cardiovascular disease (Wesseling et al. 2018; Li et al. 2021a), where it prevents the development of atherosclerosis by controlling central processes associated with atherosclerotic plaque development e.g. endothelial cell angiogenesis, endothelial dysfunction, monocyte-endothelial cell interaction, macrophage lipid accumulation, macrophage polarisation, monocyte-vascular smooth muscle cell (VSMC) interaction, VSMC proliferation and migration, and T cell proliferation (Li et al. 2021a). Why an atherosclerosis gene signature appears to be regulated by *Zeb1* in HSCs is unclear, but it may be linked to the phenomenon of clonal haematopoiesis of indeterminate potential (CHIP). CHIP is linked to acquired mutations in crucial haematopoiesis genes, including *Dnmt3a*, *Tet2*, and *Asxl1* that disrupt HSC function during ageing and cause a mutant haematopoietic clone to expand leading to a higher risk of developing cardiovascular illnesses and blood cancers (Genovese et al. 2014; Heuser et al. 2016; Bhattacharya and Bick 2021; Marnell et al. 2021). While there is yet no clear link between *Zeb1* and CHIP, it is possible to suggest that *Zeb1* mutations could allow mutated cells to be able to proliferate, expand and generate a clone, as observed in the mouse model used in this chapter. Alternatively, *Zeb1* may indirectly affect the onset or

progression of CHIP due to the crucial role it plays in regulating haematopoiesis and possible deregulation of this regulation that occurs through CHIP mutations.

We also found that *Zeb1*-deficient HSCs were enriched in the PTEN signalling pathway. One of the most frequently altered tumour suppressor genes in malignancies of humans is *PTEN* (Wang et al. 2015). PTEN is crucial for controlling hematopoietic stem cells because it inhibits the PI3K/AKT/mTOR pathway (Milella et al. 2015). PTEN is crucial for preventing leukemogenesis, particularly T-cell acute lymphoblastic leukaemia (T-ALL) (Wu et al. 2020). PTEN also gives rise to a mixed phenotype leukaemia/myeloproliferative disorder in mice depending on the Cre strain that is being used (Wu et al. 2020). In prostate cancer, *Zeb1* was found to have an immune evasive role correlated with the activation of downstream pathways modulated by PTEN and ERG (Chaves et al. 2021). p53 signalling was also activated in our RNA-seq dataset and other labs have shown that by using inhibiting p53, the inhibitive effect of ZEB1 suppression on the PTEN/PI3K/AKT signalling pathway can be effectively reversed (Li et al. 2021b). Thus, as *Zeb1* has been hypothesised to be a tumour suppressor in AML (Almotiri et al. 2021), potential therapeutic targeting of the p53/PTEN signalling axis may be effective where AML patients express *ZEB1* at reduced levels.

The data presented in this chapter further support a tumour suppressor role for ZEB1 in haematological malignancies. This is evidenced by the increased mortality of *Zeb1* KO mice, especially during ageing due to profound anaemia. When we analysed moribund *Zeb1* KO mice we found indicators of myeloid neoplasm development (Figure 4.X and data not shown) in the majority of mice and current efforts in the laboratory are placed on understanding the specific myeloid neoplasm that develops. Our working hypothesis is that aged *Zeb1* KO mice display a MDS/MPD/myelofibrosis type malignancy due to the observed (i) HSC exhaustion and BM failure (with prior HSC expansion), (ii) myeloid compartment expansion (iii) hypocellular spleen, lacking splenomegaly, with histological analysis revealing fibrosis in the spleen (data not shown) and (iv) profound anaemia. It is worth noting that *Zeb1* has been linked to ageing in other studies. Previous evidence shows that *Zeb1* plays a part in inducing senescence in fibroblasts, epithelial cells, and cancer cells (Liu et al. 2008; De Barrios et al. 2017; Swahn et al. 2023). *Zeb1* activates the p53 pathway (Li et al. 2021b) (which

is activated in our HSC RNA-seq data) and increases the production of p21, a cyclin-dependent kinase inhibitor that is a crucial senescence mediator. Moreover, *Zeb1* has been linked to the promotion of senescence in the context of ageing and age-related illnesses including atherosclerosis (Li et al. 2021a). Furthermore, EMT related genes, like *Zeb1*, have been linked to fibrosis (Imran et al. 2021) playing a critical role in the age-related development of fibrosis in the heart and lungs (Zheng et al. 2020a).

One of the aged *Zeb1* KO mice analysed displayed an atypical phenotype compared to others in the cohort and young adult mice, including splenomegaly, a startlingly high frequency of CD4+ cells in the bone marrow and a decrease in the frequency and number of CD8+ cells in the spleen. It is well known that *Zeb1* has a role in CD4+ T cell leukaemia and early mouse studies showed that *Zeb1* was essential for mediating T cell development, most likely by suppressing E box-containing genes like *Cd4, Il2, Gata3, and Itga4* (Williams et al. 1991; Brabletz et al. 1999; Grégoire and Roméo 1999; Postigo and Dean 1999). Our findings suggest that this mouse may be exhibiting a phenotype resembling CD4+ T-cell lymphoma/leukaemia, as observed in *Zeb1ΔC-fin* mice which spontaneously develop CD4+ T-cell lymphoma at an older age. In our aged *Zeb1* KO mouse, there was a decrease in the frequency of the CD150hi (myeloid biased) and CD150int (balanced) populations and an associated expansion of CD150lo (lymphoid biased) HSCs. We hypothesise that the increase of CD150lo/- HSCs could be linked to the increase of CD4 or CD4+ T-cell lymphoma/leukaemia and this requires further investigation. A future focus of further studies will also be the detailed inspection of PB and lymph nodes in this mouse model to distinguish between lymphoid leukaemia and lymphoma. In conclusion, our data currently suggest that *Zeb1* KO mice, on ageing, generate a mixed myeloid and lymphoid malignancy phenotype akin to PTEN mouse models (Lee and Pandolfi 2020) (Lee et al. 2020). The relevance to blood cancer patients expressing reduced ZEB1 is unclear. Nonetheless, the data presented here are consistent with *Zeb1* acting as a tumour suppressor in select haematological malignancies.

CHAPTER 5: EMT transcription factor *Zeb1* plays a critical role in T-cell differentiation from haematopoietic stem cells during ontogenesis.

5.1 introduction

Previous studies have demonstrated a potential role of *Zeb1* for proper T-cell development. As alluded to before, ZEB proteins are multi-domain transcription factors (Soen et al. 2018) whose different functions are domain-dependent. *Zeb1* contains seven zinc finger domains of the C2H2-type, each having around 23 amino acids. The protein, which is composed of 1117 amino acids, features four that are clustered at the N-terminal end (ranging from amino acid 150 to 272) and three located close to the C-terminal end (ranging from amino acid 88 to 959) (the numbering system corresponds to the mouse sequence). A homeobox domain is located close to the protein's core (aa 559-618). Early research by the team of H. Kondoh, utilising two separate *Zeb1*-KO mice where different sections of the *Zeb1* sequence were disrupted, provided the first evidence that *Zeb1* may fulfil one or more roles in a domain-dependent manner (Higashi et al. 1997; Takagi et al. 1998b).

In the first mouse model, the *Zeb1* homozygous null mutant mice (Null–LacZ or *Zeb1*$^{-/-}$) are born alive but die very shortly after birth (Figure 5.16) (Takagi et al. 1998a). Most defects are related to the skeleton (such as short limbs and developmental retardation). Regarding T-cell development, there is a significant drop in thymocytes at E18.5 and a smaller, hypocellular thymus with no histological distinction of the medulla and cortex, and only one-tenth as many thymocytes in comparison to wild-type mice (Takagi et al. 1998a).

Conversely, animals lacking *Zeb1's* cluster of C-terminal zinc fingers (C-fin) and Glu-rich region (*Zeb1* ΔC727/ΔC727) did not exhibit the severe skeletal abnormalities seen in *Zeb1*$^{-/-}$ mice (Figure 5.16)(Higashi et al. 1997). These zinc-finger domains are crucial for high-affinity DNA-binding in vitro (Remacle et al. 1999), unlike the homeodomain located at the centre of the protein. Homozygous C-fin mutant embryos (*Zeb1* ΔC727/ΔC727) and adults at 6 weeks old exhibit a decrease in total cell quantity in the thymus, as well as a decrease in the c-kit^{+} DN population, DN2, and DN3, in addition to a decrease in T cells in the spleen and lymph nodes (Higashi et al. 1997). Thymi of surviving *Zeb1* ΔC727/ΔC727 animals were smaller and included 0.2% to 1% of the number of thymocytes reported in wild-type mice (Higashi et al. 1997) and similar to the thymocyte

number observed in *Zeb1*^{-/-} (Null–LacZ) mice. In *Zeb1* ΔC727/ΔC727 thymus histological sections, the medulla and cortex could not be distinguished. Although there was a tendency for lower cellularity in *Zeb1* ΔC727/ΔC727 animals, spleen size and cellularity were comparable between *Zeb1* ΔC727/ΔC727 and wild-type mice (Higashi et al. 1997). In addition, the authors observed that the number of c-kit^{+} thymocytes decreased (Higashi et al. 1997). In Zeb1 ΔC727/ΔC727 mice, the majority of mature T cells were CD4^{+}, as reported by Higashi et al. in 1997. This finding is consistent with the ability of Zeb1 to bind to an E-box motif in a CD4 enhancer and inhibit transcription, as demonstrated by Brabletz et al. in 1999. Additionally, forward light scatter analysis indicated a larger population of DP thymocytes and a significantly lower population of DN thymocytes in Zeb1 ΔC727/ΔC727 mice compared to Zeb1 ΔC727/+ animals (Higashi et al. 1997).

Apart from these two initial mouse models, other *Zeb1* knockout models have been developed targeting different regions of the protein. The chemically induced (ENU) cellophane mouse model (*Zeb1* cellophane) has a point mutation (T ⇒ A) that causes a tyrosine to be changed to a stop codon in *Zeb1*. After amino acid 901, the C-terminal 216 amino acids of the CZF domain and the activation region are absent from the shorter ZEB1 protein as a result of the cellophane mutation, which truncates ZEB1. As a result, the ZEB1 protein becomes hypomorphic (Figure 5.16) (Arnold et al. 2012). The cellophane mouse model exhibits early T-cell differentiation block, alterations in thymic cell subsets, increased DN and SP thymocyte frequencies, and decreased DP thymocyte frequencies (Arnold et al. 2012). It also has tiny, hypocellular thymi. While splenic NK cell frequency is changed, splenic T cell frequency is unaffected. Similar to Zeb1 C727/C727 mice, cellophane mice have less severe skeletal defects than homozygous null mice, but they still have tiny, hypocellular thymi and more SP thymocytes than DP thymocytes (Arnold et al. 2012).

A conditional *Zeb1* knockout allele that permits gene inactivation in a tissue-specific and temporally regulated manner which is not possible in the analysis of a conventional knockout has since been generated (Brabletz et al. 2017a). Given exon 6 includes the coding sequences for a significant part of the protein core region, it was used as the foundation for creating a conditional *Zeb1* knockout

allele (*Zeb1*^{del/del}). LoxP sequences were added upstream and downstream of exon 6, consequently generating that exon 5 will be spliced into exon 7 on shortened transcripts produced by Cre-mediated deletion, leading to a premature stop of translation (Figure 5.16) (Brabletz et al. 2017a). With the use of this mouse model, *Zeb1* can be specifically deleted in mice in a way that is both tissue- and time-specific. The phenotype was consistent with previous observations using the conventional *Zeb1* knockout (*Null–LacZ* or *Zeb1*^{-/-}) with a complete block in translation (Takagi et al. 1998a).

The laboratory of Dr. Neil Rodrigues used a mouse model *Zeb1* has been genetically modified to contain conditional alleles, meaning that gene expression can be controlled. Additionally, the model includes an inducible *Mx1*-Cre system, which allows for gene deletion in response to inducersn (*Zeb1fl/fl*; *Mx1-Cre*⁺) (Figure 5.16). Here, *Zeb1* expression can be deleted in hematopoietic stem cells (HSCs) only and the function of *Zeb1* can be evaluated specifically in the hematopoietic system (Almotiri et al. 2021). The phenotypes that the authors observed in this mouse model include a smaller thymus and the absence of T-cells in *Zeb1*^{-/-} mice after transplantation of HSCs (Almotiri et al. 2021). This model of mice has shown that Zeb1 plays a crucial role in determining the fate of T cells and their ability to survive, resulting in a quick depletion of thymocytes and CD8⁺ T cell subsets. Prior research indicated that *Zeb1* is essential for the proper functioning of CD8⁺ T cells during infections (Guan et al. 2018b) and as a regulator of CD8⁺ EM in the bone marrow and peripheral blood and CD8⁺ CM T cells from the spleen (Almotiri et al. 2021). Effector memory T cells (EM cells) are located in the tissues and peripheral circulation because they lack the CCR7 lymph node-homing receptors (Woodland and Kohlmeier 2009). Central memory T cells (CM cells) are located at the lymph nodes and peripheral circulation. One characteristic used to identify effector and memory CD8⁺ T cells from naïve CD8⁺ T cells, in mice, is the enhanced expression of adhesion molecules such as CD11a and CD44 (Woodland and Kohlmeier 2009). Expression of CD62L, CCR7, and CD127 (IL-7R) is greater in naive CD8 T cells. Activated CD8⁺ T effector cells, on the other hand, downregulate these three proteins. In addition, effectors from memory T cells can be identified through the protein CD127 (Samji and Khanna 2017). The results from Almotiri et al. 2021 demonstrate that *Zeb1*

is a crucial transcriptional factor for the whole adult T cell repertoire, controlling cell survival during positive and negative selection in the thymus to early T cell commitment from HSPC BM progenitor subsets.

5.2 Aims

Zeb1 germline deletion in mice resulted in impaired T cell development (Higashi et al. 1997; Takagi et al. 1998a) and previous evidence suggests that *Zeb1* is required during adult T cell maturation in the adult haematopoietic system (Almotiri et al. 2021). However, there is a lack of evidence of the impact of *Zeb1* disruption during T-cell ontogenesis and if these impacts are intrinsic or extrinsic to *Zeb1* mediated regulation of T cell differentiation from haematopoietic stem cells (HSCs).

Therefore, the aims of this chapter are:

1. Investigate the impact of *Zeb1* deletion in HSCs at E11.5 on adult T cell development in the thymus through the use of the *Vav-iCre* system. Assess the T cell subsets and examine the early commitment of adult T cells. Specifically, the study will focus on analysing the CD4 and CD8 double negative and double positive populations in the thymus. Additionally, explore the function of *Zeb1* in T cell development in the thymus by analyze cell death, proliferation, and cell cycle.

2. Investigate how *Zeb1* deletion affects markers of both immunodeficiency and immunological ageing in adult T cell populations outside of the thymus, by analysing CD44 and CD62L expression on CD4^{+} and CD8^{+} T cells in peripheral blood, bone marrow, and spleen from both control and *Zeb1*^{-/-} mice that were eight to twelve weeks old.

3. To explore the molecular mechanism behind *Zeb1* function in common lymphoid progenitors (CLPs) and assess if transcriptional programming is perturbed in the BM prior to arriving in the thymus using Mx-Cre1 mice, with further validation of these results in the Vav-iCre model.

5.3 Results

Zeb1, a type of transcription factor belonging to the zinc finger homeobox E-box binding family, has been recognized as a crucial participant in the proper operation of hematopoietic stem cells and their ability to differentiate into multiple lineages (Almotiri et al. 2021). Previous data has shown that *Zeb1* has a key role in adult T lymphocyte development (Higashi et al. 1997; Takagi et al. 1998a; Almotiri et al. 2021), yet little is known about the function of ZEB1 in T-cells throughout ontogeny. To explore this issue, we employed a conditional genetic approach using the *Vav-iCre* system, which deletes gene expression at d11.5 of embryonic development (for more details on the generation of this model, please refer to 4.3.1). This *Vav*-iCre mouse model was used to explore the impact of *Zeb1* deletion in T-cell development.

5.3.1 *Vav-iCre* mediated *Zeb1* deletion resulted in adult impaired thymus cellularity and atrophy

Several macroscopical, immunophenotypic and histological experiments were conducted on *Zeb1$^{-/-}$* or *Zeb1$^{+/+}$* (WT) thymus initially. We obtained thymus samples from the 83.87% *Zeb1$^{-/-}$* mice that survived after weaning, aged from 8-12 weeks (Table 4.1) (Figure 5.1 A).

To assess the impact of *Zeb1* on thymocytes, we used a forward versus side scatter (FSC vs SSC) gating strategy in flow cytometry to identify cells of interest based on size and granularity. To identify lymphocytes, we drew a polygon in the bottom right corner of the plot (Figure 5.1 B) and observed a significant reduction in *Zeb1$^{-/-}$* thymus compared to WT, meaning that there are observable and significant changes in thymus cellularity (Figure 5.1 B, C). This leads to thymus atrophy with damage to the thymus architecture and no clear distinction between the medulla and cortex in *Zeb1$^{-/-}$* (Figure 5.1 D, F). Histopathological analysis shows that the cortex is absent in the *Zeb1$^{-/-}$* mice. This region is mostly made up of T-cells (Gartner and Hiatt 2011), suggesting that a lack of developing T-cells could be the cause for this absence (Figure 5.1 F). Moreover, thymus weight was reduced in *Zeb1$^{-/-}$* mice (Figure 5.1 E). Given that the thymus is the primary site

of the development of T cells, we therefore hypothesized that T-cells would be significantly altered in the *Zeb1^{-/-}* mice.
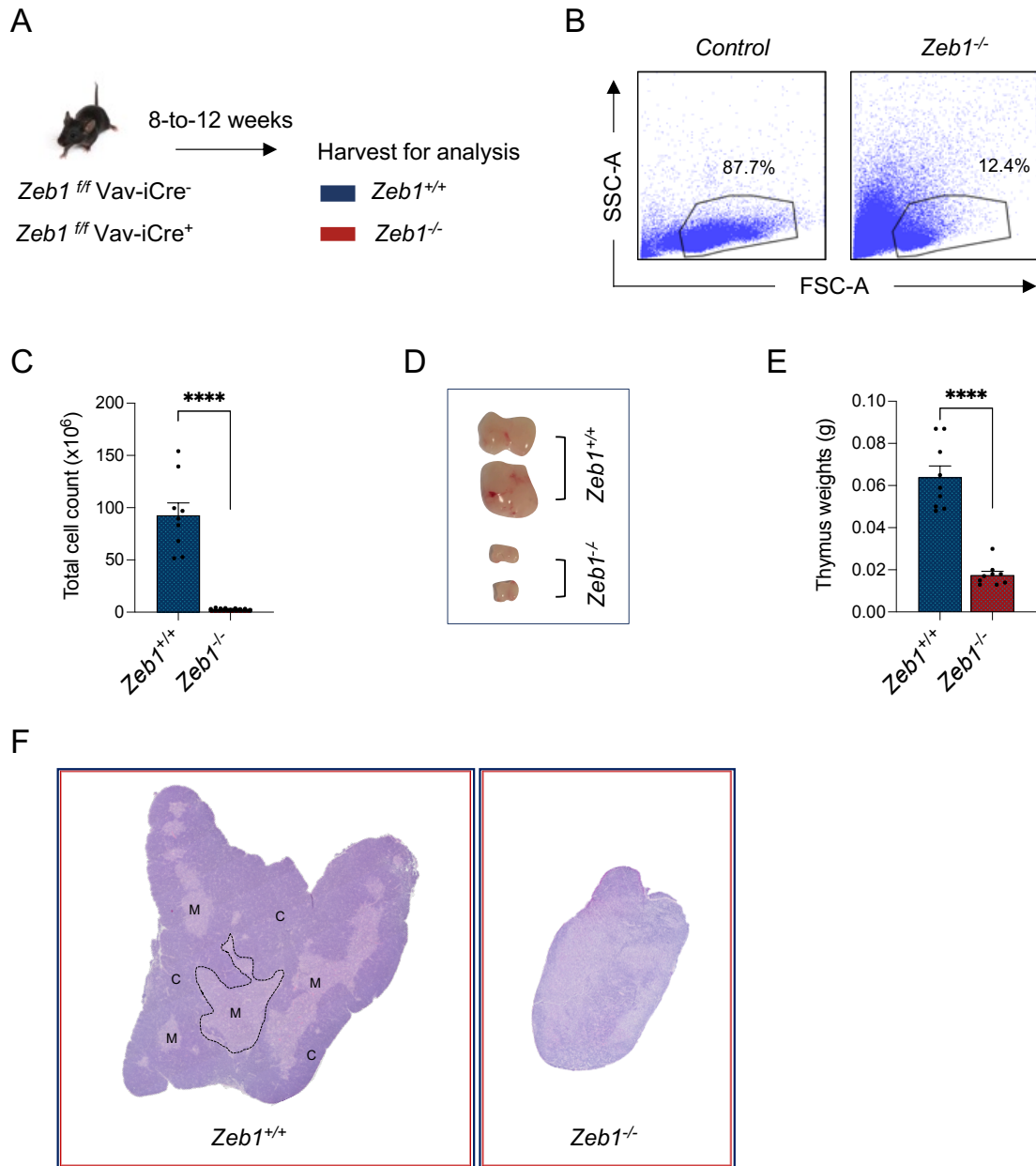
Figure 5.1 *Vav*-iCre mediated *Zeb1* deletion causes impaired thymus cellularity and thymus atrophy. 8-to-12 weeks old Zeb1f/f Vav-iCre+ and Control mice were harvested for analysis (generating experimental mice described in figure 4.1) (A). (B,C) FACS plots illustrative for the overall data of total thymocyte cells based on forward versus side scatter (FSC vs SSC) gating strategy, and total thymus cellularity. a representative picture for thymus size (D), Thymus weights (E), Thymus tissue section stained with haematoxylin and eosin, Zeb1+/+ has distinct medulla and cortex and Zeb1-/- shows damage thymus architecture (F). Data from 5-7 independent experiments (Control N=9, Knockout N=9). Error bars display the mean and SEM. Whitney U test was used to calculate significance as follows: *P < .05, **P < .01, ***P < .001, ****P <0.0001.

5.3.2 *Vav-iCre* mediated *Zeb1* deletion resulted in adult impaired T-cell development

To further explore the impact of *Zeb1* deletion on the T-cell subset, immunophenotypic analysis was performed. We used CD4 and CD8 expression to assess the developing T cell subsets in the thymus of *Vav*-iCre genetically modified mice (Resop and Uittenbogaart 2015; Kumar et al. 2018; Karimi et al. 2021).

We observed that the *Vav*-iCre mediated *Zeb1* deletion caused significant effects in the development in most T cell subpopulations (Figure 5.2). We observed an increased frequency of immature double-negative (DN) CD4– CD8$^-$ cells and mature single-positive (SP) CD4 (CD4$^+$) and SP CD8 (CD8$^+$) T cells, contrasting with a significant reduction in the proportion of double-positive (DP) CD4$^+$ CD8$^+$ cells in *Zeb1*$^{-/-}$ mice (Figure 5.2, B), suggesting a block in the DN to DP transition. Normalising for the smaller thymic cellularity observed in *Zeb1*$^{-/-}$ mice, cell counts revealed a significant reduction in DN, DP, CD4$^+$, and CD8$^+$ populations in the thymus of *Zeb1*$^{-/-}$ mice (Figure 5.2, C). The results suggest that *Zeb1* disruption during development leads to problems with differentiation at specific stages of T cell growth in the thymus. This shows that *Zeb1* is necessary for several moments in the maturation of thymocytes.
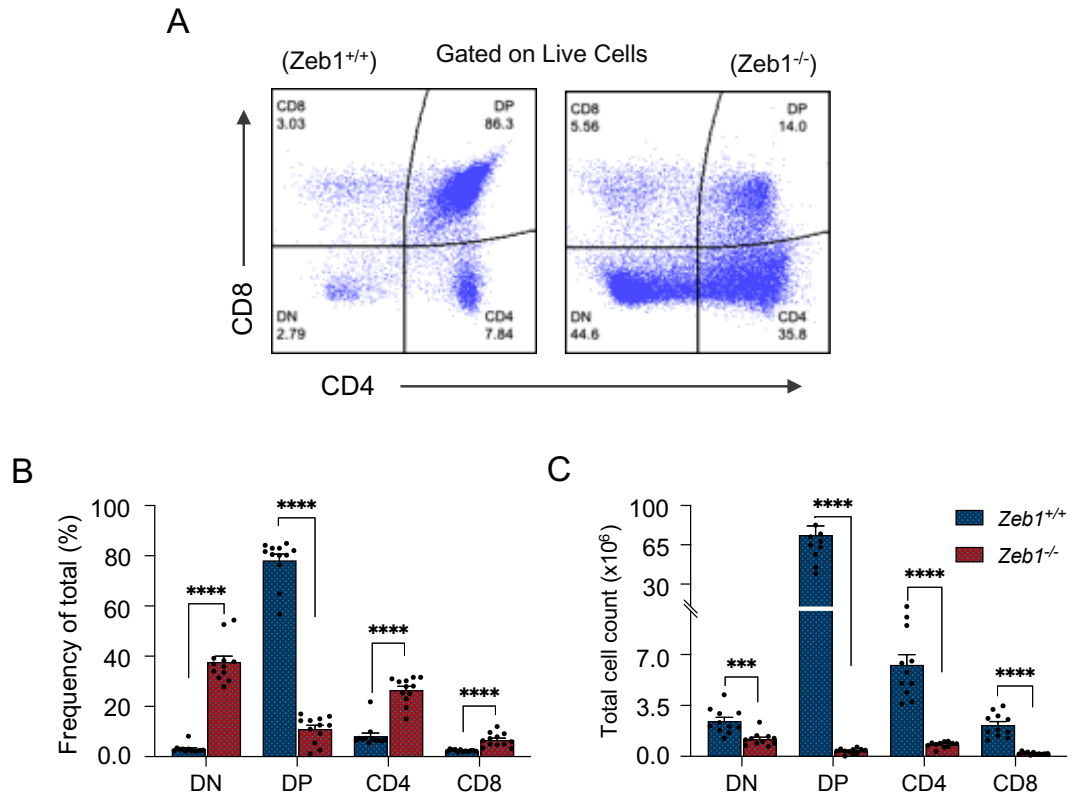
Figure 5.2 *Vav*-iCre mediated *Zeb1* deletion causes impaired T cell subsets development in thymus. FACS plots illustrative for the overall data of T cell subpopulations in the thymus of *Zeb1* deleted mice and control using CD4 and CD8 surface markers (A). T cells subset frequency in thymus (B) and total cell count (C). Data from 8 independent experiments (Control N=12, Knockout N=12). Error bars display the mean and SEM. Whitney U test was used to establish statistical significance according to the following: *P < .05, **P < .01, ***P < .001, ****P <0.0001

5.3.3 *Vav*-iCre mediated *Zeb1* deletion resulted in adult impaired DN cell subset in the thymus

Given that *Zeb1* ablation increased DN frequency, we further assessed the DN cell compartment, which represents the first stage of thymocyte selection, where immature T cell progenitors enter the thymus as double negative (DN) thymocytes that do not express CD4 or CD8 co-receptors.

The DN population can be divided into four subsets using CD44 and CD25 markers: DN1 (CD44+ CD25-), DN2 (CD44+ CD25+), DN3 (CD44- CD25+), and DN4 (CD44- CD25-) before they develop into DP cells and eventually mature into CD4⁺ or CD8⁺ cells. Analysis of cell markers showed an increase in DN1 cell frequency and a decrease in DN2 and DN3 cell frequency, as well as a decreasing trend in DN4 cell frequency in *Zeb1*⁻ᐟ⁻ mice, indicating that Zeb1 plays

a role in the differentiation of cells during the transition between DN1 and DN2/DN3 (Figure 5.3, B). Taking into account total cell count, we found additional evidence of a differentiation block in the transition between DN1 and DN2/DN3 in *Zeb1⁻/⁻* mice (Figure 5.3, C).
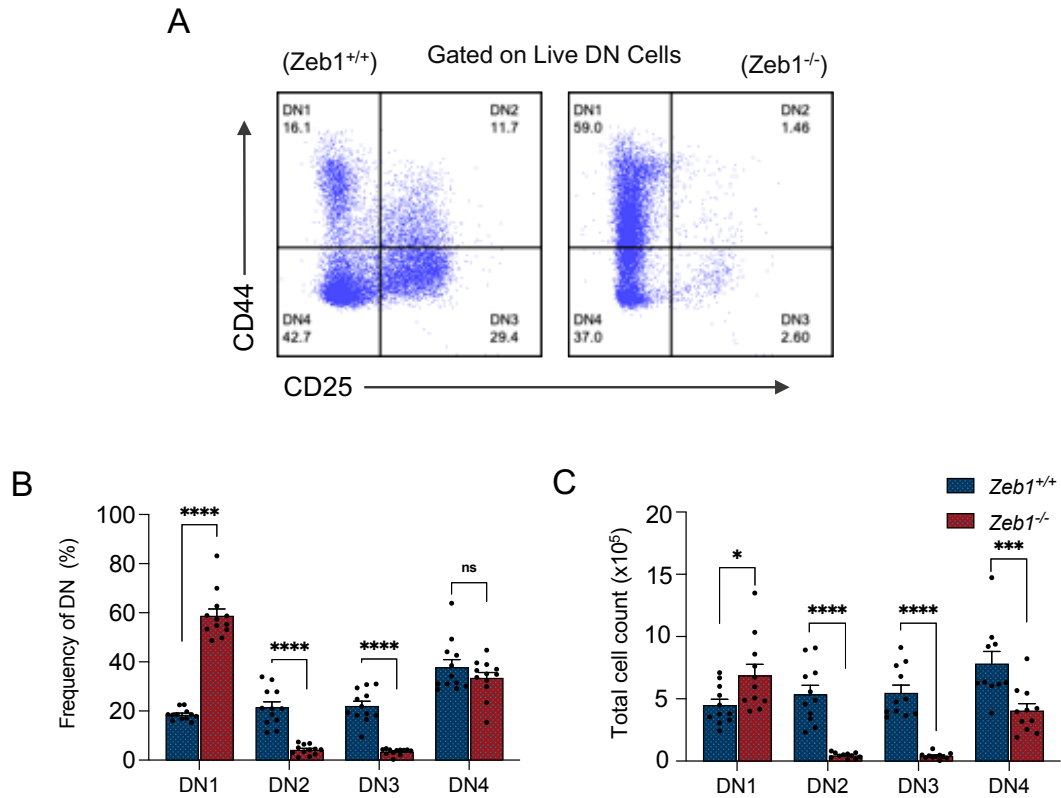
Figure 5.3 *Vav*-iCre mediated *Zeb1* deletion causes impaired DN cell subsets development in thymus. FACS plots illustrative for the overall data of DN cell subpopulations in the thymus of *Zeb1* deleted mice and control using CD44 and CD25 surface markers (A). DN cells subset frequency in the thymus (B) and total cell count (C). Data from 8 independent experiments (Control N=12, Knockout N=12). Error bars display the mean and SEM. Whitney U test was used to establish statistical significance according to the following: *P < .05, **P < .01, ***P < .001, ****P <0.0001

5.3.4 *Zeb1* is required for the survival of T-cells in the thymus and Vav-iCre mediated *Zeb1* deletion during development causes apoptosis in all subpopulations

To assess if reduced thymocyte and T-cell populations in the context of *Zeb1* deletion were caused by increased apoptosis, we next determined whether *Zeb1* is required for the survival of developing and mature T-cells in the thymus, as assessed by Annexin V assay. We found increased apoptosis in DN, DP, CD4+, and CD8+ populations (Figure 5.4, B), and also in DN1, DN2, DN3 and DN4 (Figure 5.4, C), demonstrating that *Zeb1* is indeed required for the survival of developing and mature T-cell subsets.
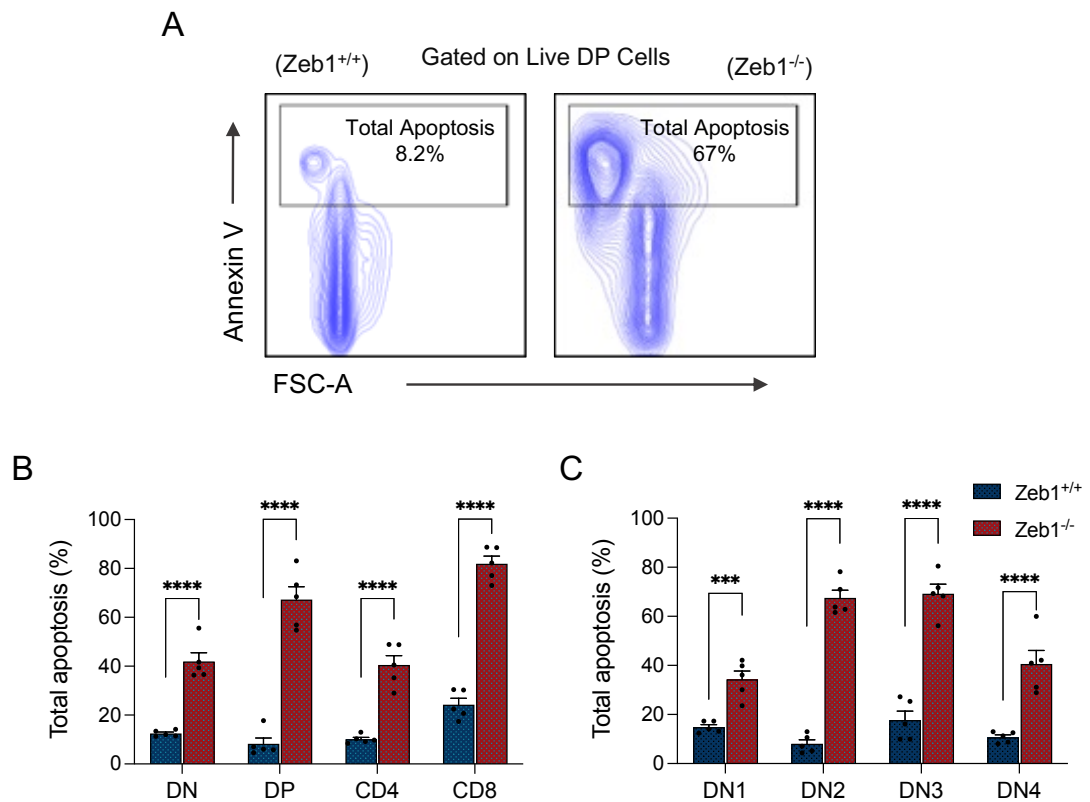
Figure 5.4 *Zeb1* is required for the survival of T cell subsets in the thymus. FACS plots illustrative for the overall data of apoptosis analysis of T cells subset using Annexin V (A). T cells subset total apoptosis (%) in thymus (B,C). Data from 3 independent experiments (Control N=5, Knockout N=5). Error bars show mean ± SEM. Holm-Šídák's multiple comparisons test was used to calculate significance as follows: *P < .05, **P < .01, ***P < .001, ****P <0.0001.

To explore the molecular mechanisms underpinning enhanced apoptosis in $Zeb1^{-/-}$ mice, we assessed the apoptotic marker FAS, a marker associated with T-cell apoptosis (Volpe et al. 2016), by flow-cytometry (representative plot in Figure 5.9, A). In a preliminary experiment using two mice from each genotype, increased apoptosis, as measured by the abundance of Fas$^+$ cells, was observed in DN, DP, CD4$^+$, and CD8$^+$ populations in $Zeb1^{-/-}$ mice (Figure 5.5, B). Analysis of FAS expression in DN subsets indicated elevated apoptotic levels in almost all DN compartments - DN1, DN2, DN3 – with the exception of DN4. (Figure 5.5, C). Thus, $Zeb1$ regulation of T-cell survival during T-cell maturation is, in part, mediated by FAS.
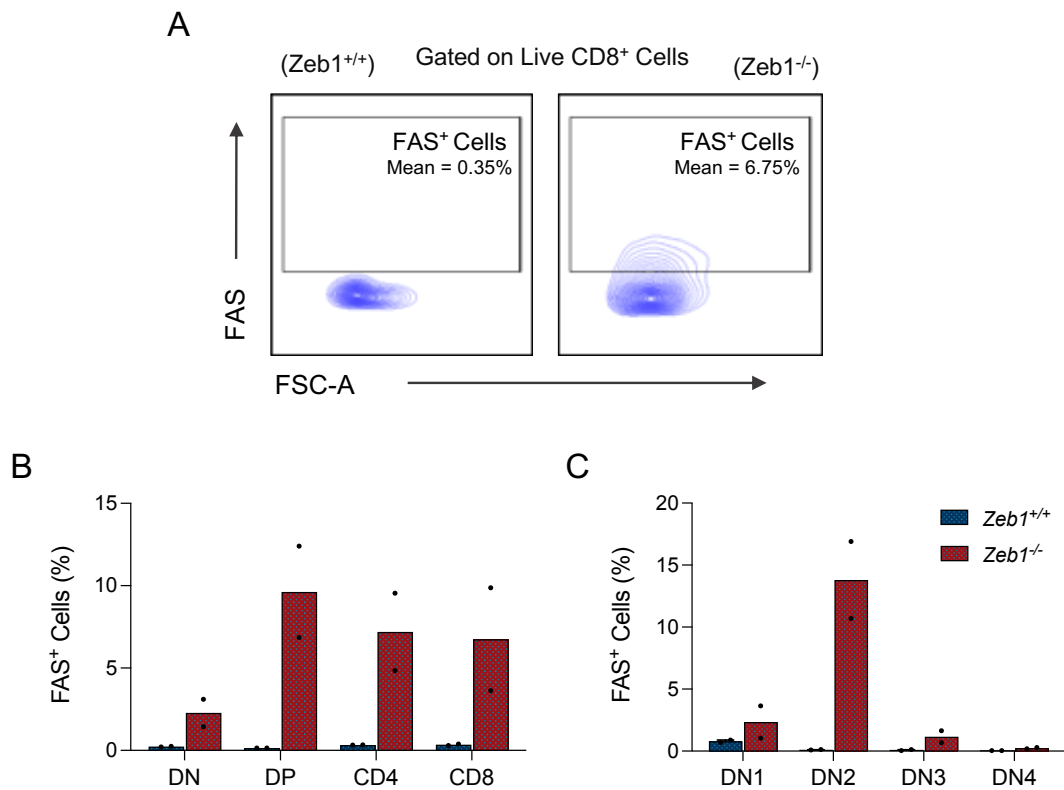
Figure 5.5 *Vav*-iCre mediated *Zeb1* deletion causes an increase in FAS+ frequency in T cell subsets cell in thymus. FACS plots illustrative for the overall data of FAS$^+$ cell gating strategy in the T cell subsets of *Zeb1* deleted mice and control (A). FAS$^+$ cells frequency in T cell subsets (B, C). Data from one independent experiment (Control N=2, Knockout N=2). Error bars show mean ± SEM.

5.3.5 Vav-iCre mediated *Zeb1* deletion during development causes cell cycle and proliferation abnormalities in developing T-cell subsets

Proliferation-associated proteins and/or nuclear proliferation antigens such as Ki-67 can distinguish between resting/quiescent and proliferating cell fractions. The Ki-67 antigen is seldom expressed in the G0 phase yet is extensively expressed in the nuclear area of proliferating cells (highest in G2 and early M phases), and rapidly destroyed throughout mitotic processes of anaphase and telophase (Gerdes et al. 1984) and is thus used as a marker for detecting proliferation. We, therefore, used Ki-67 as a marker to assess whether the diminution of T-cell subsets in mice lacking *Zeb1* was associated with a change in the state of the cell cycle.

In a preliminary analysis in two mice from each genotype, we measured proliferation using Ki67 as a marker of proliferation in T cell subsets from the thymus of *Zeb1*$^{-/-}$ mice. We found an increase in the frequency of proliferation in DP and CD4$^+$ cells, an overall reduction in the proliferation of DN cells and no change in the proliferation of CD8$^+$ cells (Figure 5.6, B). Interrogating the DN further, it was shown that DN1 and DN4 had reduced levels of Ki67$^+$ cells in *Zeb1*$^{-/-}$ mice, suggesting a more quiescent state in these compartments, while DN3 showed increased levels of Ki67$^+$ expression (Figure 5.6, C). These data demonstrate that *Zeb1* differentially regulates proliferation during the positive and negative selection of T-cells.
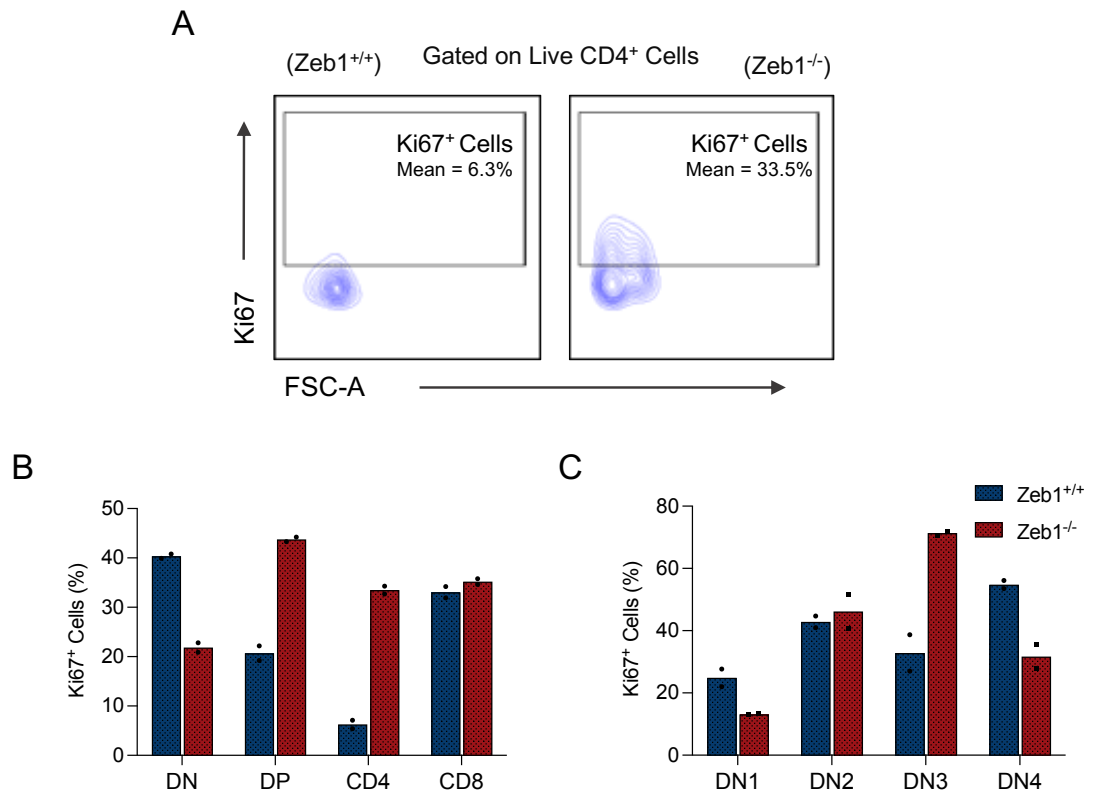
Figure 5.6 *Vav*-iCre mediated Zeb1 deletion results affect the cycle activity in the T cell subsets cells in thymus. FACS plots illustrative for the overall data of Ki67$^+$ cell gating strategy in T cell subsets (A). Frequency of Ki67$^+$ cells in T cell subset in the thymus (B,C). Data from one independent experiment (Control N=2, Knockout N=2). Error bars show mean ± SEM.

5.3.6 *Vav*-iCre mediated *Zeb1* deletion enhances the frequency of early T cell progenitors in the adult thymus

As the DN1 population increased upon *Zeb1* loss (Figure 5.2, B-C), we investigated the impact of *Zeb1* deletion on DN1 subpopulations, including ETPs, the first T-cell-restricted population to emigrate from the BM to the thymus. The frequency of the ETPs from *Zeb1*$^{-/-}$ mice was significantly increased (Figure 5.7, B) but the total cell counts of ETPs (Figure 5.7, C) from *Zeb1*$^{-/-}$ mice were unchanged in comparison to their wild-type counterparts.
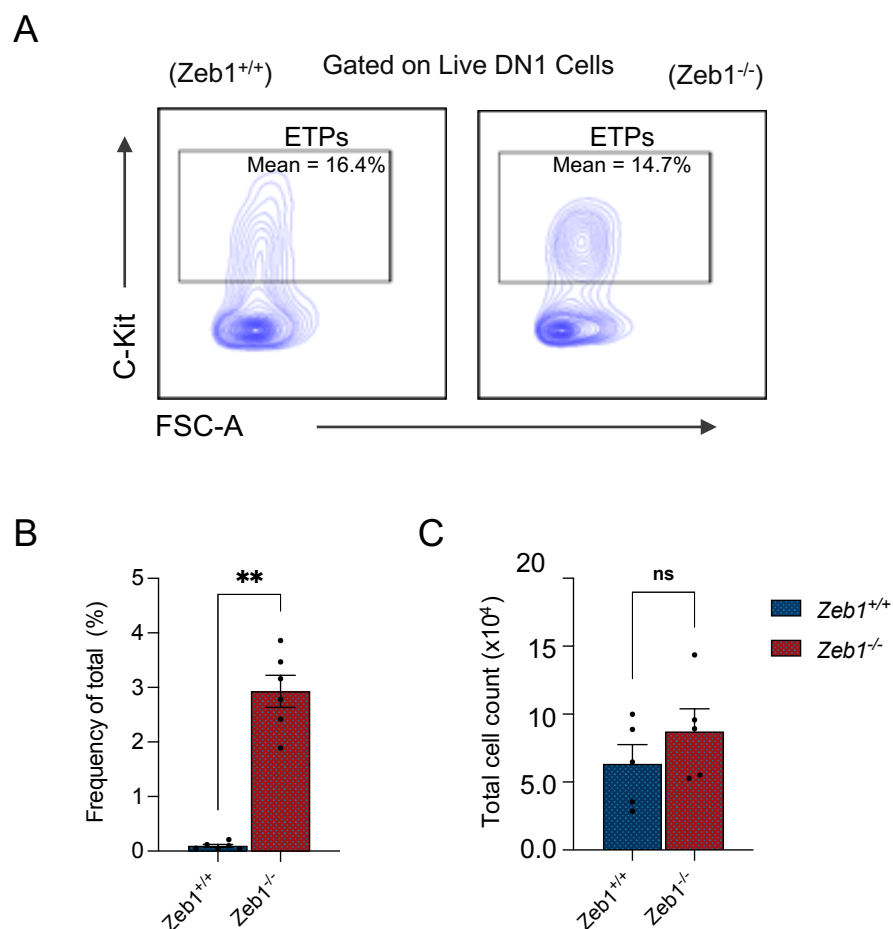
Figure 5.7 *Vav*-iCre mediated *Zeb1* deletion enhances the frequency of early T cell progenitors in the thymus. FACS plots illustrative for the overall data of ETPs in the thymus of *Zeb1* deleted mice and control using C-kit surface marker gated on DN1 (A). ETPs frequency in total thymocyte (B), and total ETPs cell count (C). Data from 3 independent experiments (Control N=6, Knockout N=6). Error bars show mean ± SEM. Mann Whitney test was used to calculate significance as follows: *P < .05, **P < .01, ***P < .001, ****P <0.0001.

5.3.7 *Vav*-iCre mediated *Zeb1* deletion causes impaired positive selection during T-cell development.

Given the impact of *Zeb1* on the potential block in the transition of cells going from DN to DP populations, we further assessed positive selection in the thymus from *Zeb1*$^{-/-}$ mice using flow cytometry-based analysis of TCRβ and CD69 expression (Hu et al. 2012). Expression of TCRβ and CD69 analysis of thymocytes gives rise to four distinct populations: The population of pre-selection DP thymocytes is represented by gate A (TCRβloCD69-), while gate B (TCRβintCD69+) represents a transitional population immediately after TCR engagement. The population of cells directly post-positive selection is represented by gate C (TCRβhiCD69+), and a more mature population of cells is represented by gate D (TCRβhiCD69-) (Figure 5.8, A) (Hu et al. 2012). Gate A (TCRβ^{lo}CD69$^-$) in a WT mouse is mostly made up of DP^{bright} cells, while gate B (TCRβ^{int}CD69$^+$) is mostly made up of DP^{bright} with some DP^{dull} and CD4$^+$CD8^{lo} cells. Gate C (TCRβ^{hi}CD69$^+$) is made up largely of DP^{dull}, CD4$^+$CD8^{lo}, and CD4SP cells, whereas gate D (TCRβ^{hi}CD69$^-$) is made up primarily of CD4SP and CD8SP cells (Figure 5.8, B). These gates are represented in a FACS plot in Figure 8, A and the frequency of results and total cell counts in Figure 5.8 C and D, respectively.

The process of positive selection initiates in the stage of DPbright and subsequently proceeds to the stage of DPdull following interaction with an antigen (Hu et al. 2012). After the DPdull stage, thymocytes undergo a transitional stage of CD4$^+$CD8lo before developing into either CD4SP or CD8SP thymocytes. If there is no presence of populations B and C, it suggests that there is no positive selection. Any alterations in the CD4SP/CD8SP ratio in population D may signify modifications in lineage commitment. The disappearance of populations C and D could be linked to issues with survival post-positive selection (Hu et al. 2012).

In Figure 5.8 (C), TCRβ^{lo}CD69$^-$ (Gate A) we observed a reduction in the frequency (Figure 5.8, C) and a significant reduction in total cell count (Figure 5.8, D) in the thymus of *Zeb1*$^{-/-}$ mice, clearly observed in a significant reduction of the DP^{bright} within the TCRβ^{lo}CD69$^-$ (Gate A) (Figure 5.8, E). This implies that

Zeb1 affects the initial stages of the positive selection process in a population of pre-selection DP thymocytes.

TCRβ^{int}CD69$^+$ (Gate B) shows an increase in the frequency (Figure 5.8, C) and a significant reduction in total cell count (Figure 5.8, D) in the *Zeb1*$^{-/-}$ genotype. As TCRβ^{int} CD69$^+$ Gate B primarily consists of DP^{bright} with some DP^{dull} and CD4$^+$CD8^{lo} cells and we found a significant reduction in total cell count (Figure 5.8, F), *Zeb1* appears to regulate the frequency of a transitional population directly after TCR engagement.

TCRβ^{hi}CD69$^+$ (Gate C) cells were decreased in frequency (Figure 5.8, C) and absolute number in *Zeb1*$^{-/-}$ mice (Figure 5.8, D). As TCRβ^{hi}CD69$^+$ (Gate C) primarily consists of DP^{dull}, CD4$^+$CD8^{lo}, and CD4SP cells, we investigated further and found a significant reduction in total cell count (Figure 5.8, G). Thus, *Vav*-iCre mediated deletion of *Zeb1* affects the population of cells directly post-positive selection.

TCRβ^{hi}CD69$^-$ (Gate D) shows no differences in the frequency (Figure 5.8, C) and a significant reduction in total cell count (Figure 5.8, D). The changes in populations C and D might imply that *Zeb1* disruption causes problems with survival following positive selection. As TCRβ^{hi}CD69$^-$ (Gate D) primarily consists of CD4SP and CD8SP cells, we further investigated this and found a significant reduction in total cell count, but no differences in the CD4:CD8 ratio within population D (figure 5.8, H, I). This latter result may indicate that ZEB1 is dispensable for lineage commitment following positive selection. Overall, the results from this analysis in our *Vav*-iCre mouse model reveal impaired positive selection in the thymus of *Zeb1*$^{-/-}$ mice.
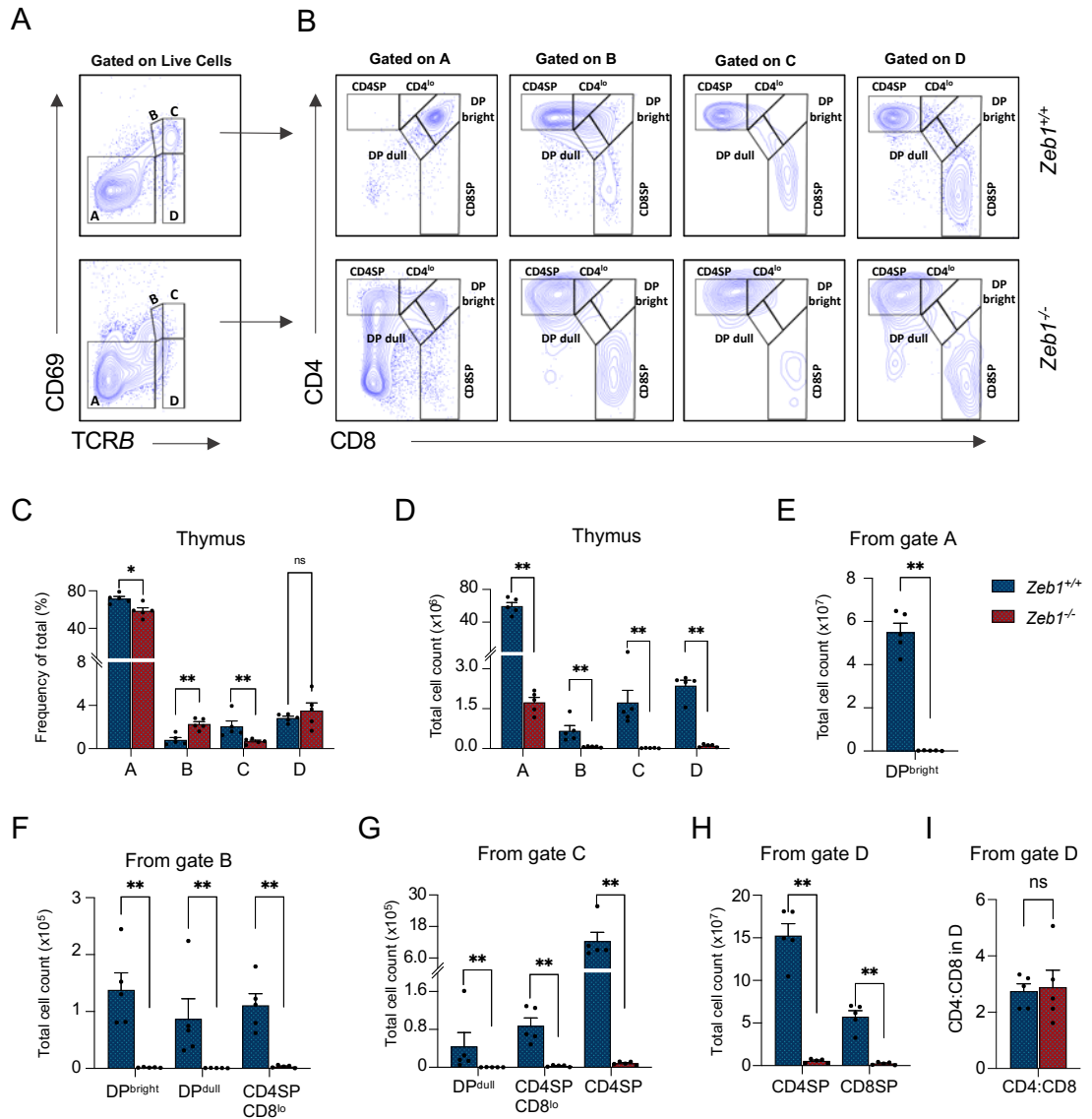
Figure 5.8 *Vav*-iCre mediated *Zeb1* deletion results in impaired positive selection in the thymus. The TCRβ by CD69 plot was used to identify four populations of thymocytes. Gate A (TCRβloCD69-) represents pre-selection DP thymocytes, gate B (TCRβintCD69+) represents transitional cells after TCR engagement, gate C (TCRβhiCD69+) represents cells after positive selection, and gate D (TCRβhiCD69-) represents mature cells. In a WT mouse, gate A is mostly made up of DPbright cells, gate B has DPbright, some DPdull, and CD4$^+$CD8lo cells, gate C has DPdull, CD4$^+$CD8lo, and CD4SP cells, and gate D has mostly CD4SP and CD8SP cells. The absence of populations B and C in *Zeb1$^{-/-}$* mice suggests a lack of positive selection, and the changes in the CD4SP/CD8SP ratio within population D may indicate changes in lineage commitment. (B). A,B,C,D gated cells frequency in thymus (C) and total cell count (D). Total cell count of DP^{bright} cells which gate A consists of (E). Total cell count of DP^{bright} with some DP^{dull} and CD4$^+$CD8^{lo} cells wich gate B primarily consists of (F). Total cell count of DP^{dull}, CD4$^+$CD8^{lo} and CD4SP cells wich gate C primarily consists of (G). Total cell count of CD4SP and CD8SP cells wich gate D primarily consists of (H), and the CD4:CD8 ratio within population D (I). Data from 4 independent experiments (Control N=5, Knockout N=5) Error bars display the mean and SEM. Whitney U test was used to calculate significance as follows: : *P < .05, **P < .01, ***P < .001, ****P <0.0001.

5.3.8 *Vav*-iCre mediated *Zeb1* deletion during development causes reduction of CD3 and TRCβ in the total thymocyte population.

The suggested evidence of impaired positive selection observed in Figure 5.8, leads us to hypothesise about an alteration of CD3 and TRCβ, for this, we further investigated the protein levels (MFI) of CD3$^+$ and TRCβ$^+$ cells in the thymus. While in the previous section, we examined TCRβ with CD69 as a marker of positive selection, here we use another method, which is to measure its protein expression via median fluorescence intensity (MFI).

CD3 is first found in the cytoplasm of pro-thymocytes, the stem cells that give birth to T-cells in the thymus (Rodewald et al. 1994). Pro-thymocytes develop into common thymocytes, and subsequently into medullary thymocytes, where the CD3 antigen starts migration to the cell membrane (Shores et al. 1994). The antigen is found attached to the membranes of all mature T-cells. Because of its great specificity, as well as the presence of CD3 at all phases of T-cell maturation, it is a suitable immunophenotypic marker for T-cells. In addition, the CD3 chains interact with the T-cell receptor TCR to provide an activation signal in T cells (Mariuzza et al. 2020; Shah et al. 2021).

We observed that there was a reduction in protein expression (median fluorescence intensity; MFI)) of CD3$^+$ and TRCβ$^+$ cells in *Zeb1$^{-/-}$* mice (Figure 5.9, A). This could be related to the fact that there are fewer total thymocytes or that the *Vav*-iCre-mediated deletion causes a reduction at early stages in pro-thymocytes. Quantitative polymerase chain reaction (qPCR) can help distinguish between lower expression levels and altered abundance by quantifying mRNA levels, providing insights into the underlying mechanisms contributing to the observed changes in protein expression.

A
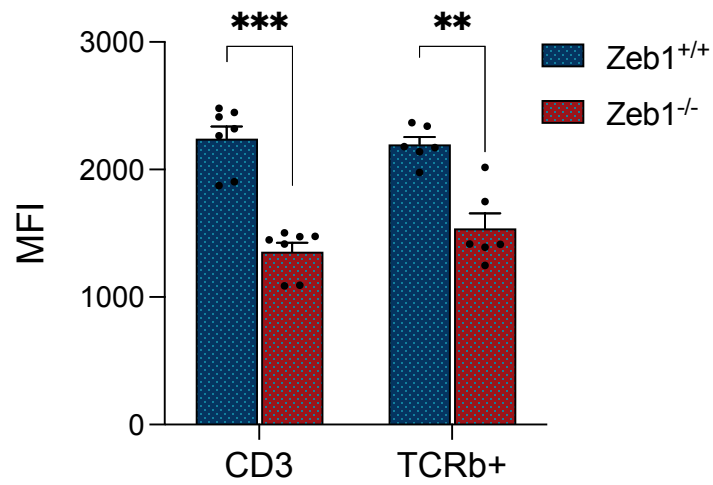
Figure 5.9 *Vav*-iCre mediated *Zeb1* deletion results in reduction of CD3 and TCRb in the thymus. MFI results of CD3 and TCRb in thymus (A). Data from 3-4 independent experiments (Control N=6-7, Knockout N=6-7). Error bars display the mean and SEM. Whitney U test was used to determine statistical significance in the following manner: : *P < .05, **P < .01, ***P < .001, ****P <0.0001.

5.3.9 *Vav*-iCre mediated *Zeb1* deletion during development causes immunological ageing in the thymus

As thymic atrophy was observed to be consistent with ageing, we next decided to evaluate if the *Zeb1*-Vav-iCre mouse model had an immunophenotype compatible with immunological ageing, as judged by CD62L as a measurement of ageing and T-cell activation in the thymus, spleen, PB and BM (Yang et al. 2011; Kolaczkowska 2016). We observed a significant reduction in the frequency of CD62L within CD3$^+$ cells in all haematopoietic organs of *Zeb1*$^{-/-}$ mice (Figure 5.10, B-E). The reduction was found not only in the frequency of CD62L within the CD3$^+$ cells but also in the MFI of CD62L except in the thymus was comparable (Figure 5.10, B). We then investigated whether the reduction observed in the frequency of CD62L in CD3$^+$ cells was observable in CD4$^+$ or CD8 only or both. We therefore further investigated these observations in each of these types separately (Figure 5.10 B-E). We observed a decreased frequency of CD62L$^+$ cells within CD3, CD4$^+$ and CD8, meaning a lower expression of CD62L protein in CD62L$^+$ cells, for spleen, PB and BM only (Figure 5.10 B-E). In sum, *Zeb1* disruption may be impacting the levels of CD62L in different T-cell subsets in the thymus and impacting T-cell activation, mimicking a phenotype similar to that observed during the natural ageing of the thymus.
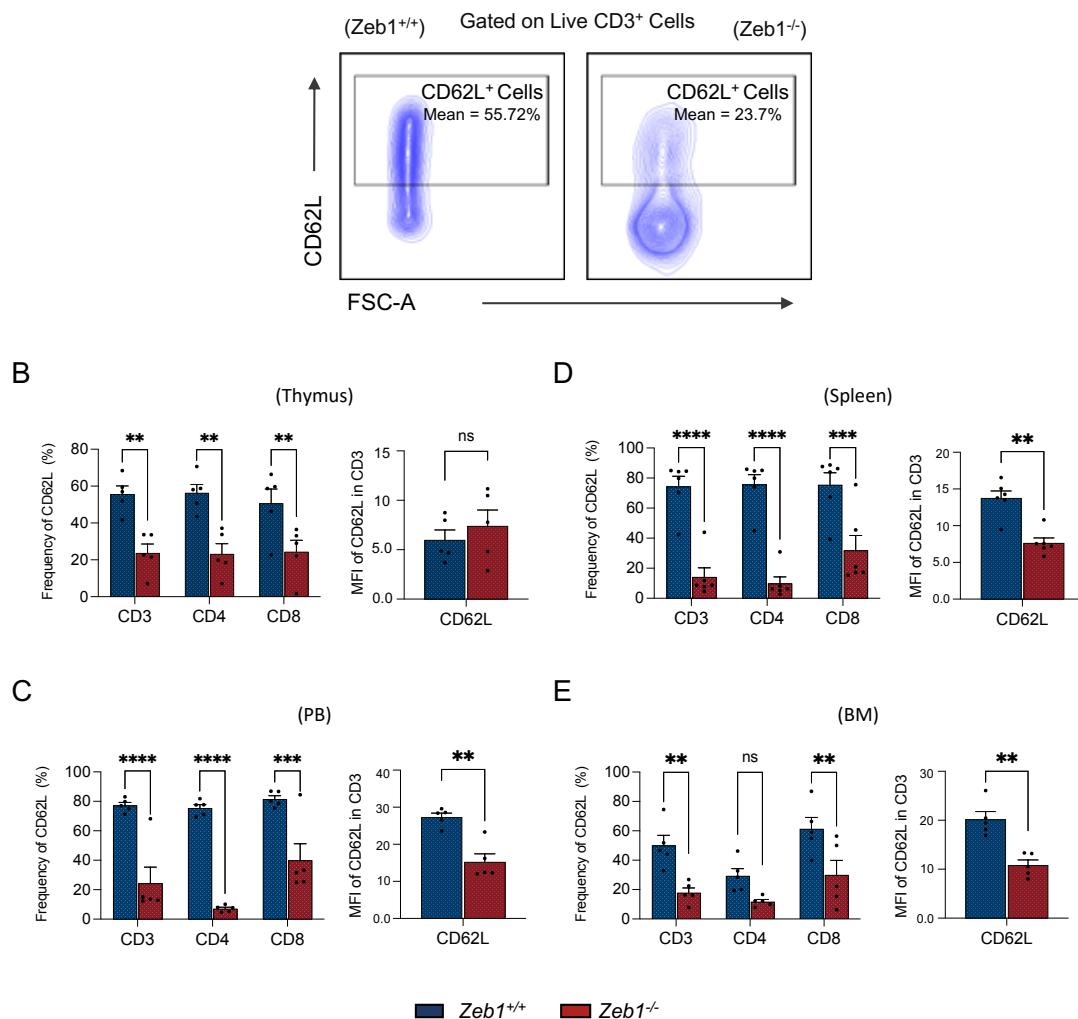
Figure 5.10 *Vav*-iCre mediated *Zeb1* deletion results in reduced CD62L frequency in the T cell subsets cells. FACS plots are illustrative for the overall data of CD62L+ cells gating strategy in T cell subsets (A). Frequency of CD62L+ Cells in T cells subsets and the CD62L MFI in CD3 in thymus (B). Frequency of CD62L+ Cells in T cell subsets and the CD62L MFI in CD3 in PB (C). Frequency of CD62L+ Cells in T cells subsets and the CD62L MFI in CD3 in SP (D). Frequency of CD62L+ Cells in T cells subsets and the CD62L MFI in CD3 in BM (E). Data from 3 independent experiments (Control N=5, Knockout N=5). Error bars display the mean and SEM. Holm-Šídák's multiple comparisons test was used (except the CD62L MFI results) Whitney U test was used to determine statistical significance in the following manner: *P < .05, **P < .01, ***P < .001, ****P <0.0001.

5.3.10 *Vav*-iCre mediated *Zeb1* deletion differentially impacts naive, CM and EM T cells

Up until they come into contact with MHC-peptide complexes that their T-cell receptors (TCR) have a strong affinity for, mature T cells are believed to be immunologically naïve (Berard and Tough 2002). The antigen recognition induces significant T-cell proliferation and effector cell differentiation. After the infection has been eradicated, the host no longer benefits from maintaining large numbers of effector cells, and the majority of activated T cells undergo apoptosis (Berard and Tough 2002). A small proportion of these cells survive (memory T cells), helping in a secondary response, which is typically faster and of greater magnitude than the primary encounter with antigen (Berard and Tough 2002). Memory T cells display significant phenotypic variety. In humans, it was discovered they may be split into $CD62L^+CCR7^+$ ("central memory") and $CD62L^-CCR7^-$ ("effector memory") subpopulations, based on the expression of lymph node homing molecules and the functional characteristics of these cells (Sallusto et al. 1999; Martin and Badovinac 2018).

As our previous results suggested a reduction in CD62L levels in $Zeb1^{-/-}$ mice (Figure 5.10), which is also a marker for the Naive and central memory (CM) populations in mice (Sallusto et al. 2004; Takada and Jameson 2009), we further investigated the $CD8^+$ and $CD4^+$ subpopulations: Naive, CM and effector memory (EM) (using the marker CD44 in addition to CD62L) for the thymus, PB, spleen and BM (Sallusto et al. 2004; Baaten et al. 2010). In the thymus of $Zeb1^{-/-}$ mice, we found a significant reduction in Naïve T cell frequency in both $CD8^+$ and $CD4^+$ and an increase of EM in the thymus (Figure 5.11, B). The frequency of Naïve T cells was reduced in $CD4^+$ and $CD8^+$ cells in the PB (Figure 5.11, C), spleen (Figure 5.11, D) and thymus (Figure 5.11, E). The frequency of EM cells was increased in $CD4^+$ and $CD8^+$ cells in the PB (Figure 5.11, C), spleen (Figure 5.11, D) and BM (Figure 5.11, E). The frequency of CM cells was unchanged in $CD4^+$ cells in the PB but significantly reduced in $CD8^+$ cells in the PB (Figure 5.11, C). The frequency of EM cells was significantly decreased in $CD4^+$ and $CD8^+$ cells in the spleen (Figure 5.11, D), while no significant differences were observed in the $CD4^+$ and $CD8^+$ cells in the BM (Figure 5.11, E). After we found a reduction in Naive and CM and an increase in EM frequency, the total cell count of each of

these subpopulations was enumerated. We found a depletion of all Naïve, CM and EM T-cells for both CD4$^+$ and CD8$^+$ populations in the thymus, spleen and BM in *Zeb1*$^{-/-}$ mice (Figure 5.12 A-F).

Overall, there are differential requirements for ZEB1 in the different T-cell subpopulations. The deletion of *Zeb1* affects naive T-cells in the thymus, bone marrow, spleen and peripheral blood, for both the CD8$^+$ and CD4$^+$ subpopulations. A large reduction of naive T-cells was observed across all haematopoietic tissues, correlating with a depletion in total cell count across all populations. In contrast, the deletion of *Zeb1* increased the frequency of effector memory cells in peripheral blood, spleen and bone marrow in the CD8$^+$ and CD4$^+$ subpopulations, and while it was significant in all cases, the impact was smaller. The effect of *Zeb1* on central memory T cells was more modest, with no significant effects on frequency on some specific subsets (e.g. CD4$^+$ peripheral blood and CD8$^+$ bone marrow) but with a depletion on total cell count.
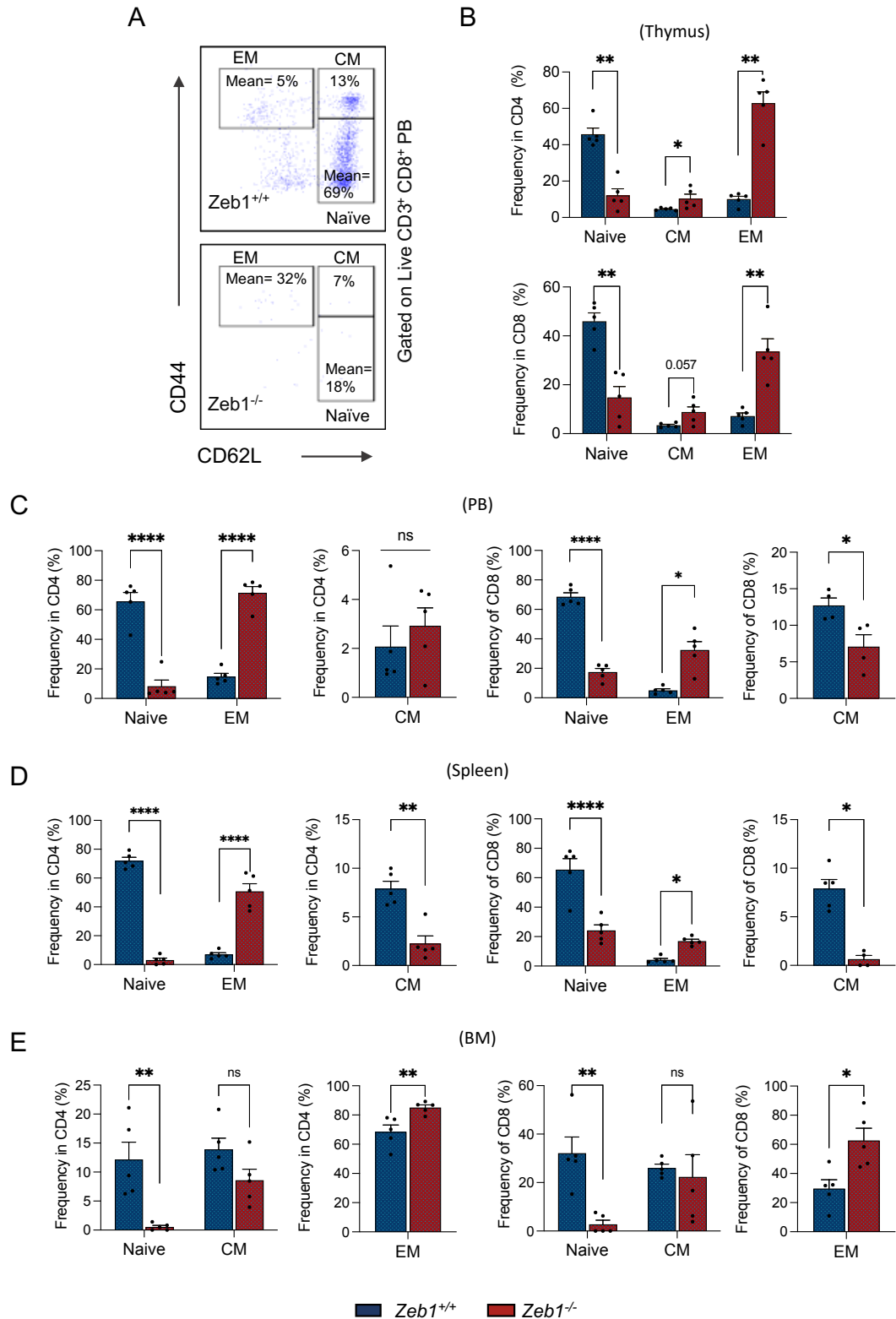
Figure 5.11 *Vav*-iCre mediated *Zeb1* deletion differentially impacts frequency of Naïve, EM and CM T cells. FACS plots illustrative for the overall data showing gating strategy of analysing the Naïve, CM and EM T cells using CD44 and CD62L surface markers gated on CD3⁺ and CD8 or CD4 T cells (A). Frequency of naïve, CM, and EM in CD4 T and CD8 cells in thymus (B), PB (C), Spleen (D) and BM (E). Data from 3 independent experiments (Control N=5, Knockout N=5). Error bars display the mean and SEM. Whitney U test was used to establish statistical significance according to the following: *P < .05, **P < .01, ***P < .001, ****P <0.0001
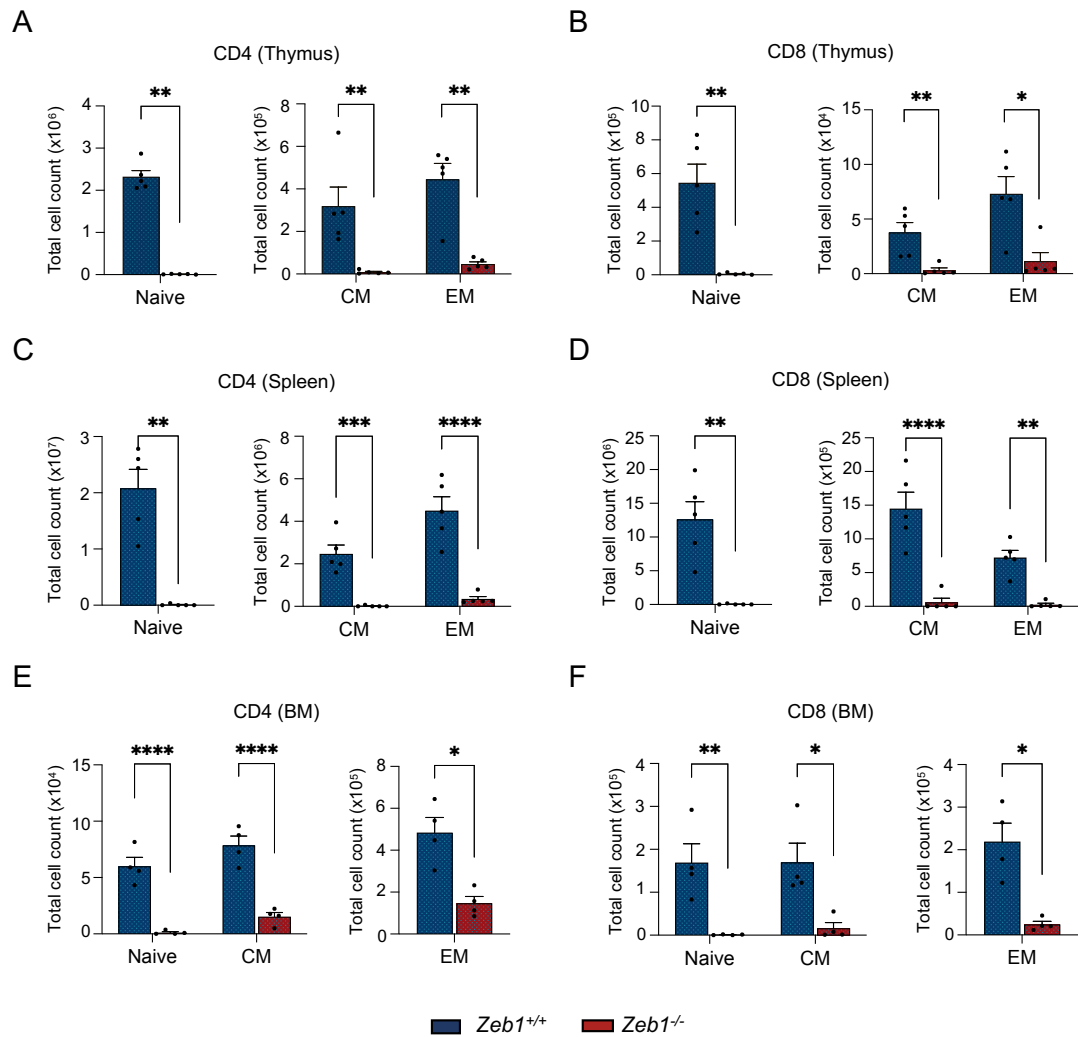
Figure 5.12 *Vav*-iCre mediated *Zeb1* deletion results in depletion of absolute numbers of Naïve, CM and EM T cells. The results of analysing the Naïve, CM and EM T cells using CD44 and CD62L surface markers gated on CD3⁺ and CD8 or CD4 T cells show a significant reduction in the total cellularity of naïve, CM, and EM of both CD4 or CD8 cells in thymus (A,B), Spleen (C,D) and BM (E,F). Data from 3 independent experiments (Control N=5, Knockout N=5). Error bars display the mean and SEM. Whitney U test was used to establish statistical significance according to the following: *P < .05, **P < .01, ***P < .001, ****P <0.0001

5.3.11 *Vav*-iCre mediated *Zeb1* deletion increases the CD4:CD8 ratio

Since having a sufficient number of naïve T cells is required for the immune system to respond to novel infections on a continual basis (Pennock et al. 2013), we additionally investigated the $CD4^+/CD8^+$ ratio. The normal $CD4^+/CD8^+$ ratio in the peripheral blood is around 2:1 and a deviation from these proportions can suggest disorders associated with immunodeficiency or autoimmune diseases (Owen, 2013). A low $CD4^+/CD8^+$ ratio (less than 1/1) implies a weakened immune system and reduced resistance to infections. As an example, patients with mutations in GATA2 leading to deficiency of its expression, have several bone marrow disorders such as reduced monocytes and inverted $CD4^+$:$CD8^+$ ratios. The haploinsufficiency observed in these patients leads to diseases such as leukaemia, monocytopenia or mycobacterial infections (Collin et al. 2015). In our Vav-iCre mouse model, we observed an increase of the $CD4^+$:$CD8^+$ ratio in the $Zeb1^{-/-}$ mice in comparison to the $Zeb1^{+/+}$ (WT) in the thymus, PB, spleen and BM (Figure 5.13 A), resembling an immunodeficient or autoimmune disease phenotype. In addition, an impaired $CD4^+/CD8^+$ ratio is linked to ageing and is a sign of immune senescence (Appay and Sauce 2014).
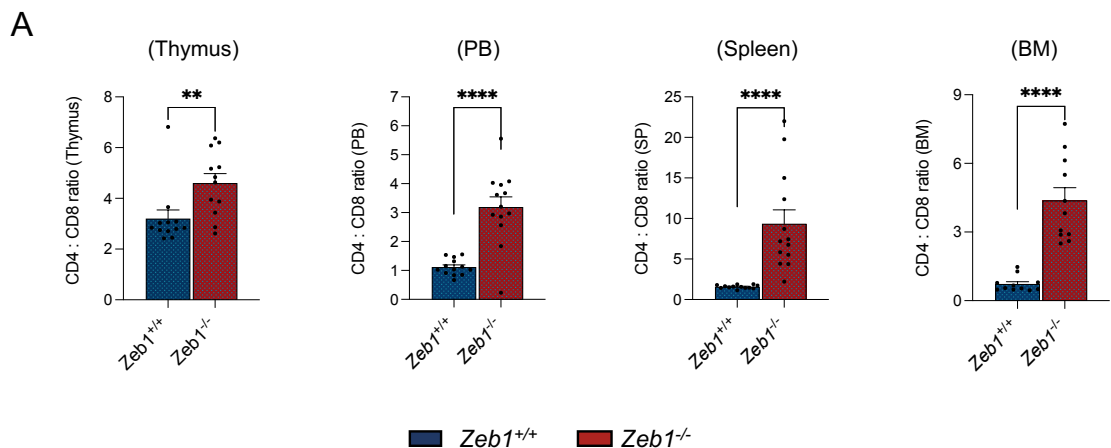
Figure 5.13 *Vav*-iCre mediated *Zeb1* deletion causes an increase in the CD4+:CD8+ ratio. Analysing the T cell subpopulations in the PB, SP and BM of Zeb1 deleted mice and control using CD4 and CD8 surface markers, CD4:CD8 ratio in thymus, PB, SP and BM (A). BM n=11, thymus n=12 and SP and PB n=13 on each genotype. Error bars display the mean and SEM. Whitney U test was used to establish statistical significance according to the following: *P < .05, **P < .01, ***P < .001, ****P <0.0001

5.3.12 Vav-iCre mediated *Zeb1* deletion during development causes an increase in PD1+ cells

Given the lower numbers of CD4$^+$ and CD8$^+$ Naive, CM, and EM T cell populations, we explored if there were increased apoptotic levels at these proteins. We used the apoptotic marker "programmed cell death protein 1", also known as PD-1, a protein found on the surface of T and B cells (Petrovas et al. 2006; Liu et al. 2009) that regulates the immune system's response by down-regulating the immune system and promoting self-tolerance by suppressing T cell inflammatory activity (Ishida et al. 1992; Francisco et al. 2010). PD-1 is an immunological checkpoint that protects against autoimmunity first by inducing apoptosis in antigen-specific T-cells in lymph nodes (Nishimura et al. 1999; Fife and Pauken 2011). In addition, it lowers the rate of apoptosis in regulatory T cells, which are anti-inflammatory, suppressive T cells (Ishida et al. 1992).

While our data is still preliminary, we found that *Zeb1$^{-/-}$* mice exhibited an increased frequency of PD-1 positive cells in both CD4$^+$ and CD8$^+$, Naive, CM and EM in the thymus. We observed this in the percentage of PD-1 frequency in CD4$^+$ subpopulations (including CD4$^+$ Naive, CD4$^+$ CM and CD4$^+$ EM) and in PD-1 frequency in CD8$^+$ subpopulations (which includes CD8 Naive, CD8 CM and CD8 EM) (Figure 5.14, B-C). This mirrors the observations in Figure 5.4, where Annexin V was performed in CD4$^+$ (which includes CD4$^+$ Naive, CD4$^+$ CM and CD4$^+$ EM) and CD8$^+$ (which includes CD8 Naive, CD8 CM and CD8 EM). Therefore, *Zeb1* disruption suggests an increase in apoptotic processes in these subpopulations, which will need further experimentation to be confirmed via Annexin V analysis in Naive, CM and EM T cell populations of *Zeb1$^{-/-}$* mice.
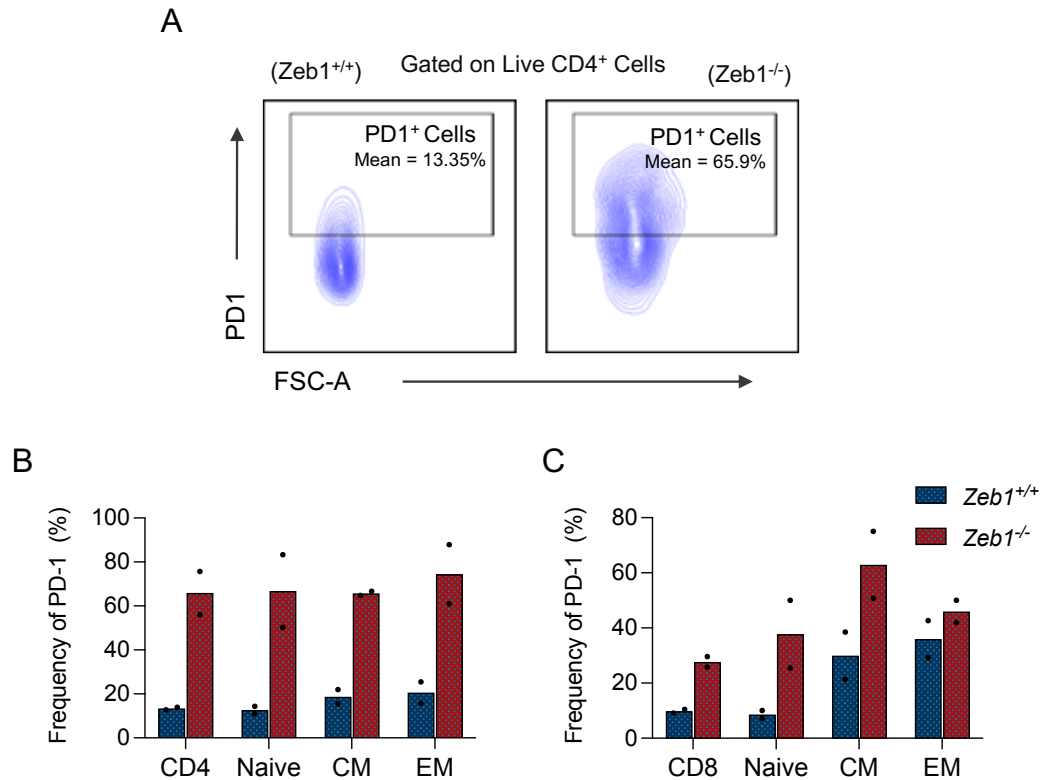
Figure 5.14 *Vav*-iCre mediated *Zeb1* deletion causes an increase in PD-1+ frequency in CD4 and CD8 subsets cell in the thymus. FACS plots are illustrative for the overall data of FAS+ cell gating strategy in the T cell subsets of Zeb1 deleted mice and control (A). FAS+ cells frequency in T cell subsets (B,C). Data from one independent experiment (Control N=2, Knockout N=2). Error bars show mean ± SEM.

5.3.13 Vav-iCre mediated *Zeb1* deletion causes global increase of cell adhesion molecules

To explore the molecular mechanism behind *Zeb1* function, we designed an RNA-Seq experiment in common lymphoid progenitors (CLPs). We focused on T-cell committed progenitors in BM which are hard-wired to form lymphoid cells exclusively because we wanted to assess if transcriptional programming is perturbed in the BM prior to arriving in the thymus in the context of *Zeb1* deficiency.

In this experiment, we used the *Mx1*-Cre mouse model to assess the effects of *Zeb1* deletion in CLPs, which allows for targeted activation of Cre and deletion of the gene in the hematopoietic system after activation of the *Mx* promoter by pIpC (Almotiri et al. 2021). FACS-purified CLPs (Lin- SCA-1^{low} C-KIT^{low} CD127$^+$) from

Zeb1^{-/-} animals (*Mx1*-Cre model) and their *Zeb1*^{+/+} (WT) controls were subjected to deep sequencing 14 days after the last dose of pIpC. We were unable to sort a large number of cells after deleting *Zeb1* due to the poor numbers of CLP in *Zeb1 Vav*-iCre; therefore, we employed an *Mx1*-Cre, and the deletion of *Zeb1* was confirmed. We additionally validated these results at the protein level in the *Zeb1 Vav*-iCre model.

In CLPs, there were 48 differentially expressed genes between *Zeb1*^{-/-} and *Zeb1*^{+/+} (WT) mice, with a significance P-value threshold of ≤ 0.05. The top overexpressed genes were Epcam, F11r, Prkcz, Cdcp1, Gyltl1b and Lsr.

The gene with the highest level of upregulation was *Epcam*, which encodes a glycoprotein that mediates cell adhesion in epithelia. EpCAM has been identified as a critical regulator of stem cell maintenance and differentiation (González et al. 2009b; Schnell et al. 2013c). The F11r (F11 receptor) gene encodes for a protein called Junctional adhesion molecule-A (JAM-A) that is involved in the formation of tight junctions between cells. The encoded member of the immunoglobulin superfamily gene can also function as a platelet receptor, integrin ligand, and reovirus receptor. It is implicated in leukocyte transmigration (Gupta et al. 2000; Sobocka et al. 2000). Many cell types, including endothelial cells, platelets, leukocytes, and epithelial cells, express the transmembrane protein JAM-A. It is essential for controlling inflammatory reactions, leukocyte migration, and cell-cell adhesion. It has also been demonstrated to play a role in the immune system's growth and inflammatory responses. It has been demonstrated that *Zeb1* controls the expression of *F11r* (Aigner et al. 2007). For instance, ZEB1 can bind to the *F11r* gene's promoter region in adult human -cells and boost the expression of the gene, increasing the quantity of F11R (Sintov et al. 2015). PKC zeta, the protein encoded by *Prkcz*, is a serine/threonine kinase that is a member of the PKC family and is involved in many cellular activities, including secretion, differentiation, and proliferation (O'Leary et al. 2016). Zeb1 mRNA expression was inversely linked with the expression of the apical-basal polarity genes *Pard6a* and *Prkcz* in cerebellar granule neuron progenitors (Singh et al. 2016b). Similarly, loss of PKCz promoted EMT through miR-200s in colorectal cancer cells, where it was also verified that there were decreased levels of E-cadherin with an increase in *Zeb1* (Shelton et al. 2018).

CDCP1 (CUB domain-containing protein 1) is a transmembrane protein that functions as a substrate for Src family kinases and has three extracellular CUB domains. The protein participates in the control of cellular activities involved in tumour invasion and metastasis that is tyrosine phosphorylation-dependent, and implicated in various cellular processes such as cell adhesion, migration, invasion, and signalling (O'Leary et al. 2016). In breast cancer cells, it has been noted that CDCP1 participates in a number of oncogenic pathways, including EGF signalling and HGF signalling, AGE-RAGE signalling, PI3K-AKT signalling, hypoxia, EMT, and TNF-signalling. The majority of these pathways have to do with how immunological checkpoints are regulated in cancer and it was suggested that EMT-activated human breast cancer cells may upregulate PD-L1 in a way dependent on ZEB1 and miR-200 (Zhao et al. 2022).

The *Gyltl1b* gene encodes a protein called LARGE2 has glucuronosyltransferase, xylosyltransferase, and dystroglycan binding activities (Brockington et al. 2005; O'Leary et al. 2016) *Lsr* is a protein-coding gene that stands for lipolysis-stimulated lipoprotein receptor. It is predicted to have a role in a number of processes, including the creation of the skin barrier, the localization of proteins to the tricellular tight junction, and the construction of the tricellular tight junction. in the extracellular exosome (O'Leary et al. 2016). In prostate cancer, results show that Snail and/or ZEB1 negatively regulate LARGE2, providing a molecular explanation for DG hypoglycosylation during growth and metastasis (Huang et al. 2015).

The most reduced genes in our analysis were *Zeb1*, as expected, and *Micu1*, and *Fbin1*. Micu1 is an EF-hand protein connected to the mitochondrial inner membrane. Under normal circumstances, this gene encodes a crucial regulator of mitochondrial Ca2+ uptake (Perocchi et al. 2010). In order to prevent mitochondrial Ca2+ overload, which can result in excessive generation of reactive oxygen species and cellular stress, the encoded protein interacts with the mitochondrial calcium uniporter, a Ca2+ channel in the inner membrane of the mitochondria (Mishra et al. 2017). It is a key regulator of the EF-hand domains on the mitochondrial calcium uniporter (MCU), which detects calcium levels. Micu1 behaves as both an activator and an inhibitor of mitochondrial calcium uptake (O'Leary et al. 2016; Bateman et al. 2021). The *Fbn1* gene encodes the

protein fibrillin-1. It is an extracellular matrix glycoprotein that acts as a structural element of calcium-binding microfibrils that are 10–12 nm in size. The body's elastic and nonelastic connective tissue is supported structurally by these microfibrils (O'Leary NA et al. 2016; Uniprot consortium 2021). Fbn1 and other fibrillins are important regulators of immunological activity (Zeyer and Reinhardt 2015). It has been shown that FBN1's cell-matrix interaction domain inactivating mutations dramatically increases the infiltration of pro-inflammatory cells and cause fibrosis in the skin (Gerber et al. 2013).

We continued to investigate the increased presence of the identified genes by utilizing pathway databases such as BioCarta, KEGG, and Reactome. The information is displayed as a negative logarithm of the p-value, with a dashed black line representing a p-value of 0.05. The analysis was conducted using GSEA software. (Figure 5.15, A). Heat maps represent the differentially expressed genes within control and $Zeb1^{-/-}$ CLPs related to the T cell, cytoskeleton and cell adhesion molecules. The heatmap scale represents the Z-score (Figure 5.15, B). GSEA plots representing tight junction organisation and cell-cell Junction assembly phenotype enriched in $Zeb1^{-/-}$ CLPs (Figure 5.15, C). In CLP, $Zeb1$ appears to regulate a transcriptional signature related to "cell junction organisation", "cell-cell communication", and "cell-cell junction organisation" (Figure 5.15, A), which were the top three enriched categories in GSEA. This data aligns with $Zeb1$ acting as a potent inducer of the EMT process (Zhang et al. 2015c; Mohammadi Ghahhari et al. 2022). In agreement with this transcriptional network, the upregulation of EpCAM, CDH1 and ITGB4, as well as the downregulation of CXCR4 in developing T-cell populations in the thymus of $Zeb1^{-/-}$ mice were confirmed independently at the protein level by flow cytometry (Figure 5.15 D-G) in the $Zeb1$ Vav-iCre mouse model. Overall, $Zeb1$ operates as a critical regulator of cell polarity, migration, adhesion, and differentiation-associated transcriptional patterns in CLPs and during thymocyte development.
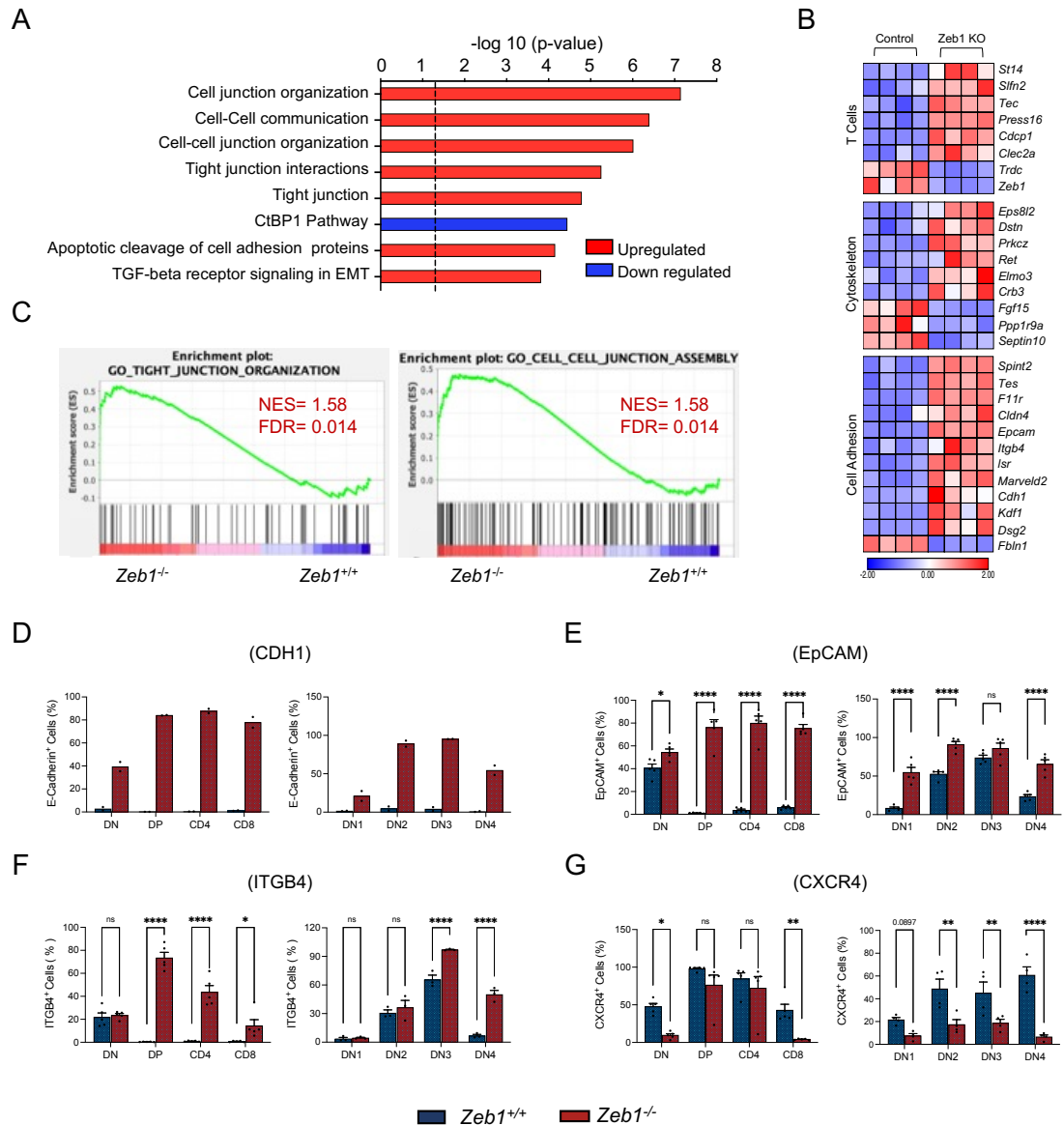
Figure 5.15 *Zeb1* deletion causes increased cell adhesion molecule expression in the common lymphoid progenitor and in developing T-cell populations in thymus. We performed RNA sequencing on sorted CLPs (Lin- SCA-1low C-KITlow CD127+) from control and Zeb1-/- mice, 14 days after the last pIpC dose (n=4 for each genotype). Pathway enrichment analysis was conducted using BioCarta, KEGG, and Reactome databases and presented as –log10 (p-value) with a dashed black line indicating p-value = 0.05. The differentially expressed genes related to T cell, cytoskeleton, and cell adhesion were displayed as a heatmap with a Z-score scale. The GSEA plots showed that tight junction organization and cell-cell junction assembly phenotype were enriched in *Zeb1*-/- CLPs.s (C). E-Cadherin+ cells frequency was validated in T cells subsets in thymus (D), EpCAM+ Cells (E), ITGB4+ Cells (F) and CXCR4+ Cells. Data from 2-3 independent experiments (Control N=2-5, Knockout N=2-5). Error bars show mean ± SEM. Holm-Šídák's multiple comparisons test was used to determine statistical significance in the following manner:s: *P < .05, **P < .01, ***P < .001, ****P <0.0001.

5.4 Discussion

In this Chapter, we explored the role of *Zeb1* during T-cell differentiation from HSCs by deleting *Zeb1* using the *Vav*-iCre system and analysing T-cell function by immunophenotyping. Unlike previous studies, we deleted *Zeb1* in at an early stage of hematopoietic development in the embryo. An additional advantage compared to other previously used mouse models is that *Vav*-iCre mediated gene deletion of *Zeb1* is largely cell-intrinsic. The results generated here are therefore obtained in the absence of any niche/accessory impacts and reflect cell intrinsic *Zeb1* mediated regulation of T-cell development rather than extrinsic impacts. In previous studies including germline models and the less specific *Mx1*-Cre model it was not possible to exclude these confounding factors. Our findings show that *Zeb1* is required for T-cell general function, thymocyte maturation, positive selection, T-cell differentiation and T-cell survival as well as for regulation of epithelium markers and cell adhesion molecules which are likely required for T-cell maturation.

After embryonic deletion of *Zeb1* in HSCs at E11.5, in adult mice, we observed a significant decrease in the total number of cells in the thymus, along with a considerable reduction in thymus weight and disruption of thymus architecture. The *Mx1*-Cre *Zeb1* null mouse (Almotiri et al. 2021 and unpublished data) model evidenced that *Zeb1* disruption causes a reduction of adult T cells in the PB and small thymi at 14 weeks after last injection, dramatically reducing total cellularity. The *Vav*-iCre *Zeb1* mouse model also shows the same pattern in PB and smaller thymi. The findings are comparable to studies that used mice embryos lacking either the complete *Zeb1* gene or the zinc finger sequence near the end of the gene, which resulted in perinatal deaths and significant decreases in thymus size and cell count at E18.5 (Higashi et al. 1997; Takagi et al. 1998a). Earlier data in the cellophane mouse model also saw a significant drop in the number of cells in the thymus (Zhang et al. 2020). All the subgroups identified by the expression of CD4, CD8, CD44, and CD25 were impacted by this drop in cell number (Zhang et al. 2020). Within Cellophane thymocytes, the CD4$^+$CD8$^+$ DP thymocyte and DN2 populations similarly saw a decline in numbers (Zhang et al. 2020).

Our data revealed that the defects in the thymus were present at different developmental stages of thymocyte selection, where cell counts revealed a significant reduction in the DN stage (early development) and the DP, CD4$^+$, and CD8$^+$ stages (late development) in cells from $Zeb1^{-/-}$ mice. In addition, similar to results from previous mouse models (Almotiri et al. 2021), we obtained evidence that suggest Zeb1 may be responsible for stopping the differentiation process between DN1 and DN2/DN3. The reduced proportions of DP cells and SP CD4$^+$, and CD8$^+$ stages could be an additional effect on the differentiation block, resulting in a dual role of $Zeb1$ in DN and DP CD4$^+$, and CD8$^+$. $Zeb1$ expression peaks throughout the DN2 and DP phases of T cell development, according to a mouse model using cellophane mice (Zhang et al. 2020). Additional data indicates that $Zeb1$ controls the transition to the SP stage by enhancing cell survival and proliferation while suppressing the production of several molecules that alter the potency of TCR signalling (Zhang et al. 2020).

We observed, for the first time, a direct impact on positive selection in T-cell development mediated by the absence of $Zeb1$. We assessed positive selection in more depth in the thymus from $Zeb1^{-/-}$ mice using TCRβ by CD69 to examine thymic positive selection by flow cytometry to show. $Zeb1$ disruption also caused impaired positive selection at different stages of DP development. We observed that there was a reduction of the MFI of CD3$^+$ and TRCβ$^+$ cells, markers of pro-thymocytes, in $Zeb1^{-/-}$ mice. Then, at the initial stages of thymocyte development $Zeb1$ had a role in a population of pre-selection DP thymocytes (TCRβ^{lo}CD69$^-$), reducing the frequency and total cell count of this population. In addition, $Zeb1$ disruption affects the total cell count of a transitional population directly after TCR engagement (TCRβ^{int}CD69$^+$) and after positive selection (TCRβ^{hi}CD69$^+$), which means that there could be reduced positive selection. Most interestingly, $Zeb1$ disruption does not impact lineage commitment following positive selection (TCRβ^{hi}CD69$^-$). The lower levels of T cells during DN and DP development are correlated with increased apoptosis in DN, DP, CD4$^+$, and CD8$^+$ populations, and, also in DN1, DN2, DN3 and DN4. On the development of SP thymocytes throughout ontogeny, positive and negative selection have different impacts. Positive selection may predominantly control the size of the thymic SP cell population during newborn life because negative selection is known to be

ineffective early in ontogeny and becomes more effective with age (He et al. 2013). TCR signalling was evaluated in the cellophane mouse model in developing thymocytes (Zhang et al. 2020). Starting with newly isolated thymocytes in steady state or after TCR engagement by cross-linking with anti-CD3 antibodies, they measured the phosphorylation (p) levels of a number of signalling proteins implicated in TCR-mediated activation (Zhang et al. 2020).Thus, when compared to control animals, the MAPK and PI3K/Akt pathways were found to be more active in thymocytes going through selection in Cellophane mice. As a result, it is thought that *Zeb1* regulates the intensity of the signalling downstream of the activated TCR at the DP stage, and Cellophane DP cells exhibit enhanced TCR signalling (Zhang et al. 2020). This may increase negative selection and hence explain why T-cell development is faulty in Cellophane animals (Zhang et al. 2020). However, we think that this mechanistic explanation may only apply to the cellophane model, since the *Vav*-iCre model more likely reflects cell intrinsic haematopoietic activity as alluded to above.

We noticed a connection between *Zeb1*'s influence on T-cell differentiation and alterations in cell cycle and cell death. These modifications began at the DN1 phase, which marks the initial stages of T cell lineage determination (Wu et al. 1996) and was present through maturation in all compartments (DN1, DN2, DN3), especially in DN2. It was previously observed that early in CD4$^-$CD8 double-negative (DN2) stage 2 T cell development, *Zeb1* reaches its maximum expression (Zhang et al. 2020). The absence of populations C and D might be due to problems with cell survival after positive selection (Figure 8). Therefore, we decided to quantify apoptosis in T-cells across several developmental stages, using an Annexin V assay. Analysis of cell cycle and apoptosis revealed that *Zeb1* is required differently in distinct thymus populations. We observed a reduction in DN and an increase in DP for both CD4$^+$ and CD8$^+$ cells as measured by using Ki67 as a proliferation marker. DN1/DN4 showed reduced levels of proliferation in contrast to DN2 and DN3 which showed increased levels of proliferation cells. Cells in the DN1 compartment become more quiescent in comparison to the WT, which could imply that they accumulate and don't differentiate towards DN2. Overall, *Zeb1* differentially regulate proliferation during positive and negative selection of T-cells. Different results were observed

in the cellophane mouse model (Zhang et al. 2020). The authors of this study examined the EdU incorporation in vivo as a measure of proliferation in WT and Cellophane thymocytes. Cellophane cells proliferate more than WT DN3 cells, but Cellophane DN2 and DP cells proliferated less than their WT counterparts (Zhang et al. 2020). These results were supported by Ki67 staining (Zhang et al. 2020). It was concluded that the Cellophane mutation impairs the survival and proliferation of DN2 and DP thymocytes as they mature, which may explain why there are fewer of these cells in the Cellophane thymi (Zhang et al. 2020). The opposite proliferation levels in the DN2 between our mouse model and cellophane may be due to our small sample size or due to characteristics intrinsic biological or technical characteristics of each model.

We observed that the initial stages of T cell progenitors, measured as the frequency of ETPs, were significantly affected by the absence of *Zeb1*. However, the total cell count was not statistically affected, but slight increases were observed, and additional evidence of a differentiation block in the transition between DN1 and DN2/DN3. Summed to the fact that the DN1 consists of ETPs (approximately 16 % of DN1; CD4$^-$ CD8$^-$ CD44$^+$ CD25$^-$ C-KIT$^+$) and have a reduction in Ki67 (i.e. quiescence), we could argue that the ETPs may expand, proliferate and accumulate but fail to differentiate. The increasing non-significant trend observed indeed suggests that ETPs increase proliferation and try to compensate or, alternatively, that there is a block of differentiation at this stage, which might explain why we observe an increase in frequency and total cell count of DN1 and no change in the absolute number of ETPs seeded from BM. Further work would be needed to elucidate those aspects. While we observed that CLPs and LMPPs are significantly reduced in our mouse model **(**Chapter 4**),** a phenotype that was also observed in the *Mx*-Cre1 mouse model (Almotiri et al. 2021), In the study using *Mx*-Cre1, we noticed a decrease in early thymic progenitors (ETPs) that initiate thymus formation, which could be responsible for a nearly significant decrease in ETPs in the thymus. This is one of the main aspects that are different between the data obtained in the *Vav*-iCre and *Mx*-Cre1 model to data, that will need to be further explored. However, the data may reflect differences between the deletion of *Zeb1* in embryonic development (in *Vav*-Cre) versus adult (in *Mx1*-Cre) and the duration of *Zeb1* loss, which is longer in *Vav*-

Cre than in the *Mx1*-Cre model, where *Zeb1* was deleted acutely. Thus, the result in the *Vav*-Cre model suggests that the *Zeb1* mediated effects produced in the thymus most likely are due to a role of *Zeb1* in during T cell ontogenesis.

We also observed a dramatic reduction in the frequency of Naïve T cells and depletion of Naïve, CM and EM T cells in the thymus. These changes resemble immune senescence, a natural process that leads to a decline in immune function, thus affecting various aspects of immune functional networks and increasing cancer risk (Lian et al. 2020)

Some of the impacts of ageing include a gradual decrease in the generation of young, naive T cells, a more constrained T cell receptor (TCR) repertoire, and weaker T cell activation (Salam et al. 2013) and the replacement of naive T cells by memory T cells. Thymic involution, a slow deterioration in the structural integrity of the thymus with ageing that results in an atrophic thymus, is one of the major causes of ageing (Salam et al. 2013). Thymic involution causes a continuous drop in the number of naive T cells produced, which leads to a constrained TCR repertoire. Due to a lack of naive T cells in the elderly, there is an increased chance of developing a serious infection when more naive T cells become memory cells as a result of ongoing antigenic stimulation (Salam et al. 2013). Ageing causes a build-up of memory T cell subsets, many of which are dysfunctional, such as fatigued, terminally differentiated, or T effector memory cells that re-express CD45RA (Quinn et al. 2019b).

We observed a significant reduction in Naïve T cells frequency in both CD8 and CD4^{+} and an increase of EM in the thymus, correlated with an increased frequency of PD-1 positive cells in both CD4^{+} and CD8^{+}, Naive, CM, EM in the thymus. In turn, *Zeb1* Vav-iCre deletion is not only affecting the levels of naive T cell production in the thymus, resembling a normal thymus involution phenotype during ageing (Gruver et al. 2007; Nikolich-Žugich 2014), but it also affects the compensating mechanisms that might arise during the ageing process, such as peripheral proliferation or homeostatic proliferation of naive T cells that emigrated from the thymus earlier in life (Min 2018). This is observed by the lower levels in the frequency of naive T cells in PB, spleen and BM and the depletion of Naïve, CM and EM T-cells in thymus, spleen and BM.

An explanation for why the frequency of naive and CM is reduced while EM is increased could be that because most naïve T cells are depleted, the increase of EM frequency is a compensatory mechanism. The ultimate fate of a T cell is influenced by a variety of environmental stimuli, such as cytokines, inflammatory and immune-modulatory substances, and tissue-specific elements, among others (Pennock et al. 2013). These signals then affect the T cell's transcriptional profile, affecting the developmental options (Pennock et al. 2013). Eomes/Bcl-6 and IL-7/15/21 are often thought to tilt the scale in favour of memory. IL-2/12, inflammatory substances, and T-bet/Blimp-1, on the other hand, favour terminal differentiation and effectors (Pennock et al. 2013). When T cells are exposed to these substances too vigorously or for too long, exhaustion may develop (Pennock et al. 2013). As an example, infections with the influenza virus A/H1N1 show that while distinct memory and effector subsets rise with age, the fraction of naive T cells decreases (Zhou and McElhaney 2011). The molecular mechanism behind this behaviour might lie in a coordinate expression pattern of *miR-200*, *Zeb1* and *Zeb2* during an immune response (Guan et al. 2018a). It was found that miR-200 selectively targets *Zeb2* in CD8^{+} T cells after, allowing for *Zeb1* re-expression and memory cell formation and persistence (Guan et al. 2018a). In particular, the study demonstrated that *Zeb1* and miR-200 allow for the establishment of a long-lived pool of memory CD8^{+} T cells and central memory T cell differentiation (Guan et al. 2018a). Numerous peripheral T cell subsets, including iNKT cells, NK1.1^{+} T cells, and Ly49-expressing CD8^{+} T cells, are absent in Cellophane homozygous mice (Zhang et al. 2020) (refer to Chapter 4 for a more detailed analysis of NK1.1^{+} T cells in *Vav*-iCre mice, which was depleted in the thymus, SP, BM and PB). Therefore, it can be said that there is an intrinsic function of *Zeb1* in T cell development which regulates innate-like T cells (Zhang et al. 2020).

Likewise, comparable findings were reported in the *Mx1*-Cre mouse model, where *Zeb1* was identified as a regulator of CD8^{+} EM in BM and PB as well as CD8^{+} CM T cells in the spleen. This indicates the crucial role of *Zeb1* in the functioning of CD8^{+} T cells during infection (Almotiri et al. 2021). These observations have implications for the role of *Zeb1* in cancer. Given that the immune system performs a crucial immune surveillance role in the antitumor

response while simultaneously being linked to tumour genesis and development (Hu et al. 2012), it could be postulated that lowering the expression of *Zeb1* might result in a decrease in CD62L+ naïve/central memory phenotype, which is more effective in managing the growth of solid tumours compared to CD62L− cytotoxic T cells in mice (Watson et al. 2019). Therefore, the decrease of the naïve/central memory of CD62L$^+$ T cells will lead to missing control of pre-leukaemia cells in *Zeb1*$^{-/-}$ mice (see other data presented in Chapter 4).

Through positive and negative selection of thymocytes mediated by T cell receptor (TCR) signalling intensity, central tolerance is produced (Xing and Hogquist 2012). As a result, autoimmunity frequently results from thymic selection process dysregulation. The elimination of potentially autoreactive thymocytes by apoptosis during thymus development is a key strategy to maintain immunological tolerance (Xing and Hogquist 2012; Farhangnia and Akbarpour 2022). The immune system primarily acquires the ability to distinguish between self and non-self through central tolerance (Nemazee 2017). To stop the immune system from overreacting to different environmental factors, peripheral tolerance is essential (Xing and Hogquist 2012). Central tolerance is achieved through the positive and negative selection of thymocytes. The majority of thymocytes express the TNFR family member Fas (CD95). Previous studies have demonstrated that in addition to TCR triggering, Fas signals are necessary for peripheral T lymphocytes to undergo apoptosis. When thymocytes are being negatively selected, Fas can influence apoptosis in combination with antigen-specific signals (Castro et al. 1996). It has been postulated that the Fas system influences the negative/positive selection of thymocytes as they are developing inside the thymus. Through a mechanism known as activation-induced cell death, the Fas system also helps to eliminate peripheral lymphocytes following the clonal growth phase and the autoreactive lymphocytes in the periphery (Villa-Morales et al. 2010). Fas-mediated apoptosis of peripheral T cells is a crucial mechanism for maintaining immunological tolerance. By using this process, called activation-induced cell death (AICD), peripheral autoreactive or excessively active T cells are eliminated (Roberts et al. 2003). In mutant mice lacking Fas, there is a failure in the elimination of peripheral T cells, which results in an increase in autoreactive T cells and the production of autoimmune lesions

in several organs. Thus, dysregulation of the thymic selection process often leads to autoimmunity. It is possible that *Zeb1* deficit during thymic T cell maturation results in autoreactive T cells, causing autoimmunity because deficiencies in thymic selection promote the breakdown of central tolerance (Xing and Hogquist 2012). In our mouse model, we observed that FAS expression in DN subsets revealed higher apoptotic levels in almost all DN compartments, suggesting that FAS is a partial mediator of Zeb1 regulation of T-cell survival during T-cell maturation. In addition, *Zeb1*$^{-/-}$ mice exhibited an increased frequency of PD-1 positive cells in both CD4$^+$ and CD8$^+$ subpopulations in the thymus, which suggests an increase in apoptotic processes in these subpopulations.

Interestingly, during COVID-19 infection an increase in FAS and PD-1 expression was noted, resulting in T cells increasing their propensity to apoptosis and exhaustion and therefore becoming a link between the adaptive and innate immune response (Bellesi et al. 2020). Interestingly, *Zeb1* is among the top genes found to be upregulated at the whole transcriptome level during recovery from COVID-19, which suggests a role for *Zeb1* in immune antiviral response (Zheng et al. 2020b) and adds another layer of evidence to the fact that *Zeb1* mediates positive selection through apoptosis.

RNA-Seq analysis of transcriptome differences reveals that there is an increase in cell adhesion molecules in CLPs from *Zeb1*-deleted mice, associated with upregulation of *Cdh1*, *EpCAM* and *Itgb4* and dysregulation of epithelial markers in developing thymocytes and T-cells in the thymus. Furthermore, in the thymus, *Zeb1* deletion leads to a reduction of the receptor CXCR4, associated with cellular migration. A previous study revealed that deleting CXCR4 at the DN2 and DN3 stages with a Cre recombinase under the control of the *Lck* promoter results in marked inhibition of the transition from the DN3 to the DN4 stage as well as the transition from the DN4 to the DP stage, resulting in thymic atrophy, accumulation of DN3 cells, and reduced numbers of DP cells (Trampont et al. 2010). Furthermore, CXCR4-deficient CD25$^+$ DN cells (DN2 and DN3 cells) aggregated in the lower inner cortical area rather than the SCZ, where WT counterparts were recruited, indicating that CXCR4 is important in the polarised migration of the DN2 and DN3 cells to the SCZ (Janas et al. 2010). We observed that the reduction of CXCR4 happens in the immature T cells at DN1-2-3-4 which

would be linked to the previous phenotype described, where this impairment takes place in the cortex and the migration to the medulla. Studies conducted on chimeric mice, where adult bone marrow cells from lck[Cre]/CXCR4loxP/loxP mice were transplanted, resulting in the CXCR4 deficiency of the transplanted cells after entering the thymus. The results indicate that CXCR4 signalling is necessary to facilitate the migration of DN1 progenitors from the CMJ, and cells without CXCR4 are unable to differentiate beyond the DN1 stage (Misslitz et al. 2004). The block of differentiation at DN1 observed in our studies, similar to the chimeric mice, could suggest that *Zeb1* is mediating the CXCR4 reduction.

In addition, it is interesting to note that the upregulation of EpCAM in our model could be linked to an increased activity of epithelial thymocytes (González et al. 2009c; Imrich et al. 2012). We could hypothesise that the increase of epithelial markers in T cells, in the absence of *Zeb1*, might affect the guidance mechanisms and therefore the cells become adherent or attached to the thymus epithelium cells (Smith and Bhowmick 2016). The reduced expression of the receptor CXCR4, needed for cellular migration, would also affect these mechanisms in the T cell migration (Bianchi and Mezzapelle 2020).

In sum, *Vav*-iCre mediated *Zeb1* knockout mice have smaller thymi coupled with reduced cell numbers. We also discovered a significant increase in DN1 at both frequency and total cell count and a decrease in all T cell populations in the thymus from DN2 to final maturation stages CD4$^+$ and CD8$^+$ T cells, which was associated with distinct cell cycle regulation and increased cell death. These T cell changes are likely to be inherent to T cells and are not due to early progenitors seeding the thymus. In addition, we observe, for the first time, how changes leading to T cell dysfunction in Naive, EM and CM CD4$^+$ and CD8$^+$ imply that *Zeb1* malfunction may contribute to premature immunological ageing, characterised by immunosenescence (including decrease of naive T cells and CD62L) and exhaustion of T-cells (high levels of PD-1 and FAS). Altogether, we show that ZEB1 is a transcription factor required not only in the adult stage but also from early developmental stages to regulate adult T cell development. Our research suggests that Zeb1 plays an essential role as a transcription factor in the development of thymic T cells. Furthermore, our results suggest that Zeb1 is involved in various stages of T cell development and differentiation (Figure 5.17).

Mouse Model	Protein Structure	Target tissue	Sites affected
Wild-type	N-fin HD C-fin	None	None
Zeb1 Null-LacZ (Takagi et al., 1998)		All	Thymus and severe skeletal defects
Zeb1 flox/flox (Brabletz et al. 2017)		All	Thymus and skeletal defects
Zeb1 Mx1-Cre (Almotiri et al. 2021)		Haematopoietic Stem Cells	Thymus
Zeb1 Vav-iCre (This Study)		Haematopoietic Stem Cells	Thymus
Zeb1 ΔC727/ΔC727 (Higashi et al., 1997)		All	Thymus and less severe skeletal defects
Cellophane (Arnold et al. 2012)		All	Thymus and less severe skeletal defects

Figure 5.16 Summary of *Zeb1* mouse models generated to date and the deletion caused at the protein structure level. In addition, targeted tissue within each model is highlighted, as well as the organs affected by the deletion.

195
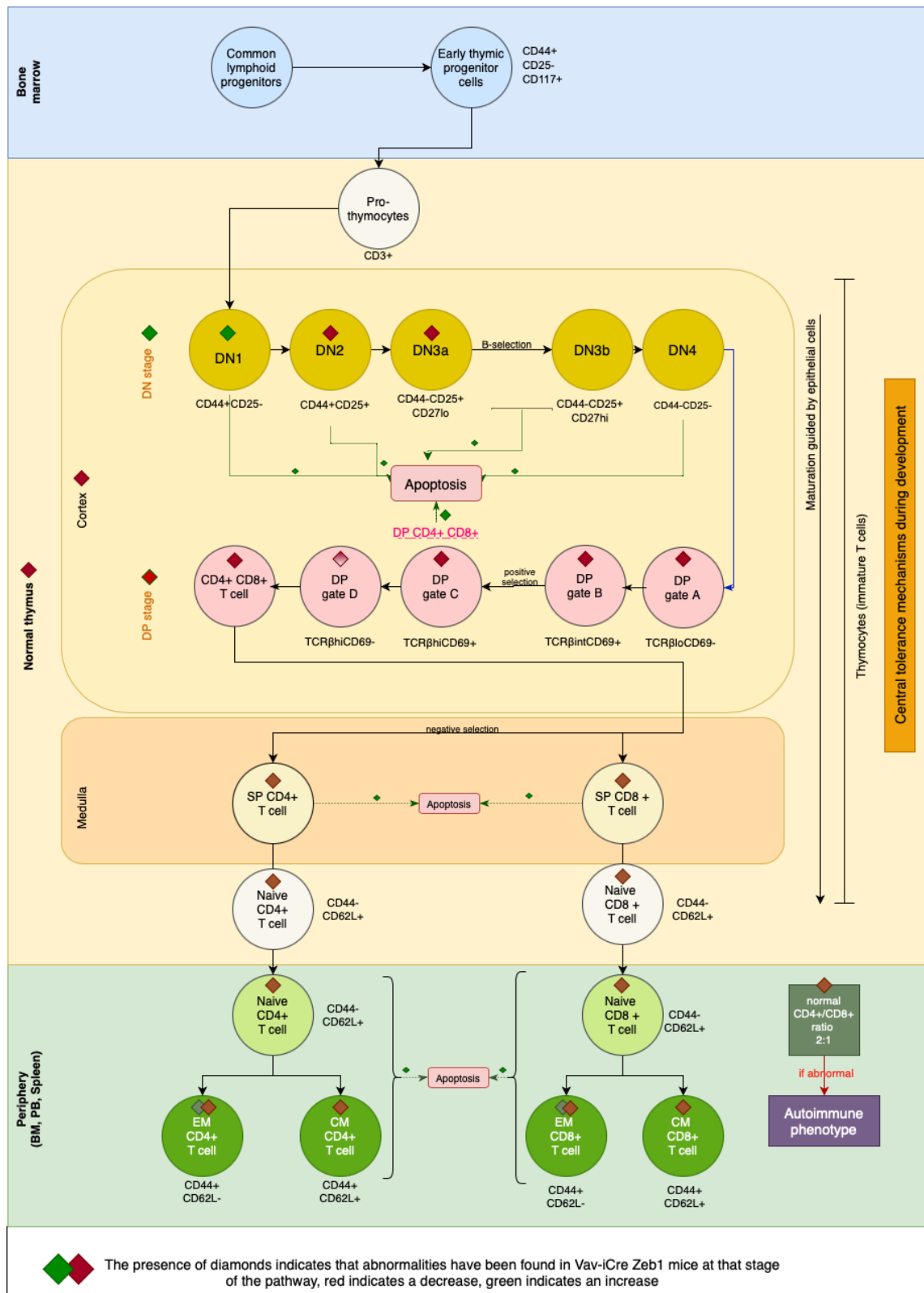
Figure 5.17 Summary of the role of *Zeb1* in T cell development from haematopoietic stem cells during ontogenesis.

CHAPTER 6: Discussion

The current study aimed to investigate the role of the transcription factor *Zeb1* in haematopoiesis. An understanding of the molecular mechanisms regulating haematopoiesis is crucial for the development of new therapeutic strategies for these disorders. In order to evaluate the role of *Zeb1* in regulating haematopoiesis, we generated and characterised a new mouse model using the *Vav*-iCre system (Georgiades et al. 2002; Siegemund et al. 2015). Our work found that the deletion of *Zeb1* in mice leads to partial lethality, hypochromic normocytic anaemia, a significant reduction in the number of blood cells, including immature myeloid cells in peripheral blood and spleen and erythroid cells, and bone marrow hypocellularity consistent with a pre-leukaemic/bone marrow failure phenotype.

The major findings suggest that *Zeb1* plays a crucial role in regulating stem-cell function, maintenance, and multilineage differentiation during haematopoiesis with a vital role in regulating stem-cell fate decisions (Almotiri et al. 2021). In the context of the haematopoietic system, we have found novel results that suggest that *Zeb1* likely regulates adult T cell maturation and differentiation and plays a crucial role in HSPCs in the bone marrow. *Zeb1* KO mice are able to generate HSCs, but they are functionally perturbed. As *Vav*-iCre deletes *Zeb1* during HSC generation in the embryo, the results of this study support the hypothesis that *Zeb1* is essential for both HSC generation in the embryo and long-term maintenance of HSPCs in the bone marrow. Our study adds to the growing evidence that EMT-TFs (such as *Twist1*, *Snail* and *Zeb* families) are essential for controlling the development of the haematopoietic system (Peinado et al. 2007; Beck et al. 2015; Liao and Yang 2017). However, the precise stages of where *Zeb1* is required during HSC ontogenesis (e.g., placenta, AGM, foetal liver) merits further investigation.

6.1 Immunophenotypic markers that mediate *Zeb1* regulated control haematopoiesis.

Our study found that *Zeb1* plays a role in inhibiting HSCs from differentiating into their progenitors at a later stage, with an increased frequency of CD34- and CD135- cells, consistent with an expansion of the HSC pool. CD135, the cytokine Flt3 ligand-receptor, plays roles in lymphoiesis, B cell development and maturation, and humoral immunity. CD34, on the other hand, is a transmembrane phosphoglycoprotein protein which is selectively expressed in haematopoietic progenitor cells, small vessel endothelial cells, embryonic fibroblasts, areolar tissue cells, adipocytes, and tumour cells of endothelial origin (Krause et al. 1996; Lanza et al. 2001). These findings suggest that *Zeb1* may be adversely regulating the differentiation of CD135- and CD34- HSCs into downstream progenitors.

Another factor involved in the growth and operation of immune cells is CD150, a receptor from the SLAM family of signalling lymphocyte activation molecules. The CD150 (SLAM) family of immunoglobulin superfamily cell-surface receptors control a number of leukocyte activities (Engel et al. 2003; Veillette 2006) such as cell-cell contact and signalling receptors (Romero et al. 2004). In particular, CD150 is known to have a role in the proliferation and maintenance of HSCs as well as the control of haematopoiesis by encouraging HSC differentiation into distinct lineages. In our studies, CD150 appears to be a *ZEB1* target gene, which may be related to the function of *ZEB1* in regulating immune cell function, as we discovered an increase in CD150lo (lymphoid-biased) HSC frequency in *Zeb1*$^{-/-}$ mice.

6.2 The role of *Zeb1* in anaemia

Anaemia can be caused by a dysregulation in the modulation of erythrocyte (red blood cell) synthesis and maturation. Transcription factors are essential in controlling the process of erythrocyte synthesis, which is carried out in the bone marrow by a particular population of stem cells known as erythroid precursors (Hattangadi et al. 2011). The findings of this thesis support that *Zeb1* is required for the development of an anaemia phenotype in a mouse model, which is defined by a reduction in the frequency and number of erythroid cells overall in the bone

marrow and spleen. The prevalence of anaemia in this mouse model is further supported by the whiter colour of tibia and femur bones, indicators of anaemia and low erythroid cells. Previous research found that *Zeb1* and E2f1 mRNA were significantly increased in all anaemia cases in canines with immune-mediated haemolytic anaemia (Berghorst 2018). It was also demonstrated that after tamoxifen-induced *Zeb1*/2 double knockout, mice with inducible KO of both *Zeb1* and *Zeb2* experience further blockages in haematopoiesis, substantial increases in the number of HSPCs, and die from fatal anaemia/cytopenia within two weeks (Wang et al. 2021a). Through the preservation of a single wild-type (wt) *Zeb2* allele, these deficiencies are selectively repaired, which also points to the fundamental role of *Zeb1* in anaemia (Wang et al. 2021a).

Zeb1 likely regulates the maturation and growth of erythroid cells as suggested by our findings. The resuts of our *Zeb1* knockout mouse model show downregulating in the expression of transcription regulators, including *Meis2, Irf7, Mycn* and *Nfkb2,* and an increase in the expression of *Erf.* These transcription regulators have demonstrated involvement in the progression of anaemia, especially during embryonic development (Edwards et al. 2015; Machon et al. 2015; Kuehn et al. 2017; Peraki et al. 2017; Li et al. 2022). For example, *Meis2* knockout mice develop smaller livers and severe anaemia (Wang et al. 2018a).

6.3 The role of *Zeb1* as a model of immunodeficiency

Our *Zeb1* mouse model is also reminiscent of Severe Combined Immunodeficiency (SCID), a genetic condition that weakens the immune system. Similar to humans, a genetic flaw that impairs T cell and B cell development and function is used to model SCID in mice (Vladutiu 1993). We have observed that transmembrane receptor expression, including that of *Il2rb* and *Csf2rb*, was upregulated in the absence of *Zeb1*. *IL2RB* encodes for the interleukin-2 receptor (IL-2), which is present in T cells, natural killer cells, and B cells on their cell surface (Ramirez et al. 2015), and in cases of dysregulation, these cells cannot grow or work properly and SCID can develop (Zhang et al. 2019).

In addition, we observed that in *Zeb1 Vav*-iCre mice, the percentage of pre-pro-B cells is significantly reduced in the bone marrow, suggesting a developmental

block between the pre-pro and pro-B cell stages. The role of *Zeb* transcription factors in B cell development has been demonstrated for *Zeb2* (Li et al. 2017) using an interferon-inducible *Mx1*-Cre *Zeb2* KO mouse model, which led to B cell lineage differentiation in the adult haematopoietic system (Li et al. 2017). It could therefore be speculated that *Zeb1 and Zeb2* have different roles in B-cells, with *Zeb1* acting earlier in B-cell development and *Zeb2* regulating the maturation of B-cells (Scott and Omilusik 2019). Further evidence comes from B cells isolated from mice with a mutation in the *Zeb1* gene, which could not effectively proliferate or respond to immune-activating stimuli like LPS (Arnold et al. 2012). Overall, studies suggest that *Zeb1* and 2 may both be vital for the development and maturation of B cells.

6.4 *Zeb1* mediated control of inflammation and atherosclerosis

Atherosclerosis is believed to originate and progress because of inflammation. The build-up of LDL (low-density lipoprotein) cholesterol and other lipids in the artery wall attracts immune cells including monocytes and T cells (Tabas and Lichtman 2017). Following their migration into the artery wall, these immune cells undergo differentiation to become macrophages, which consume LDL cholesterol and other lipids to form foam cells (Moore et al. 2013b). A chronic inflammatory response is brought on by the production of inflammatory mediators from the foam cells, which further recruit immune cells (Angelovich et al. 2015).

We found that in *Zeb1* KO mice, there is an upregulation of IL6, which plays a role in inflammation. High levels of IL6 have been associated with an increased risk of atherosclerosis, although depending on the type of damage and the organ or cell it is working on, this molecule exhibits both pro-inflammatory and anti-inflammatory effects (Kamimura et al. 2003; Reiss et al. 2017b; Villar-Fincheira et al. 2021). The general pro-atherogenic signature observed in *Zeb1*^{-/-} HSCs suggests that the lack of *Zeb1* in HSCs may contribute to the development of atherosclerosis. How this happens is unclear, but it may occur by altering the levels of various molecules involved in lipid metabolism and inflammation. This would need to be tested in future experiments using high-fat diet and atherosclerosis-prone mouse models (e.g. *Ldlr-/-* mouse model) (Ishibashi et al. 1993; Jawień et al. 2004), using a genetic or RNAi knockdown of *Zeb1*. It would

be interesting to investigate the requirement for *Zeb1* in the differentiation of HSC progeny; specifically, the effector cells of inflammation, the monocyte/macrophage lineage – a lineage for which *Zeb1* is required (Almotiri et al. 2021). Deletion of *Zeb1* using LysM-Cre would enable gene deletion predominantly in the myeloid lineage, in combination with disease progression models of atherosclerosis (Ye et al. 2003).

6.5 The role of *Zeb1* in malignancy

The expression of both *Zeb1* and *Zeb2* proteins has been found to be increased in various cancers and displays associations with the severity of the disease or invasiveness. *Zeb1* has been previously shown to modulate tumour metastasis in breast, lung, and colorectal cancers (Wang et al. 2014; Larsen et al. 2016). In AML patients, one study found that high *Zeb1* correlated with poorer prognosis (Li et al. 2021b). In contrast, our group recently found lower expression of *Zeb1* in AML patients (Almotiri et al. 2021). Thus, it was speculated in these patients that *Zeb1* may act as a tumour suppressor (Almotiri et al. 2021). In a study of AML patients, *Zeb1* was found to bind directly to p53 and the *Zeb1* silencing led to alterations in the PTEN signalling pathway (Li et al. 2021b). The results in this thesis also point to a role of *Zeb1* in the activation of PTEN signalling in HSCs as well. In addition, and in accordance with the mouse model created by Hidaka et al. (2008), we found that animals without *Zeb1* exhibit severe thymus atrophy, and CD4 T cell lymphoma develops at an advanced age. Additionally, the case study using our mouse model revealed a much higher percentage of CD4$^+$ cells. The molecular mechanism behind this phenotype could be related to the intricate network of proteins involved in controlling T cell development.

Our experiments found activation in the tumour suppressor protein TP53B1, essential for controlling cell growth and division and preventing the development of cancer cells. In healthy cells, TP53 and TP53B1 aid in the detection and repair of DNA damage, but if DNA damage is permanent, these proteins induce cell death (Wu et al. 2005). However, mutations in TP53 and TP53B1 which are often identified in many forms of cancer, including T-cell malignancy can result in the loss of their tumour suppressor activity. We also found upregulation and activation of PIM2 in HSCs. PIM2 is overexpressed in many cancers, including

T-cell malignancies (Daenthanasanmak et al. 2018). PIM proteins have been shown to support cancer cell survival, proliferation, and resistance to apoptosis and are frequently overexpressed in T-cell acute lymphoblastic leukaemia (T-ALL), (Padi et al. 2017; Wu et al. 2021). PIM2 has the potential to be a therapeutic target in T-cell malignancy because it is also linked to a poor prognosis in AML patients (Hamed et al. 2022).

These briefly mentioned roles showcase the significance of *Zeb1* and *Zeb2* in malignancy. It is worth mentioning a very recent study that contributed towards the understanding of the potentially synergistic effects of *Zeb1* and *Zeb2*. Wang et al (2021) found distinct differences in *Zeb1* and *Zeb2* expression during differentiation of HSCs and progenitor cells (Wang et al. 2021c). Overexpression of both induced the development of monocytes and inactivation resulted in increased survival of acute myeloid leukaemia model mice. It is critical to verify these mechanisms and interplay in other cancer models, animal models, and translationally in human patients. Additionally, the development of a CD4+ T-cell-driven lymphoproliferative syndrome in a single-aged Zeb1 KO mouse warrants further investigation. It is crucial to replicate this finding in a larger cohort of aged *Zeb1* KO mice to determine the characteristics of this disorder. Detailed immunophenotyping, functional assays, and genetic profiling of the affected CD4+ T cells would provide insights into the underlying mechanisms and its relationship with Zeb1 depletion.

6.6 Future directions

In future experiments to extend the observations presented in this thesis, to understand the functional role of EpCAM in *Zeb1*-deficient and normal haematopoiesis, I propose performing knockdown experiments and examining the effect of EpCAM knockdown in both $Zeb1^{-/-}$ and $Zeb1^{+/+}$ mice. We hypothesise that the HSCs expansion and block of differentiation phenotype observed in $Zeb1^{-/-}$ mice could be rescued in this setting. Additionally, we should aim to investigate the role of EpCAM in normal haematopoiesis by performing EpCAM knockdown in wild-type mice, as it is not yet clear.

EPCAM exhibits significant upregulation in acute myeloid leukemia (AML), indicating its high expression in this disease. This increased EPCAM expression is particularly notable and may suggest a potential role of EPCAM in driving leukemic progression (Huang et al. 2018). The crucial role of EpCAM in AML is also suggested as it promotes tumorigenicity and chemoresistance (Huang et al. 2018). CAR T cell therapy targeting EpCAM has shown promise in AML treatment by enhancing treatment efficacy and improving migration capabilities (Huang et al. 2018; Liu et al. 2022b). In our future research, we will investigate the specific involvement of the Zeb1/EpCAM axis in AML using the *Mx1*-Cre mouse model, allowing us to avoid the confounding effects of the *Vav*-iCre-mouse model, which develops a leukemic phenotype independently. Although exploring the role of Zeb1/EpCAM in the Vav background is also a possibility, caution is warranted due to the inherent bias resulting from concurrent pre-leukemia/leukemia development in this model. Thus, our focus remains on comprehending the complexities of the Zeb1/EpCAM axis in AML without interference from pre-existing biases.

It will be of interest to perform further experiments in *Zeb1* KO mice in the *Vav*-Cre model to identify the specific cause of fatality during ageing, including the possibility of both myeloid and lymphoid malignancy. Finally, to further our understanding of the role of *Zeb1* in T-cell development, we should investigate the mechanism of *Zeb1* in early T cell progenitors by performing RNA-seq on ETPs/DN/DP populations and further investigation/validation of Zeb1 targets genes from these studies.

References

Adams, J.M. and Cory, S. 2007. Bcl-2-regulated apoptosis: mechanism and therapeutic potential. *Current opinion in immunology* 19(5), pp. 488–496.

Adolfsson, J. et al. 2001. Upregulation of Flt3 expression within the bone marrow Lin(-)Sca1(+)c-kit(+) stem cell compartment is accompanied by loss of self-renewal capacity. *Immunity* 15(4), pp. 659–669.

Adolfsson, J. et al. 2005. Identification of Flt3+ lympho-myeloid stem cells lacking erythro-megakaryocytic potential: A revised road map for adult blood lineage commitment. *Cell* 121(2), pp. 295–306. doi: 10.1016/j.cell.2005.02.013.

Ager, A. 2012. ADAMs and Ectododomain Proteolytic Shedding in Leucocyte Migration: Focus on L-Selectin and ADAM17. *Current Immunology Reviews* 8(2), pp. 103–117. doi: 10.2174/157339512800099657.

Aigner, K. et al. 2007. The transcription factor ZEB1 (deltaEF1) promotes tumour cell dedifferentiation by repressing master regulators of epithelial polarity. *Oncogene* 26(49), pp. 6979–6988.

Aiman Mohtar, M., Syafruddin, S.E., Nasir, S.N. and Yew, L.T. 2020. Revisiting the Roles of Pro-Metastatic EpCAM in Cancer. *Biomolecules 2020, Vol. 10, Page 255* 10(2), p. 255.

Akala, O.O. and Clarke, M.F. 2006. Hematopoietic stem cell self-renewal. *Current Opinion in Genetics & Development* 16(5), pp. 496–501. doi: 10.1016/J.GDE.2006.08.011.

Akashi, K., Traver, D., Miyamoto, T. and Weissman, I.L. 2000. A clonogenic common myeloid progenitor that gives rise to all myeloid lineages. *Nature* 404(6774), pp. 193–197.

Akdis, M. et al. 2011. Interleukins, from 1 to 37, and interferon-γ: Receptors, functions, and roles in diseases. *Journal of Allergy and Clinical Immunology* 127(3), pp. 701-721.e70. doi: 10.1016/j.jaci.2010.11.050.

Aksentijevich, M., Lateef, S.S., Anzenberg, P., Dey, A.K. and Mehta, N.N. 2020. Chronic inflammation, cardiometabolic diseases and effects of treatment: Psoriasis as a human model. *Trends in Cardiovascular Medicine* 30(8), pp. 472–478. doi: 10.1016/J.TCM.2019.11.001.

Alanazi, B. et al. 2020. Integrated nuclear proteomics and transcriptomics identifies S100A4 as a therapeutic target in acute myeloid leukemia. *Leukemia* 34(2), pp. 427–440.

Alberts, B., A, J. and Lewis J. 2002. Analyzing Protein Structure and Function. *Molecular Biology of the Cell*.

Almotiri, A. et al. 2021. Zeb1 modulates hematopoietic stem cell fates required for suppressing acute myeloid leukemia. *Journal of Clinical Investigation* 131(1), pp. 1–17. doi: 10.1172/JCI129115.

Alpert, A. et al. 2019. A clinically meaningful metric of immune age derived from high-dimensional longitudinal monitoring. *Nature Medicine* 25(3), pp. 487–495.

Ambrogini, E. et al. 2010. FoxO-Mediated Defense against Oxidative Stress in Osteoblasts Is Indispensable for Skeletal Homeostasis in Mice. *Cell Metabolism* 11(2), pp. 136–146.

Angelovich, T.A., Hearps, A.C. and Jaworowski, A. 2015. Inflammation-induced foam cell formation in chronic inflammatory disease. *Immunology and cell biology* 93(8), pp. 683–693.

Antas, V.I., Al-Drees, M.A., Prudence, A.J.A., Sugiyama, D. and Fraser, S.T. 2013. Hemogenic endothelium: a vessel for blood production. *The international journal of biochemistry & cell biology* 45(3), pp. 692–695.

Appay, V. and Sauce, D. 2014. Naive T cells: The crux of cellular immune aging? *Experimental Gerontology* 54, pp. 90–93. doi: 10.1016/J.EXGER.2014.01.003.

Arnold, C.N. et al. 2012. A forward genetic screen reveals roles for Nfkbid, Zeb1, and Ruvbl2 in humoral immunity. *Proceedings of the National Academy of Sciences of the United States of America* 109(31), pp. 12286–12293.

Artis, D. and Spits, H. 2015. The biology of innate lymphoid cells. *Nature* 517(7534), pp. 293–301.

Ash, P., Loutit, J.F. and Townsend, K.M.S. 1980. Osteoclasts derived from haematopoietic stem cells. *Nature* 283(5748), pp. 669–670.

Athyala, P.K., Chitipothu, S., Kanwar, J.R., Krishnakumar, S. and Narayanan, J. 2019. Synthesis of saporin–antibody conjugates for targeting EpCAM positive tumour cells. *IET Nanobiotechnology* 13(1), pp. 90–99.

Baaten, B.J.G., Li, C.R. and Bradley, L.M. 2010. Multifaceted regulation of T cells by CD44. *Communicative & Integrative Biology* 3(6), p. 508.

Baeza, A.V., Dobson-Stone, C., Rampoldi, L., Bader, B., Walker, R.H., Danek, A. and Monaco, A.P. 2019. Chorea-Acanthocytosis. *The Curated Reference Collection in Neuroscience and Biobehavioral Psychology*, pp. 217–219.

Bakir, B., Chiarella, A.M., Pitarresi, J.R. and Rustgi, A.K. 2020. EMT, MET, Plasticity, and Tumor Metastasis. *Trends in cell biology* 30(10), pp. 764–776.

Balazs, A.B., Fabian, A.J., Esmon, C.T. and Mulligan, R.C. 2006. Endothelial protein C receptor (CD201) explicitly identifies hematopoietic stem cells in murine bone marrow. *Blood* 107(6), pp. 2317–2321.

Barrientos, S., Stojadinovic, O., Golinko, M.S., Brem, H. and Tomic-Canic, M. 2008. Growth factors and cytokines in wound healing. *Wound Repair and Regeneration* 16(5), pp. 585–601. doi: 10.1111/j.1524-475X.2008.00410.x.

De Barrios, O. et al. 2017. ZEB1-induced tumourigenesis requires senescence inhibition via activation of DKK1/mutant p53/Mdm2/CtBP and repression of macroH2A1. *Gut* 66(4), pp. 666–682.

Barthlott, T., Kohler, H. and Eichmann, K. 1997. Asynchronous coreceptor downregulation after positive thymic selection: Prolonged maintenance of the double positive state in CD8 lineage differentiation due to sustained biosynthesis of the CD4 coreceptor. *Journal of Experimental Medicine* 185(2), pp. 357–362. doi: 10.1084/jem.185.2.357.

Bateman, A. et al. 2021. UniProt: the universal protein knowledgebase in 2021. *Nucleic acids research* 49(D1), pp. D480–D489.

Beck, B. et al. 2015. Different levels of Twist1 regulate skin tumor initiation, stemness, and progression. *Cell stem cell* 16(1), pp. 67–79.

Becker, D.A.J., Mcculloch, E.A. and Till, J.E. 1963. CYTOLOGICAL DEMONSTRATION OF THE CLONAL NATURE OF SPLEEN COLONIES DERIVED FROM TRANS-PLANTED MOUSE MARROW CELLS. 197(4866), pp. 452–454.

Beerman, I., Bhattacharya, D., Zandi, S., Sigvardsson, M., Weissman, I.L., Brydere, D. and Rossia, D.J. 2010. Functionally distinct hematopoietic stem cells modulate hematopoietic lineage potential during aging by a mechanism of clonal expansion. *Proceedings of the National Academy of Sciences of the United States of America* 107(12), pp. 5465–5470.

Bellesi, S. et al. 2020. Increased CD95 (Fas) and PD-1 expression in peripheral blood T lymphocytes in COVID-19 patients. *British Journal of Haematology* 191(2), p. 207.

Benz, C. et al. 2012. Hematopoietic stem cell subtypes expand differentially during development and display distinct lymphopoietic programs. *Cell stem cell* 10(3), pp. 273–283.

Berard, M. and Tough, D.F. 2002. Qualitative differences between naïve and memory T cells. *Immunology* 106(2), pp. 127–138.

Berghorst, F.E. 2018. Bmi-1 expression is increased in dogs suffering from immune-mediated haemolytic anaemia.

Bertoli, C., Skotheim, J.M. and De Bruin, R.A.M. 2013. Control of cell cycle transcription during G1 and S phases. *Nature Reviews Molecular Cell Biology* 14(8), pp. 518–528. doi: 10.1038/nrm3629.

Bhandoola, A. and Sambandam, A. 2006. From stem cell to T cell: one route or many? *Nature reviews. Immunology* 6(2), pp. 117–126.

Bhattacharya, R. and Bick, A.G. 2021. Clonal Hematopoiesis of Indeterminate Potential: an Expanding Genetic Cause of Cardiovascular Disease. *Current atherosclerosis reports* 23(11).

Bianchi, M.E. and Mezzapelle, R. 2020. The Chemokine Receptor CXCR4 in Cell Proliferation and Tissue Regeneration. *Frontiers in Immunology* 11, p. 2109. doi: 10.3389/FIMMU.2020.02109/BIBTEX.

Bick, A.G. et al. 2022. Increased prevalence of clonal hematopoiesis of indeterminate potential amongst people living with HIV. *Scientific Reports 2022 12:1* 12(1), pp. 1–7.

Von Boehmer, H. and Fehling, H.J. 1997. Structure and function of the pre-T cell receptor. *Annual review of immunology* 15, pp. 433–452.

de Boer, J. et al. 2003. Transgenic mice with hematopoietic and lymphoid specific expression of Cre. *European Journal of Immunology* 33(2), pp. 314–325. doi: 10.1002/IMMU.200310005.

Brabletz, S. and Brabletz, T. 2010. The ZEB/miR-200 feedback loop--a motor of cellular plasticity in development and cancer? *EMBO reports* 11(9), pp. 670–677.

Brabletz, S., Lasierra Losada, M., Schmalhofer, O., Mitschke, J., Krebs, A., Brabletz, T. and Stemmler, M.P. 2017a. Generation and characterization of mice for conditional inactivation of Zeb1. *Genesis* 55(4), pp. 1–7. doi: 10.1002/dvg.23024.

Brabletz, S., Lasierra Losada, M., Schmalhofer, O., Mitschke, J., Krebs, A., Brabletz, T. and Stemmler, M.P. 2017b. Generation and characterization of mice for conditional inactivation of Zeb1. *Genesis* 55(4), pp. 1–7. doi: 10.1002/dvg.23024.

Brabletz, T., Jung, A., Hlubek, F., Löhberg, C., Meiler, J., Suchy, U. and Kirchner, T. 1999. Negative regulation of CD4 expression in T cells by the transcriptional repressor ZEB. *International Immunology* 11(10), pp. 1701–1708. doi: 10.1093/intimm/11.10.1701.

Bremer, E. and Helfrich, W. 2008. EpCAM-targeted induction of apoptosis. *Frontiers in bioscience : a journal and virtual library* 13(13), pp. 5042–5049.

BRILL, J.R. and BAUMGARDNER, D.J. 2000. Normocytic Anemia. *American Family Physician* 62(10), pp. 2255–2263.

Brockington, M. et al. 2005. Localization and functional analysis of the LARGE family of glycosyltransferases: significance for muscular dystrophy. *Human molecular genetics* 14(5), pp. 657–665.

de Bruijn, M.F.T.R. 2000. Definitive hematopoietic stem cells first develop within the major arterial regions of the mouse embryo. *The EMBO Journal* 19(11), pp. 2465–2474.

Busch, K. et al. 2015. Fundamental properties of unperturbed haematopoiesis from stem cells in vivo. *Nature 2015 518:7540* 518(7540), pp. 542–546.

van Buul, J.D. et al. 2002. Migration of Human Hematopoietic Progenitor Cells Across Bone Marrow Endothelium Is Regulated by Vascular Endothelial Cadherin. *The Journal of Immunology* 168(2), pp. 588–596.

Cabezas-Wallscheid, N. et al. 2014. Identification of regulatory networks in HSCs and their immediate progeny via integrated proteome, transcriptome, and DNA methylome analysis. *Cell Stem Cell* 15(4), pp. 507–522. doi: 10.1016/j.stem.2014.07.005.

Cai, X. et al. 2015. Runx1 Deficiency Decreases Ribosome Biogenesis and Confers Stress Resistance to Hematopoietic Stem and Progenitor Cells. *Cell stem cell* 17(2), pp. 165–177.

Cano, R.L.E. and Lopera, H.D.E. 2013. Introduction to T and B lymphocytes.

Caocci, G., Greco, M. and La Nasa, G. 2017. Bone marrow homing and engraftment defects of human hematopoietic stem and progenitor cells. *Mediterranean Journal of Hematology and Infectious Diseases* 9(1). doi: 10.4084/MJHID.2017.032.

Cardoso, V. et al. 2017. Neuronal regulation of type 2 innate lymphoid cells via neuromedin U. *Nature* 549(7671), pp. 277–281.

Cariappa, A., Chase, C., Liu, H., Russell, P. and Pillai, S. 2007. Naive recirculating B cells mature simultaneously in the spleen and bone marrow. *Blood* 109(6), pp. 2339–2345.

Carman, C. V. and Martinelli, R. 2015. T lymphocyte-endothelial interactions: Emerging understanding of trafficking and antigen-specific immunity. *Frontiers in Immunology* 6(NOV), p. 603. doi: 10.3389/FIMMU.2015.00603/BIBTEX.

Carpenter, G. and Cohen, S. 1990. Epidermal growth factor. *Journal of Biological Chemistry* 265(14), pp. 7709–7712.

Carstanjen, D., Gross, A., Kosova, N., Fichtner, I. and Salama, A. 2005. The α4β1 and α5β1 integrins mediate engraftment of granulocyte–colony-stimulating factor–mobilized human hematopoietic progenitor cells. *Transfusion* 45(7), pp. 1192–1200.

Castro, J.E. et al. 1996. Fas modulation of apoptosis during negative selection of thymocytes. *Immunity* 5(6), pp. 617–627.

Cell, H.S. 1996. Long-Term Lymphohematopoietic. 273(1995), pp. 242–245.

Ceredig, R., Dialynas, D.P., Fitch, F.W. and Robson Macdonald, H. 1983. Precursors of T cell growth factor producing cells in the thymus: ontogeny, frequency, and quantitative recovery in a subpopulation of phenotypically mature thymocytes defined by monoclonal antibody GK-1.5. *Journal of Experimental Medicine* 158(5), pp. 1654–1671.

Ceredig, R. and Rolink, T. 2002. A positive look at double-negative thymocytes. *Nature reviews. Immunology* 2(11), pp. 888–896.

Chakrabarti, S., Hoque, M., Jamil, N.Z., Singh, V.J., Pollacksmith, D., Meer, N. and Pezzano, M.T. 2022. Bone Marrow-Derived Cells Contribute to the Maintenance of Thymic Stroma including TECs. *Journal of Immunology Research* 2022. doi: 10.1155/2022/6061746.

Challen, G.A., Boles, N., Lin, K.K.Y. and Goodell, M.A. 2009. Mouse hematopoietic stem cell identification and analysis. *Cytometry Part A* 75A(1), pp. 14–24.

Challen, G.A., Boles, N.C., Chambers, S.M. and Goodell, M.A. 2010. Distinct hematopoietic stem cell subtypes are differentially regulated by TGF-beta1. *Cell stem cell* 6(3), pp. 265–278.

Chao, R., Gong, X., Wang, L., Wang, P. and Wang, Y. 2015. CD71(high) population represents primitive erythroblasts derived from mouse embryonic stem cells. *Stem cell research* 14(1), pp. 30–38.

Chapple, R.H., Tseng, Y.J., Hu, T., Kitano, A., Takeichi, M., Hoegenauer, K.A. and Nakada, D. 2018. Lineage tracing of murine adult hematopoietic stem cells reveals active contribution to steady-state hematopoiesis. *Blood Advances* 2(11), p. 1220.

Charles A Janeway, J., Travers, P., Walport, M. and Shlomchik, M.J. 2001. Generation of lymphocytes in bone marrow and thymus.

Chaves, L.P., Caliari, A.L., Melo, C.M., Saggioro, F.P. and Squire, J.A. 2021. Abstract 1818: ZEB1 expression is associated with the PTEN loss and TMPRSS2 ERG fusion immune evasion phenotype in prostate cancer. *Cancer Research* 81(13_Supplement), pp. 1818–1818.

Chen, L. et al. 2021. Dynamic changes in murine erythropoiesis from birth to adulthood: implications for the study of murine models of anemia. *Blood Advances* 5(1), p. 16.

Chen, T., You, Y., Jiang, H. and Wang, Z.Z. 2017. Epithelial-mesenchymal transition (EMT): A biological process in the development, stem cell differentiation, and tumorigenesis. *Journal of cellular physiology* 232(12), pp. 3261–3272.

Chen, Y. and Ernst, P. 2019. Hematopoietic transformation in the absence of MLL1/KMT2A: distinctions in target gene reactivation. *Cell cycle (Georgetown, Tex.)* 18(14), pp. 1525–1531.

Cheng, H., Zheng, Z. and Cheng, T. 2020. New paradigms on hematopoietic stem cell differentiation. *Protein & cell* 11(1), pp. 34–44.

Cheung, A.M. and Mak, T.W. 2006. PTEN in the haematopoietic system and its therapeutic indications. *Trends in Molecular Medicine* 12(11), pp. 503–505. doi: 10.1016/J.MOLMED.2006.09.002.

Clark, S.G. and Chiu, C. 2003. C. elegans ZAG-1, a Zn-finger-homeodomain protein, regulates axonal development and neuronal differentiation. *Development* 130(16), pp. 3781–3794.

Collin, M., Dickinson, R. and Bigley, V. 2015. Haematopoietic and immune defects associated with GATA2 mutation. *British Journal of Haematology* 169(2), pp. 173–187.

Croft, D. et al. 2014. The Reactome pathway knowledgebase. *Nucleic acids research* 42(Database issue).

Croker, B.A. et al. 2004. SOCS3 Is a Critical Physiological Negative Regulator of G-CSF Signaling and Emergency Granulopoiesis. *Immunity* 20(2), pp. 153–165. doi: 10.1016/S1074-7613(04)00022-6.

Crowley, L.C., Marfell, B.J., Scott, A.P. and Waterhouse, N.J. 2016. Quantitation of Apoptosis and Necrosis by Annexin V Binding, Propidium Iodide Uptake, and Flow Cytometry. *Cold Spring Harbor protocols* 2016(11), pp. 953–957.

Cupit-Link, M.C., Arora, M., Wood, W.A. and Hashmi, S.K. 2018. Relationship between Aging and Hematopoietic Cell Transplantation. *Biology of Blood and Marrow Transplantation* 24(10), pp. 1965–1970. doi: 10.1016/J.BBMT.2018.08.015.

Daenthanasanmak, A. et al. 2018. PIM-2 protein kinase negatively regulates T cell responses in transplantation and tumor immunity. *The Journal of clinical investigation* 128(7), pp. 2787–2801.

Diefenbach, A., Colonna, M. and Koyasu, S. 2014. Development, differentiation, and diversity of innate lymphoid cells. *Immunity* 41(3), pp. 354–365.

Dishowitz, M.I., Mutyaba, P.L., Takacs, J.D., Barr, A.M., Engiles, J.B., Ahn, J. and Hankenson, K.D. 2013. Systemic inhibition of canonical Notch signaling results in sustained callus inflammation and alters multiple phases of fracture healing. *PloS one* 8(7).

Dollé, L., Theise, N.D., Schmelzer, E., Boulter, L., Gires, O. and Van Grunsven, L.A. 2015. Intestinal Stem Cells in GI Physiology and Disease: EpCAM and the biology of hepatic stem/progenitor cells. *American Journal of Physiology - Gastrointestinal and Liver Physiology* 308(4), p. G233.

Dong, F. et al. 2020. Differentiation of transplanted haematopoietic stem cells tracked by single-cell transcriptomic analysis. *Nature Cell Biology 2020 22:6* 22(6), pp. 630–639.

Doulatov, S., Notta, F., Laurenti, E. and Dick, J.E. 2012. Cell Stem Cell Hematopoiesis: A Human Perspective. doi: 10.1016/j.stem.2012.01.006.

Drake, J.M., Strohbehn, G., Bair, T.B., Moreland, J.G. and Henry, M.D. 2009. ZEB1 Enhances Transendothelial Migration and Represses the Epithelial Phenotype of Prostate Cancer Cells. *Molecular Biology of the Cell* 20(8), p. 2207.

Drápela, S., Bouchal, J., Jolly, M.K., Culig, Z. and Souček, K. 2020. ZEB1: A Critical Regulator of Cell Plasticity, DNA Damage Response, and Therapy Resistance. *Frontiers in Molecular Biosciences* 7(March), pp. 1–10. doi: 10.3389/fmolb.2020.00036.

Dudley, E.C., Petrie, H.T., Shah, L.M., Owen, M.J. and Hayday, A.C. 1994. T cell receptor beta chain gene rearrangement and selection during thymocyte development in adult mice. *Immunity* 1(2), pp. 83–93.

Dunn, I.F., Heese, O. and Black, P.M. 2000. Growth factors in glioma angiogenesis: FGFs, PDGF, EGF, and TGFs. *Journal of Neuro-Oncology* 50(1–2), pp. 121–137. doi: 10.1023/A:1006436624862.

Dutta, A., Zhao, B. and Love, P.E. 2021. New insights into TCR β-selection. *Trends in immunology* 42(8), pp. 735–750.

Dykstra, B. et al. 2006. High-resolution video monitoring of hematopoietic stem cells cultured in single-cell arrays identifies new features of self-renewal. *Proceedings of the National Academy of Sciences of the United States of America* 103(21), pp. 8185–8190.

Dykstra, B., Olthof, S., Schreuder, J., Ritsema, M. and Haan, G. De. 2011. Clonal analysis reveals multiple functional defects of aged murine hematopoietic stem cells. *Journal of Experimental Medicine* 208(13), pp. 2691–2703.].

Dzhagalov, I. and Phee, H. 2012. How to find your way through the thymus: A practical guide for aspiring T cells. *Cellular and Molecular Life Sciences* 69(5), pp. 663–682. doi: 10.1007/s00018-011-0791-6.

Eaves, C.J. 2015. Hematopoietic stem cells: concepts, definitions, and the new reality. *Blood* 125(17), pp. 2605–2614.

Edwards, C.L. et al. 2015. Spatiotemporal requirements for IRF7 in mediating type I IFN-dependent susceptibility to blood-stage Plasmodium infection. *European Journal of Immunology* 45(1), pp. 130–141.

Elmore, S. 2007. Apoptosis: a review of programmed cell death. *Toxicologic pathology* 35(4), pp. 495–516.

Elyahu, Y. et al. 2019. Aging promotes reorganization of the CD4 T cell landscape toward extreme regulatory and effector phenotypes. *Science Advances* 5(8). doi: 10.1126/sciadv.aaw8330.

Ema, H., Morita, Y. and Suda, T. 2014. Anniversary Review Series: Perspectives on the modern exploration of Experimental Hematology Heterogeneity and hierarchy of hematopoietic stem cells.

Ema, M., Yokomizo, T., Wakamatsu, A., Terunuma, T., Yamamoto, M. and Takahashi, S. 2006. Primitive erythropoiesis from mesodermal precursors expressing VE-cadherin, PECAM-1, Tie2, endoglin, and CD34 in the mouse embryo. *Blood* 108(13), pp. 4018–4024.

Engel, P., Eck, M.J. and Terhorst, C. 2003. The SAP and SLAM families in immune responses and X-linked lymphoproliferative disease. *Nature reviews. Immunology* 3(10), pp. 813–821.

Engel, P., Zhou, L.J., Ord, D.C., Sato, S., Koller, B. and Tedder, T.F. 1995. Abnormal B lymphocyte delevopment, activation, and differentiation in mice that lack or overexpress the CD19 signal transduction molecule. *Immunity* 3(1), pp. 39–50. doi: 10.1016/1074-7613(95)90157-4.

Fabre, M.A. et al. 2021. The Longitudinal Dynamics and Natural History of Clonal Hematopoiesis. *Blood* 138(Supplement 2), p. LBA-2.

Fadeev, R.S. et al. 2015. The inhibition of NF-kB activation decreases the resistance of acute myeloid leukemia cells to TRAIL-induced apoptosis in multicellular aggregates. *Biophysics (Russian Federation)* 60(6), pp. 953–956.

Famili, F., Wiekmeijer, A.S. and Staal, F.J. 2017. The development of T cells from stem cells in mice and humans. *Future Science OA* 3(3).

Fan, T. et al. 2022. CDH1 overexpression predicts bladder cancer from early stage and inversely correlates with immune infiltration. *BMC Urology* 22(1).

Fang, Y. and Fullwood, M.J. 2016. Roles, Functions, and Mechanisms of Long Non-coding RNAs in Cancer. *Genomics, proteomics & bioinformatics* 14(1), pp. 42–54.

Farhangnia, P. and Akbarpour, M. 2022. Immunological Tolerance. *Encyclopedia of Infection and Immunity*, pp. 206–220.

Fife, B.T. and Pauken, K.E. 2011. The role of the PD-1 pathway in autoimmunity and peripheral tolerance. *Annals of the New York Academy of Sciences* 1217(1), pp. 45–59.

Filippi, M.D. and Ghaffari, S. 2019. Mitochondria in the maintenance of hematopoietic stem cells: new perspectives and opportunities. *Blood* 133(18), pp. 1943–1952.

Fleming, H.E., Janzen, V., Lo Celso, C., Guo, J., Leahy, K.M., Kronenberg, H.M. and Scadden, D.T. 2008. Wnt signaling in the niche enforces hematopoietic stem cell quiescence and is necessary to preserve self-renewal in vivo. *Cell stem cell* 2(3), p. 274.

Francisco, L.M., Sage, P.T. and Sharpe, A.H. 2010. The PD-1 Pathway in Tolerance and Autoimmunity. *Immunological reviews* 236(1), p. 219.

Gao, J., Yan, Q., Liu, S. and Yang, X. 2014. Knockdown of EpCAM Enhances the Chemosensitivity of Breast Cancer Cells to 5-fluorouracil by Downregulating the Antiapoptotic Factor Bcl-2. *PLOS ONE* 9(7), p. e102590.

Gartner, L.P. and Hiatt, J.L. 2011. Lymphoid (Immune) System. *Concise Histology*, pp. 168–187. doi: 10.1016/B978-0-7020-3114-4.00012-9.

Genovese, G. et al. 2014. Clonal Hematopoiesis and Blood-Cancer Risk Inferred from Blood DNA Sequence. *New England Journal of Medicine* 371(26), pp. 2477–2487.

Georgiades, P., Ogilvy, S., Duval, H., Licence, D.R., Charnock-Jones, D.S., Smith, S.K. and Print, C.G. 2002. vavCre Transgenic mice: A tool for mutagenesis in hematopoietic and endothelial lineages. *genesis* 34(4), pp. 251–256.

Gerdes, J., Lemke, H., Baisch, H., Wacker, H.H., Schwab, U. and Stein, H. 1984. Cell cycle analysis of a cell proliferation-associated human nuclear antigen defined by the monoclonal antibody Ki-67. *The Journal of Immunology* 133(4), pp. 1710–1715.

Geske, F.J., Lieberman, R., Strange, R. and Gerschenson, L.E. 2001. Early stages of p53-induced apoptosis are reversible. *Cell Death & Differentiation 2001 8:2* 8(2), pp. 182–191.

Ghaedi, M., Steer, C.A., Martinez-Gonzalez, I., Halim, T.Y.F., Abraham, N. and Takei, F. 2016. Common-Lymphoid-Progenitor-Independent Pathways of Innate and T Lymphocyte Development. *Cell Reports* 15(3), pp. 471–480.

Gheldof, A., Hulpiau, P., Van Roy, F., De Craene, B. and Berx, G. 2012. Evolutionary functional analysis and molecular regulation of the ZEB transcription factors. *Cellular and Molecular Life Sciences 2012 69:15* 69(15), pp. 2527–2541.

Godfrey, D.I., Kennedy, J., Suda, T. and Zlotnik, A. 1993. A developmental pathway involving four phenotypically and functionally distinct subsets of CD3-CD4-CD8- triple-negative adult mouse thymocytes defined by CD44 and CD25 expression. *Journal of Immunology (Baltimore, Md. : 1950)* 150(10), pp. 4244–4252.

González, B., Denzel, S., Mack, B., Conrad, M. and Gires, O. 2009a. EpCAM Is Involved in Maintenance of the Murine Embryonic Stem Cell Phenotype. *STEM CELLS* 27(8), pp. 1782–1791.

González, B., Denzel, S., Mack, B., Conrad, M. and Gires, O. 2009b. EpCAM is involved in maintenance of the murine embryonic stem cell phenotype. *Stem cells (Dayton, Ohio)* 27(8), pp. 1782–1791.

González, B., Denzel, S., Mack, B., Conrad, M. and Gires, O. 2009c. EpCAM is involved in maintenance of the murine embryonic stem cell phenotype. *Stem Cells* 27(8), pp. 1782–1791. doi: 10.1002/STEM.97.

Goodell, M.A., Brose, K., Paradis, G., Conner, A.S. and Mulligan, R.C. 1996. Isolation and functional properties of murine hematopoietic stem cells that are replicating in vivo. *The Journal of experimental medicine* 183(4), pp. 1797–1806.

Goronzy, J.J. and Weyand, C.M. 2013. Understanding immunosenescence to improve responses to vaccines. *Nature Immunology* 14(5), pp. 428–436. doi: 10.1038/ni.2588.

Goronzy, J.J. and Weyand, C.M. 2017. Successful and Maladaptive T Cell Aging. *Immunity* 46(3), pp. 364–378. doi: 10.1016/j.immuni.2017.03.010.

Goronzy, J.J. and Weyand, C.M. 2019. Mechanisms underlying T cell ageing. *Nature reviews. Immunology* 19(9), pp. 573–583.

Grégoire, J.M. and Roméo, P.H. 1999. T-cell expression of the human GATA-3 gene is regulated by a non-lineage-specific silencer. *The Journal of biological chemistry* 274(10), pp. 6567–6578.

Gruver, A.L., Hudson, L.L. and Sempowski, G.D. 2007. Immunosenescence of ageing. *The Journal of pathology* 211(2), pp. 144–156.

Guan, T. et al. 2018a. ZEB1, ZEB2, and the miR-200 family form a counterregulatory network to regulate CD8+ T cell fates. *The Journal of Experimental Medicine* 215(4), p. 1153.

Guan, T. et al. 2018b. ZEB1, ZEB2, and the miR-200 family form a counterregulatory network to regulate CD8+ T cell fates. *Journal of Experimental Medicine* 215(4), pp. 1153–1168.

Guo, Y. et al. 2022. Opposing roles of ZEB1 in the cytoplasm and nucleus control cytoskeletal assembly and YAP1 activity In brief Opposing roles of ZEB1 in the cytoplasm and nucleus control cytoskeletal assembly and YAP1 activity. *CellReports* 41, p. 111452.

Gupta, B. et al. 2021. The transcription factor ZEB1 regulates stem cell self-renewal and cell fate in the adult hippocampus. *Cell reports* 36(8).

Gupta, S.K., Pillarisetti, K. and Ohlstein, E.H. 2000. Platelet agonist F11 receptor is a member of the immunoglobulin superfamily and identical with junctional adhesion molecule (JAM): regulation of expression in human endothelial cells and macrophages. *IUBMB life* 50(1), pp. 51–56.

Gutiérrez, L., Caballero, N., Fernández-Calleja, L., Karkoulia, E. and Strouboulis, J. 2020. Regulation of GATA1 levels in erythropoiesis. *IUBMB Life* 72(1), pp. 89–105.

De Haan, G. and Lazare, S.S. 2018. Aging of hematopoietic stem cells. *Blood* 131(5), pp. 479–487.

Hale, J.S. and Fink, P.J. 2009. Back to the Thymus: Peripheral T Cells Come Home. *Immunology and cell biology* 87(1), p. 58.

Hamed, G., Omar, H.M., Sarhan, A.M. and Salah, H.E. 2022. Proviral Integration of Moloney Virus-2 (PIM-2) Expression Level as a Prognostic Marker in Patients with Acute Myeloid Leukemia. *International Journal of General Medicine* 15, pp. 4247–4258.

Hamidi, S. and Sheng, G. 2018. Epithelial-mesenchymal transition in haematopoietic stem cell development and homeostasis. *The Journal of Biochemistry* 164(4), pp. 265–275.

Hansford, S. et al. 2015. Hereditary Diffuse Gastric Cancer Syndrome: CDH1 Mutations and Beyond. *JAMA oncology* 1(1), pp. 23–32.

Hardy, R.R., Carmack, C.E., Shinton, S.A., Kemp, J.D. and Hayakawa, K. 1991. Resolution and characterization of pro-B and pre-pro-B cell stages in normal mouse bone marrow. *The Journal of experimental medicine* 173(5), pp. 1213–1225.

Harjunpää, H., Asens, M.L., Guenther, C. and Fagerholm, S.C. 2019. Cell adhesion molecules and their roles and regulation in the immune and tumor microenvironment. *Frontiers in Immunology* 10(MAY). doi: 10.3389/fimmu.2019.01078.

Hartman, J. and Frishman, W.H. 2014. Inflammation and atherosclerosis: a review of the role of interleukin-6 in the development of atherosclerosis and the potential for targeted drug therapy. *Cardiology in review* 22(3), pp. 147–151.

Hattangadi, S.M., Wong, P., Zhang, L., Flygare, J. and Lodish, H.F. 2011. From stem cell to red cell: regulation of erythropoiesis at multiple levels by multiple proteins, RNAs, and chromatin modifications. *Blood* 118(24), p. 6258.

Haug, J.S. et al. 2008. N-Cadherin Expression Level Distinguishes Reserved versus Primed States of Hematopoietic Stem Cells. *Cell Stem Cell* 2(4), pp. 367–379. doi: 10.1016/J.STEM.2008.01.017.

Hayashi, S., Lewis, P., Pevny, L. and McMahon, A.P. 2002. Efficient gene modulation in mouse epiblast using a Sox2Cre transgenic mouse strain. *Gene Expression Patterns* 2(1–2), pp. 93–97.

He, Q. et al. 2013. Thymic development of autoreactive T cells in NOD mice is regulated in an age-dependent manner. *Journal of immunology (Baltimore, Md. : 1950)* 191(12), pp. 5858–5866.

Heisterkamp, N., Groffen, J., Warburton, D. and Sneddon, T.P. 2008. The human gamma-glutamyltransferase gene family. *Human Genetics* 123(4), pp. 321–332.

Herreros-Pomares, A., Aguilar-Gallardo, C., Calabuig-Fariñas, S., Sirera, R., Jantus-Lewintre, E. and Camps, C. 2018. EpCAM duality becomes this molecule in a new Dr. Jekyll and Mr. Hyde tale. *Critical Reviews in Oncology/Hematology* 126, pp. 52–63. doi: 10.1016/J.CRITREVONC.2018.03.006.

Heuser, M., Thol, F. and Ganser, A. 2016. Clonal Hematopoiesis of Indeterminate Potential: A Risk Factor for Hematologic Neoplasms. *Deutsches Ärzteblatt International* 113(18), p. 317.

Hidaka, T. et al. 2008. Down-regulation of TCF8 is involved in the leukemogenesis of adult T-cell leukemia/lymphoma. *Blood* 112(2), pp. 383–393.

Higashi, Y., Moribe, H., Takagi, T., Sekido, R., Kawakami, K., Kikutani, H. and Kondoh, H. 1997. Impairment of T Cell Development in δEF1 Mutant Mice. *Journal of Experimental Medicine* 185(8), pp. 1467–1480.

Hiraga, T., Ito, S. and Nakamura, H. 2016. EpCAM expression in breast cancer cells is associated with enhanced bone metastasis formation. *International journal of cancer* 138(7), pp. 1698–1708.

Holmes, C. and Stanford, W.L. 2007. Concise review: stem cell antigen-1: expression, function, and enigma. *Stem cells (Dayton, Ohio)* 25(6), pp. 1339–1347.

Hosokawa, K. et al. 2007. Function of oxidative stress in the regulation of hematopoietic stem cell-niche interaction. *Biochemical and Biophysical Research Communications* 363(3), pp. 578–583. doi: 10.1016/J.BBRC.2007.09.014.

Hosokawa, K. et al. 2010. Cadherin-based adhesion is a potential target for niche manipulation to protect hematopoietic stem cells in adult bone marrow. *Cell stem cell* 6(3), pp. 194–198.

Hu, Q., Nicol, S.A., Suen, A.Y.W. and Baldwin, T.A. 2012. Examination of thymic positive and negative selection by flow cytometry. *Journal of Visualized Experiments* (68). doi: 10.3791/4269.

Huang, L., Yang, Y., Yang, F., Liu, S., Zhu, Z., Lei, Z. and Guo, J. 2018. Functions of EpCAM in physiological processes and diseases (Review). *International Journal of Molecular Medicine* 42(4), pp. 1771–1785. doi: 10.3892/ijmm.2018.3764.

Huang, Q., Miller, M.R., Schappet, J. and Henry, M.D. 2015. The glycosyltransferase LARGE2 is repressed by Snail and ZEB1 in prostate cancer. *Cancer biology & therapy* 16(1), pp. 125–136.

Huang, R.Y.J., Guilford, P. and Thiery, J.P. 2012. Early events in cell adhesion and polarity during epithelial-mesenchymal transition. *Journal of Cell Science* 125(19), pp. 4417–4422.

Hussain, S., Plückthun, A., Allen, T.M. and Zangemeister-Wittke, U. 2006. Chemosensitization of carcinoma cells using epithelial cell adhesion molecule–targeted liposomal antisense against bcl-2/bcl-xL. *Molecular Cancer Therapeutics* 5(12), pp. 3170–3180.

Ichikawa, M. et al. 2004. AML-1 is required for megakaryocytic maturation and lymphocytic differentiation, but not for maintenance of hematopoietic stem cells in adult hematopoiesis. *Nature medicine* 10(3), pp. 299–304.

Imran, S.A.M., Yazid, M.D., Idrus, R.B.H., Maarof, M., Nordin, A., Razali, R.A. and Lokanathan, Y. 2021. Is There an Interconnection between Epithelial–Mesenchymal Transition (EMT) and Telomere Shortening in Aging? *International Journal of Molecular Sciences 2021, Vol. 22, Page 3888* 22(8), p. 3888.

Imrich, S., Hachmeister, M. and Gires, O. 2012. EpCAM and its potential role in tumor-initiating cells. *Cell Adhesion & Migration* 6(1), p. 30.

Indra, A.K., Warot, X., Brocard, J., Bornert, J.M., Xiao, J.H., Chambon, P. and Metzger, D. 1999. Temporally-controlled site-specific mutagenesis in the basal layer of the epidermis: Comparison of the recombinase activity of the tamoxifen-inducible Cre-ER(T) and Cre-ER(T2) recombinases. *Nucleic Acids Research* 27(22). doi: 10.1093/nar/27.22.4324.

IRF7 protein expression summary - The Human Protein Atlas. [no date].

Irion, S., Luche, H., Gadue, P., Fehling, H.J., Kennedy, M. and Keller, G. 2007. Identification and targeting of the ROSA26 locus in human embryonic stem cells. *Nature Biotechnology* 25(12). doi: 10.1038/nbt1362.

Ishibashi, S., Brown, M.S., Goldstein, J.L., Gerard, R.D., Hammer, R.E. and Herz, J. 1993. Hypercholesterolemia in low density lipoprotein receptor knockout mice and its reversal by adenovirus-mediated gene delivery. *The Journal of clinical investigation* 92(2), pp. 883–893.

Ishida, Y., Agata, Y., Shibahara, K. and Honjo, T. 1992. Induced expression of PD-1, a novel member of the immunoglobulin gene superfamily, upon programmed cell death. *The EMBO Journal* 11(11), p. 3887.

Ito, K., Bonora, M. and Ito, K. 2018. Metabolism as master of hematopoietic stem cell fate. *International Journal of Hematology 2018 109:1* 109(1), pp. 18–27.

Ito, K. and Frenette, P.S. 2016. HSC Contribution in Making Steady-State Blood. *Immunity* 45(3), pp. 464–466. doi: 10.1016/J.IMMUNI.2016.09.002.

Ito, K. and Suda, T. 2014. Metabolic requirements for the maintenance of self-renewing stem cells. *Nature Reviews Molecular Cell Biology 2014 15:4* 15(4), pp. 243–256.

Ivanovs, A., Rybtsov, S., Ng, E.S., Stanley, E.G., Elefanty, A.G. and Medvinsky, A. 2017. Human haematopoietic stem cell development: from the embryo to the dish. *Development (Cambridge, England)* 144(13), pp. 2323–2337.

Ivanovs, A., Rybtsov, S., Welch, L., Anderson, R.A., Turner, M.L. and Medvinsky, A. 2011. Highly potent human hematopoietic stem cells first emerge in the

intraembryonic aorta-gonad-mesonephros region. *Journal of Experimental Medicine* 208(12), pp. 2417–2427.

Ivetic, A., Green, H.L.H. and Hart, S.J. 2019. L-selectin: A major regulator of leukocyte adhesion, migration and signaling. *Frontiers in Immunology* 10(MAY), p. 1068. doi: 10.3389/FIMMU.2019.01068/BIBTEX.

Jacobson, L.O., Simmons, E.L., Marks, E.K. and Eldredge, J.H. 1951. Recovery from radiation injury. *Science* 113(2940), pp. 510–511.

Jacome-Galarza, C.E. et al. 2019. Developmental origin, functional maintenance and genetic rescue of osteoclasts. *Nature* 568(7753), pp. 541–545.

Janas, M.L., Varano, G., Gudmundsson, K., Noda, M., Nagasawa, T. and Turner, M. 2010. Thymic development beyond β-selection requires phosphatidylinositol 3-kinase activation by CXCR4. *The Journal of Experimental Medicine* 207(1), p. 247.

Jawień, J., Nastałek, P. and Korbut, R. 2004. Mouse models of experimental atherosclerosis. *Journal of Physiology and Pharmacology : an Official Journal of the Polish Physiological Society* 55(3), pp. 503–517.

Jiang, Y. et al. 2018. Zinc finger E-box–binding homeobox 1 (ZEB1) is required for neural differentiation of human embryonic stem cells. *The Journal of Biological Chemistry* 293(50), p. 19317.

Joseph, C., Quach, J.M., Walkley, C.R., Lane, S.W., Lo Celso, C. and Purton, L.E. 2013. Deciphering Hematopoietic Stem Cells in Their Niches: A Critical Appraisal of Genetic Models, Lineage Tracing, and Imaging Strategies. *Cell Stem Cell* 13(5), pp. 520–533. doi: 10.1016/J.STEM.2013.10.010.

Kahlert, U.D. et al. 2015. ZEB1 Promotes Invasion in Human Fetal Neural Stem Cells and Hypoxic Glioma Neurospheres. *Brain pathology (Zurich, Switzerland)* 25(6), pp. 724–732.

Kalluri, R. and Weinberg, R.A. 2009. The basics of epithelial-mesenchymal transition. *The Journal of clinical investigation* 119(6), pp. 1420–1428.

Kamimura, D., Ishihara, K. and Hirano, T. 2003. IL-6 signal transduction and its physiological roles: the signal orchestration model. *Reviews of physiology, biochemistry and pharmacology* 149, pp. 1–38.

Kanehisa, M. and Goto, S. 2000. KEGG: kyoto encyclopedia of genes and genomes. *Nucleic acids research* 28(1), pp. 27–30.

Kanz, D., Konantz, M., Alghisi, E., North, T.E. and Lengerke, C. 2016. Endothelial-to-hematopoietic transition: Notch-ing vessels into blood. *Annals of the New York Academy of Sciences* 1370(1), pp. 97–108.

Karimi, M.M. et al. 2021. The order and logic of CD4 versus CD8 lineage choice and differentiation in mouse thymus. *Nature Communications 2021 12:1* 12(1), pp. 1–14.

Kataoka, K. et al. 2011. Evi1 is essential for hematopoietic stem cell self-renewal, and its expression marks hematopoietic cells with long-term multilineage repopulating activity. *The Journal of experimental medicine* 208(12), pp. 2403–2416.

Kato, T. 2021. Hematopoietic growth factors. *Handbook of Hormones: Comparative Endocrinology for Basic and Clinical Research*, pp. 453–455. doi: 10.1016/B978-0-12-820649-2.00116-9.

Kavanagh, D.P.J., Robinson, J. and Kalia, N. 2014. Mesenchymal stem cell priming: fine-tuning adhesion and function. *Stem cell reviews and reports* 10(4), pp. 587–599.

Keller, L., Werner, S. and Pantel, K. 2019. Biology and clinical relevance of EpCAM. *Cell Stress* 3(6), p. 165.

Kemp, R., Ireland, H., Clayton, E., Houghton, C., Howard, L. and Winton, D.J. 2004. Elimination of background recombination: somatic induction of Cre by combined transcriptional regulation and hormone binding affinity. *Nucleic acids research* 32(11).

Kent, D.G. et al. 2009. Prospective isolation and molecular characterization of hematopoietic stem cells with durable self-renewal potential. *Blood* 113(25), pp. 6342–6350.

Khacho, M. et al. 2016. Mitochondrial Dynamics Impacts Stem Cell Identity and Fate Decisions by Regulating a Nuclear Transcriptional Program. *Cell Stem Cell* 19(2), pp. 232–247.

Kiel, M.J., Radice, G.L. and Morrison, S.J. 2007. Lack of evidence that hematopoietic stem cells depend on N-cadherin-mediated adhesion to osteoblasts for their maintenance. *Cell stem cell* 1(2), pp. 204–217.

Kim, C.H. et al. 2011. Conditioning for hematopoietic transplantation activates the complement cascade and induces a proteolytic environment in bone marrow: a novel role for bioactive lipids and soluble C5b-C9 as homing factors. *Leukemia 2012 26:1* 26(1), pp. 106–116.

Kim, H., Kim, M., Im, S.-K. and Fang, S. 2018. Mouse Cre-LoxP system: general principles to determine tissue-specific roles of target genes. *Laboratory Animal Research* 34(4), p. 147.

Kisanuki, Y.Y., Hammer, R.E., Miyazaki, J. ichi, Williams, S.C., Richardson, J.A. and Yanagisawa, M. 2001. Tie2-Cre transgenic mice: A new model for endothelial cell-lineage analysis in vivo. *Developmental Biology* 230(2). doi: 10.1006/dbio.2000.0106.

Kissa, K. and Herbomel, P. 2010. Blood stem cells emerge from aortic endothelium by a novel type of cell transition. *Nature* 464(7285), pp. 112–115.

Klose, C.S.N. et al. 2014. Differentiation of type 1 ILCs from a common progenitor to all helper-like innate lymphoid cell lineages. *Cell* 157(2), pp. 340–356.

Klose, C.S.N. et al. 2017. The neuropeptide neuromedin U stimulates innate lymphoid cells and type 2 inflammation. *Nature 2017 549:7671* 549(7671), pp. 282–286.

Köhler, G., Hering, U., Zschörnig, O. and Arnold, K. 1997. Annexin V Interaction with Phosphatidylserine-Containing Vesicles at Low and Neutral pH†. *Biochemistry* 36(26), pp. 8189–8194.

Kolaczkowska, E. 2016. The older the faster: aged neutrophils in inflammation. *Blood* 128(19), pp. 2280–2282.

Koltsova, E.K., Hedrick, C.C. and Ley, K. 2013. Myeloid cells in atherosclerosis: a delicate balance of anti-inflammatory and proinflammatory mechanisms. *Current opinion in lipidology* 24(5), p. 371.

Kondo, M., Weissman, I.L. and Akashi, K. 1997. Identification of clonogenic common lymphoid progenitors in mouse bone marrow. *Cell* 91(5), pp. 661–672.

Koulnis, M., Pop, R., Porpiglia, E., Shearstone, J.R., Hidalgo, D. and Socolovsky, M. 2011a. Identification and analysis of mouse erythroid progenitors using the CD71/TER119 flow-cytometric assay. *Journal of visualized experiments : JoVE* (54).

Koulnis, M., Pop, R., Porpiglia, E., Shearstone, J.R., Hidalgo, D. and Socolovsky, M. 2011b. Identification and Analysis of Mouse Erythroid Progenitors using the CD71/TER119 Flow-cytometric Assay. *JoVE (Journal of Visualized Experiments)* (54), p. e2809.

Kovacic, J.C., Dimmeler, S., Harvey, R.P., Finkel, T., Aikawa, E., Krenning, G. and Baker, A.H. 2019. Endothelial to Mesenchymal Transition in Cardiovascular Disease. *Journal of the American College of Cardiology* 73(2), p. 190.

Krause, D., Fackler, M., Civin, C. and May, W. 1996. CD34: Structure, Biology, and Clinical Utility. *Blood* 87(1), pp. 1–13. doi: 10.1182/BLOOD.V87.1.1.1.

Krueger, A., Ziętara, N. and Łyszkiewicz, M. 2017. T Cell Development by the Numbers. *Trends in immunology* 38(2), pp. 128–139.

Kuehn, H.S. et al. 2017. Novel nonsense gain-of-function NFKB2 mutations associated with a combined immunodeficiency phenotype. *Blood* 130(13), p. 1553.

Kühn, R., Schwenk, F., Aguet, M. and Rajewsky, K. 1995. Inducible gene targeting in mice. *Science* 269(5229). doi: 10.1126/science.7660125.

Kulkeaw, K. et al. 2017. Twist1 regulates embryonic hematopoietic differentiation through binding to Myb and Gata2 promoter regions. *Blood advances* 1(20), pp. 1672–1681.

Kumar, B. V., Connors, T.J. and Farber, D.L. 2018. Human T Cell Development, Localization, and Function throughout Life. *Immunity* 48(2), pp. 202–213. doi: 10.1016/J.IMMUNI.2018.01.007.

Kumaravelu, P. et al. 2002. Quantitative developmental anatomy of definitive haematopoietic stem cells/long-term repopulating units (HSC/RUs): role of the aorta-gonad-mesonephros (AGM) region and the yolk sac in colonisation of the mouse embryonic liver. *Development (Cambridge, England)* 129(21), pp. 4891–4899.

Laffont, S. et al. 2017. Androgen signaling negatively controls group 2 innate lymphoid cells. *The Journal of experimental medicine* 214(6), pp. 1581–1592.

Lagasse, E. and Weissman, I.L. 1996. Flow cytometric identification of murine neutrophils and monocytes. *Journal of immunological methods* 197(1–2), pp. 139–150.

Lambert, S.A. et al. 2018. The Human Transcription Factors. *Cell* 172(4), pp. 650–665.

Lanza, F., Healy, L. and Sutherland, D.R. 2001. Structural and functional features of the CD34 antigen: an update. *Journal of Biological Regulators and Homeostatic Agents* 15(1), pp. 1–13.

Lanzkowsky, P. 2016. Chapter 3 - Classification and Diagnosis of Anemia in Children. In: Lanzkowsky, P., Lipton, J. M., and Fish, J. D. B. T.-L. M. of P. H. and O. (Sixth E. eds. San Diego: Academic Press, pp. 32–41.

Larsen, J.E. et al. 2016. ZEB1 drives epithelial-to-mesenchymal transition in lung cancer. *The Journal of Clinical Investigation* 126(9), p. 3219.

Latchman, D.S. 2001. Transcription factors: bound to activate or repress. *Trends in biochemical sciences* 26(4), pp. 211–213.

Laurenti, E. et al. 2008. Hematopoietic Stem Cell Function and Survival Depend on c-Myc and N-Myc Activity. *Cell stem cell* 3(6), p. 611.

Lazer, G. and Katzav, S. 2011. Guanine nucleotide exchange factors for RhoGTPases: good therapeutic targets for cancer therapy? *Cellular signalling* 23(6), pp. 969–979.

Lee Hyung-Suk, T., Kooshesh, F., Sauder, D.N. and Kondo, S. 1997. Modulation of TGF-β1 production from human keratinocytes by UVB. *Experimental Dermatology* 6(2), pp. 105–110. doi: 10.1111/j.1600-0625.1997.tb00155.x.

Lee, T.I. and Young, R.A. 2013. Transcriptional regulation and its misregulation in disease. *Cell* 152(6), pp. 1237–1251.

Lee, Y.R. and Pandolfi, P.P. 2020. PTEN Mouse Models of Cancer Initiation and Progression. *Cold Spring Harbor Perspectives in Medicine* 10(2).

Leffers, H. et al. 1993. Molecular cloning and expression of the transformation sensitive epithelial marker stratifin. A member of a protein family that has been involved in the protein kinase C signalling pathway. *Journal of molecular biology* 231(4), pp. 982–998.

Lenardo, M., Chan, F.K.M., Hornung, F., McFarland, H., Siegel, R., Wang, J. and Zheng, L. 1999. Mature T lymphocyte apoptosis--immune regulation in a dynamic and unpredictable antigenic environment. *Annual review of immunology* 17, pp. 221–253.

Lenardo, M.J. 1996. Fas and the art of lymphocyte maintenance. *The Journal of Experimental Medicine* 183(3), p. 721.

Lévesque, J.P., Helwani, F.M. and Winkler, I.G. 2010. The endosteal 'osteoblastic' niche and its role in hematopoietic stem cell homing and mobilization. *Leukemia 2010 24:12* 24(12), pp. 1979–1992.

Lewandoski, M. 2001. Conditional control of gene expression in the mouse. *Nature reviews. Genetics* 2(10), pp. 743–755.

Lewis, K., Yoshimoto, M. and Takebe, T. 2021. Fetal liver hematopoiesis: from development to delivery. *Stem Cell Research and Therapy* 12(1), pp. 1–8.

Li, H., Zou, J., Yu, X.H., Ou, X. and Tang, C.K. 2021a. Zinc finger E-box binding homeobox 1 and atherosclerosis: New insights and therapeutic potential. *Journal of cellular physiology* 236(6), pp. 4216–4230.

Li, J. et al. 2017. The EMT transcription factor Zeb2 controls adult murine hematopoietic differentiation by regulating cytokine signaling. *Blood* 129(4), pp. 460–472.

Li, L. et al. 2021b. ZEB1 serves as an oncogene in acute myeloid leukaemia via regulating the PTEN/PI3K/AKT signalling pathway by combining with P53. *Journal of Cellular and Molecular Medicine* 25(11), p. 5295.

Li, M., Wang, D., He, J., Chen, L. and Li, H. 2020. Bcl-XL: A multifunctional anti-apoptotic protein. *Pharmacological research* 151.

Li, Y., Farmer, R.W., Yang, Y. and Martin, R.C.G. 2016. Epithelial cell adhesion molecule in human hepatocellular carcinoma cell lines: a target of chemoresistence. *BMC Cancer* 16(1).

Li, Y.F. et al. 2022. Mycn regulates intestinal development through ribosomal biogenesis in a zebrafish model of Feingold syndrome 1. *PLOS Biology* 20(11), p. e3001856.

Li, Y.S., Wasserman, R., Hayakawa, K. and Hardy, R.R. 1996. Identification of the earliest B lineage stage in mouse bone marrow. *Immunity* 5(6), pp. 527–535. doi: 10.1016/S1074-7613(00)80268-X.

Li, Z. et al. 2012. Mouse embryonic head as a site for hematopoietic stem cell development. *Cell stem cell* 11(5), pp. 663–675.

Lian, J., Yue, Y., Yu, W. and Zhang, Y. 2020. Immunosenescence: a key player in cancer development. *Journal of hematology & oncology* 13(1).

Liang, Z., Dong, X., Zhang, Z., Zhang, Q. and Zhao, Y. 2022. Age-related thymic involution: Mechanisms and functional impact. *Aging Cell* 21(8), p. e13671.

Liao, T.T. and Yang, M.H. 2017. Revisiting epithelial-mesenchymal transition in cancer metastasis: the connection between epithelial plasticity and stemness. *Molecular Oncology* 11(7), p. 792.

Liesveld, J.L., Rosell, K., Panoskaltsis, N., Belanger, T., Harbol, A. and Abboud, C.N. 2004. Response of Human CD34+ Cells to CXC, CC, and CX3C Chemokines: Implications for Cell Migration and Activation. *https://home.liebertpub.com/scd* 10(5), pp. 643–655.

Linton, M.F. et al. 2019. The Role of Lipids and Lipoproteins in Atherosclerosis. *Science* 111(2877), pp. 166–186.

Liu, W., Chua, C., Wu, X., Wang, D., Ying, D., Cui, L. and Cao, Y. 2005. Inhibiting scar formation in rat wounds by adenovirus-mediated overexpression of truncated TGF-β receptor II. *Plastic and Reconstructive Surgery* 115(3), pp. 860–870. doi: 10.1097/01.PRS.0000153037.12900.45.

Liu, Y. et al. 2009. Regulation of arginase I activity and expression by both PD-1 and CTLA-4 on the myeloid-derived suppressor cells. *Cancer immunology, immunotherapy : CII* 58(5), pp. 687–697.

Liu, Y. et al. 2022a. Understanding the versatile roles and applications of EpCAM in cancers: from bench to bedside. *Experimental Hematology & Oncology 2022 11:1* 11(1), pp. 1–19.

Liu, Y. et al. 2022b. Understanding the versatile roles and applications of EpCAM in cancers: from bench to bedside. *Experimental Hematology and Oncology* 11(1), pp. 1–19.

Liu, Y., El-Naggar, S., Darling, D.S., Higashi, Y. and Dean, D.C. 2008. Zeb1 links epithelial-mesenchymal transition and cellular senescence. *Development (Cambridge, England)* 135(3), pp. 579–588. doi: 10.1242/dev.007047.

Loo, L.S.W. et al. 2020. BCL-xL/BCL2L1 is a critical anti-apoptotic protein that promotes the survival of differentiating pancreatic cells from human pluripotent stem cells. *Cell Death & Disease 2020 11:5* 11(5), pp. 1–18.

Look, A.T. 1997. Oncogenic transcription factors in the human acute leukemias. *Science* 278(5340), pp. 1059–1064. doi: 10.1126/SCIENCE.278.5340.1059.

Love, P.E. and Bhandoola, A. 2011. Signal integration and crosstalk during thymocyte migration and emigration. *Nature Reviews Immunology* 11(7), pp. 469–477. doi: 10.1038/nri2989.

Machon, O., Masek, J., Machonova, O., Krauss, S. and Kozmik, Z. 2015. Meis2 is essential for cranial and cardiac neural crest development. *BMC Developmental Biology* 15(1).

Mal, A. et al. 2021. EpCAM-Mediated Cellular Plasticity Promotes Radiation Resistance and Metastasis in Breast Cancer. *Frontiers in Cell and Developmental Biology* 8, p. 1637. doi: 10.3389/FCELL.2020.597673/BIBTEX.

Mandich, P. et al. 2009. Clinical features and molecular modelling of novel MPZ mutations in demyelinating and axonal neuropathies. *European Journal of Human Genetics* 17(9), p. 1129.

Manfredini, R. et al. 2005. The kinetic status of hematopoietic stem cell subpopulations underlies a differential expression of genes involved in self-renewal, commitment, and engraftment. *Stem cells (Dayton, Ohio)* 23(4), pp. 496–506.

Mariuzza, R.A., Agnihotri, P. and Orban, J. 2020. The structural basis of T-cell receptor (TCR) activation: An enduring enigma. *Journal of Biological Chemistry* 295(4), pp. 914–925. doi: 10.1016/S0021-9258(17)49904-2.

van der Mark, V.A., Oude Elferink, R.P.J. and Paulusma, C.C. 2013. P4 ATPases: flippases in health and disease. *International journal of molecular sciences* 14(4), pp. 7897–7922.

Marnell, C.S., Bick, A. and Natarajan, P. 2021. Clonal hematopoiesis of indeterminate potential (CHIP): Linking somatic mutations, hematopoiesis, chronic inflammation and cardiovascular disease. *Journal of molecular and cellular cardiology* 161, pp. 98–105.

Martin, M.D. and Badovinac, V.P. 2018. Defining memory CD8 T cell. *Frontiers in Immunology* 9(NOV), p. 2692. doi: 10.3389/FIMMU.2018.02692/BIBTEX.

McInnes, I.B. and Gravallese, E.M. 2021. Immune-mediated inflammatory disease therapeutics: past, present and future. *Nature Reviews Immunology 2021 21:10* 21(10), pp. 680–686.

McRae, H.M., Voss, A.K. and Thomas, T. 2019. Are transplantable stem cells required for adult hematopoiesis? *Experimental Hematology* 75, pp. 1–10. doi: 10.1016/J.EXPHEM.2019.05.007.

Medvinsky, A., Rybtsov, S. and Taoudi, S. 2011. Embryonic origin of the adult hematopoietic system: advances and questions. *Development (Cambridge, England)* 138(6), pp. 1017–1031.

Michael N. Hall, S.G.& A.C.W.Z.S.K.M.S.F.N.E.K.R.H.G.C.R.W.L.E.P.M.A.R. 2018. mTORC1 plays an important role in osteoblastic regulation of B-lymphopoiesis. (August), pp. 1–10.

Michie, A.M. and Zúñiga-Pflücker, J.C. 2002. Regulation of thymocyte differentiation: Pre-TCR signals and β-selection. *Seminars in Immunology* 14(5), pp. 311–323.

Miettinen, M. and Lasota, J. 2005. KIT (CD117): A review on expression in normal and neoplastic tissues, and mutations and their clinicopathologic correlation. *Applied Immunohistochemistry and Molecular Morphology* 13(3), pp. 205–220.

Mikkola, H.K.A., Klintman, J., Yang, H., Hock, H., Schlaeger, T.M., Fujiwara, Y. and Orkin, S.H. 2003. Haematopoietic stem cells retain long-term repopulating activity and multipotency in the absence of stem-cell leukaemia SCL/tal-1 gene. *Nature* 421(6922), pp. 547–551.

Milella, M. et al. 2015. PTEN: Multiple Functions in Human Malignant Tumors. *Frontiers in Oncology* 5(FEB).

Min, B. 2018. Spontaneous T cell proliferation: A physiologic process to create and maintain homeostatic balance and diversity of the immune system. *Frontiers in Immunology* 9(MAR), p. 547. doi: 10.3389/FIMMU.2018.00547/BIBTEX.

Mishra, J., Jhun, B.S., Hurst, S., O-Uchi, J., Csordás, G. and Sheu, S.S. 2017. The Mitochondrial Ca2+ Uniporter: Structure, Function and Pharmacology. *Handbook of experimental pharmacology* 240, p. 129.

Misslitz, A., Pabst, O., Hintzen, G., Ohl, L., Kremmer, E., Petrie, H.T. and Förster, R. 2004. Thymic T Cell Development and Progenitor Localization Depend on CCR7. *Journal of Experimental Medicine* 200(4), pp. 481–491.

Mitchell, E. et al. 2022. Clonal dynamics of haematopoiesis across the human lifespan. *Nature 2022 606:7913* 606(7913), pp. 343–350.

Miyawaki, K. et al. 2015. CD41 Marks the Initial Myelo-Erythroid Lineage Specification in Adult Mouse Hematopoiesis: Redefinition of Murine Common Myeloid Progenitor. *Stem Cells* 33(3), pp. 976–987.

Mohammadi Ghahhari, N., Sznurkowska, M.K., Hulo, N., Bernasconi, L., Aceto, N. and Picard, D. 2022. Cooperative interaction between ERα and the EMT-inducer ZEB1 reprograms breast cancer cells for bone metastasis. *Nature Communications 2022 13:1* 13(1), pp. 1–19.

Momiuchi, Y. et al. 2021. Group 2 innate lymphoid cells in bone marrow regulate osteoclastogenesis in a reciprocal manner via RANKL, GM-CSF and IL-13. *International Immunology* 33(11), pp. 573–585.

Mooney, C.J., Cunningham, A., Tsapogas, P., Toellner, K.M. and Brown, G. 2017. Selective Expression of Flt3 within the Mouse Hematopoietic Stem Cell Compartment. *International Journal of Molecular Sciences 2017, Vol. 18, Page 1037* 18(5), p. 1037.

Moore, K.J., Sheedy, F.J. and Fisher, E.A. 2013a. Macrophages in atherosclerosis: a dynamic balance. *Nature reviews. Immunology* 13(10), p. 709.

Moore, K.J., Sheedy, F.J. and Fisher, E.A. 2013b. Macrophages in atherosclerosis: a dynamic balance. *Nature reviews. Immunology* 13(10), p. 709.

Mori, T. and Osumi, T. 2022. Hematopoietic Stem Cell Transplantation. *Non-Hodgkin's Lymphoma in Childhood and Adolescence*, pp. 305–313.

Morita, Y., Ema, H. and Nakauchi, H. 2010. Heterogeneity and hierarchy within the most primitive hematopoietic stem cell compartment. *The Journal of experimental medicine* 207(6), pp. 1173–1182.

Moro, K. et al. 2009. Innate production of TH2 cytokines by adipose tissue-associated c-Kit+Sca-1+ lymphoid cells. *Nature 2009 463:7280* 463(7280), pp. 540–544.

Morrison, S.J., Andycz1, A.M.W. and Weissman, I.L. 1996. The aging of hematopoietic stem cells AMIELA GLOBERSON 2 & Progenitor cells in mouse populations. *Nature Medicine* 2(9), pp. 2–7.

Morrison, S.J. and Scadden, D.T. 2014. The bone marrow niche for haematopoietic stem cells. *Nature 2014 505:7483* 505(7483), pp. 327–334.

Munz, M., Baeuerle, P.A. and Gires, O. 2009. The emerging role of EpCAM in cancer and stem cell signaling. *Cancer Research* 69(14), pp. 5627–5629.

n, Eunsung Mouradian, M.M. 2008. CD19 as a molecular target in CNS autoimmunity. *Bone* 23(1), pp. 1–7. doi: 10.1038/nature08365.Reconstructing.

Nagasawa, T. 2006. Microenvironmental niches in the bone marrow required for B-cell development. *Nature reviews. Immunology* 6(2), pp. 107–116.

Nagata, S. and Suda, T. 1995. Fas and Fas ligand: lpr and gld mutations. *Immunology Today* 16(1), pp. 39–43. doi: 10.1016/0167-5699(95)80069-7.

Nagy, A. 2000. Cre Recombinase: The Universal Reagent for Genome Tailoring.

Naka, K. and Hirao, A. 2011. Maintenance of genomic integrity in hematopoietic stem cells. *International Journal of Hematology* 93(4), pp. 434–439.

Nakahara, F., Weiss, C.N. and Ito, K. 2014. The role of PML in hematopoietic and leukemic stem cell maintenance. *International journal of hematology* 100(1), p. 18.

Nakamura-Ishizu, A., Ito, K. and Suda, T. 2020. Hematopoietic Stem Cell Metabolism during Development and Aging. *Developmental Cell* 54(2), pp. 239–255. doi: 10.1016/J.DEVCEL.2020.06.029.

Nakayama, T. et al. 2002. The Generation of Mature, Single-Positive Thymocytes In Vivo Is Dysregulated by CD69 Blockade or Overexpression. *The Journal of Immunology* 168(1), pp. 87–94. doi: 10.4049/jimmunol.168.1.87.

Nelson, A.J., Dunn, R.J., Peach, R., Aruffo, A. and Farr, A.G. 1996. The murine homolog of human Ep-CAM, a homotypic adhesion molecule, is expressed by thymocytes and thymic epithelial cells. *European journal of immunology* 26(2), pp. 401–408.

Nemazee, D. 2017. Mechanisms of central tolerance for B cells. *Nature Reviews Immunology 2017 17:5* 17(5), pp. 281–294.

Ng, V.Y., Ang, S.N., Chan, J.X. and Choo, A.B.H. 2010. Characterization of Epithelial Cell Adhesion Molecule as a Surface Marker on Undifferentiated Human Embryonic Stem Cells. *STEM CELLS* 28(1), pp. 29–35.

Nieto, M.A., Huang, R.Y.Y.J., Jackson, R.A.A. and Thiery, J.P.P. 2016. EMT: 2016. *Cell* 166(1), pp. 21–45.

Nikolich-Žugich, J. 2014. Aging of the T cell compartment in mice and humans: from no naive expectations to foggy memories. *Journal of immunology (Baltimore, Md. : 1950)* 193(6), pp. 2622–2629.

Nikolich-Žugich, J. 2017. The twilight of immunity: emerging concepts in aging of the immune system. *Nature Immunology 2017 19:1* 19(1), pp. 10–19.

Nikolich-Žugich, J. 2018. The twilight of immunity: Emerging concepts in aging of the immune system review-article. *Nature Immunology* 19(1), pp. 10–19. doi: 10.1038/s41590-017-0006-x.

Nishimura, H., Nose, M., Hiai, H., Minato, N. and Honjo, T. 1999. Development of lupus-like autoimmune diseases by disruption of the PD-1 gene encoding an ITIM motif-carrying immunoreceptor. *Immunity* 11(2), pp. 141–151.

Notta, F. et al. 2016. Distinct routes of lineage development reshape the human blood hierarchy across ontogeny. *Science (New York, N.Y.)* 351(6269).

Notta, F., Doulatov, S., Laurenti, E., Poeppl, A., Jurisica, I. and Dick, J.E. 2011. Isolation of single human hematopoietic stem cells capable of long-term multilineage engraftment. *Science (New York, N.Y.)* 333(6039), pp. 218–221.

Nutt, S.L. and Kee, B.L. 2007. The Transcriptional Regulation of B Cell Lineage Commitment. *Immunity* 26(6). doi: 10.1016/j.immuni.2007.05.010.

O'Connell, K.E. et al. 2015. Practical Murine Hematopathology: A Comparative Review and Implications for Research. *Comparative Medicine* 65(2), p. 96.

Ogawa, M., Ten Boekel, E. and Melchers, F. 2000. Identification of CD19(-)B220(+)c-Kit(+)Flt3/Flk-2(+)cells as early B lymphoid precursors before pre-B-I cells in juvenile mouse bone marrow. *International immunology* 12(3), pp. 313–324.

Ogilvy, S., Metcalf, D., Gibson, L., Bath, M.L., Harris, A.W. and Adams, J.M. 1999. Promoter Elements of vav Drive Transgene Expression In Vivo Throughout the Hematopoietic Compartment. *Blood* 94(6), pp. 1855–1863.

Oguro, H., Ding, L. and Morrison, S.J. 2013. SLAM family markers resolve functionally distinct subpopulations of hematopoietic stem cells and multipotent progenitors. *Cell stem cell* 13(1), pp. 102–116.

Oh, M. and Nör, J.E. 2015. The perivascular niche and self-renewal of stem cells. *Frontiers in Physiology* 6(DEC), p. 367. doi: 10.3389/FPHYS.2015.00367/BIBTEX.

Okada, S., Nakauchi, H., Nagayoshi, K., Nishikawa, S.I., Miura, Y. and Suda, T. 1992. In vivo and in vitro stem cell function of c-kit- and Sca-1-positive murine hematopoietic cells. *Blood* 80(12). doi: 10.1182/blood.v80.12.3044.bloodjournal80123044.

Olariu, V. and Peterson, C. 2019. Kinetic models of hematopoietic differentiation. *Wiley interdisciplinary reviews. Systems biology and medicine* 11(1).

O'Leary, N.A. et al. 2016. Reference sequence (RefSeq) database at NCBI: current status, taxonomic expansion, and functional annotation. *Nucleic acids research* 44(D1), pp. D733–D745.

Olsson, I., Bergh, G., Ehinger, M. and Gullberg, U. 1996. Cell differentiation in acute myeloid leukemia. *European Journal of Haematology* 57(1), pp. 1–16.

Orkin, S.H. 2000. Diversification of haematopoietic stem cells to specific lineages. *Nature reviews. Genetics* 1(1), pp. 57–64.

Orkin, S.H. 2003. Priming the Hematopoietic Pump. *Immunity* 19(5), pp. 633–634. doi: 10.1016/S1074-7613(03)00302-9.

Orkin, S.H. and Zon, L.I. 2008a. Hematopoiesis: An Evolving Paradigm for Stem Cell Biology. *Cell* 132(4), pp. 631–644. doi: 10.1016/j.cell.2008.01.025.

Orkin, S.H. and Zon, L.I. 2008b. Hematopoiesis: an evolving paradigm for stem cell biology. *Cell* 132(4), pp. 631–644.

Osawa, M., Hanada, K.I., Hamada, H. and Nakauchi, H. 1996. Long-term lymphohematopoietic reconstitution by a single CD34-low/negative hematopoietic stem cell. *Science (New York, N.Y.)* 273(5272), pp. 242–245.

Osmond, D.G., Rolink, A. and Melchers, F. 1998. Murine B lymphopoiesis: towards a unified model. *Immunology today* 19(2), pp. 65–68.

Ottersbach, K. and Dzierzak, E. 2005. The murine placenta contains hematopoietic stem cells within the vascular labyrinth region. *Developmental cell* 8(3), pp. 377–387.

Padi, S.K.R. et al. 2017. Targeting the PIM protein kinases for the treatment of a T-cell acute lymphoblastic leukemia subset. *Oncotarget* 8(18), pp. 30199–30216.

Park, D. et al. 2012. Endogenous bone marrow MSCs are dynamic, fate-restricted participants in bone maintenance and regeneration. *Cell Stem Cell* 10(3), pp. 259–272.

Parker, M.P. and Peterson, K.R. 2018. Mouse Models of Erythropoiesis and Associated Diseases. *Methods in molecular biology (Clifton, N.J.)* 1698, p. 37.

Patton, D.T., Plumb, A.W. and Abraham, N. 2014. The Survival and Differentiation of Pro-B and Pre-B Cells in the Bone Marrow Is Dependent on IL-7Rα Tyr449. *The Journal of Immunology* 193(7), pp. 3446–3455. doi: 10.4049/jimmunol.1302925.

Payne, S., De Val, S. and Neal, A. 2018. Endothelial-Specific Cre Mouse Models. *Arteriosclerosis, Thrombosis, and Vascular Biology* 38(11). doi: 10.1161/atvbaha.118.309669.

Pearce, D.J., Anjos-Afonso, F., Ridler, C.M., Eddaoudi, A. and Bonnet, D. 2007. Age-Dependent Increase in Side Population Distribution Within Hematopoiesis: Implications for Our Understanding of the Mechanism of Aging. *Stem Cells* 25(4), pp. 828–835. doi: 10.1634/stemcells.2006-0405.

Pei, D., Shu, X., Gassama-Diagne, A. and Thiery, J.P. 2019. Mesenchymal-epithelial transition in development and reprogramming. *Nature cell biology* 21(1), pp. 44–53.

Peikert, K. et al. 2022. Commentary: Acanthocytes identified in Huntington's disease. *Frontiers in Neuroscience* 16, p. 1920. doi: 10.3389/FNINS.2022.1049676/BIBTEX.

Peinado, H., Olmeda, D. and Cano, A. 2007. Snail, Zeb and bHLH factors in tumour progression: an alliance against the epithelial phenotype? *Nature reviews. Cancer* 7(6), pp. 415–428.

Pennock, N.D., White, J.T., Cross, E.W., Cheney, E.E., Tamburini, B.A. and Kedl, R.M. 2013. T cell responses: naïve to memory and everything in between. *Advances in Physiology Education* 37(4), p. 273.

Peraki, I., Palis, J. and Mavrothalassitis, G. 2017. The Ets2 Repressor Factor (Erf) Is Required for Effective Primitive and Definitive Hematopoiesis. *Molecular and cellular biology* 37(19).

Pereira, B.I. et al. 2020. Sestrins induce natural killer function in senescent-like CD8+ T cells. *Nature Immunology 2020 21:6* 21(6), pp. 684–694.

Perez-Oquendo, M. and Gibbons, D.L. 2022. Regulation of ZEB1 Function and Molecular Associations in Tumor Progression and Metastasis. *Cancers* 14(8).

Pernas, L. and Scorrano, L. 2016. Mito-Morphosis: Mitochondrial Fusion, Fission, and Cristae Remodeling as Key Mediators of Cellular Function. *https://doi.org/10.1146/annurev-physiol-021115-105011* 78, pp. 505–531.

Perocchi, F., Gohil, V.M., Girgis, H.S., Bao, X.R., McCombs, J.E., Palmer, A.E. and Mootha, V.K. 2010. MICU1 encodes a mitochondrial EF hand protein required for Ca2+ uptake. *Nature* 467(7313), p. 291.

Persa, O.D. and Niessen, C.M. 2019. Epithelial polarity limits EMT. *Nature Cell Biology 2019 21:3* 21(3), pp. 299–300.

Petrovas, C. et al. 2006. PD-1 is a regulator of virus-specific CD8+ T cell survival in HIV infection. *The Journal of Experimental Medicine* 203(10), p. 2281.

Phillips, M.C. 2018. Thematic Review Series: Lipid Transfer Proteins: Is ABCA1 a lipid transfer protein? *Journal of Lipid Research* 59(5), p. 749.

Pimanda, J.E. et al. 2007. Gata2, Fli1, and Scl form a recursively wired gene-regulatory circuit during early hematopoietic development. *Proceedings of the National Academy of Sciences of the United States of America* 104(45), p. 17692.

Pinho, S. and Frenette, P.S. 2019. Haematopoietic stem cell activity and interactions with the niche. *Nature Reviews Molecular Cell Biology 2019 20:5* 20(5), pp. 303–320.

Postigo, A.A. and Dean, D.C. 1999. Independent repressor domains in ZEB regulate muscle and T-cell differentiation. *Molecular and cellular biology* 19(12), pp. 7961–7971.

Postigo, A.A., Depp, J.L., Taylor, J.J. and Kroll, K.L. 2003. Regulation of Smad signaling through a differential recruitment of coactivators and corepressors by ZEB proteins. *EMBO Journal* 22(10), pp. 2453–2462. doi: 10.1093/emboj/cdg226.

Postigo, A.A., Sheppard, A.M., Mucenski, M.L. and Dean, D.C. 1997. c-Myb and Ets proteins synergize to overcome transcriptional repression by ZEB. *The EMBO Journal* 16(13), pp. 3924–3934.

Pouzolles, M., Oburoglu, L., Taylor, N. and Zimmermann, V.S. 2016. Hematopoietic stem cell lineage specification. *Current opinion in hematology* 23(4), pp. 311–317.

Pronk, C.J.H. et al. 2007. Elucidation of the phenotypic, functional, and molecular topography of a myeloerythroid progenitor cell hierarchy. *Cell stem cell* 1(4), pp. 428–442.

Pucella, J.N., Upadhaya, S. and Reizis, B. 2020. The Source and Dynamics of Adult Hematopoiesis: Insights from Lineage Tracing. *Annual review of cell and developmental biology* 36, pp. 529–550.

Quinn, K.M., Palchaudhuri, R., Palmer, C.S. and La Gruta, N.L. 2019a. The clock is ticking: the impact of ageing on T cell metabolism. *Clinical & Translational Immunology* 8(11), p. e01091.

Quinn, K.M., Palchaudhuri, R., Palmer, C.S. and La Gruta, N.L. 2019b. The clock is ticking: the impact of ageing on T cell metabolism. *Clinical & Translational Immunology* 8(11), p. e01091.

Raabe, B.M., Artwohl, J.E., Purcell, J.E., Lovaglio, J. and Fortman, J.D. 2011. Effects of Weekly Blood Collection in C57BL/6 Mice. *Journal of the American Association for Laboratory Animal Science : JAALAS* 50(5), p. 680.

Ramirez, N.;, Woytschak, J.; and Boyman, O. 2015. Interleukin-2: biology, design and application. *Trends in Immunology* 36(12), pp. 763–777. doi: 10.1016/j.it.2015.10.003.

Rashighi, M. and Harris, J.E. 2017. 乳鼠心肌提取 HHS Public Access. *Physiology & behavior* 176(3), pp. 139–148. doi: 10.1053/j.gastro.2016.08.014.CagY.

Ratajczak, W., Niedźwiedzka-Rystwej, P., Tokarz-Deptuła, B. and Deptuła, W. 2018. Immunological memory cells. *Central-European Journal of Immunology* 43(2), p. 194.

Redman, C., Huima, T., Robbins, E., Lee, S. and Marsh, W. 1989. Effect of phosphatidylserine on the shape of McLeod red cell acanthocytes. *Blood* 74(5), pp. 1826–1835. doi: 10.1182/BLOOD.V74.5.1826.1826.

Reiss, A.B., Siegart, N.M. and De Leon, J. 2017a. Clinical Lipidology Interleukin-6 in atherosclerosis: atherogenic or atheroprotective? Interleukin-6 in atherosclerosis: atherogenic or atheroprotective?

Reiss, A.B., Siegart, N.M. and De Leon, J. 2017b. Clinical Lipidology Interleukin-6 in atherosclerosis: atherogenic or atheroprotective? Interleukin-6 in atherosclerosis: atherogenic or atheroprotective?

Remacle, J.E. et al. 1999. New mode of DNA binding of multi-zinc finger transcription factors: deltaEF1 family members bind with two hands to two target sites. *The EMBO Journal* 18(18), p. 5073.

Resop, R.S. and Uittenbogaart, C.H. 2015. Human T-Cell Development and Thymic Egress: An Infectious Disease Perspective. *Forum on immunopathological diseases and therapeutics* 6(1–2), p. 33.

Reutelingsperger, C.P.M. and Van Heerde, W.L. 1997. Annexin V, the regulator of phosphatidylserine-catalyzed inflammation and coagulation during apoptosis. *Cellular and Molecular Life Sciences* 53(6), pp. 527–532.

Rix, B., Maduro, A.H., Bridge, K.S. and Grey, W. 2022. Markers for human haematopoietic stem cells: The disconnect between an identification marker and its function. *Frontiers in physiology* 13.

Roberts, A.I. et al. 2003. The role of activation-induced cell death in the differentiation of T-helper-cell subsets. *Immunologic research* 28(3), pp. 285–293.

Roberts, O. and Paraoan, L. 2020. PERP-ing into diverse mechanisms of cancer pathogenesis: Regulation and role of the p53/p63 effector PERP. *Biochimica et Biophysica Acta (BBA) - Reviews on Cancer* 1874(1), p. 188393. doi: 10.1016/J.BBCAN.2020.188393.

Robin, C. et al. 2009. Human placenta is a potent hematopoietic niche containing hematopoietic stem and progenitor cells throughout development. *Cell stem cell* 5(4), pp. 385–395.

Rodewald, H.R., Kretzschmar, K., Takeda, S., Hohl, C. and Dessing, M. 1994. Identification of pro-thymocytes in murine fetal blood: T lineage commitment can precede thymus colonization. *The EMBO journal* 13(18), pp. 4229–4240.

Rodriguez, I.J. et al. 2021. Immunosenescence Study of T Cells: A Systematic Review. *Frontiers in Immunology* 11, p. 3460. doi: 10.3389/FIMMU.2020.604591/BIBTEX.

Romero, X., Benítez, D., March, S., Vilella, R., Miralpeix, M. and Engel, P. 2004. Differential expression of SAP and EAT-2-binding leukocyte cell-surface molecules CD84, CD150 (SLAM), CD229 (Ly9) and CD244 (2B4). *Tissue antigens* 64(2), pp. 132–144.

Ross, R. 1986. The pathogenesis of atherosclerosis--an update. *The New England journal of medicine* 314(8), pp. 488–500.

Rossi, L. et al. 2012. Less is More: unveiling the functional core of hematopoietic stem cells through knockout mice. *Cell stem cell* 11(3), p. 302.

Van Roy, F. and Berx, G. 2008. The cell-cell adhesion molecule E-cadherin. *Cellular and Molecular Life Sciences* 65(23), pp. 3756–3788.

Sahin, A.O. and Buitenhuis, M. 2012. Molecular mechanisms underlying adhesion and migration of hematopoietic stem cells. *https://doi.org/10.4161/cam.18975* 6(1), pp. 39–48.

Salam, N. et al. 2013. T cell ageing: Effects of age on development, survival & function. *The Indian Journal of Medical Research* 138(5), p. 595.

Sallusto, F., Geginat, J. and Lanzavecchia, A. 2004. Central memory and effector memory T cell subsets: function, generation, and maintenance. *Annual review of immunology* 22, pp. 745–763.

Sallusto, F., Lenig, D., Förster, R., Lipp, M. and Lanzavecchia, A. 1999. Two subsets of memory T lymphocytes with distinct homing potentials and effector functions. *Nature* 401(6754), pp. 708–712.

Salnikov, A. V. et al. 2009. Targeting of cancer stem cell marker EpCAM by bispecific antibody EpCAMxCD3 inhibits pancreatic carcinoma. *Journal of cellular and molecular medicine* 13(9B), pp. 4023–4033.

Samji, T. and Khanna, K.M. 2017. Understanding Memory CD8+ T cells. *Immunology letters* 185, p. 32.

Sam-Yellowe, T.Y. 2021. Leukocyte Homing, Migration and Recirculation. *Immunology: Overview and Laboratory Manual*, pp. 55–58. doi: 10.1007/978-3-030-64686-8_7.

Sato, T., Onai, N., Yoshihara, H., Arai, F., Suda, T. and Ohteki, T. 2009. Interferon regulatory factor-2 protects quiescent hematopoietic stem cells from type i interferon-dependent exhaustion. *Nature Medicine* 15(6). doi: 10.1038/nm.1973.

Sawai, C.M. et al. 2016. Hematopoietic stem cells are the major source of multilineage hematopoiesis in adult animals. *Immunity* 45(3), p. 597.

Schaefer, C.F., Anthony, K., Krupa, S., Buchoff, J., Day, M., Hannay, T. and Buetow, K.H. 2009. PID: the Pathway Interaction Database. *Nucleic acids research* 37(Database issue).

Schnell, U., Cirulli, V. and Giepmans, B.N.G. 2013a. EpCAM: Structure and function in health and disease. *Biochimica et Biophysica Acta (BBA) - Biomembranes* 1828(8), pp. 1989–2001. doi: 10.1016/J.BBAMEM.2013.04.018.

Schnell, U., Cirulli, V. and Giepmans, B.N.G. 2013b. EpCAM: Structure and function in health and disease. *Biochimica et Biophysica Acta - Biomembranes* 1828(8), pp. 1989–2001.

Schnell, U., Cirulli, V. and Giepmans, B.N.G. 2013c. EpCAM: structure and function in health and disease. *Biochimica et biophysica acta* 1828(8), pp. 1989–2001.

Schwartz, R.H. 2003. T cell anergy. *Annual review of immunology* 21, pp. 305–334.

Scott, C.L. and Omilusik, K.D. 2019. ZEBs: Novel Players in Immune Cell Development and Function. *Trends in Immunology* 40(5), pp. 431–446. doi: 10.1016/J.IT.2019.03.001.

Shah, K., Al-Haidari, A., Sun, J. and Kazi, J.U. 2021. T cell receptor (TCR) signaling in health and disease. *Signal Transduction and Targeted Therapy 2021 6:1* 6(1), pp. 1–26.

Shelton, P.M. et al. 2018. The Secretion of miR-200s by a PKCζ/ADAR2 Signaling Axis Promotes Liver Metastasis in Colorectal Cancer. *Cell reports* 23(4), pp. 1178–1191.

Shim, Y.A., Campbell, T., Weliwitigoda, A., Dosanjh, M. and Johnson, P. 2020. Regulation of CD71+TER119+ erythroid progenitor cells by CD45. *Experimental Hematology* 86, pp. 53-66.e1. doi: 10.1016/J.EXPHEM.2020.05.005.

Shimshek, D.R. et al. 2002. Codon-improved Cre recombinase (iCre) expression in the mouse. *genesis* 32(1), pp. 19–26.

Shores, E.W., Van Ewijk, W. and Singer, A. 1994. Maturation of medullary thymic epithelium requires thymocytes expressing fully assembled CD3-TCR complexes. *International immunology* 6(9), pp. 1393–1402.

Siegemund, S., Shepherd, J., Xiao, C. and Sauer, K. 2015. hCD2-iCre and Vav-iCre Mediated Gene Recombination Patterns in Murine Hematopoietic Cells. *PLoS ONE* 10(4).

Siminovitch, L., Mcculloch, E.A. and Till, J.E. 1963. The Distribution of Colony-forming Cells Among Spleen Colonies. *JOURNAL OF CELLULAR AND COMPARATIVE PHYSIOLOGY* 62(3).

Singh, D.K. et al. 2017. Oncogenes Activate an Autonomous Transcriptional Regulatory Circuit That Drives Glioblastoma. *Cell reports* 18(4), pp. 961–976.

Singh, S. et al. 2016a. Zeb1 controls neuron differentiation and germinal zone exit by a mesenchymal-epithelial-like transition. *eLife* 5(MAY2016).

Singh, S. et al. 2016b. Zeb1 controls neuron differentiation and germinal zone exit by a mesenchymal-epithelial-like transition. *eLife* 5(MAY2016).

Sintov, E., Nathan, G., Knoller, S., Pasmanik-Chor, M., Russ, H.A. and Efrat, S. 2015. Inhibition of ZEB1 expression induces redifferentiation of adult human β cells expanded in vitro. *Scientific Reports* 5, pp. 13024–13024.

Smith, B.N. and Bhowmick, N.A. 2016. Role of EMT in Metastasis and Therapy Resistance. *Journal of Clinical Medicine* 5(2), p. 17.

Sobocka, M.B. et al. 2000. Cloning of the human platelet F11 receptor: a cell adhesion molecule member of the immunoglobulin superfamily involved in platelet aggregation: Presented in part at the XVIIth Congress of the International Society on Thrombosis and Haemostasis, Washington, DC, August 14-21, 1999. *Blood* 95(8), pp. 2600–2609. doi: 10.1182/BLOOD.V95.8.2600.

Soen, B., Vandamme, N., Berx, G., Schwaller, J., Van Vlierberghe, P. and Goossens, S. 2018. ZEB Proteins in Leukemia: Friends, Foes, or Friendly Foes? *HemaSphere* 2(3).

Sonawane, A.R. et al. 2017. Understanding Tissue-Specific Gene Regulation. *Cell reports* 21(4), pp. 1077–1088.

Song, Y. et al. 2017. H19 promotes cholestatic liver fibrosis by preventing ZEB1-mediated inhibition of epithelial cell adhesion molecule. *Hepatology* 66(4), pp. 1183–1196.

Spizzo, G. et al. 2011. EpCAM expression in primary tumour tissues and metastases: an immunohistochemical analysis. *Journal of Clinical Pathology* 64(5), pp. 415–420.

Stadtfeld, M. and Graf, T. 2005. Assessing the role of hematopoietic plasticity for endothelial and hepatocyte development by non-invasive lineage tracing. *Development* 132(1), pp. 203–213.

Stemmler, M.P., Eccles, R.L., Brabletz, S. and Brabletz, T. 2019. Non-redundant functions of EMT transcription factors. *Nature Cell Biology 2019 21:1* 21(1), pp. 102–112.

Sumide, K. et al. 2018. A revised road map for the commitment of human cord blood CD34-negative hematopoietic stem cells. *Nature Communications 2018 9:1* 9(1), pp. 1–17.

Sun, J. et al. 2014. Clonal dynamics of native haematopoiesis. *Nature* 514(7522), pp. 322–327.

Sunderkötter, C., Nikolic, T., Dillon, M.J., van Rooijen, N., Stehling, M., Drevets, D.A. and Leenen, P.J.M. 2004. Subpopulations of Mouse Blood Monocytes Differ in Maturation Stage and Inflammatory Response. *The Journal of Immunology* 172(7), pp. 4410–4417. doi: 10.4049/JIMMUNOL.172.7.4410.

Swahn, H. et al. 2023. Senescent cell population with ZEB1 transcription factor as its main regulator promotes osteoarthritis in cartilage and meniscus. *Annals of the Rheumatic Diseases* 82(3), pp. 403–415.

Swain, S.L. and Blomberg, B.B. 2013. Immune senescence: New insights into defects but continued mystery of root causes. *Current Opinion in Immunology* 25(4), pp. 495–497.

Tabas, I. and Lichtman, A.H. 2017. Monocyte-Macrophages and T Cells in Atherosclerosis. *Immunity* 47(4), p. 621.

Takada, K. and Jameson, S.C. 2009. Naive T cell homeostasis: from awareness of space to a sense of place. *Nature reviews. Immunology* 9(12), pp. 823–832.

Takagi, T., Moribe, H., Kondoh, H. and Higashi, Y. 1998a. DeltaEF1, a zinc finger and homeodomain transcription factor, is required for skeleton patterning in multiple lineages. *Development (Cambridge, England)* 125(1), pp. 21–31.

Takagi, T., Moribe, H., Kondoh, H. and Higashi, Y. 1998b. DeltaEF1, a zinc finger and homeodomain transcription factor, is required for skeleton patterning in multiple lineages. *Development (Cambridge, England)* 125(1), pp. 21–31.

Takahama, Y. 2006. Journey through the thymus: Stromal guides for T-cell development and selection. *Nature Reviews Immunology* 6(2), pp. 127–135. doi: 10.1038/nri1781.

Talayero, B.G. and Sacks, F.M. 2011. The Role of Triglycerides in Atherosclerosis. *Current cardiology reports* 13(6), p. 544.

Tall, A.R. and Yvan-Charvet, L. 2015. Cholesterol, inflammation and innate immunity. *Nature reviews. Immunology* 15(2), pp. 104–116.

Thiery, J.P. and Sleeman, J.P. 2006. Complex networks orchestrate epithelial–mesenchymal transitions. *Nature Reviews Molecular Cell Biology 2006 7:2* 7(2), pp. 131–142.

TILL, J.E. and McCULLOCH, E.A. 1961. A direct measurement of the radiation sensitivity of normal mouse bone marrow cells. *Radiation research* 14, pp. 213–222. doi: 10.2307/3570892.

Tissue expression of EPCAM - Summary - The Human Protein Atlas. [no date].

Tousoulis, Di., Oikonomou, E., Economou, E.K., Crea, F. and Kaski, J.C. 2016. Inflammatory cytokines in atherosclerosis: current therapeutic approaches. *European Heart Journal* 37(22), pp. 1723–1732.

Trampont, P.C. et al. 2010. CXCR4 acts as a costimulator during thymic β selection. *Nature immunology* 11(2), p. 162.

Uhlén, M. et al. 2015. Proteomics. Tissue-based map of the human proteome. *Science (New York, N.Y.)* 347(6220).

Upadhaya, S. et al. 2018. Kinetics of adult hematopoietic stem cell differentiation in vivo. *The Journal of experimental medicine* 215(11), pp. 2815–2832.

Vandewalle, C., Van Roy, F. and Berx, G. 2009. The role of the ZEB family of transcription factors in development and disease. *Cellular and Molecular Life Sciences* 66(5), pp. 773–787.

Vannier, C., Mock, K., Brabletz, T. and Driever, W. 2013. Zeb1 Regulates E-cadherin and Epcam (Epithelial Cell Adhesion Molecule) Expression to Control Cell Behavior in Early Zebrafish Development. *The Journal of Biological Chemistry* 288(26), p. 18643.

Vasquez, C.G., De la Serna, E.L. and Dunn, A.R. 2021. How cells tell up from down and stick together to construct multicellular tissues - interplay between apicobasal polarity and cell-cell adhesion. *Journal of cell science* 134(21).

Veillette, A. 2006. Immune regulation by SLAM family receptors and SAP-related adaptors. *Nature Reviews Immunology 2006 6:1* 6(1), pp. 56–66.

Velasco-Hernandez, T., Säwén, P., Bryder, D. and Cammenga, J. 2016. Potential Pitfalls of the Mx1-Cre System: Implications for Experimental Modeling of Normal and Malignant Hematopoiesis. *Stem cell reports* 7(1), pp. 11–18.

Velten, L. et al. 2017. Human haematopoietic stem cell lineage commitment is a continuous process. *Nature cell biology* 19(4), pp. 271–281.

Villa-Morales, M., González-Gugel, E., Shahbazi, M.N., Santos, J. and Fernández-Piqueras, J. 2010. Modulation of the Fas-apoptosis-signalling

pathway by functional polymorphisms at Fas , FasL and Fadd and their implication in T-cell lymphoblastic lymphoma susceptibility. *Carcinogenesis* 31(12), pp. 2165–2171.

Villar-Fincheira, P. et al. 2021. Role of Interleukin-6 in Vascular Health and Disease. *Frontiers in Molecular Biosciences* 8, p. 79. doi: 10.3389/FMOLB.2021.641734/BIBTEX.

Vladutiu, A.O. 1993. The severe combined immunodeficient (SCID) mouse as a model for the study of autoimmune diseases. *Clinical and Experimental Immunology* 93(1), p. 1.

Voermans, C., Rood, P.M.L., Hordijk, P.L., Gerritsen, W.R. and Schoot, C.E. van der. 2000. Adhesion Molecules Involved in Transendothelial Migration of Human Hematopoietic Progenitor Cells. *STEM CELLS* 18(6), pp. 435–443.

Volpe, E., Sambucci, M., Battistini, L. and Borsellino, G. 2016. Fas-fas ligand: Checkpoint of t cell functions in multiple sclerosis. *Frontiers in Immunology* 7(SEP), p. 382. doi: 10.3389/FIMMU.2016.00382/BIBTEX.

Volpe, G. et al. 2015. Regulation of the flt3 gene in haematopoietic stem and early progenitor cells. *PLoS ONE* 10(9), pp. 1–18. doi: 10.1371/journal.pone.0138257.

Wahren-Herlenius, M. and Dörner, T. 2013. Immunopathogenic mechanisms of systemic autoimmune disease. *The Lancet* 382(9894), pp. 819–831. doi: 10.1016/S0140-6736(13)60954-X.

Wallberg, F., Tenev, T. and Meier, P. 2016. Analysis of Apoptosis and Necroptosis by Fluorescence-Activated Cell Sorting. *Cold Spring Harbor protocols* 2016(4), pp. 347–352.

Wallrapp, A. et al. 2017. The neuropeptide NMU amplifies ILC2-driven allergic lung inflammation. *Nature 2017 549:7672* 549(7672), pp. 351–356.

Wang, H., Xiao, Z., Zheng, J., Wu, J., Hu, X.L., Yang, X. and Shen, Q. 2019a. ZEB1 Represses Neural Differentiation and Cooperates with CTBP2 to

Dynamically Regulate Cell Migration during Neocortex Development. *Cell Reports* 27(8), pp. 2335-2353.e6. doi: 10.1016/J.CELREP.2019.04.081.

Wang, H., Xiao, Z., Zheng, J., Wu, J., Hu, X.L., Yang, X. and Shen, Q. 2019b. ZEB1 Represses Neural Differentiation and Cooperates with CTBP2 to Dynamically Regulate Cell Migration during Neocortex Development. *Cell Reports* 27(8), pp. 2335-2353.e6. doi: 10.1016/J.CELREP.2019.04.081.

Wang, J. et al. 2021a. Interplay between the EMT transcription factors ZEB1 and ZEB2 regulates hematopoietic stem and progenitor cell differentiation and hematopoietic lineage fidelity. *PLOS Biology* 19(9), p. e3001394.

Wang, J. et al. 2021b. Interplay between the EMT transcription factors ZEB1 and ZEB2 regulates hematopoietic stem and progenitor cell differentiation and hematopoietic lineage fidelity. *PLoS biology* 19(9).

Wang, J. et al. 2021c. *Interplay between the EMT transcription factors ZEB1 and ZEB2 regulates hematopoietic stem and progenitor cell differentiation and hematopoietic lineage fidelity*.

Wang, J., Lee, S., Teh, C.E.Y., Bunting, K., Ma, L. and Shannon, M.F. 2009. The transcription repressor, ZEB1, cooperates with CtBP2 and HDAC1 to suppress IL-2 gene activation in T cells. *International Immunology* 21(3), pp. 227–235. doi: 10.1093/intimm/dxn143.

Wang, M. et al. 2018a. MEIS2 regulates endothelial to hematopoietic transition of human embryonic stem cells by targeting TAL1. *Stem Cell Research & Therapy* 9(1).

Wang, M. et al. 2018b. MEIS2 regulates endothelial to hematopoietic transition of human embryonic stem cells by targeting TAL1 06 Biological Sciences 0604 Genetics. *Stem Cell Research and Therapy* 9(1), pp. 1–13.

Wang, M.H. et al. 2018c. Epithelial cell adhesion molecule overexpression regulates epithelial-mesenchymal transition, stemness and metastasis of nasopharyngeal carcinoma cells via the PTEN/AKT/mTOR pathway. *Cell Death & Disease 2018 9:1* 9(1), pp. 1–16.

Wang, X. et al. 2020. Identification of a Zeb1 expressing basal stem cell subpopulation in the prostate. *Nature Communications* 11(1).

Wang, X., Huang, H. and Young, K.H. 2015. The PTEN tumor suppressor gene and its role in lymphoma pathogenesis. *Aging* 7(12), pp. 1032–1049.

Wang, Y. et al. 2014. CUL4A induces epithelial-mesenchymal transition and promotes cancer metastasis by regulating ZEB1 expression. *Cancer Research* 74(2), pp. 520–531.

Watson, H.A. et al. 2019. L-selectin enhanced T cells improve the efficacy of cancer immunotherapy. *Frontiers in Immunology* 10(JUN), pp. 1–20. doi: 10.3389/fimmu.2019.01321.

Wei, Y. et al. 2020. Targeting Bcl-2 Proteins in Acute Myeloid Leukemia. *Frontiers in Oncology* 10, p. 2137. doi: 10.3389/FONC.2020.584974/BIBTEX.

Wellner, U. et al. 2009. The EMT-activator ZEB1 promotes tumorigenicity by repressing stemness-inhibiting microRNAs. *Nature cell biology* 11(12), pp. 1487–1495.

Werner, S., Keller, L. and Pantel, K. 2020. Epithelial keratins: Biology and implications as diagnostic markers for liquid biopsies. *Molecular Aspects of Medicine* 72, p. 100817. doi: 10.1016/J.MAM.2019.09.001.

Wesseling, M., Sakkers, T.R., de Jager, S.C.A., Pasterkamp, G. and Goumans, M.J. 2018. The morphological and molecular mechanisms of epithelial/endothelial-to-mesenchymal transition and its involvement in atherosclerosis. *Vascular Pharmacology* 106, pp. 1–8. doi: 10.1016/J.VPH.2018.02.006.

Williams, T.M. et al. 1991. Identification of a zinc finger protein that inhibits IL-2 gene expression. *Science (New York, N.Y.)* 254(5039), pp. 1791–1794.

Wilson, A. et al. 2008. Hematopoietic Stem Cells Reversibly Switch from Dormancy to Self-Renewal during Homeostasis and Repair. *Cell* 135(6), pp. 1118–1129. doi: 10.1016/j.cell.2008.10.048.

Wilson, N.K. et al. 2010. Combinatorial Transcriptional Control In Blood Stem/Progenitor Cells: Genome-wide Analysis of Ten Major Transcriptional Regulators. *Cell Stem Cell* 7(4), pp. 532–544. doi: 10.1016/J.STEM.2010.07.016.

Wilson, N.K., Calero-Nieto, F.J., Ferreira, R. and Göttgens, B. 2011. Transcriptional regulation of haematopoietic transcription factors. *Stem Cell Research and Therapy* 2(1), pp. 1–8.

Wognum, A.W., Eaves, A.C. and Thomas, T.E. 2003. Identification and isolation of hematopoietic stem cells. *Archives of medical research* 34(6), pp. 461–475.

Woodland, D.L. and Kohlmeier, J.E. 2009. Migration, maintenance and recall of memory T cells in peripheral tissues. *Nature Reviews Immunology 2009 9:3* 9(3), pp. 153–161.

Woolthuis, C.M. and Park, C.Y. 2016a. Hematopoietic stem/progenitor cell commitment to the megakaryocyte lineage. *Blood* 127(10), pp. 1242–1248.

Woolthuis, C.M. and Park, C.Y. 2016b. Hematopoietic stem/progenitor cell commitment to the megakaryocyte lineage. *Blood* 127(10), pp. 1242–1248.

Wright, D.E., Bowman, E.P., Wagers, A.J., Butcher, E.C. and Weissman, I.L. 2002. Hematopoietic Stem Cells Are Uniquely Selective in Their Migratory Response to Chemokines. *Journal of Experimental Medicine* 195(9), pp. 1145–1154.

Wu, J., Motto, D.G., Koretzky, G.A. and Weiss, A. 1996. Vav and SLP-76 interact and functionally cooperate in IL-2 gene activation. *Immunity* 4(6), pp. 593–602.

Wu, W.S., Heinrichs, S., Xu, D., Garrison, S.P., Zambetti, G.P., Adams, J.M. and Look, A.T. 2005. Slug antagonizes p53-mediated apoptosis of hematopoietic progenitors by repressing puma. *Cell* 123(4), pp. 641–653.

Wu, Y., Tian, L., Mealer, C., Choi, H.-J. and Yu, X.-Z. 2021. Targeting Pim2 for Improving T-Cell Effector Function and Promoting Cancer Immunotherapy. *Blood* 138(Supplement 1), pp. 1720–1720.

Wu, Y., Zhu, H. and Wu, H. 2020. PTEN in Regulating Hematopoiesis and Leukemogenesis. *Cold Spring Harbor Perspectives in Medicine* 10(10), p. a036244.

Xia, L., McDaniel, J.M., Yago, T., Doeden, A. and McEver, R.P. 2004. Surface fucosylation of human cord blood cells augments binding to P-selectin and E-selectin and enhances engraftment in bone marrow. *Blood* 104(10), pp. 3091–3096.

Xing, Y. and Hogquist, K.A. 2012. T-Cell Tolerance: Central and Peripheral. *Cold Spring Harbor Perspectives in Biology* 4(6), pp. 1–15.

Xiong, J. et al. 2021. Integrins regulate stemness in solid tumor: an emerging therapeutic target. *Journal of Hematology & Oncology 2021 14:1* 14(1), pp. 1–18.

Xue, L. et al. 2014. Prostaglandin D2 activates group 2 innate lymphoid cells through chemoattractant receptor-homologous molecule expressed on TH2 cells. *The Journal of allergy and clinical immunology* 133(4).

Yamamoto, R. et al. 2013. Clonal analysis unveils self-renewing lineage-restricted progenitors generated directly from hematopoietic stem cells. *Cell* 154(5).

Yang, J., Zhao, S. and Ma, D. 2019. Biological Characteristics and Regulation of Early Megakaryocytopoiesis. *Stem Cell Reviews and Reports* 15(5), pp. 652–663.

Yang, L., Bryder, D., Adolfsson, J., Nygren, J., Månsson, R., Sigvardsson, M. and Jacobsen, S.E.W. 2005. Identification of Lin–Sca1+kit+CD34+Flt3– short-term hematopoietic stem cells capable of rapidly reconstituting and rescuing myeloablated transplant recipients. *Blood* 105(7), pp. 2717–2723.

Yang, S., Liu, F., Wang, Q.J., Rosenberg, S.A. and Morgan, R.A. 2011. The Shedding of CD62L (L-Selectin) Regulates the Acquisition of Lytic Activity in Human Tumor Reactive T Lymphocytes. *PLoS ONE* 6(7), p. 22560.

Yavropoulou, M.P. and Yovos, J.G. 2008. Osteoclastogenesis--current knowledge and future perspectives. *Journal of Musculoskeletal & Neuronal Interactions* 8(3), pp. 204–216.

Ye, M. et al. 2003. Hematopoietic stem cells expressing the myeloid lysozyme gene retain long-term, multilineage repopulation potential. *Immunity* 19(5), pp. 689–699.

Yokomizo, T., Ng, C.E.L., Osato, M. and Dzierzak, E. 2011. Three-dimensional imaging of whole midgestation murine embryos shows an intravascular localization for all hematopoietic clusters. *Blood* 117(23), pp. 6132–6134.

Young, K., Borikar, S., Bell, R., Kuffler, L., Philip, V. and Trowbridge, J.J. 2016. Progressive alterations in multipotent hematopoietic progenitors underlie lymphoid cell loss in aging. *Journal of Experimental Medicine* 213(11), pp. 2259–2267.

Yu, M. and Cantor, A.B. 2012. Megakaryopoiesis and thrombopoiesis: an update on cytokines and lineage surface markers. *Methods in molecular biology (Clifton, N.J.)* 788, pp. 291–303.

Yu, X.J., Guo, X.Z., Li, C., Chong, Y., Song, T.N., Pang, J.F. and Shao, M. 2019. SIRT1-ZEB1-positive feedback promotes epithelial-mesenchymal transition process and metastasis of osteosarcoma. *Journal of cellular biochemistry* 120(3), pp. 3727–3735.

Zavadil, J., Cermak, L., Soto-Nieves, N. and Böttinger, E.P. 2004. Integration of TGF-β/Smad and Jagged1/Notch signalling in epithelial-to-mesenchymal transition. *The EMBO Journal* 23(5), pp. 1155–1165.

Zeisberg, M. and Neilson, E.G. 2009. Biomarkers for epithelial-mesenchymal transitions. *The Journal of Clinical Investigation* 119(6), pp. 1429–1437.

Zeyer, K.A. and Reinhardt, D.P. 2015. Fibrillin-containing microfibrils are key signal relay stations for cell function. *Journal of cell communication and signaling* 9(4), pp. 309–325.

Zhang, J. et al. 2020. Zeb1 represses TCR signaling, promotes the proliferation of T cell progenitors and is essential for NK1.1+ T cell development. *Cellular and Molecular Immunology* 18(9), pp. 2140–2152.

Zhang, J., He, T., Xue, L. and Guo, H. 2021. Senescent T cells: a potential biomarker and target for cancer therapy. *eBioMedicine* 68.

Zhang, K. et al. 2022a. Zeb1 sustains hematopoietic stem cell functions by suppressing mitofusin-2-mediated mitochondrial fusion. *Cell Death and Disease* 13(8). doi: 10.1038/s41419-022-05194-w.

Zhang, K. et al. 2022b. Zeb1 sustains hematopoietic stem cell functions by suppressing mitofusin-2-mediated mitochondrial fusion. *Cell Death & Disease 2022 13:8* 13(8), pp. 1–12.

Zhang, N., Hartig, H., Dzhagalov, I., Draper, D. and He, Y.W. 2005a. The role of apoptosis in the development and function of T lymphocytes. *Cell Research 2005 15:10* 15(10), pp. 749–769.

Zhang, N., Hartig, H., Dzhagalov, I., Draper, D. and He, Y.W. 2005b. The role of apoptosis in the development and function of T lymphocytes. *Cell Research 2005 15:10* 15(10), pp. 749–769.

Zhang, P., Sun, Y. and Ma, L. 2015a. ZEB1: At the crossroads of epithelial-mesenchymal transition, metastasis and therapy resistance. *Cell Cycle* 14(4), p. 481.

Zhang, P., Sun, Y. and Ma, L. 2015b. ZEB1: At the crossroads of epithelial-mesenchymal transition, metastasis and therapy resistance. *https://doi.org/10.1080/15384101.2015.1006048* 14(4), pp. 481–487.

Zhang, P., Sun, Y. and Ma, L. 2015c. ZEB1: At the crossroads of epithelial-mesenchymal transition, metastasis and therapy resistance. *Cell Cycle* 14(4), p. 481.

Zhang, Z. et al. 2019. Human interleukin-2 receptor β mutations associated with defects in immunity and peripheral tolerance. *The Journal of Experimental Medicine* 216(6), p. 1311.

Zhao, E. et al. 2012. Bone marrow and the control of immunity. *Cellular and Molecular Immunology* 9(1), pp. 11–19. doi: 10.1038/cmi.2011.47.

Zhao, J. et al. 2022. Overexpression of CDCP1 is Associated with Poor Prognosis and Enhanced Immune Checkpoints Expressions in Breast Cancer. *Journal of Oncology* 2022.

Zhao, Y., Shao, Q. and Peng, G. 2020. Exhaustion and senescence: two crucial dysfunctional states of T cells in the tumor microenvironment. *Cellular and Molecular Immunology* 17(1), p. 27.

Zheng, H. et al. 2020a. Glycogen synthase kinase-3β: a promising candidate in the fight against fibrosis. *Theranostics* 10(25), pp. 11737–11753.

Zheng, H.Y. et al. 2020b. Longitudinal transcriptome analyses show robust T cell immunity during recovery from COVID-19. *Signal Transduction and Targeted Therapy 2021 5:1* 5(1), pp. 1–12.

Zhou, C. et al. 2017. ZEB1 confers stem cell-like properties in breast cancer by targeting neurogenin-3. *Oncotarget* 8(33), p. 54388.

Zhou, X. and McElhaney, J.E. 2011. Age-related changes in memory and effector T cells responding to influenza A/H3N2 and pandemic A/H1N1 strains in humans. *Vaccine* 29(11), p. 2169.